

# Genotype-Phenotype Correlations in Fuchs Corneal Endothelial Dystrophy

*Kirithika Muthusamy*  
*MBChB MRCOphth*

A Thesis Submitted to the  
University College London  
for the degree of  
Doctor Of Medicine

## Abstract

Fuchs endothelial corneal dystrophy (FECD) is the most common form of corneal dystrophy and the leading indication of corneal transplant surgery worldwide. Over the past decade, greater insight into the genetic changes causative of FECD has provided clinicians with an opportunity to improve our understanding of this dystrophy and to explore new potential therapeutic avenues.

In this thesis, I investigate the genotype-phenotype correlations identified in a cohort of 342 FECD patients recruited from Moorfields Eye Hospital. By first studying the CTG trinucleotide repeat expansion within the *TCF4* gene (termed CTG18.1), the causal variant in the majority of FECD patients, I have shown the existence of significant demographic differences between FECD patients who carry this mutation (ExpPos) and those who do not (ExpNeg). I have also demonstrated a significant correlation between repeat expansion size and disease severity in ExpPos subjects, as longer repeat length was associated with younger age at transplantation.

I then carried out phenotype analysis on ExpNeg patients who were identified to harbour other FECD-associated variants via whole exome sequencing. The findings within this subgroup support the classification of corneal decompensation secondary to mutations in the *COL8A2* gene as a clinical entity distinct from FECD, in view of significant differences in both disease onset and severity.

Investigation of the FECD cohort further highlighted the rare concurrent presentation of keratoconus in this population. Although we found no definitive genetic link between the two diseases, this study highlights the clinical challenges that arise in the diagnosis and management of patients presenting with the dual pathology.

Finally, to translate the advances made in the field of molecular genetics into improved treatment options for FECD patients, I discuss the design of a Phase 1 clinical trial to evaluate the therapeutic potential and safety of an antisense oligonucleotide therapy targeting ExpPos FECD.

## **Impact Statement**

### **A New Approach to FECD**

This study enhances our understanding of Fuchs Endothelial Corneal Dystrophy (FECD) genetic heterogeneity and highlights that although corneal oedema secondary to endothelial dysfunction is the final common pathological outcome for patients clinically diagnosed as FECD, at the molecular level the basis for their disease may vary considerably.

Through detailed evaluation of phenotypic characteristics of patients harbouring different mutations, this study highlights clinically significant variations in disease onset, severity and progression within genetically defined subgroups of FECD. These findings not only contribute to an evolving understanding of this common sight threatening disease but also signals the need for a shift in clinical perspective when evaluating patients with FECD. This study contributes to the development of a personalised genetic medical model that informs FECD patients in regards to disease prognosis and potential new treatments. By clearly defining genotype-phenotype correlations and understanding the natural history of the disease, we can begin to identify optimal treatment windows for new and emerging gene-based FECD therapeutics.

Through the collaborative work of the clinicians and scientists, we have been able to channel the knowledge gained through this project along the following avenues:

### **Successful Design and Development of the First in Human Antisense Oligonucleotide Therapy Trial For FECD**

In September 2021, Moorfields Eye Hospital, the Institute of Ophthalmology and ProQr therapeutics opened recruitment to the FuchsFocus Phase I Clinical Trial of an antisense oligonucleotide aimed at ameliorating the pathological changes observed in FECD. This open-label, single dose exploratory study represents the world's first trial to evaluate the safety and tolerability of a gene-based therapy for the treatment of FECD.

### **Validating genetic testing for FECD in the presence of emerging therapies**

As we work to translate new gene-based treatments from bench to bedside, we have also begun to increase awareness of the value of identifying the underlying genetic cause of FECD in clinical practice. To support the effort to build a genetic risk profile of patients with FECD in routine NHS practice so that

we can identify patient sub-populations that are likely to receive the greatest benefit from current or new therapies and determine optimal therapeutic windows, we have applied for the most common genetic cause of this condition (CTG18.1 repeat expansion within the *TCF4* gene) to be included in the National Genomic Testing Directory.

#### **Ongoing Research into the Genotype-Phenotype correlations underlying FECD**

The insight gained from this study has highlighted the need for to build a phenotypic database of patients with FECD to support future work and improve our understanding of this disease. We continue to work with colleagues in academia and pharmaceutical industry to better understand the natural history of this disease, evaluate new parameters by which to define disease progression, and identify potential new therapeutic targets for this condition.

## Statement of Originality

The work presented in this thesis submitted for the degree of Doctor of Medicine is my own work composition and except where otherwise stated the data presented here is my own original work.

*Kirithika Muthusamy*

## Acknowledgements

I would like to thank my supervisors Professor Steven Tuft, Dr Alice Davidson and Professor Alison Hardcastle for their unwavering support and guidance through every stage of this work. I was also fortunate to receive a great amount of support from all members of the UCL team, particularly Beatriz Sanchez-Pintado, Nathaniel J Hafford Tear, Amanda Sadan and Nihar Bhattacharyya to whom I am very grateful as this work would not have been possible without them. Dr Petra Liskova through her collaboration from the Charles University and General University Hospital in Prague, Dr Caroline Thaung from the Ophthalmic Pathology Department of the Institute of Ophthalmology and Mr Scott Hau as the head of Imaging for the MEH Corneal Service have also played an invaluable role in sharing their time and expertise in guiding this thesis.

Finally, I must thank the patients and their families for their selfless contribution towards the ongoing research in the field of corneal genetic disease.

## Table of Contents

Abstract .....	2
Impact Statement.....	3
Statement of Originality.....	5
Acknowledgments.....	6
1.0 Introduction.....	19
1.1 Background.....	20
1.2 The Normal Cornea.....	21
1.2.1 Basic Anatomy and Function of Cornea.....	21
1.3 Fuchs Endothelial Corneal Dystrophy.....	26
1.3.1 Clinical presentation of FECD.....	26
1.3.2 Pathophysiology of FECD.....	28
1.3.2.1 Endothelial Cell Dysfunction.....	28
1.3.2.2 Abnormalities of Descemet’s Membrane in FECD.....	29
1.3.3 Classification of Fuchs Endothelial Corneal Dystrophy.....	30
1.3.4 Advances in the field of genetics and the study of FECD.....	35
1.3.4.1 The Human Genome Project.....	35
1.3.4.2 The Human Genome.....	35
1.3.4.3 Genetic Variants.....	37
1.3.4.4 Mechanisms of Mutational Effect.....	38
1.3.4.5 Genetic Variation and Population Genetics.....	40
1.3.4.6 Next Generation Sequencing.....	41
1.3.4.7 Genome Databases and Bioinformatics.....	41
1.3.4.8 In silico prediction tools.....	42
1.3.4.9 Genome-Wide Association Studies.....	43
1.3.4.10 Application of WES to identify disease causing mutations.....	44
1.3.5 Fuchs Endothelial Corneal Dystrophy associated Genes.....	44
1.3.5.1 <i>ZEB1/TCF8</i> .....	45
1.3.5.2 <i>LOXHD1</i> .....	46
1.3.5.3 <i>SLC4A11</i> .....	46
1.3.5.4 <i>COL8A2</i> .....	47
1.3.5.5 <i>TCF4 CTG18.1</i> .....	47
1.3.5.5.1 Pathophysiology of Repeat Expansion Positive FECD.....	48
1.3.5.5.1.1 RNA Toxicity.....	49
1.3.5.5.1.2 Dysregulation expression of TCF4.....	50

1.3.5.5.1.3	RAN translation.....	51
1.3.5.6	Recently associated genes with FECD by GWAS.....	52
1.3.5.6.1	<i>LINC00970/ATP1B1</i> .....	53
1.3.5.6.2	<i>LAMC1</i> rs3768617.....	53
1.3.5.6.3	<i>KANK4</i> .....	53
1.4	Aims and Hypothesis.....	54
<b>2.0</b>	<b>Genotype-Phenotype Correlation of the TCF4 CTG18.1 Triplet Repeat Expansion.....</b>	<b>55</b>
2.1	Background.....	56
2.2	Aims.....	57
2.3	Methods.....	61
2.3.1	Patient Recruitment.....	61
2.3.2	Consent.....	61
2.3.3	Phenotyping.....	61
2.3.4	TCF4 Genotyping.....	62
2.3.5	Statistical Analysis.....	63
2.4	Results.....	65
2.4.1	Comparisons Between the Repeat Expansion Positive Cohort.....	65
	and the Repeat Expansion Negative Cohort	
2.4.1.1	Patient Demographics.....	66
2.4.1.1.1	Ethnicity.....	66
2.4.1.1.2	Gender.....	67
2.4.1.1.3	Ocular Co-morbidities.....	67
2.4.1.1.4	Family History.....	69
2.4.1.1.5	Age of Diagnosis.....	69
2.4.1.2	Surrogate markers of disease severity.....	70
2.4.1.2.1	Age at the time of first corneal transplantation.....	70
a.	Influence of <i>CTG18.1</i> repeat expansion status on the age at first corneal transplant surgery.....	71
b.	Correlation between age at first corneal transplant surgery and <i>CTG18.1</i> repeat length within the expansion-positive cohort.....	71
c.	Comparison of age at first corneal transplant surgery within the repeat expansion-positive cohort stratified	



	to exclude prior cataract surgery.....	72
2.4.1.2.2	Modified clinical grading score.....	73
2.4.1.2.3	Central Corneal Thickness at time of first corneal graft surgery.....	73
2.5	Discussion.....	74
2.6	Limitations.....	81
2.7	Conclusion.....	83
<b>3</b>	<b>Analysis of the CTG18.1 Expansion Negative FECD Cohort.....</b>	<b>84</b>
3.1	Introduction.....	85
3.2	Methods.....	86
3.2.1	Whole Exome Sequencing.....	86
3.2.1.1	Alignment of read data.....	86
3.2.1.2	Variant filtering.....	86
3.2.2	Pathogenicity prediction tools.....	86
3.2.2.1	In silico prediction.....	86
3.2.2.2	Variant effect predictor.....	87
3.2.2.3	OMIM.....	87
3.2.2.4	BioEdit Alignment Editor.....	87
3.2.3	Filtering strategy applied in investigating ExpNeg cohort.....	88
3.2.4	Patient Recruitment.....	91
3.2.5	Phenotyping.....	91
3.2.5.1	Clinical Data Collection.....	91
3.2.5.2	Imaging and structural analysis.....	92
3.2.5.3	Pathology.....	92
3.3	Results.....	93
3.3.1	Early Onset FECD and Collagen VIII.....	94
3.3.1.1	<i>COL8A2</i> .....	95
3.3.1.1.1	Background.....	95
3.3.1.1.2	Genotyping.....	97
3.3.1.1.3	Phenotyping.....	99
3.3.1.1.4	Corneal Imaging and Histology.....	102
3.3.1.1.5	Discussion.....	106
3.3.1.2	<i>COL8A1</i> .....	111

3.3.1.2.1	Background.....	111
3.3.1.2.2	Genotyping.....	112
3.3.1.2.3	Phenotyping.....	113
3.3.1.2.4	Corneal Imaging and Histology.....	114
3.3.1.2.5	Discussion.....	115
3.3.2	Genes Previously Associated with FECD.....	120
3.3.2.1	<i>SLC4A11</i> .....	121
3.3.2.1.1	Background.....	121
3.3.2.1.2	Genotyping.....	122
3.3.2.1.3	Phenotyping.....	125
3.3.2.1.4	Discussion.....	127
3.3.2.2	<i>ZEB1</i> .....	128
3.3.2.2.1	Background.....	128
3.3.2.2.2	Genotyping.....	129
3.3.2.2.3	Phenotyping.....	130
3.3.2.2.4	Discussion.....	130
3.3.3	GWAS associated FECD Genes.....	131
3.3.3.1	<i>LAMC1</i> .....	132
3.3.3.1.1	Background.....	132
3.3.3.1.2	Genotyping.....	132
3.3.3.1.3	Phenotyping.....	135
3.3.3.1.4	Discussion.....	136
3.3.3.2	<i>KANK4</i> .....	138
3.3.3.2.1	Background.....	138
3.3.3.2.2	Genotyping.....	138
3.3.3.2.3	Phenotyping.....	140
3.3.3.2.4	Discussion.....	140
3.4	Conclusion.....	141
<b>4</b>	<b>Investigating the Dual Presentation of FECD and Keratoconus.....</b>	<b>142</b>
4.1	Background.....	143
4.2	Aims.....	149
4.3	Methods.....	150

4.4 Results.....	151
4.4.1 Genetic Analysis.....	152
4.4.2 Surgical Intervention.....	156
4.4.2.1 Case studies.....	156
4.4.3 Histopathology.....	166
4.5 Discussion.....	167
4.6 Limitations.....	172
4.7 Conclusion.....	172
<b>5 Phase I Clinical Trial to Investigate an Antisense Oligonucleotide based therapy for FECD.....</b>	<b>173</b>
5.1 Ocular Gene Based Therapies.....	174
5.2 Developing a novel gene based therapy for FECD.....	176
5.2.1 Background.....	176
5.2.2 Developing an ASO to Treat Repeat Expansion Positive FECD.....	177
5.3 Potential pathways for ASO delivery to the corneal endothelium.....	181
5.4 Understanding the FECD Patient Population.....	186
5.4.1 Patient engagement.....	186
5.4.2 Evaluating Patient Burden in Trial Participation.....	186
5.4.3 Assessing the potential recruitment base of MEH FECD patients.....	187
5.5 Considerations when choosing trial outcome measures.....	189
5.5.1 Objective assessment of visual function.....	191
5.5.2 Anatomical Assessment of Outcome Measure.....	192
5.5.3 Assessment of Bioavailability.....	194
5.5.4 Patient Reported Outcomes Measure.....	194
5.6 Study Design.....	195
<b>References.....</b>	<b>198</b>
<b>Appendix.....</b>	<b>217</b>
A Genotyping for TCF4 CTG18.1 Repeat Expansion.....	217
B Statistical analysis Chapter 2.....	219
C Legend to pedigree symbols.....	227
D Moorfields corneal cross linking protocol.....	228

E	Clinical Trial Subject Inclusion and Exclusion Criteria.....	230
F	Clinical trial schedule of events of investigations.....	233

## List of Tables

<b>Chapter 1</b>	<b>Introduction</b>	
Table 1	Population based prevalence of FECD.....	26
Table 2	Krachmer grading score of FECD.....	30
Table 3	Summary of studies suggesting new modalities by which to measure and stage FECD.....	32
<b>Chapter 2</b>	<b>Genotype-Phenotype Correlation of <i>TCF4</i> CTG18.1 triplet repeat expansion in the MEH FECD Cohort</b>	
Table 1	Summary of publications investigating the genotype-phenotype correlation of <i>TCF4</i> CTG18.1 Triplet Repeat Expansion on disease severity.....	58
Table 2	Modified Clinical Staging (MCS) score of Fuchs Endothelial Corneal Dystrophy.....	62
Table 3	Ethnicity of FECD patients subdivided by repeat expansion status.....	66
Table 4	Table of family members reported to show symptoms of FECD within the MEH FECD study cohort.....	69
Table 5	Summary of publications investigating the prevalence of Keratoconus in predominantly Caucasian populations.....	76
Table 6	Summary of FECD disease characteristics that were shown to correlate significantly with repeat expansion status or length.....	80
<b>Chapter 3</b>	<b>Analysis of CTG18.1 Expansion Negative FECD</b>	
Table 1	Summary of genes and loci associated with FECD.....	89
Table 2	A summary of published phenotypic characteristics of subjects identified as harbouring disease-associated heterozygous missense variants within the <i>COL8A2</i> gene.....	109
Table 3	Three heterozygous variants in <i>SLC4A11</i> were identified through whole exome sequencing.....	122
Table 4	Summary of associated <i>ZEB1</i> variants reported in late and early onset FECD.....	128

Table 5 Identification of rare variants in LAMC1 within the CTG18.1 ExpNeg cohort.....133

**Chapter 4 Investigating the Dual Presentation of FECD and Keratoconus**

Table 1 Literature review of combined cases of Keratoconus and FECD.....146

Table 2 Tabulation of demographic data, CTG18.1 repeat expansion status, surgical intervention and other ocular co-morbidities within the KC FECD patient Population.....153

Table 3 Follow up and progression data of KCFED patients documenting changes in corneal curvature and central corneal thickness.....155

Table 4 Summary of surgical outcomes following both DMEK and DSEK surgery in patients with combined keratoconus and FECD.....171

**Chapter 5 Phase I Clinical Trial Design to Investigate an Antisense Oligonucleotide-Based Therapy for FECD**

Table 1 Emerging techniques in the field of ocular drug delivery.....184

## List of Figures

<b>Chapter 1</b>	<b>Introduction</b>	
Figure 1	Illustration depicting the multiple mechanisms that are hypothesised to contribute to the pathophysiology of Fuchs Endothelial Corneal Dystrophy.....	45
Figure 2	Three pathogenic mechanism contributing to the pathophysiology of <i>TCF4</i> CTG18.1 expansion mediated FECD.....	48
Figure 3	RNA toxicity secondary to sequestration of vital RNA-binding protein MBNL1.....	50
Figure 4	Overview of potential proteins products produced by RAN translation of a CTG expansion transcript.....	51
Figure 5	Results from Genome Wide Association study by Afshari et al. 2017.....	52
<b>Chapter 2</b>	<b>Genotype-Phenotype Correlation of <i>TCF4</i> CTG18.1 triplet repeat expansion in the MEH FECD Cohort</b>	
Figure 1	<i>TCF4</i> CTG18.1 repeat expansion distribution.....	65
Figure 2	Distribution of FECD patients based on gender and expansion status.....	67
Figure 3	Ocular Co-morbidities within the FECD cohort.....	68
Figure 4	Bee swarm plot of age of first corneal transplantation within the MEH FECD cohort in accordance with expansion status.....	71
Figure 5	Correlation analysis of the relationship between age of first corneal transplant surgery and repeat expansion length in the Expansion Positive FECD cohort .....	72
<b>Chapter 3</b>	<b>Analysis of CTG18.1 Expansion Negative FECD</b>	
Figure 1	Whole exome sequencing (WES) filtering strategy employed by this study to identify potential FECD-associated variants and enable genotype-phenotype correlation analysis.....	90
Figure 2	Pie chart depicting the percentage of the FECD repeat-expansion negative subjects investigated by Whole Exome Sequencing that were found to harbour rare variants in genes associated with FECD as well as genes	

	reported in a genome wide association study (GWAS) as promising candidate genes.....	91
Figure 3	Multiple Sequencing Alignment showing conservation of amino acid residue p.Q455 COL8A2 across orthologues.....	97
Figure 4	Molecular model of Collagen VIII mutant.....	98
Figure 5	Pedigree of Proband COL-A (IV.3), a 51 year old Caucasian female who is heterozygous for the p.Q455K missense variant.....	100
Figure 6	Pedigree of Proband COL-B (II.2), a 25 year old Caucasian male who is heterozygous for the p.Q455K missense variant.....	101
Figure 7	Slitlamp images of Proband A's unoperated right eye.....	103
Figure 8	Corneal endothelial cell imaging of three subjects harbouring mutations in COL8A2.....	104
Figure 9	Magnified image of histology specimen obtained from Proband COL-B.....	105
Figure 10	Multiple Sequencing Alignment showing conservation of amino acid residue p.I207 COL8A1 across orthologues.....	112
Figure 11	Familial Segregation of unique COL8A1 variant in Proband COL-C.....	116
Figure 12	Slitlamp biomicroscopy images of first-degree relatives of proband COL-C affected by FECD.....	117
Figure 13	Imaging of Proband COL-C's 38-year-old sister.....	118
Figure 14	Confocal images of Proband IT_1639's affected siblings and father.....	119
Figure 15	Descemet's membrane and endothelial cell layer removed at the time of partial thickness endothelial keratoplasty from Proband COL-C stained with haematoxylin and eosin.....	119
Figure 16	Multiple Sequencing Alignment showing conservation of amino acid across orthologues corresponding to 3 nonsynonymous heterozygous variants in the SLC4A11 gene in 3 individuals.....	123
Figure 17	Molecular model of SLC4A11 protein homodimer.....	124
Figure 18	Sanger sequencing chromatogram and familial pedigree of proband SLC-C.....	126
Figure 19	Multiple Sequencing Alignment showing conservation of amino acid residue p.T212 in ZEB1 across orthologues.....	129
Figure 20	Multiple Sequencing Alignment showing conservation of amino acid across orthologues corresponding to 3 nonsynonymous heterozygous variants in the LAMC1 gene in 3 individuals.....	134
Figure 21	Identification and segregation analysis of the rare LAMC1 variant c.1836C>T.....	137



Figure 22	Multiple Sequencing Alignment showing conservation of amino acid across orthologues corresponding to 2 nonsynonymous heterozygous variants in the KANK4 gene in 2 individuals.....	139
-----------	--	-----

**Chapter 4      Investigating the Dual Presentation of FECD and Keratoconus**

Figure 1	Pre-operative Scheimpflug corneal tomography (Pentacam) scans of KF13’s right eye at the age of 69 years.....	157
Figure 2	Comparative Scheimpflug corneal tomography (Pentacam) scans performed 25 months following Right DMEK surgery in subject KF13.....	158
Figure 3	Scheimpflug corneal tomography (Pentacam) scans obtained from KF12 on presentation at the age of 52 years.....	159
Figure 4	Scheimpflug corneal tomography (Pentacam) obtained from KF12 following left DMEK surgery.....	160
Figure 5	Scheimpflug corneal tomography (Pentacam) of KF12 following right corneal transplant surgery (DSAEK) surgery and intraocular lens implantation.....	162
Figure 6	Left eye Scheimpflug corneal tomography (Pentacam) of KF8, a 44 year old white Caucasian male taken at the time of diagnosis.....	163
Figure 7	The right Scheimpflug corneal tomography (Pentacam) of KF8, a 44 year old white Caucasian male taken at the time of diagnosis.....	164
Figure 8	Scheimpflug corneal tomography (Pentacam) of KF8’s right cornea pre and post DMEK surgery.....	165
Figure 9	Histopathology samples obtained at the time of penetrating keratoplasty.....	166

**Chapter 5      Phase I Clinical Trial Design to Investigate an Antisense Oligonucleotide-Based Therapy for FECD**

Figure 1	Timeline of milestones in ocular gene therapy.....	174
Figure 2	Schematic representation of factors that were evaluated in the design of a Phase I clinical trial for the treatment of Expansion Positive	

	Fuchs Endothelial Corneal Dystrophy with a targeted gene based therapy.....	175
Figure 3	Oligonucleotide Based Gene Therapy.....	176
Figure 4	mRNA splicing factors MBNL1and MBNL2 are sequestered to RNA foci of corneal endothelial cells derived from FECD patients.....	178
Figure 5	ASO-Mediated treatment of CECs significantly reduces foci number and rescues MBNL1 nuclear localization.....	179
Figure 6	Planned patient treatment pathway over the period of enrolment in the FuchFocus Phase I Clinical Trial.....	197

# INTRODUCTION

## 1.1 Background

Fuchs endothelial corneal dystrophy (FECD) was the first identified as a progressive bilateral corneal degeneration by Ernst Fuchs in 1910. Although first assumed to be a bilateral disease of the epithelial layer and described by Fuchs as Dytrophia Epithelialis, FECD is primarily a disease of the corneal endothelium. This common corneal dystrophy leads to considerable visual morbidity and presents a significant burden of disease across the world. It is the fourth leading indication for corneal transplant surgery internationally (Gain, Jullienne et al. 2016). Given the global shortage of appropriate donor corneal tissue, this treatment is not easily accessible to the majority of FECD patients. Even following successful transplantation, the grafted endothelial cells are susceptible to immune mediated rejection episodes and eventual graft failure. Consequently, there exists a drive for alternative therapeutic strategies to treat this patient population.

In the century since the condition was first described, we have begun to develop a deeper understanding of both the genetics and the pathophysiology of FECD. It is hoped that a finer understanding of the disease, as well as an appreciation of its natural history, will guide the development of future preventative treatments that could negate the need for surgical intervention.

As we continue to witness breakthroughs in the field of gene-based therapy in ocular disease, we hope to translate these successes to FECD. This study aims to contribute towards an improved understanding of FECD genotype-phenotype correlation and guide future treatment strategies for this disease.

## 1.2 The Normal Cornea

### 1.2.1. Basic Anatomy and Function of the Cornea

The adult cornea is 11-12mm in diameter horizontally and 9-11mm vertically. It is approximately 500  $\mu\text{m}$  thick centrally and increases in thickness towards the periphery to a depth of approximately 700 $\mu\text{m}$  (Fares, Otri et al. 2012). The cornea is a convex structure that flattens from the apex to the periphery. The central cornea is therefore steeper relative to the peripheral cornea. It possesses a refractive index of 1.376 and along with the overlying tearfilm forms the major refractive component of the eye (Helmholtz and Southall 1924).

The cornea is made up of 5 distinct layers:

#### a) Epithelial Layer

The corneal epithelial layer is formed by non-keratinized, squamous epithelial cells that create a transparent defensive barrier on the ocular surface. This layer is an even thickness of 50 $\mu\text{m}$  across the surface of the cornea. The epithelial cell population consists of 3 subtypes: Superficial cells, wing cells and columnar basal cells. The basal cells are the only epithelial cells that are able to proliferate. Through secondary differentiation, basal cells give rise to wing cells that remain in an intermediate state of differentiation as well as terminally differentiated superficial.

Multiple junctional complexes exist between the different epithelial cells. Tight junctions between the superficial cells create a barrier to the tear film and chemicals within the ocular surface environment. In addition, cell adhesion proteins such as occludins, desmosomes and hemidesmosomes are found throughout the epithelial multilayer that provide a further barrier function to external solutes. However, within the deeper basal and wing cell layers, gap-junctions do allow selective permeability to small molecules. Gap junctions in the basal cell layers are believed to mediate intercellular communication and play an important role in cell differentiation (Mantelli, Mauris et al. 2013).

In response to injury, epithelial cells in the vicinity of the damaged cells lose junctional complexes and begin to flatten and spread to cover the area of epithelial defect. Epithelial cell proliferation and migration occurs from the limbus towards the site of injury. In the final stage,

hemidesmosomes and gap junctions are reformed followed by synthesis and assembly of extracellular matrix (Thoft and Friend 1983).

b) Epithelial Basement Membrane

The epithelial basement membrane lies posterior to epithelium and is secreted from basal epithelial cells. The anterior layer of the basement membrane, the lamina lucida, is made up of laminins and is structurally distinct from the posterior lamina densa which consist of collagen, laminins, glycoproteins and proteoglycans. This layer provides an anchoring point for the epithelial cells to the stroma (Saikia, Medeiros et al. 2018). The corneal basal epithelial cells have small protuberances on the basal surface known as hemidesmosomes. The hemidesmosomes (Bourne, Johnson et al. 1982) attach to anchoring filaments of laminin and Type VII collagen within the lamina lucida and lamina densa respectively to form the “hemidesmosome-stable adhesion complex” (Torricelli, Singh et al. 2013).

c) Bowman’s layer

Corneal epithelial cells are anchored to an underlying basement membrane layer known as Bowman’s layer. This acellular layer is approximately 8-12µm thick and is formed primarily of Collagen Type I and Type III as well as proteoglycans (Wilson 2020). Bowman’s layer is secreted by the stromal keratocytes and the posterior layer of the membrane is noted to be continuous with the anterior stroma. As Bowman’s layer is routinely removed during refractive laser procedures with little detriment to the corneal structure and function, the exact role of this layer is not fully understood. Although it has been hypothesized that this acellular layer contributes to the structural integrity of the epithelial layer and may provide a physical barrier to microbial penetration (Wilson and Hong 2000).

d) Stroma

The corneal stromal layer account for 90% of the corneal thickness. Keratocytes are the main cellular component of the stroma but make up approximately only 3 % of the stromal volume. These cells secrete collagen, glycosaminoglycans and matrix metalloproteinases to maintain the structural integrity of the stromal layer. The stroma is made up predominantly of Type I and Type IV collagen, although small amounts of Collagen III and V are also present (Ihanamaki, Pelliniemi et al. 2004). The highly ordered structure of the collagen fibres is essential to the transparency of the cornea (Meek and Boote 2004). The mean diameter of the collagen fibres and the mean

distance between these fibres is maintained at less than half the wavelength of visible light (400-700nm). This exact arrangement leads to a pattern of interference from scattered light rays that enables passage of an incident ray of light through the cornea (West-Mays and Dwivedi 2006). If this highly ordered structure is altered by oedema or scarring, the cornea loses its transparency.

Proteoglycans form the extracellular matrix of the stroma and consist of a core protein (keratocan, lumican, mimecan, decorin or biglycan) attached to glycosaminoglycans (GAGs). The primary GAG in the stroma is keratan sulphate dermatan sulphate (Xuan, Wang et al. 2016). The role of the highly charged extracellular matrix components is to provide both structural stability and to aid intrafibrillar spacing that is essential to corneal clarity (Kao and Liu 2002).

e) Descemet's membrane (DM)

Descemet's Membrane is composed primarily of Collagen Type VIII in addition to Collagen Type IV, fibronectin and laminin (Levy, Moss et al. 1996). Type VIII collagen is a short-chain protein that forms both heterotrimers and homotrimers made up of two alpha chains,  $\alpha 1(VIII)$  and  $\alpha 2(VIII)$  (Greenhill, Rugar et al. 2000). In healthy adult DM, collagen forms a highly ordered transparent structure (Levy, Moss et al. 1996). The anterior banded layer (ABL) of the DM is made up of wide spaced collagen fibres that are identified as Collagen VIII. In the healthy adult human cornea, the collagen fibrils in the ABL exhibit a characteristic banded pattern and remain static in the postnatal period. The posterior non-banded layer (PNBL) is a fine granular layer that continues to increase in size in the post-natal period through the secretion of amorphous material from corneal endothelial cells. In FECD, increased secretion of an abnormal amorphous material by CECs leads to formation of a pathological posterior collagenous layer on the inner DM (Levy, Moss et al. 1996, Gottsch, Zhang et al. 2005).

f) Endothelium

The endothelium is a monolayer of cells that form the innermost layer of the cornea. As the cells mature, they arrest in the G1 phase of mitosis and possess limited proliferative capacity. The cells are held in a non-mitotic state by a combination of factors that prevent transition to S phase (p27kip1, TGF- $\beta$ ) and cell-cell contact inhibition (Joyce, Harris et al. 2002, Joyce, Zhu et al. 2009). To enable the most efficient coverage of the posterior corneal surface, this limited number of cells forms a hexagonal mosaic in which cells are connected by tight junctions and desmosomes (Rao, Lohman et al. 1982, Waring, Bourne et al. 1982). In adults, the endothelial layer is approximately

1.5-2.5  $\mu\text{m}$  thick. At birth, the human cornea consists on average of 3000-4000 cells/ $\text{mm}^2$ , with this number continuing to decline with age (Bourne, Nelson et al. 1997, Gambato, Longhin et al. 2015). Physiological CEC loss is known to occur at an exponential rate, with a greater decrease in density occurring up to approximately 18 years of age. The observed decrease in CEC density occurs in part due to normal ocular growth and increase in corneal size (Joyce 2003). The rate of decline plateaus and stabilises in adulthood to a rate of 0.3%-0.6% per year. (Murphy, Alvarado et al. 1984, Bourne, Nelson et al. 1997, Hollingsworth, Perez-Gomez et al. 2001). The average CEC density in a 15 year old is 3400/ $\text{mm}^2$  versus 2300/ $\text{mm}^2$  in an 85 year old (Bourne 2003).

Corneal endothelium cells (CECs) play a crucial role in maintaining the transparency of the cornea. The hydrophilic, glycosaminoglycan rich content of the corneal stroma creates a negative osmotic pressure gradient between the stroma and aqueous in the anterior chamber. This osmotic gradient induces fluid flow from aqueous into the corneal tissue. The normal stromal swelling pressure of approximately 50mmHg is counterbalanced by the CECs that act both as a physical barrier to fluid as well as an active pump which drives fluid out of the stroma to create a relative state of dehydration. The dual mechanism by which endothelial cells maintain corneal deturgence was first postulated more than 30 years ago and is known as the "Pump-Leak hypothesis" (Riley 1985).

The fluid pump function of the corneal endothelial cell layer is coordinated by a combination of ion pumps, channels and exchangers that are located on the apical and basolateral cell surface (Maurice 1972). The  $\text{Na}^+/\text{K}^+$ -ATPase active co-transporter forms the main endothelial pump working in concordance with  $\text{HCO}_3^-$ ,  $\text{Cl}^-$  and carbonic anhydrase transporter (Fischbarg and Lim 1974). In addition, aquaporin (AQP) water channels (Kenney, Atilano et al. 2004) and SLC4A11 sodium borate cotransporters are both intrinsic membrane proteins that contribute to the maintenance of corneal deturgence by allowing active transport of  $\text{H}_2\text{O}$  from CECs (Vilas, Loganathan et al. 2013). At present, the exact interplay between the ion and water channels of the CEC pump is not fully understood, but the importance of individual components is beginning to come to light (Bonanno 2012). A proposed mechanism is that the  $\text{Na}^+/\text{K}^+$ -ATPase pump creates a low intracellular concentration of  $\text{Na}^+$  and high intracellular concentration  $\text{K}^+$  to enable efflux of fluid from the cornea. The pump's ability to maintain the osmotic gradient is dependent on the bioavailability of  $\text{HCO}_3^-$ ,  $\text{Cl}^-$  and carbonic anhydrase. Experimental models that deprive CECs of these three chemical components demonstrate an inhibitory effect on the endothelial pump mechanism (Winkler, Riley et al. 1992, Riley, Winkler et al. 1995).



Knock-out *Slc4a11* mouse models have been shown to develop corneal oedema associated with increased concentration of NaCl in the stroma, thus supporting the role of this transmembrane cotransporter in maintaining the corneas fluid-ion balance (Groger, Frohlich et al. 2010). In contrast, the exact function of AQP channels in corneal dehydration remains controversial. Although it has been shown that AQP1 channels are reduced in FECD (Macnamara, Sams et al. 2004) (Kenney, Atilano et al. 2004), knockout mouse models of this channel did not exhibit corneal oedema (Agre 1998).

In addition to the CEC active transport mechanisms, evaporation is also known to increase the osmolality of the tear film leading to passive egress of fluid from the stroma to the ocular surface (Bourassa, Benjamin et al. 1991).

As the proliferative capacity of human CECs is limited, damage or loss of these cells can only be compensated for by the migration and spread of existing endothelial cells. As this occurs, the cells are more variable in size (polymegathism) and begin to lose the normal hexagonal structure leading to greater variability in shape (polymorphism)(Rao, Lohman et al. 1982). When the cell loss results in CEC density below 400-500/mm<sup>2</sup>, the cornea decompensates leading to accumulation of fluid within the stroma, loss of clarity and subsequent visual loss (Waring, Bourne et al. 1982, Crawford, Ernst et al. 1995).

### 1.3 Fuchs Endothelial Corneal Dystrophy (FECD)

Fuchs Endothelial Corneal Dystrophy (FECD) accounted for thirty nine percent of transplants performed in 116 countries in 2012, making it the leading indication for corneal transplantation across the globe (Gain, Jullienne et al. 2016).

#### 1.3.1 Clinical Presentation of FECD

FECD is a disease that can be differentiated into a more common late-onset form and a rarer early onset form. Prevalence of the disease in patients above the age of 50 years ranges between 3.7-11%, depending on region and ethnicity, Table 1 (Lorenzetti, Uotila et al. 1967, Nagaki, Hayasaka et al. 1996, Kitagawa, Kojima et al. 2002, Zoega, Fujisawa et al. 2006, Higa, Sakai et al. 2011, Eghrari, McGlumphy et al. 2012). Late-onset FECD is recognized to exhibit a female to male preponderance of approximately 2.5: 1 – 3.5:1 (Krachmer, Purcell et al. 1978, Afshari, Pittard et al. 2006, Elhalis, Azizi et al. 2010).

Population studied	Prevalence (%) of late onset FECD/ Primary corneal guttate			Female:Male Ratio	Publication
	Overall	Female	Male		
Singaporean Chinese	6.7	8.5	4.4	2:1	(Kitagawa, Kojima et al. 2002)
Japan:					
Southwestern Island	4.1	5.8	2.4	2.4:1	(Higa, Sakai et al. 2011)
Monzen-machi	3.7	5.5	1.5	3.7:1	(Kitagawa, Kojima et al. 2002)
Iceland	9.2	11	7	1.6:1	(Zoega, Fujisawa et al. 2006)
USA:					
Florida	3.9	4	3.8	1.05:1	(Lorenzetti, Uotila et al. 1967)
Tangier Island	11	25.3	14.1	1.79:1	(Eghrari, McGlumphy et al. 2012)

Table 1: Population based prevalence of FECD. Cross sectional population studies of FECD have shown that the disease exhibits variation in prevalence across different regions and ethnicities. The cross sectional population-based studies tabulated here investigated the presence of late onset FECD in patients above 40-years of age. Primary central corneal guttata were the main outcome measure in all the quoted/ mentioned/ referenced/ studies.

FECD typically presents with blurring of vision that exhibits a diurnal variation, with more pronounced loss of acuity on waking that improves slightly throughout the day (Adamis, Filatov et al. 1993). As the eyelids are closed during sleep, no evaporation of fluid occurs from the ocular surface and absorption of atmospheric oxygen is reduced. Even in healthy corneas, this causes a reduction in tear osmolality as well as tissue hypoxia that leads to an increase in corneal thickness on waking (Mandell and Fatt 1965, Leung, Bonanno et al. 2011). In FECD, the diurnal variation is more pronounced due to the additional underlying dysfunction of corneal hydration control (Mandell, Polse et al. 1989, Fritz, Grewing et al. 2019) .

The formation of central guttata on Descemet's membrane also contribute to visual compromise as patients report symptoms of glare due to diffraction of light by these excrescences (Wacker, McLaren et al. 2015). Studies have also noted that even early in the course of the disease the anterior corneal anatomy is altered by loss of stromal keratocytes and abnormal subepithelial cells (Amin, Baratz et al. 2014). These anterior corneal changes in FECD are believed to contribute to decreased visual function occurs due to an increase in forward scatter of light as well as optical aberrations from the cornea (van der Meulen, Patel et al. 2011, Amin, Baratz et al. 2014, Wacker, McLaren et al. 2015). As the disease progresses, the central guttata become more confluent and progressive endothelial cell loss eventually leads to the failure to maintain a balanced fluid exchange between the corneal stroma and aqueous. As stromal oedema accumulates, the highly ordered equidistant spacing of collagen fibrils is lost and the cornea's refractive capacity is compromised (Cristol, Edelhauser et al. 1992, Wacker, McLaren et al. 2015).

As the stromal oedema progresses, epithelial and subepithelial bullae begin to form both within and under the water logged epithelial surface respectively (Adamis, Filatov et al. 1993). The rupture of these superficial bullae within the highly innervated epithelial layer leads to increased ocular discomfort (Elhalis, Azizi et al. 2010). In the most advanced stages of FECD, patients can develop large epithelial bullae that are prone to rupture causing not only significant pain but also an increased risk of infection due to the mechanical breakdown of the corneal epithelial barrier (Elhalis, Azizi et al. 2010). Longstanding disruption of normal stromal architecture in addition to epithelial breakdown leads to formation of subepithelial fibrous scar tissue deposition between the epithelium and Bowmans membrane (Waring, Bourne et al. 1982, Adamis, Filatov et al. 1993). As a result, the cornea opacifies and patients suffer from significant visual loss (Elhalis, Azizi et al. 2010).

### 1.3.2 Pathophysiology of FECD

This bilateral disease of the posterior cornea results in progressive corneal endothelial cell loss and abnormal deposition of extracellular matrix posterior to Descemet's membrane, causing it to thicken and leading to formation of focal excrescences known as guttata. It is hypothesized that in the early stage of the disease, endothelial cell loss occurs due to a combination of intrinsic cellular dysfunction as well as an increased susceptibility to oxidative stress. Although the underlying pathology of endothelial cell death and thickening of Descemet's membrane in FECD is not yet fully understood, certain distinct mechanisms are thought to contribute to the endothelial dysfunction:

#### 1.3.2.1 Endothelial Cell Dysfunction in FECD

##### a. Epithelial to Mesenchymal Transformation

Epithelial to mesenchymal transition (EMT) is a normal physiological process observed in both normal development as well as wound healing. However, this change in cellular morphology is also recognized to occur in pathological process, including FECD. Early electron micrograph studies have shown that endothelial cells in FECD undergo fibroblastic change resulting in an epithelial-like morphology (Iwamoto and DeVoe 1971). This was further confirmed by the identification of epithelial cell markers (pancytokeratin, CK7 and vimentin) within the endothelial cells of FECD tissue (Hidayat and Cockerham 2006).

##### b. Oxidative Stress

Oxidative stress leading to DNA damage and accelerated apoptosis have both been linked to the more common late-onset FECD, which manifests clinically after the 4<sup>th</sup> decade of life. As endothelial cells are arrested in a post-mitotic state, these cells are highly susceptible to oxidative damage. Jurukunas et al have demonstrated that markers of oxidative damage are co-localized to corneal guttae in FECD tissue (Jurkunas, Bitar et al. 2010). The same study further highlighted that mitochondrial DNA (mtDNA) damage was increased in FECD suggesting a role in the pathogenesis of the disease. Further gene expression studies corroborate a reduction of mitochondrial DNA expression as well as downregulation of proteins that play a protective role against oxidative stress (nuclear ferritin, glutathione S-transferase- $\pi$ , heat shock protein 70-kDa) in FECD tissue (Gottsch, Bowers et al. 2003).

### c. Apoptosis

DNA damage, such that occurs as a result of oxidative stress, is a major trigger of apoptosis (Roos and Kaina 2013). Apoptosis, a highly regulated form of programmed cell death, is known to occur in FECD (Borderie, Baudrimont et al. 2000). Apoptosis of endothelial cells, evidenced by condensed nucleus, decreased cell size and DNA fragmentation were demonstrated in more than 75% of FECD samples (Borderie, Baudrimont et al. 2000, Li, Ashraf et al. 2001). However, it remains unclear if this mode of cell death plays a primary or secondary role in the disease process.

#### 1.3.2.2 Abnormalities of Descemet's Membrane in FECD

In adult onset FECD, the DM becomes thickened by the pathological deposition of wide spaced collagen and amorphous material by CECs to form an abnormal posterior collagenous layer (PCL) between DM and endothelial cells (Levy, Moss et al. 1996, Gottsch, Zhang et al. 2005). As a result, the regular array of co-localized collagen fibres (collagen VIII $\alpha$ 1 and collagen VIII $\alpha$ 2) becomes disorganised. Nodules consisting mainly of collagen VIII develop from the PCL and form refractile excrescences on the posterior DM, known as guttata (Gottsch, Zhang et al. 2005). Guttata create a barrier to normal ion transport and disrupt the solute barrier function of the endothelium. (Chiou, Kaufman et al. 1999, Li, Ashraf et al. 2001).

In advanced cases of FECD a retrocorneal fibrous membrane can develop and is believed to derive from corneal endothelial mesenchymal transformation into fibroblasts (Michels, Kenyon et al. 1972, Roy, Leclerc et al. 2015). This fibrous change is not unique to FECD though as it has also been observed in pseudophakic bullous keratopathy as well as following surgical removal of DM, indicating it is a common feature of advanced endothelial cell dysfunction (de Oliveira and Wilson 2020).

### 1.3.3 Classification of Fuchs Endothelial Corneal Dystrophy

Over the years, a variety of anatomical and morphological grading systems have been proposed to allow staging of FECD. The Krachmer grading system was developed in 1978 and is a morphological grading scale that remains the most commonly applied method of evaluating severity of FECD, Table 2 (Krachmer, Purcell et al. 1978, Louttit, Kopplin et al. 2012):

Krachmer Grade	Slit lamp biomicroscopy findings
Grade 0	No apparent disease. Up to 11 central guttae on each cornea.
Grade 1	Definitive onset of the disease. Twelve or more central, nonconfluent guttae in at least one eye.
Grade 2	A zone of confluent central guttae 1 to 2 mm in horizontal width.
Grade 3	A zone of confluent central guttae 2 to 5 mm wide.
Grade 4	A zone of confluent central guttae greater than 5 mm wide.
Grade 5	A zone of confluent central guttae greater than 5 mm wide plus oedema of the corneal stroma and/or corneal epithelium.

Table 2: Krachmer grading scale of Fuchs Endothelial Corneal Dystrophy. The table details the 5 levels of the Krachmer grading scale used to evaluate clinical severity of FECD on the basis of morphological changes observed on slit lamp biomicroscopy. This grading system prioritises the occurrence and distribution of corneal guttae, while the existence of corneal oedema is only assigned to the most advanced stage of FECD.

One of the drawbacks of this subjective grading scale that it is susceptible to interobserver variation (Repp, Hodge et al. 2013). Also, in cases of early FECD, the staging criteria for Grade 1-4 do not account for the possibility of mild corneal oedema early in the course of the disease .

Recent studies have introduced a Krachmer Grade 6 for eyes that have undergone corneal transplantation (Soliman et al 2015). However, this stage reflects the high threshold for surgical intervention that was applied to patients when Penetrating Keratoplasty (PK) was the only available treatment. With the advent of less invasive Endothelial Keratoplasty (EK), the threshold for performing surgical intervention in FECD has decreased to reflect the lower risk and improved post-operative outcome of this technique (Price and Price 2017). As glare due to central guttata or diurnal variation with even mild corneal oedema can adversely affect a patient's ability to perform everyday tasks, EK surgery is now offered earlier in the course of FECD. Even a patient with a Krachmer Grade of 2 who was having difficulty with glare secondary to confluent central guttata could be offered the option of endothelial keratoplasty if visual disability was significantly interfering with activities such as driving.

To address these limitations, various studies have been performed to define new anatomical and optical measures of FECD (Table 3). Efforts to improve the repeatability of slit lamp assessment of the cornea, to evaluate the changing distribution of corneal oedema and to assess the pattern of aberrant refraction of light through the cornea in FECD, have all been proposed to improve staging of this disease. Further to this, there is now a greater emphasis on measuring the patients' own experience of the disease through Patient Reported Outcome Measures (PROMs). The Visual Function and Corneal Health Status (V-FUCHS) is a standardized and validated questionnaire developed to allow patient-reported quantification of visual disability specifically in the FECD patient population (Wacker, Baratz et al. 2018)

Author	Modality of assessment	Baseline Grading System	Conclusion	Limitation
Kopplin <i>et al</i> 2012 (Kopplin, Przepyszny <i>et al.</i> 2012)	Central corneal thickness measured by ultrasonographic pachymetry	Siltlamp biomicroscopy assessment of central or paracentral guttae were graded according to the confluence of guttae and presence of corneal epithelial or stromal oedema  Kraemer grading score applied	An increase in CCT occurs with increasing severity of FECD, including at lower FECD grades in which clinically observable oedema is not present	<ul style="list-style-type: none"> <li>- Does not consider repeatability of CCT measured by ultrasonic pachymetry</li> <li>- The measurement of thickness only in the central cornea may underestimate of the thickest area of the cornea when more severe disease is located in the paracentral region</li> <li>- Study does not account for diurnal variation</li> </ul>
Amin <i>et al</i> 2014 (Amin, Baratz <i>et al.</i> 2014)	Anterior and posterior corneal high-order aberrations (HOAs) measured from the confocal image light intensity profile	Siltlamp biomicroscopy assessment of central or paracentral guttae were graded according to the confluence of guttae and presence of corneal epithelial or stromal oedema  Grade 0: Normal corneas, devoid of any central guttae Grades 1–2: Mild Grades 3–4: Moderate Grade 5–6: Severe  (If corneas had clinically detectable corneal oedema, they were assigned to grade 6 irrespective of the distribution of guttae)	Anterior corneal cellular and structural abnormalities begin early in the course of FECD, before the onset of clinically evident oedema	<ul style="list-style-type: none"> <li>- Confocal microscopy shows a higher level of variation than Scheimpflug imaging when assessing backscatter</li> <li>- Specular reflection in confocal images limited the sensitivity to detect subtle posterior changes in the mild stages of the disease previously</li> </ul>



Eghrari <i>et al</i> 2015 (Eghrari, Garrett <i>et al.</i> 2015)	Retrillumination photography analysis of slit-lamp flash photography after pupillary dilation	Slitlamp biomicroscopy assessment of central or paracentral guttae were graded according to the confluence of guttae and presence of corneal epithelial or stromal oedema Grade 0: Normal corneas, devoid of any central guttae Grades 1–2: Mild Grades 3–4: Moderate Grade 5–6: Severe (If corneas had clinically detectable corneal oedema, they were assigned to grade 6 irrespective of the distribution of guttae)	Retrillumination photography analysis provides an objective assessment of the number and distribution of guttae in FECD and demonstrates enhanced definition of severity at advanced stages of disease	<ul style="list-style-type: none"> <li>- Clinically time consuming methodology</li> <li>- Counting of guttata are dependent on quality of images obtained</li> <li>- Measurement remains dependent on classification based on guttata rather than presence of oedema, thus significant overlap between eyes with 4+ and 5+ grading</li> </ul>
Wacker <i>K et al</i> 2015 (Wacker, McLaren <i>et al.</i> 2015)	Wavefront errors from the anterior and posterior corneal surfaces were derived from Scheimpflug images and expressed as Zernike polynomials	As per Eghrari <i>et al</i> 2015	<p>Anterior corneal HOAs were increased in moderate and advanced FECD prior to clinically visible corneal oedema</p> <p>Posterior cornea HOAs and corneal backscatter was increased even in mild FECD</p> <p>Increased posterior corneal HOAs and anterior and posterior corneal backscatter were associated with lower endothelial cell count and thicker corneas in FECD</p>	<ul style="list-style-type: none"> <li>- Suggests new measure of visual compromise in FECD, highlighting changes occurring on the anterior corneal surface early in the course of the disease, but does not provide a grading system</li> <li>- Wavefront measurement requires use of a rotating Scheimpflug camera but fixation and imaging can be difficult in more advanced disease</li> <li>- The study did not quantify the level of corneal oedema and therefore could not assess the influence of stromal oedema on HOA and backscatter</li> </ul>
McLaren <i>et al</i> 2014 (McLaren, Bachman <i>et al.</i> 2014)	Local contiguous cell density determined using a variable frame measure of confocal microscopy images of the endothelium	As per Eghrari <i>et al</i> 2015	Effective Endothelial Cell Density in confocal images provides an objective means of assessing the corneal endothelium in FECD Allows a larger sample area reducing sample bias	<ul style="list-style-type: none"> <li>- Assume that the local ECD is representative of viable cell density in all areas of the image</li> <li>- In advanced disease guttata became more confluent, brightness of their images</li> </ul>

				<p>became less uniform and assessment is more challenging</p> <ul style="list-style-type: none"> <li>- Endothelial cell density and viability assumes that the area covered by guttae is non-functional, although we did not measure either pump or barrier function.</li> <li>- Manual counting of cells introduces a margin of human error and is labour intensive</li> <li>- In advance cases, the "Region of Interest" was selected to allow for at least a single countable cell introducing an inconsistency in defining an area of as central or peripheral</li> </ul>
Syed <i>et al</i> 2017 (Syed, Tran et al. 2017)	Endothelial photographs of central and peripheral in vivo confocal microscopy were used to perform manual cell counts centrally and peripherally in advanced FECD	Grade 1 – nonconfluent guttae Grade 2 – presence of any area of confluent guttae, but without oedema or clinical thickening Grade 3 – confluent guttae with oedema or clinical thickening Grade 4 – oedema associated with whitening or haze	In advanced FECD, severity is best determined by the peripheral ECC compared with the central ECC, visual acuity, clinical disease grade, and CCT	
Wacker <i>et al</i> 2018 (Wacker, Baratz <i>et al</i> . 2018)	Measuring patient-reported visual disability to validate a new patient-reported visual disability questionnaire, the Visual Function and Corneal Health Status (V-FUCHS) instrument	As per Eghrari <i>et al</i> 2015	The V-FUCHS instrument allows standardized, comprehensive, and rapid assessment of disease-specific visual disability in FECD, with a particular focus on the effect of glare on visual disability	<ul style="list-style-type: none"> <li>- Assumes that participants can estimate abstract concepts, such as glare, and can transform these to numerical scales relative to what is considered normal</li> <li>- Margin of error in interpretation as responses can be influenced by socio-economic background (eg. ability to drive, vocation)</li> </ul>

Abbreviations: QOV- quality of vision, FECD – Fuchs Endothelial Corneal Dystrophy, V-FUCHS- Visual Function and Corneal Health Status,

Table 3: A summary of studies that suggest new modalities by which to measure and stage the severity of FECD.

To improve the accuracy and validity of the evaluation of severity of FECD, a variety of imaging modalities, anatomical measures and patients reported outcome measures have been implemented to provide a more comprehensive view of the disease process both on an anatomical and morphological level as well as in regards to the patient experience.

### 1.3.4 Advances in the field of genetics and the study of FECD

#### 1.3.4.1 The Human Genome Project

The Human Genome Project (HGP) was launched on the 1<sup>st</sup> of October 1990 with the goal of analysing the full human genome (Green, Watson et al. 2015)( <https://www.genome.gov/human-genome-project/results>). By the very nature of scientific methodology required to achieve such large scale sequencing, the HGP was also able to pioneer the development of industrial scale resources for gene mapping and sequencing across the globe. The project was biology's first example of "big-science" with 20 different centres across 6 different countries working together towards a common goal. On the 14<sup>th</sup> of April 2003 (the 50<sup>th</sup> anniversary of the discovery of the DNA double helix), the HGP published a near complete sequence of the human genome (International Human Genome Sequencing 2004).

#### 1.3.4.2 The Human Genome

The human genome is comprised of the complete set of genetic information stored within deoxyribonucleic acid (DNA). Four nucleotide bases make up DNA: adenine (A), cytosine (C), guanine (G) and thymine (T) (Read 2019). The human genome is made of approximately 3.2 billion base pairs of DNA, with nuclear DNA forming 99.9995% of the coded genetic information while mitochondrial DNA contributes to the remaining 0.0005% (International Human Genome Sequencing 2004).

Within the nucleus of the cell, DNA is coiled into packages of 22 chromosome pairs and an additional X and Y sex chromosome(Read 2019). The chromosomes comprise units of DNA known as genes that encode for the formation of proteins. Within each somatic chromosome there exists corresponding allele pairs: each allele carries a variant form of a given gene, meaning it is one of two or more versions of the gene sequence at the same location on a chromosome. Genes are divided into coding and non-coding sequences known as exons and introns, respectively. Before genes are transcribed into proteins introns are typically spliced out leaving only the protein-coding portion of DNA. Although introns may be referred to as 'non-coding' they are known to perform important regulatory functions in directing gene expression and can themselves encode functional RNAs. The human nuclear genome is estimated to contain between 20,000 and 25,000 genes. In addition to the nuclear genome, the mitochondrial genome contributes a further 37 known genes that are important in regulation of oxidative phosphorylation, cellular metabolism apoptosis and regulation of proteins for energy production.

An estimated 8000 protein coding genes, sometimes referred to as house-keeping genes, are expressed in almost all cell types. These genes are ubiquitously expressed as they play a vital role in the routine maintenance of gene expression such as transcription, translation, RNA processing and metabolism. However, the majority of genes are transcribed only in specific tissues in accordance with their biological function within the cell. Therefore, at any given timepoint, only a fraction of genes are expressed through transcription.

The process of interpreting the genetic code to enable protein formation begins with transcription of the DNA sequence into messenger RNA (mRNA) (Read 2019). An RNA polymerase enzyme first binds to a promoter site on the DNA sequence, upstream from the target gene. By proceeding in one direction (3' to 5'), the polymerase enzyme unwinds the DNA strand, exposing DNA base pairs to allow attachment of complementary mRNA nucleotides. The process continues until a termination sequence is reached. The mRNA molecule is referred to as a primary transcript at this stage.

Before the primary mRNA leaves the cell nucleus to enter the cytoplasm, it must undergo splicing to form a functional mRNA sequence. Splicing involves the removal of non-coding intron sequences to leave only the protein coding section to form mature protein-coding mRNA. Most genes also contain alternative-splice-sites that allow specific but varied combinations of the genes exons to be transcribed. These variations are known as isoforms. The process of alternative splicing allows different proteins to be created from the same original gene sequence. The expression of a specific isoform may be tissue specific. In the human genome, 95% of multi-exonic genes are alternatively spliced to allow an increased diversity of proteins encoded by the genome. The resulting proteins from a single gene may therefore have similar structures and but perform different functions.

Once the primary mRNA has been spliced, it is a mature transcript that can move from the nucleus into the cytoplasm where translation begins. Translation is a process by which amino acids are assembled along the mRNA strand-to form a polypeptide chain. Transfer RNA (tRNA) molecules are an essential component of this process as each specific amino acid must first bind to its corresponding 3' end site before being transported to the corresponding site on the mRNA template. The ribosome is the cytoplasmic site of protein synthesis. Ribosomes initiate translation by binding to the AUG site of the mRNA. This is followed by the binding of the tRNA-amino acid complex to its surface to enable base pairing to occur. The ribosome then zips along the mRNA template, creating peptide bonds between adjacent amino acids forming a polypeptide chain until a stop codon is reached.

Further diversity can be introduced to protein formation through posttranslational modification (PTM) of the newly synthesized peptide chain. Modifications that can occur at this stage include cleavage into smaller polypeptides or combination with other peptide chains to form larger protein structures. The exact modifications are catalysed by enzyme recognition of specific binding sites to allow alteration not only of the protein structure but also its functional capabilities.

#### 1.3.4.3 Genetic Variants

A mutation is a permanent change that occurs within the DNA sequence. Mutations can be broadly classified under two headings (Read 2019):

- Hereditary (germline) mutations: These changes in the DNA sequence are inherited from a parent and can be found in every nucleated cell in the body
- Acquired (somatic) mutations: The change within the DNA sequence occurs at a particular timepoint in a person life and presents only in certain affected cells. These mutations can be the result of environmental factors such as UV light or exposure to carcinogens. These changes cannot be passed on to the next generation

A mutation can occur either on a single allele leaving a normal corresponding gene sequence on the paired allele (heterozygous) or be found on both alleles meaning that no normal gene sequence could be potentially expressed (homozygous).

Mutations occur on either a small or large scale. Large scale mutations include chromosomal anomalies such as trisomy (the presence of an extra chromosome), and structural breakage of a chromosome leading to errors in re-joining. These relatively rare abnormalities can be observed through cytogenetic studies such as karyotyping, analysis of G,C,R-banded chromosomes and visualisation via fluorescent *in situ* hybridisation (FISH) or comparative genomic hybridisation (CGH).

Small scale mutations are more common and can be divided into three main classes:

- Substitution

Substitutions commonly occur in the form of replacing a singly base which is known as a point mutation. Due to the degenerate nature of the genetic code that allows different codons to code for the same amino acid, not all point mutations result in an amino acid change. Such substitutions are called silent mutations. A mutation point mutation that does result in a change can either be a

missense mutation, resulting in a single amino acid change, or a nonsense mutation, which forms the code of a stop codon (UAA,UAG, or UGA) resulting in premature termination of the polypeptide chain formation.

- Deletion or insertion

Deletion or insertion of a base pair into the genetic sequence can result in an additional or missing amino acid in the polypeptide chain. As a sequence of three base codons (a “reading-frame”) codes for a single amino acid, if the number of base pairs is disrupted by a number that is not divisible by three it leads to a significant disruption of the DNA template. This resulting “frameshift mutation” alters the downstream sequence and fails to code for the correct protein.

- Duplication

A duplication is made up of one or more nucleotides that have been abnormally copied and repeated one or more times. Repeat expansions (multiplication of a repetitive base sequences within DNA) are a form of mutation that fall under this subcategory.

- Inversion

An inversion occurs when two or more nucleotides are reversed within the original sequence to create a mirrored complement of DNA

#### 1.3.4.4 Mechanisms of Mutational Effect

The majority of mutations in the human genome occur within non-coding regions of the genome and therefore do not result in changes to the phenotype (Anthony Griffiths 2020). Should an alteration in the gene sequence lead to a change in the protein polypeptide sequence formation, a downstream change in phenotype can occur as a result of either a gain-of-function or a loss-of-function of the encoded protein.

Should a mutation in both alleles lead to a total loss in gene function (as seen in recessive disorders), a complete loss of the gene product would occur (Read 2019, Anthony Griffiths 2020). However, if the mutation was heterozygous, thus allowing for the presence of one functioning allele, a partial loss of function would be observed. Whether or not this mutation would result in a clinical manifestation of disease phenotype would depend on the quantity of gene product required to sustain normal function. Should only half of the normal gene product be required for physiological function to be maintained, then a heterozygous mutation may not lead to a change in phenotype. Conversely, if half the normal gene product is not adequate for normal functioning (haploinsufficiency), then even a heterozygous

mutation can lead to abnormal phenotypic characteristics and create the impression of autosomal dominant inheritance.

Gain-of-function mutations are not strictly a mutation that leads to the attainment of an entirely new capability. It is most often the result of a change in regulation that leads to a protein being expressed in erroneous tissue or at the wrong time. For example, a mutation could lead to a receptor activating in the absence of a ligand or an alteration in an enzyme's structure that allows it to respond to a different substrate. Mutations in growth promoting genes such as oncogenes are commonly observed in cancer where the gain of function manifests as abnormal amplification of a specific gene product. Another sub-type of this mutation is through the production of an RNA with novel toxic properties. In addition to causing defects in RNA molecules that play an essential role in cell homeostasis, RNA toxicity can occur as a result of abnormal RNA transcription. This is a common feature of dynamic RNA mutations whereby microsatellite repeats within a gene sequence become unstable. This instability leads to expansion of the repeat sequence through multiplication of tandem repeats. When this expanded sequence is transcribed it may form an RNA sequence containing the expanded tandem repeat that can be toxic to the host cell. In these cases the pathological effect on the cell is not directly related to the function of the mutated gene.

Differentiating between gain and loss-of-function can be difficult, for example in cases of a mutation leading to a decreased expression of an inhibitory molecule which in turn causes aberrant increase in expression of its intended target. It is important therefore to not only understand the molecular changes that occur as a result of a change in the gene sequence, but also the downstream effect on the individual's phenotype.

Single nucleotide variants due to nucleotide substitution are the most common form of point mutation. The presence of such a change to the genetic sequence may or may not have an impact on the encoded protein. Within the human genome, there are 64 different codons that encode just 20 different amino acids (Read 2019). It is therefore possible that a single point mutation could lead to a change in sequence within a codon, that still allows it to code for the same amino acid (a synonymous substitution).

A point mutation that does lead to a change in amino acid (non-synonymous variation) can exert an effect on protein structure via a few different pathways (Read 2019):

- a. Polarity: The presence of side chains on the amino acids allows them to be classified as non-polar, charged polar and un-charged polar. Should a change in sequence result in an amino acid being substituted for one within its own class, the effect on the overall structure of the protein would be less than that of an amino acid from a different class.
- b. Steric effect: A substitution of an amino acid for one of varying size can also have significant implications on protein structure. For example, glycine is the smallest amino acid and if a substitution with a larger amino acid occurs the protein folding structure may be significantly altered.
- c. Molecular bond formation and compatibility: Cysteine is an amino acid that is able to form disulphide bonds that form strong covalent bonds and reinforce the protein structure. A point mutation that leads to loss of a cysteine molecule can therefore have significant impact on the integrity of the protein structure. Similarly, proline is known to be incompatible with certain folding patterns and can therefore cause disruption if substituted into a protein structure.

#### 1.3.4.5 Genomic Variation and Population Genetics

Changes in the base sequence are termed variants. Traditionally, if the population frequency of a DNA variant is  $>0.01$  it would be considered “common” and known as a polymorphism. Changes resulting in point mutations are also referred to as single nucleotide polymorphisms or SNPs. Should the frequency of the variant fall below 0.01 it was described as a “rare” variant (Anthony Griffiths 2020). The application of 0.01 as the cut-off for labelling the commonality of a change in sequence was however an arbitrary value. To provide a more accurate assessment of the frequency of SNPs, an international project was developed with the aim of developing a haplotype map of the human genome. A haplotype refers to a genotype sequence of a short segment of a chromosome. The International HapMap Project was an organization that aimed to develop a haplotype map (HapMap) of the human genome, to describe common patterns of human genetic variation (Haiman and Stram 2008) (<https://www.genome.gov/10001688/international-hapmap-project>). A genome wide map of SNPs was developed to show the frequency of  $10^6$  SNPs derived from 11 different populations. The findings of the HapMap study lead to a refined classification of SNPs as a minority DNA variant with a frequency  $>0.05$ . Following the completion of the HapMap project, further study into human genetic variation has been undertaken by The 1000 Genomes Project (abbreviated as 1KGP).



Based on the map of SNP variation, candidate genes for each SNP could then be studied to investigate an association to a particular disease phenotype. Statistical analysis of the association between an SNP and a particular phenotype can then provide an “odds ratio”: the probability of a phenotype corresponding to a genotype relative to the whole population (Haiman and Stram 2008, Anthony Griffiths 2020). Although the identification of a rare SNP can mean a direct causative relationship with a disease phenotype, in most cases the SNP allele lies adjacent to a non-SNP allele that is the cause of the disease manifestation (Anthony Griffiths 2020).

#### **1.3.4.6 Next Generation Sequencing**

In addition to the deeper understanding of the human genome and the function of various the nucleotide sequences, the Human Genome Project lead to a surge of technological advances that revolutionised the speed and efficiency of gene sequencing. The late 1990s witnessed the introduction of new sequencing methodologies that lead to the development of commercial “Next Generation Sequencing” (NGS) modalities (Yohe and Thyagarajan 2017).

The development of NGS sequencing has enabled large scale sequencing of whole exomes and whole genomes in a time and cost efficient manner. The term “massively parallel DNA sequencing” is eponymous with NGS as it described the basis of the technology that is employed: the sequencing of millions of DNA fragments simultaneously (Read 2019). NGS platforms are fully automated and are able to record the sequence during the sequencing reaction itself. While older techniques allowed scientist to sequence up to 800 bases, this new technology enabled read lengths of up to 14,000 nucleotides (Reuter, Spacek et al. 2015).

#### **1.3.4.7 Genome Databases and Bioinformatics**

As advances in mapping and sequencing of the human genome were made, large computer based repositories were developed to store the generated data. This lead to the formation of large open-access genome databases as well as software to enable gene mapping and detailed searches of gene sequence data (Wang, Kong et al. 2013). These shared genome browsers allow the user to navigate the human genome to the level of a single nucleotide and also to draw comparisons with other

genomes to assess for levels of gene conservation. Examples of eukaryotic genome browsers available online include Ensembl, NCBI Genome Data Viewer and UCSC Genome Browser.

In addition to genome browsers, more clinical databases have been created to report on genotyped phenotype correlations. The Clinvar database (<https://www.ncbi.nlm.nih.gov/clinvar/>) for example is an open access online resource that aims to provide data on whether a variant is either known to be associated with a disease and if so, what the clinical significance of the variant is to the phenotype. In addition to providing links to relevant publications on the variant, the database also provides an assessment of the likely pathogenicity.

#### 1.3.4.8 In silico prediction tools

Once a missense mutation has been identified, the next question that needs to be answered is whether or not the change leads to a disruptive effect on the encoded protein (Read 2019). As it would be difficult to develop functional assays to study every missense variant identified, in silico prediction tools have been developed to perform this task. The term "in silico" describes a computational analysis of multiprotein alignments to predict the likely effect of a missense mutation. By comparing related proteins known as "paralogs" within a species and "orthologs" between species, the relative consistency of an amino acid placement is assessed (Read 2019). If all studied proteins show the same amino acid at the same position (highly conserved), it is inferred that the peptide has a vital role and a change at that point would have a significant effect. To further understand the potential consequence of the amino acid substitution on the polypeptide structure, computer analysis of the 3-dimensional structure can be carried out through comparisons to similar known protein homolog templates (Xiang 2006). Such analysis can identify if the change has potentially affected an active site of functional importance.

Examples of open-access in silico programs that are able to carry out such high throughput multialignment assessments include:

- SIFT (Sorting Intolerant From Tolerant): <http://sift-dna.org/>
- POLYPHEN-2: <http://genetics.bwh.harvard.edu/pph2/>
- PROVEAN: <http://provean.jcvi.org/index.php>
- Align-GVGD: <https://agvgd.iarc.fr>
- SNPs&GO: <https://snps.biofold.org/snps-and-go/snps-and-go.html>

As each of these programs is able to produce a prediction that is approximately 70% accurate, it is best to run at least two programs to allow a consensus approach to the prediction of mutational effect. Two commonly used combination of programs for deriving an accurate prediction are SIFT and PolyPhen-2. The SIFT matrix predicts the impact of a substitution based on the assumption that the more conserved a sequence is across species, the less likely it is to tolerate a mutation (Sim, Kumar et al. 2012). In addition to predicting the impact of the substitution on protein function, Polyphen-2 can be used to supplement the SIFT findings assessing the effect on the 3 dimensional protein structure. Following assessment of the level of disruption that occurs as a result of an amino acid change, we are also able to assess the level to which the amino acid is conserved across orthologues. Disruption of a highly conserved protein would be expected to have greater consequence than that occurring in an amino acid chain that shows a higher degree of variability across species (Read 2019).

#### 1.3.4.9 Genome -wide Association Studies

With the development of high-density SNP genotyping chips, it is now possible to perform genotyping of 500,000 or more SNPs across a genome in a single session. Genome wide association studies are performed by applying this technology to sequence a phenotyped cohort who display signs and symptoms of the same disease compared to a matched control cohort. Study participants are screened for selected markers of genetic variation obtained from the HapMap project database of common SNPs within the population (Tam, Patel et al. 2019).

Should a genetic variant be found to be more common in the cohort of patients suffering from the disease, it is considered to be “associated” with the condition. GWAS report the measure of risk of the variant being associated with the disease in the form of an odds ratio (Read 2019, Tam, Patel et al. 2019). It should be noted that although a variant may be shown to be associated with the disease, it could be an indication that the variant is situated adjacent to the disease causing mutation and not necessarily that it is the cause of the pathology. To investigate the association further, sequencing of the effected region is required to identify the disease causing mutation.

#### 1.4.4.10 Application of whole exome sequencing (WES) to identify disease causing mutations

Sequencing of the protein-coding exome provides information on both coding-DNA and protein variants. As the exome makes up approximately 1% of the genome, it is easier to carry out sequencing of this section of DNA compared to the whole genome (Read 2019). Whole exome sequencing therefore provides an efficient way of analysing the DNA sequence of patients to identify changes within the protein coding region of their genome (Petersen, Fredrich et al. 2017).

When an alternative sequence of DNA is identified, it is termed a DNA variant. The term polymorphism is used to describe a common DNA variant that does not lead to phenotypic changes. A sequence variation that is known to be disease causing however is termed a mutation (Read 2019).

To allow us to predict the effect of a specific change in amino acid, protein sequence similarity searching programs such as SIFT and Polyphen-2 are then applied. Once a variant is identified as potentially disease causing, familial aggregation analysis should be sought to confirm that the same genetic change can be identified in other affected family members. Demonstrating segregation of the variant with the disease phenotype provides confirmation of a disease causing mutation (Read 2019).

### 1.3.5 Fuchs Endothelial Corneal Dystrophy Associated Genes

FECD is recognized as a multifactorial disease with complex underlying genetic changes. Although it has been attributed to an autosomal dominant mutations in certain forms of early-onset disease (Biswas, Munier et al. 2001), the majority of cases display a more heterogenous but still typically autosomal dominant inheritance pattern with reduced penetrance (Cross, Maumenee et al. 1971, Krachmer, Purcell et al. 1978, Louttit, Kopplin et al. 2012). It has now been shown that the majority of FECD cases are attributed to a mutation in the *TCF4* gene (Wieben, Aleff et al. 2012, Xing, Gong et al. 2014, Nakano, Okumura et al. 2015, Zarouchlioti, Sanchez-Pintado et al. 2018). The clinical picture of the disease in both early and late onset also demonstrate variable severity, manifesting as mild to severe corneal decompensation. To date, 16 genetic variations have been associated with early and late onset FECD.

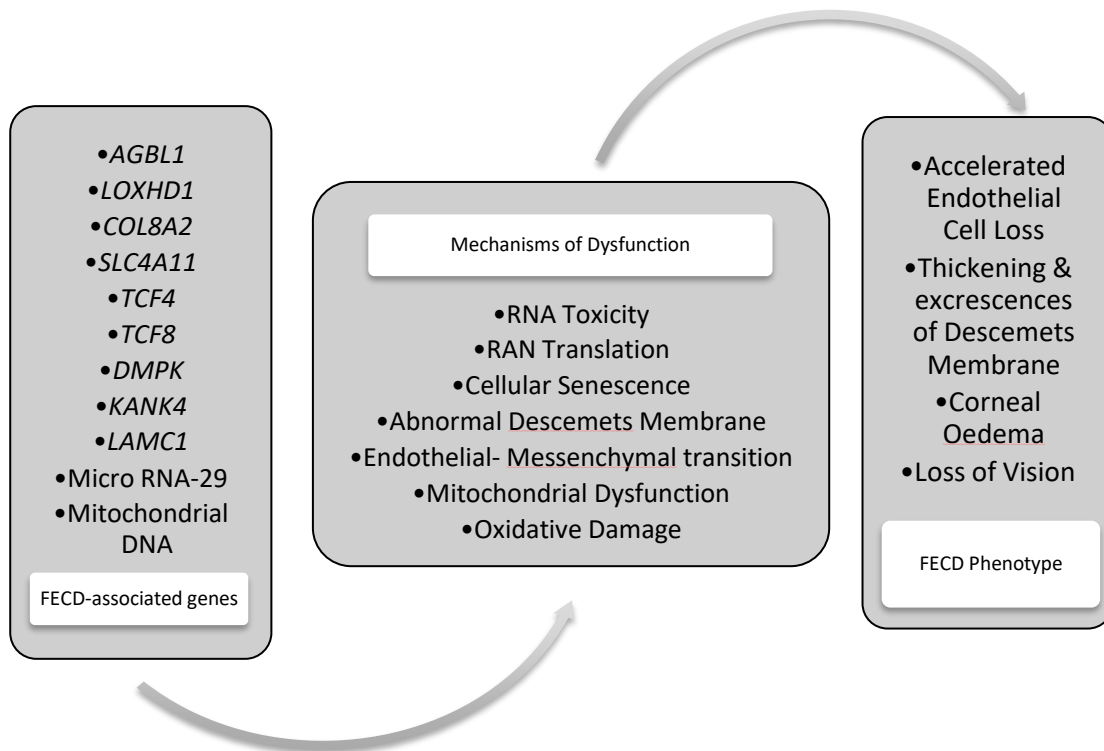


Figure 1: Illustration depicting the multiple mechanisms that are hypothesised to contribute to the pathophysiology of Fuchs Endothelial Corneal Dystrophy. A wide array of genetic variants have been associated with FECD and are believed to contribute directly or be associated with disease through multiple pathways. The resultant cellular dysfunction presents as a common phenotype of corneal endothelial decompensation that leads to progressive visual loss.

#### 1.3.5.1 ZEB1

The *ZEB1* gene, previously known as *TCF8*, is located on chromosome 9. The gene encodes for a zinc finger transcription factor and is upregulated by the E2-2 protein encoded by *TCF4* (Cano and Portillo 2010). Loss-of-function mutations of *ZEB1* are known to result in endothelial dysfunction as a result of haploinsufficiency and present clinically as posterior polymorphous dystrophy (PPCD) (Krafchak, Pawar et al. 2005). Heterozygous missense *ZEB1* variants have also been associated with late-onset FECD (Riazuddin, Zaghoul et al. 2010). Although the exact role of the *ZEB1* protein is unknown, PPCD-associated *ZEB1* mutations have been associated with *COL4A3* overexpression (Krafchak, Pawar et al. 2005). Further to this, dysregulation of  $\alpha$ -type IV collagens represents a common link between *ZEB1* mutations and the clinical phenotypes of PPCD3, FECD and keratoconus (Lechner, Dash et al. 2013). It is therefore postulated that aberrant collagen production may be the underlying cause of disease in FECD associated with *ZEB1* mutation.

ZEB1 is also believed to play a role in epithelial-mesenchymal transition by repressing E-cadherin expression in non-corneal pathology (Eger, Aigner et al. 2005). Similarly, the E2-2 protein encoded by *TCF4* induces EMT through indirect mechanisms, including upregulation of *ZEB1* expression (Sobrado, Moreno-Bueno et al. 2009). Given that *TCF4* is involved in *ZEB1* regulation and that both transcription factors regulate EMT this unifying feature of EMT dysregulation has been noted as a common feature of both PPCD and FECD (Baratz, K.H. et al., 2010; Li, Y.J. et al., 2011; Riazuddin, S.A. et al., 2011; Thalamuthu, A. et al., 2011). However, the exact mechanism of pathogenesis for both diseases remain unresolved.

#### 1.3.5.2 *LOXHD1*

Lipoxygenase homology domain-containing 1 (*LOXHD1*) gene codes for a protein localized to the plasma membrane (Grillet, Schwander et al. 2009). It is a highly conserved protein that is not commonly expressed in healthy corneal endothelial tissue (Riazuddin, Parker et al. 2012). Riazuddin *et al.* identified 15 heterozygous missense variants in the *LOXHD1* gene associated with late-onset FECD. The study reported one presumed causal variant in *LOXHD1* that was transmitted in an autosomal dominant pattern by affected members of a multigenerational family with autosomal dominant late-onset FECD. The study presented immunohistochemical evidence that a heterozygous point mutation led to an upregulation *LOXHD1* with the resulting protein products forming toxic aggregates within endothelial cells. To date, the findings of this study have not been replicated.

#### 1.3.5.3 *SLC4A11*

*SLC4A11* encodes a sodium borate cotransporter located within the corneal endothelium (Vilas, Loganathan et al. 2013). Heterozygous mutations within this gene have been suggested to cause late-onset FECD in a small number of individuals (Vithana, Morgan et al. 2008). Both homozygous and compound heterozygous mutations in this gene are well established to cause autosomal recessive childhood-onset congenital hereditary endothelial dystrophy (CHED) and Harboyan syndrome, a combination of CHED and progressive sensorineural deafness (Vithana, Morgan et al. 2006, Ramprasad, Ebenezer et al. 2007). In FECD patients harboring mutations in the *SLC4A11* gene, it hypothesized that intracellular retention leads to failure of protein to correctly localize on the basolateral membrane of the endothelial cell (Vilas, Morgan et al. 2011). In studies of *Slc4a11* knock-out mouse models, one group demonstrated normal corneal endothelial phenotype, although the corneal thickness was noted to be slightly increased (Lopez, Rosenblatt et al. 2009). Two other groups reported that the knock-out

mouse model did exhibit corneal pathology: Han *et al.* showed that corneas exhibited progressive corneal oedema secondary to decreased endothelial cell density (Han, Ang *et al.* 2013), while Zhang *et al.* reported abnormal ion transport activity in knock-out mouse models along with reduced endothelial cell proliferative capacity and EMT transformation (Zhang, Ogando *et al.* 2017).

#### 1.3.5.4 COL8A2

In 2001 an early-onset endothelial disease was mapped to the short arm of chromosome 1 (1p34.3-p32) in a three-generation family. The disease was subsequently attributed to a heterozygous missense mutation, c.1363C>A p.Q455K (Ensembl transcript: ENST00000397799) in COL8A2 (Biswas, Munier *et al.* 2001). Subsequently, two further missense mutations in COL8A2 were attributed to early-onset FECD, c.1349T>G p.L450W (Ensembl transcript: ENST00000397799) (Gottsch, Sundin *et al.* 2005, Liskova, Prescott *et al.* 2007, Eghrari, Riazuddin *et al.* 2016) and c.1363\_1364CA>GT p.Q455V (Ensembl transcript: ENST00000397799). Further reports by Liskova *et al.* and Mok *et al.* supported the role of this mutation in FECD in British and Korean probands (Liskova, Prescott *et al.* 2007) (Mok, Kim *et al.* 2009).

Identification of missense mutations in COL8A2 led to the development of knock-in mouse models for both the p.Gln455Lys and p.Gln450Trp substitutions (Jun, Meng *et al.* 2012, Meng, Matthaei *et al.* 2013). *Col8a2*<sup>Q455K/Q455K</sup> mice show a phenotype highly similar to FECD with progressive endothelial cell loss, morphologic changes of the endothelial cells and characteristic DM guttae (Jun, Meng *et al.* 2012). The p.Gln450Trp mouse model exhibited a milder disease phenotype with less endothelial cell loss and fewer guttae compared to the p.Gln455Val mice (Meng, Matthaei *et al.* 2013).

#### 1.3.5.5 TCF4 CTG18.1

In 2010, a GWAS by Baratz *et al.* identified a loci on chromosome 18 spanning the transcription factor 4 gene (*TCF4*) that showed a strong association with FECD (Baratz, Tosakulwong *et al.* 2010). The study suggested that the pathway regulated by the transcription factor TCF4 was a major contributor to the disease process of FECD.

The initial findings of the GWAS was followed by a ground breaking study by Wieben *et al.* that identified a trinucleotide CTG repeat expansion within the third intron of *TCF4* gene on Chromosome 18, as the causative mutation in adult onset FECD (Wieben, Aleff *et al.* 2012). At least one expanded

copy of the CTG repeat (termed CTG18.1) exceeding the threshold of 50 repeats was found in 79% of FECD patients in the cohort compared to 3% of controls. A CTG expansion size of >50 was therefore suggested as a causative mutation in FECD. This finding has since been replicated in various multi-ethnic patient populations worldwide (Mootha, Gong et al. 2014, Nanda, Padhy et al. 2014, Wieben, Aleff et al. 2014, Xing, Gong et al. 2014, Nakano, Okumura et al. 2015, Vasanth, Eghrari et al. 2015, Eghrari, Vahedi et al. 2017, Foja, Luther et al. 2017, Rao, Tharigopala et al. 2017, Zarouchlioti, Sanchez-Pintado et al. 2018).

The discovery of an underlying trinucleotide repeat mutation suggests that FECD shares a similar pathophysiology to other neurodegenerative disease such as Huntington’s disease and myotonic dystrophy (Hannan 2018). A study by Winkler *et al.* has since identified the presence of clinical and cellular hallmarks of FECD in patients with myotonic dystrophy, further elucidating a shared disease pathway (Winkler, Milone et al. 2018).

#### 1.3.5.5.1 Pathophysiology of Repeat Expansion Positive FECD

To date, there exists 3 mechanisms by which the CTG18.1 repeat expansion is hypothesized to lead to endothelial dysfunction in FECD (Figure 2). Although all three pathways could cause cellular dysfunction independently, it is possible that all three mechanisms occur concurrently in repeat expansion mediated FECD.

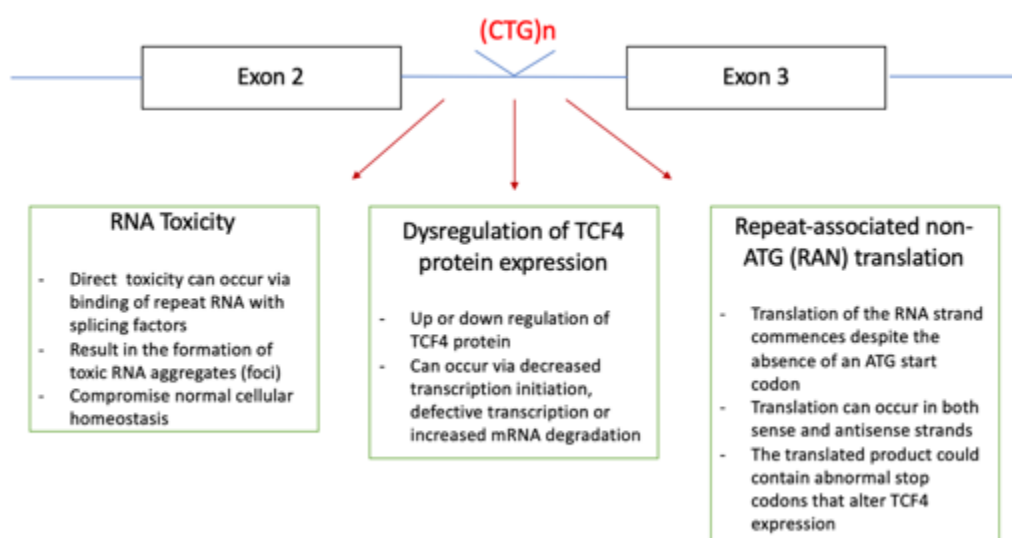


Figure 2: Three pathogenic mechanism contributing to the pathophysiology of TCF4 CTG18.1 expansion mediated Fuchs Endothelial Corneal Dystrophy (FECD). Direct and indirect RNA toxicity, dysregulation of



TCF4 protein expression and repeat-associated non-ATG (RAN translation) are three independent mechanisms of cellular dysfunction that could occur concurrently in the development of FECD. (Adapted from Foja *et al.* 2017 and Zarouchlioti *et al.* 2018)

#### 1.4.5.5.1.1 RNA Toxicity

RNA toxicity as a mechanism of disease was first characterized in myotonic dystrophy type 1 (DM1) and has since been described in other repeat-expansion (microsatellite)-mediated diseases (Fragile X-associated tremor/ataxia syndrome, amyotrophic lateral sclerosis/ Frontotemporal Degeneration (Duan, Sharma *et al.* 2014). RNA toxicity can be considered a gain-of-function mutation as the product of the mutant RNA has a toxic effect on the cell. When a tandem repeat expansion is transcribed it forms an elongated RNA molecule. This enlarged molecule can exert a toxic effect either by directly binding vital RNA-binding proteins or the abnormal molecule chain can form a foci that is toxic due to its ability to sequester other RNA-binding proteins. Trapping of freely circulating RNA binding proteins such as Muscleblind Like Splicing Regulator 1 (MBNL1) and Nuclear Mitotic Apparatus protein 1 (NUMA1) can disrupt their normal function of splicing gene transcripts. In DM1, the process of MBNL1 sequestration to RNA CTG repeat sequences was shown to lead to downstream mis-splicing events and cellular toxicity (Du, Cline *et al.* 2010). It was therefore hypothesized that a similar pathological process may occur in FECD.

Studies have since confirmed that, similar to DM1, nuclear RNA foci are present within endothelial cells derived from patients with CTG18.1 expansion. Immunofluorescence staining has demonstrated that these RNA aggregates sequester RNA binding proteins MBNL1 and MBNL2 (Figure 3) (Du, Aleff *et al.* 2015, Zarouchlioti, Sanchez-Pintado *et al.* 2018). Further evidence was provided by RT-PCR of RNA extracted from expansion-positive cultured endothelial cells which revealed aberrant splicing events in MBNL1, MBNL2 and NUMA1 (Zarouchlioti, Sanchez-Pintado *et al.* 2018, Rong, Hu *et al.* 2019). In subjects harboring the repeat expansion, it was shown that depletion of the RNA binding proteins lead to abnormal splicing resulting in the formation of truncated gene products within the endothelial cell.

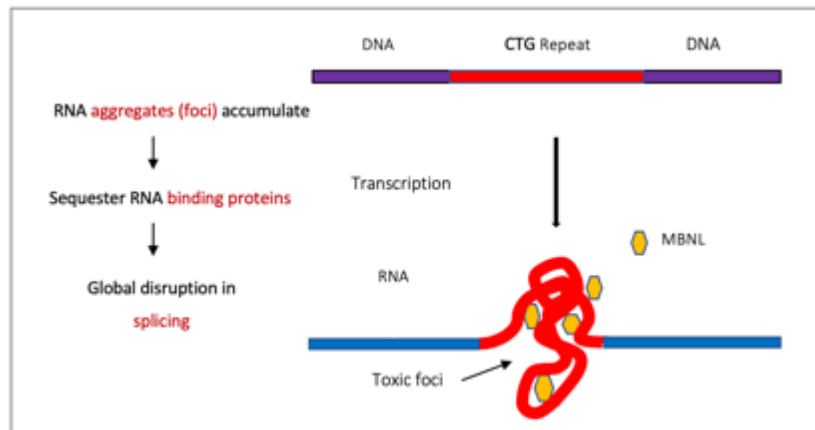


Figure 3: RNA toxicity secondary to sequestration of vital RNA-binding protein MBNL1. RNA binding proteins such as MBNL play a vital role in the correct splicing of gene transcripts. The transcription of the abnormal CTG tandem repeat leads to the formation of mutant RNA hairpin loops that sequester MBNL leading to the formation of toxic foci within the corneal endothelial cell. The resulting decrease in freely available MBNL leads to aberrant splicing events downstream.

#### 1.3.5.5.1.2 Dysregulation expression of *TCF4*

The *TCF4* gene comprises 20 annotated coding exons. Expression of the gene is known to be highly varied as a result of alternative splicing as well as the generation of multiple first exons that vary with each isoform. Multiple isoforms of *TCF4* have been identified in the corneal endothelium, some of which are thought to be tissue specific (Eghrari, Vasanth et al. 2018). Due to the highly variable nature of the isoforms, it has proven difficult to determine specifically which transcripts are affected in expansion-positive disease. However, it is hypothesized that the CTG18.1 expansion may specifically affect the expression of CEC-specific *TCF4* isoforms and hence explain the tissue specificity of the disease.

Intron retention has been postulated as a possible underlying cause for the reduced expression of *TCF4*. An intron would normally be spliced out of a primary transcript to allow to formation of the final RNA product prior to translation. However, in the event of intron retention of the CTG18.1 tandem repeat, the repeat sequence would not be removed and would remain un-spliced in the mature mRNA (Sznajder, Thomas et al. 2018). Intron retention can lead to reduced gene expression by activating nonsense mediated decay via the introduction of premature stop codons and also by reducing the export of mRNA from the cell nucleus. This mechanism may therefore contribute to the pathophysiology of CTG18.1 expansion mediated FECD.

### 1.3.5.5.1.3 RAN translation

The process of protein translation can only be initiated by a ribosome binding to the ATG start codon of a mRNA strand. Repeat associated non-ATG (RAN) translation in an unconventional protein translation mechanism whereby translation is initiated despite the absence of an ATG initiation codon. RAN translation therefore has the potential to lead to the repeat expansion being translated in a variety of reading frames, as well as in both the sense and antisense direction. This aberrant form of translation is recognized to occur in DNA repeat disorders such as spinocerebellar ataxia types 8 (SCA8) and 31 (SCA31), familial forms of amyotrophic lateral sclerosis, frontotemporal dementia, Huntington disease and myotonic dystrophy type 2 (Zu, Pattamatta et al. 2018) as well as non-coding repeat expansion diseases, including myotonic dystrophy type 1 (Zu, Gibbens et al. 2011).

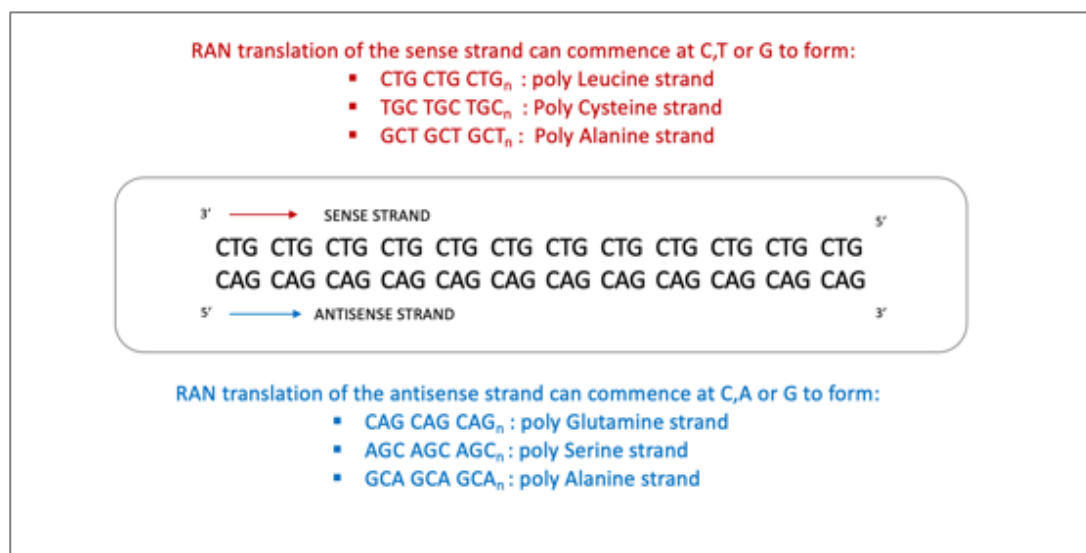


Figure 4: Overview of potential proteins products produced by RAN translation of a CTG expansion transcript. Initiation of mRNA translation at different start points, in both the sense and antisense direction can lead to aberrant formation of poly- Leucine, -Cysteine, -Alanine, -Glutamine and -Serine proteins as shown above. Formation of these homopolymeric polypeptides can lead to the formation of nuclear and cytoplasmic inclusions that are thought to contribute to disease pathogenesis.

Soragni *et al.* have shown that RAN translation occurs in FECD CTG18.1 expansion positive tissue (Figure 4). Their study reports that RAN peptides are translated from the sense but not antisense strand of RNA transcripts (Soragni, Petrosyan et al. 2018). Transfection of the RAN translation polypeptides into healthy corneal endothelial cells was shown to induce cytotoxicity, thus supporting the concept that

toxicity is a result of transcription of the non-coding CTG.CAG expansion. The study also confirmed the finding that a repeat length threshold needs to be exceeded to allow the formation of RAN translation product (Zu, Gibbens et al. 2011). This would in part explain the association of repeat lengths of >50 with FECD.

### 1.3.5.6 Genes recently associated with FECD by GWAS

In 2017, Afshari *et al.* reported the results of a GWAS analysing 2075 FECD cases and 3342 control subjects that not only validated the previously identified effect of the *TCF4* locus, but also identified 3 novel loci of genome-wide significance ( $P < 5 \times 10^{-8}$ ) (Figure 5) (Afshari, Igo et al. 2017):

- I. LINC00970/*ATP1B1* rs1022114 (intergenic region)
- II. *LAMC1* rs3768617 (intronic region)
- III. *KANK4* rs79742895 (intronic region)

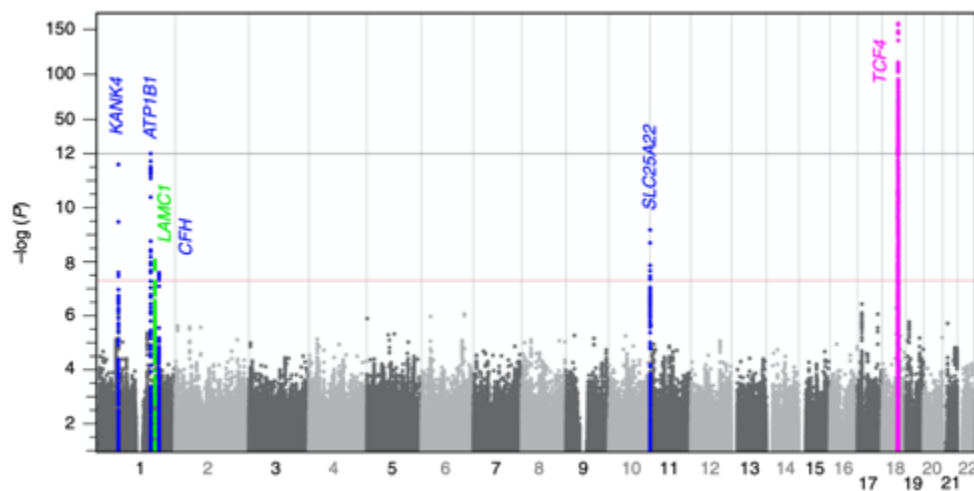


Figure 5 : Results from Genome Wide Association study by Afshari, Igo *et al.* 2017. The vertical axis shows the negative log P values from 8 680 745 single nucleotide polymorphisms. The horizontal axis is marked by a red line to indicate the cut off for genome-wide significance ,  $P = 5 \times 10^{-8}$ . Three novel loci, LINC00970/*ATP1B1* rs1022114, *LAMC1* rs3768617 and *KANK4* rs79742895, are shown to exceed the threshold of significance in addition to the already established *TCF4* locus (PMID 28358029).

#### 1.3.5.6.1 LINC00970/*ATP1B1*

A SNP in the intergenic region between LINC00970 and *ATP1B1* was noted to have a strong association to FECD, with a meta-P value of  $9.9 \times 10^{-19}$  at rs1022114 (Afshari, Igo et al. 2017). In transcriptomic data profiles from the same study, LINC00970 gene has not been shown to be expressed in the cornea while *ATP1B1* is highly expressed in normal corneal endothelium. *ATP1B1* encodes the beta subunit of  $\text{Na}^+/\text{K}^+$ ATPase pump that plays a role in transmembrane ion transport modulation (Li, Yang et al. 2011). It is therefore plausible to hypothesize that variants modulating this expression of function of *ATP1B1* could result in failure of the ion pump mechanism leading to increased corneal hypertonicity and subsequent corneal oedema. It has not however been shown to contribute to formation or maintenance of Descemet's membrane components to imply a role in DM thickening seen in FECD

#### 1.3.5.6.2 *LAMC1*

Laminins are an extracellular matrix glycoprotein that play an integral structural role in the formation of basement membranes. Laminins are heterotrimers formed by three separate non-identical short chains that are each encoded by distinct genes: alpha, beta and gamma. Multiple isoforms have been described for each of these chains. *LAMC1* encodes laminin subunit gamma 1 that is highly expressed in the corneal DM and endothelial cells (Afshari, Igo et al. 2017).

#### 1.3.5.6.3 *KANK4*

The GWAS by Afshari et al was the first study to show that *KANK4* rs79742895 was significantly associated with FECD (Afshari, Igo et al. 2017). The gene is a member of the *KANK* family (*KANK1-4*) which encode ankyrin-repeat domain containing proteins (Kakinuma, Zhu et al. 2009). *KANK* genes have mainly been found to be expressed in kidney cell lines where they have been shown to regulate actin cytoskeleton formation, but recent studies have shown *KANK4* can be localized to the corneal endothelial cytoplasm (Sarkar, Roy et al. 2002).

#### 1.4 Aims and Hypothesis

The primary objective of this study is to investigate genotype-phenotype correlations in patients diagnosed with FECD. A total of 342 FECD patients recruited from Moorfields Eye Hospital were initially genotyped for the FECD associated *TCF4* CTG18.1 expansion. Whole exome sequencing (WES) was subsequently performed for patients found to be repeat-expansion negative to allow identification of other possible underlying disease-causing variants. The phenotype of both the repeat expansion-positive and repeat expansion-negative groups was then analyzed to understand the influence of the underlying genetic changes on the clinical manifestation, natural progression of the disease, along with associations to concurrent corneal pathology. The findings of this study were then applied to designing a robust clinical trial protocol to guide future gene based therapies for the treatment of Fuchs Endothelial Corneal Dystrophy.

Genotype-Phenotype Correlation of  
*TCF4* CTG18.1 Triplet Repeat Expansion  
in the Moorfields Eye Hospital  
Fuchs Endothelial Corneal Dystrophy Cohort

## 2.1 Background

The identification of the CTG18.1 triplet repeat expansion as a genetic cause of FECD raises the possibility that repeat length may influence phenotypic characteristics of the disease. A recognised feature of repeat expansion diseases is the presence of a correlation between the length of the repeat region with disease severity and age-of-onset (Furtado, Suchowersky et al. 1996, Rosenblatt, Abbott et al. 2003). For example, Huntington's disease is a neurodegenerative condition caused by an expanded CAG repeat on chromosome 4 (Gusella, Wexler et al. 1983, 1993). The size of the CAG repeat displays an inverse correlation to the age of disease presentation, with longer expansions resulting in a younger age of onset (Andrew, Goldberg et al. 1993, Duyao, Ambrose et al. 1993). The neuromuscular degeneration Myotonic dystrophy type 1 (DM1) is caused by an unstable CTG intron repeat expansion within the dystrophin myotonia protein kinase (DMPK) gene on chromosome 19. In DM1, the size of the triplet expansion exhibits a positive correlation with muscular disability and an inverse correlation with age of onset (Jaspert, Fahsold et al. 1995, Groh, Groh et al. 2011, Overend, Legare et al. 2019).

To date, several studies have investigated CTG18.1 expansion status and how this correlates with various phenotypic outcomes related to severity of disease in FECD. Four previous studies reported a significant positive correlation between the presence of a CTG18.1 triplet repeat >40 and disease severity in FECD (Soliman, Xing et al. 2015, Vasanth, Eghrari et al. 2015, Eghrari, Vasanth et al. 2017, Soh, Peh Swee Lim et al. 2019). All four studies applied different thresholds for the assessment of disease severity (Table 1). Eghrari *et al* demonstrated that a higher proportion of patients harbouring the repeat expansion had undergone keratoplasty while Vasanth *et al* reported that the presence of the intron repeat lead to an increased Krachmer score with respect to age, within the same cohort of patients. Neither of the two studies analysed the impact of repeat expansion length as a continuous variable, to assess the effect of longer repeat length on disease severity. Soliman *et al* is the only study to show that within their repeat expansion positive cohort, longer CTG18.1 repeat length correlated to a higher proportion of patients requiring keratoplasty.

All three studies by Vasanth *et al*, Eghrari *et al* and Soliman *et al* respectively, did not comment on whether subjects had undergone cataract surgery prior to the assessment of disease severity. Soh *et al* is currently the only publication that has addressed the issue of cataract surgery accelerating corneal decompensation by excluding post-cataract surgery patients from their analysis (Seitzman 2005, Soh, Peh Swee Lim et al. 2019). In their prospective study of 51 FECD patients, a threshold of "significant clinical progression" was defined as: central corneal thickness increased to >700µm,



endothelial cell count decreased to <700 cells/ mm<sup>2</sup> or undergoing keratoplasty for treatment of FECD. These three criteria were assessed in two cohorts of FECD that were classified as expansion positive versus expansion negative status. The repeat expansion length (defined as  $\geq 40$ ) and the age of subjects at the time of reaching threshold severity were not analysed. Soh et al reported that although a higher rate of disease progression was noted in the repeat expansion group compared to the expansion negative group in the first 5 years of from diagnosis, the association was no longer statistically significant at 8 years and 10 year follow up. This finding is however of limited value as no correction was made for the age of the subject at the time of diagnosis or follow up. Table 1 summarises the 4 published studies on the genotype-phenotype correlation of *TCF4* CTG18.1 repeat expansion status in FECD.

To date, no study has investigated the impact of *TCF4* CTG18.1 repeat expansion length on the phenotype of an FECD cohort adequately stratified to account for prior surgical intervention.

## 2.2 Aims

The aim of this study is to determine if *TCF4* CTG18.1 triplet repeat expansion status correlates with disease severity of FECD in a Moorfields Eye Hospital FECD patient cohort. In addition to comparing the demographic and clinical characteristics of the expansion-positive versus expansion-negative FECD subjects, the effect of the CTG18.1 repeat length on disease severity will also be investigated. By gaining a deeper understanding of how the CTG18.1 triplet repeat expansion correlates with the disease phenotype, this study aims to improve our ability to advise patients regarding the natural course of their disease based on genotyping of CTG18.1. A secondary outcome of this study is to identify the limitations of assessment of FECD patients in daily clinical practice so as to inform future trial design for gene based therapies.

<b>Author</b>	<b>Population</b>	<b>Categorisation of CTG18.1 Intron Repeat Expansion Status</b>	<b>Threshold of severity applied</b>	<b>Findings</b>	<b>Limitations of study</b>
Soliman <i>et al</i> 2015	139 index cases with FECD Sub-analysis on the white population of FECD cases as they represented the vast majority of the re-reported cohort (n = 122)	The alleles were separated into 4 groups based on the CTG triplet repeat length of the largest allele: – < 40 – 40 - 84 – 85 - 120 – > 120	Traditional Krachmer grading of 1-5 (ref) with an additional Grade 6 for patients who had undergone keratoplasty	The Krachmer grade of disease severity was greater in FECD cases with the CTG18.1 triplet repeat expansion in TCF4 than in those without the expansion.  The CTG triplet repeat allele length was positively correlated with the Krachmer grade of severity	– Assigning of a Krachmer grade 6 to patients post keratoplasty does not take into consideration modern surgical techniques that would allow earlier surgical intervention (ref)  – No data was provided to indicate type of keratoplasty surgery and subject's cataract surgery status at time of grading
Vasanth <i>et al</i> 2015	574 late-onset FECD cases and 354 controls	Expansion-positive: any allele with $\geq 40$ CTG repeats Expansion negative: $< 40$ CTG	Traditional Krachmer grading of 1-5 (ref) with an additional Grade 6 for patients who had undergone keratoplasty	Regression analyses demonstrated a significant correlation between disease severity and age in individuals who harbour repeat expansion $> 40$ in both homozygous (p=0.008) and heterozygous (p=0.021) carriers of the repeat expansion	– Impact of variation in length of repeat expansion $\geq 40$ as a continuous variable was not analysed – Assigning of a Krachmer grade 6 to patients post keratoplasty does not take into consideration modern surgical techniques that would allow earlier surgical intervention (ref) – No data was provided to indicate form of keratoplasty surgery and subject's cataract surgery status at time of grading
Eghrari <i>et al</i> 2017	Retrospective case-control study of the	Expansion-positive: any allele	Analysed relationship between age, gender,	Higher proportion of expansion positive subjects had undergone transplantation (21.8%) compared	– Impact of variation in length of repeat expansion $\geq 40$ as a continuous variable was not analysed

	same patient population studied by Vasanth <i>et al</i> 2015	with $\geq 40$ CTG repeats Expansion negative: $< 40$ CTG	triplet expansion, and keratoplasty	to those without the expanded allele (12.9%), a significant association ( $p=0.007$ ).  Also noted a significant difference in survival function over time ( $p=0.027$ ) indicating earlier age of surgery in expansion positive subjects.	– No data was provided to indicate form of keratoplasty surgery and subject's cataract surgery status at time of grading
Soh <i>et al</i> 2019	Prospective study of 51 subjects followed up to assess the time from diagnosis to development of "significant" clinical progression defined as <i>Threshold Disease</i>  Follow-up period: 12 years  Average follow up period 4.32 years	Subjects with newly diagnosed FECD with minimal disease severity Krachmer Grade 4 were divided into: – Expansion- positive: any allele with $\geq 40$ CTG repeats – Expansion negative: $< 40$ CTG	<i>Threshold disease</i> was met by meeting any of the 3 criteria defined below in at least one eye assessed yearly:  – CCT increased to $> 700\mu\text{m}$  – CCT increased to $> 700\mu\text{m}$  – All measurements were acquired between 10am to 3pm, to account for diurnal variations in CCT – ECD decreased to $< 700$ cells/ $\text{mm}^2$ – Keratoplasty for treatment of FECD  – Eyes that underwent cataract extraction surgery during the course of follow-up were excluded from analysis	– $\geq 40$ patients are at greater risk of FECD progression and development of <i>Threshold disease</i> within the first 5 years following diagnosis – <i>Threshold Disease</i> rates at the 5-year time point were 87.5% for the $\geq 40$ group and 47.8% for the $< 40$ group ( $p = 0.012$ )  – The difference between cohorts was no longer statistically significant at the 8-years (92.9% vs 78.9%, $p = 0.278$ ) and 10-years (92.9% vs 84.2%, $p = 0.426$ ) time points	– No indication of subject age at given timepoint of severity assessment. Assessment of clinical progression is based on limited follow up period and not the natural history of the disease over a subject's lifetime – Impact of variation in length of repeat expansion $\geq 40$ as a continuous variable was not analysed – Average follow up period of 4.32 years and only 33 subjects at final review – natural variation in central corneal thickness in the normal population was not accounted for

Table 1: Summary of publications investigating the genotype-phenotype correlation of TCF4 CTG18.1 Triplet Repeat Expansion on disease severity. All four studies reported a significant positive correlation between the presence of the CTG18.1 repeat expansion and increased disease severity. Soliman *et al* is the only study to show that longer repeat length was associated with more severe disease based on Krachmer score. In analysing expansion status as a binary value (expansion-positive versus expansion-negative ), Eghrari *et al* showed that a higher proportion of patients harbouring the mutation had undergone keratoplasty while Vasanth *et al* reported that the presence of the intron repeat lead to an increased Krachmer score with respect to age in the same cohort of patients. Soh *et al* are the only publication to date to exclude subjects who had undergone cataract surgery when analysing disease progression in FECD. However, when Soh *et al* studied the more stratified cohort, the impact of repeat length  $\geq 40$  as a continuous variable was not considered and patient age was not corrected for in the analysis of disease progression.

## 2.3 Methods

### 2.3.1 Patient recruitment

Three hundred and forty-two probands with a clinical diagnosis of FECD were enrolled for genotyping and retrospective review of the disease phenotype. FECD diagnosis was made on the basis of slit lamp biomicroscopy examination findings of Descemet's membrane guttae and evidence of endothelial dysfunction in the form of central corneal oedema. I personally reviewed the notes and available images of all patient that had been recruited top the study, spoke patients personally in order to ascertain missing information in regards to demographics and disease progression. Where relevant I contacted effected family members and obtained additional imaging.

Approval for this study was obtained from the Moorfields Eye Hospital Research and Ethics Committee [ Moorfields Eye Hospital (MEH) ethics committee (REC reference 09/H0724/25)]

### 2.3.2 Consent

All patients involved in the study gave informed written consent for analysis of genetic data, storage of genetic data and access to medical records.

### 2.3.3 Phenotyping

The clinical data collected by retrospective case review of medical records included slit lamp biomicroscopy findings of guttae and corneal oedema as well as clinical history of patient visual symptoms. Due the retrospective nature of data analysis performed in this study, it was not possible to obtain objective measures of the number of guttata as per traditional Krachmer grading. In addition, as the incidence of visually-significant cataracts is high amongst patients in this study cohort whose average age was above 60 years old, visual acuity was not taken as a reliable gauge of FECD severity. Instead, where possible, acuity and assessment of guttata were utilised as part of a Modified Clinical Staging (MCS) score adapted from Suh et al , shown below in Table 2 (Leejee H. Suh 2008).

Clinical notes and correspondence from opticians and general practitioners were used to ascertain the time of diagnosis of FECD and the time at which the patients first reported onset of symptoms (e.g. Diurnal variation in vision, blurring of vision in the absence of other ocular co-morbidities). Demographic data such as ethnicity and family history were recorded and patients were contacted directly when this data was not documented in the medical records.

Stage	Symptoms	Clinical Findings	Visual Acuity (Snellen)
Stage I	No symptoms	Few to moderate corneal guttae	Normal (6/6)
Stage II	Mild to moderate loss of vision, no pain	Moderate to numerous corneal guttae, mild corneal oedema	Mild to moderate reduction (6/9 to 6/24 )
Stage III	Moderate to severe loss of vision and pain	Confluent corneal guttae, moderate to severe corneal oedema, epithelial bullae	Moderate to severe reduction (6/30 to 6/120)
Stage IV	Severe loss of vision, reduced pain	Subepithelial scar, fewer epithelial bullae	Severe reduction (6/120 or worse)

Table 2: Modified Clinical Staging (MCS) score of Fuchs Endothelial Corneal Dystrophy.

The clinical staging system shown here is a modification of the clinical staging system adapted from Adamis *et al.* by Suh *et al.* in the 2008 edition of *Cornea and External Eye Disease* (Adamis, Filatov *et al.* 1993, Leejee H. Suh 2008). The application of symptoms in relation to gross clinical findings on slit lamp examination and range of visual acuity were easily adaptable as a retrospective staging criterion in the analysis of FECD.

Patients' surgical history of all ocular surgery was noted with particular attention to date of first corneal transplantation for treatment of FECD and date of first cataract surgery. When available, central corneal thickness data (ultrasound pachymetry data device, Pachymate DGH55 DGH Technology) was obtained at the time of listing for corneal transplant surgery.

#### 2.3.4 *TCF4* CTG18.1 Genotyping

DNA extraction was performed from blood samples to enable sequencing of the CTG18.1 trinucleotide repeat region within the *TCF4* gene. A short tandem repeat (STR) assay was performed to genotype the CTG18.1 allele, in accordance with methods previously published by Wieben *et al.*<sup>9</sup> In brief, genomic DNA was amplified using a 5' FAM conjugated primer (5' -CAGATGAGTTTGGTGTAAGAT-3' ) and an unlabelled reverse primer (5' -ACAAGCAGAAAGGGGGCTGCAA-3'). Post PCR product separation was

performed on the ABI 3730 Electrophoresis 96 capillary DNA analyser (Applied Biosystems). Data analysis was performed using GeneMarker software (SoftGenetics).

Genotyping work was performed by Beatriz Sanchez-Pintado, Nathaniel J Hafford Tear, Amanda Sadan as part of the publication by Zarouchlioti *et al* with additional samples processed by myself (Zarouchlioti, Sanchez-Pintado et al. 2018). Details of genotyping are provided in Appendix A.

### 2.3.5 Statistical Analysis

Statistical analysis was performed to investigate the potential differences in disease characteristics between CTG18.1 expansion-positive and CTG18.1 expansion-negative FECD cohort.

Ethnicity and gender were treated as nominal data sets and cross-tabulated against expansion status. The cross-tabulation compared the observed and expected frequencies in each cell of the table. It then determined whether there was a statistically significant difference between the observed and the expected values. Adjusted residuals of  $< -2.5$  or  $> 2.5$  were considered statistically significant.

The statistical test applied was then determined according to the number of variables investigated. As per the gold standard method if the expected value was less than 5, then the Fisher exact test used but if expected value greater than 5 then the Chi-squared test was used.

To determine the presence of a statistically significant relationship between ocular comorbidity distribution in the expansion-positive cohort compared to the expansion-negative cohort, the Chi square test was applied ( $p < 0.05$  indicated significance).

Further analysis was performed on the expansion-positive cohort to determine the effect of repeat expansion length on disease phenotype. To characterise disease severity, the following parameters of disease severity were investigated: age of first corneal transplant, central corneal thickness at time of listing for surgery and modified clinical grading (MCG) score. Three patients with keratoconus were excluded from the analysis of disease progression as this form of corneal ectasia causes thinning of the stroma which could potentially mask/offset the corneal thickening seen in FECD secondary to stromal oedema.

Ordinal regression analysis was used to determine if there was an association between expansion length and MCG score after accounting for age. Linear regression was performed to determine if there

was an association between CCT and expansion length after accounting for age at the time of first corneal graft.

To further stratify the cohort of FECD patients, patients with corneal decompensation following cataract surgery were excluded to allow analysis of FECD patients with spontaneous corneal decompensation with no prior intraoperative damage to the cornea. Spearman correlation analysis was used to study non-parametric correlations with a Fisher Z transformation to compare differences between correlations.

Non-parametric continuous and ordinal data sets were analysed using a Mann-Whitney U test to determine if there was a difference between the expansion positive and negative groups. Mann-Whitney U test was used when the dependent variable was ordinal (MCG score) and the independent variable was dichotomous categorical variable (expansion-positive or negative). A p value of  $<0.05$  would suggest a statistically significant difference between both groups.



## 2.4 Results

### 2.4.1 Comparisons Between the Repeat Expansion Positive Cohort and the Repeat Expansion Negative Cohort

The FECD cohort of 342 patients was first divided into CTG18.1 expansion-positive and expansion-negative subgroups depending on the longest allele detected in each patient. Based on findings of a previous study that investigated Caucasian FECD patients from the MEH population, an expanded allele was defined as one carrying a trinucleotide repeat sequence with  $\geq 50$  CTG repeats (Zarouchlioti, Sanchez-Pintado et al. 2018). Patients with at least one allele in the CTG18.1 locus with a length that was equal to or greater than 50 repeats were categorised as expansion-positive, while those with both alleles found to have fewer than 50 repeats were categorised as expansion-negative. Within this current study of the MEH FECD population, no patients were found to have repeat lengths between 37 and 50. Therefore, the more conservative threshold of 50 repeats was applied when defining expansion positive FECD. Zarouchlioti et al had previously reported a highly significant association between  $\geq 50$  repeats on at least one allele and FECD (OR = 76.47; 95% CI: 47.45–123.2;  $p = 5.69 \times 10^{-71}$ ) (Zarouchlioti, Sanchez-Pintado et al. 2018). More than three quarters of this study cohort ( $n = 265, 77.4\%$ ) was found to be expansion-positive (Figure 1).

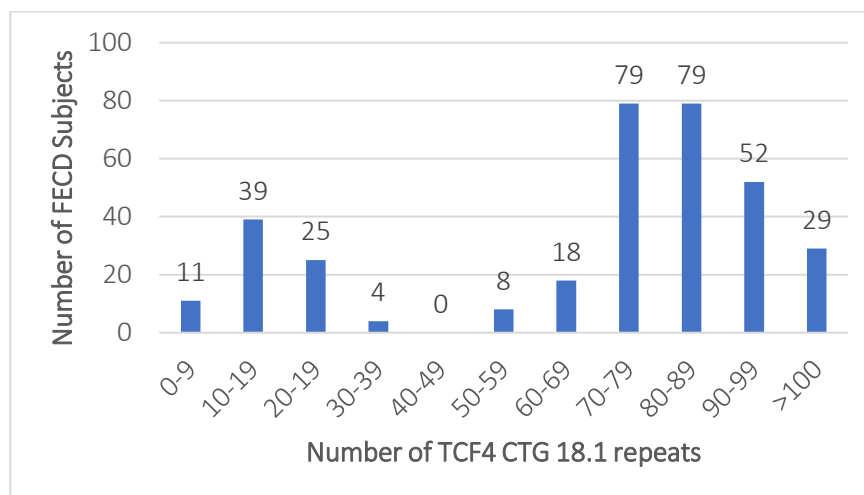


Figure 1: TCF4 CTG18.1 repeat expansion distribution. The histogram displays the frequency distribution of CTG repeat length when considering the number of repeats in the longer allele of the Moorfields Eye Hospital Fuchs Corneal Endothelial Dystrophy study subjects. Two hundred and sixty five (77.48%) of the patients in this study were found to be repeat expansion positive defined as  $\geq 50$  CTG repeats.

## 2.4.1.1 Patient Demographics

### 2.4.1.1.1 Ethnicity

The FECD cohort was predominantly Caucasian, with 302 subjects (88.3%) self-identifying as white British or white other. Collectively, the non-Caucasian cohort constituted 24.7% of the expansion negative cohort and only 7.9% of the expansion positive cohort (Table 3). A statistically significant association was found between the ethnicity and expansion status ( $X^2 = 31.57$ ,  $p < 0.001$ ). Specifically, Black/Afro-Caribbean patients were more likely to be expansion negative than positive (75% vs. 25%) while White Caucasian patients were more likely to expansion positive (81% vs. 19%) (Table 3). The distribution of subjects of South Asian ethnicity showed a greater proportion were repeat expansion positive while an almost equal distribution of patients of Chinese ethnicity were found in both groups. The numbers of Chinese and Asian patients in this study were however too small to draw statistically significant conclusions regarding FECD in subjects of this ethnicities. No statistically significant relationship was found between expansion status and other ethnic groups (Appendix B, Table 1).

	Number	Repeat Expansion Negative	Repeat Expansion Positive
Total FECD cohort	342	77/342 (22.5%)	265/342 (77.5%)
Females	188/342 (55%)	53/188 (28.2%)	135/188 (71.8%)
Males	154/342 (45%)	24/154 (15.6%)	130/154 (84.4%)
Patient Ethnicity:			
Caucasian	302/342 (88.3%)	58/302 (19.2%)	244/302 (80.8%)
Black/ Afro-Caribbean	16/342 (4.7%)	12/16 (75.0%)	4/16 (25.0%)
South Asian	12/342 (3.5%)	6/12 (50.0%)	6/12 (50.0%)
Other	8/342 (2.3%)	0/8 (0%)	8/8 (100%)
Chinese	4/342 (1.2%)	1/4 (25.0%)	3/4 (75.0%)

Table 3: Ethnicity of FECD patients subdivided by repeat expansion status. The majority of patients within the MEH FECD Fuchs cohort were Caucasian (88.3%), 92.1% of whom were found to be repeat expansion positive. The repeat expansion-negative cohort of was more ethnically diverse (24.7% non-Caucasian) than the repeat expansion-positive cohort (7.9% non-Caucasian).

#### 2.4.1.1.2 Gender

The FECD cohort was noted to be predominantly female, as women accounted for 55.0% (188/342) of individuals in the study. Males were more likely to be expansion positive than females (84.4% vs 71.8%) (Figure 2). A statistically significant association was shown between the gender and expansion status :  $\chi^2 (1, N=342) = 7.71, p < 0.005$  (Appendix B, Table 2).

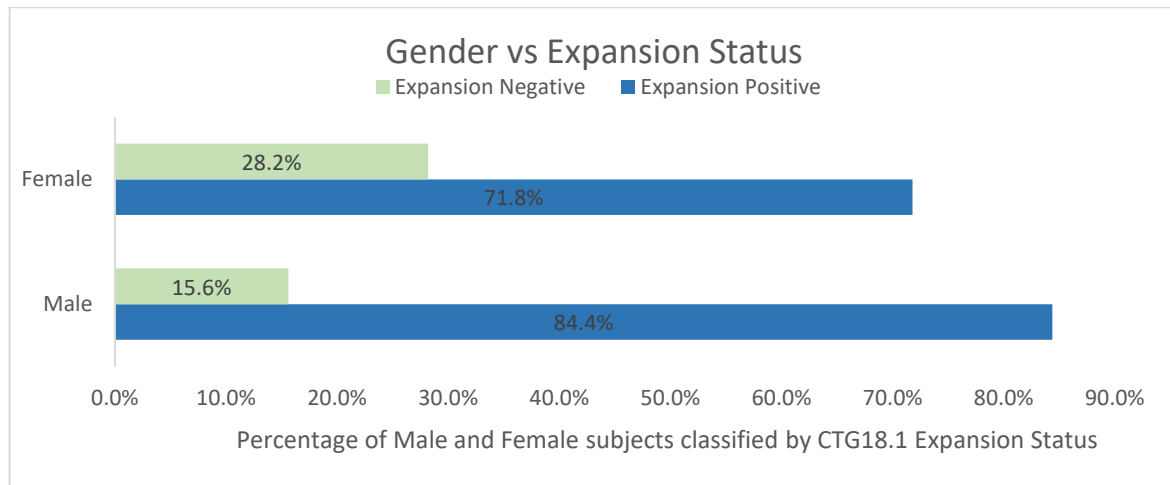


Figure 2: Distribution of FECD patients based on gender and expansion status. A higher percentage of male subjects were noted to be an expansion positive (84.4%) compared to female subjects who carried the mutation (71.8%).

#### 2.4.1.1.3 Ocular Comorbidities

The most common ocular comorbidity apart from cataract noted in the FECD cohort was glaucoma (n=27, 7.9%). Figure 3 shows the breakdown of ocular comorbidities according to expansion status. Overall, a greater incidence of concomitant ocular disease was noted in the expansion negative cohort (n=16, 20.7%) than the expansion positive cohort (n= 37, 13.9%), although the difference was not statistically significant (Appendix B, Table 3).

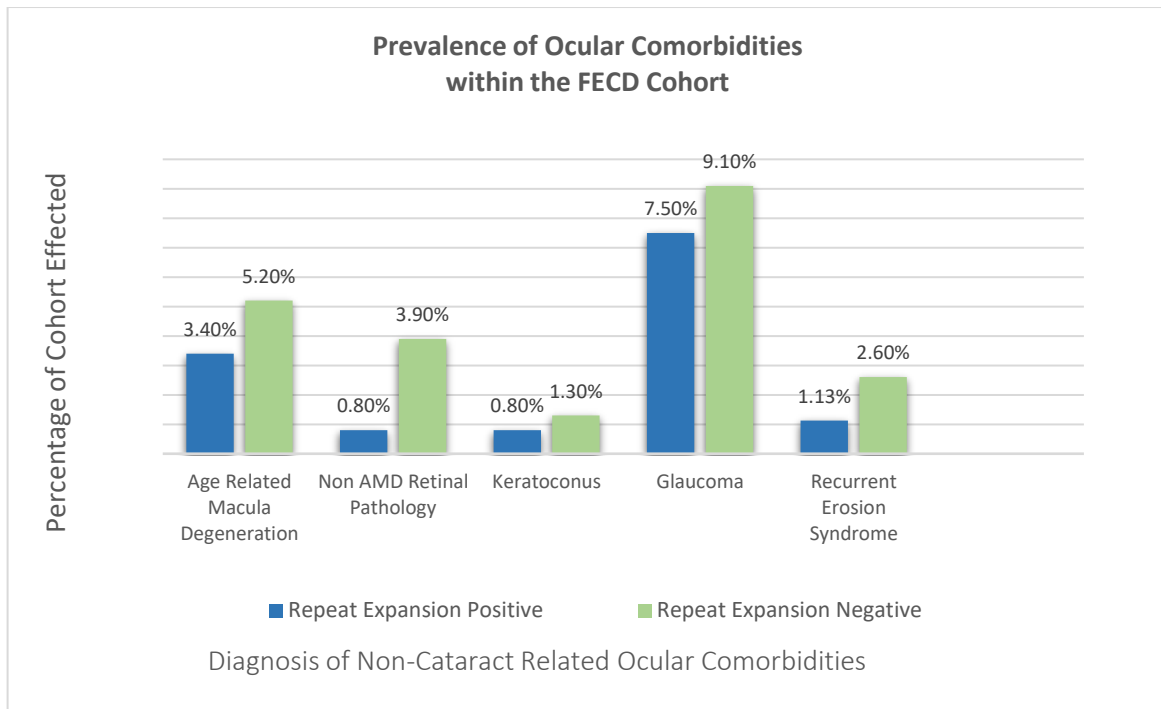


Figure 3: Ocular Co-morbidities within the FECD cohort. The percentage of patients effected by non-cataract related ocular comorbidities is shown for both the expansion positive and expansion negative cohorts. A greater prevalence of comorbidity was noted within the expansion negative cohort compared to the expansion positive cohort but no statistically relationship was noted between disease status and ocular pathology.

(AMD: age-related macular degeneration, FECD: Fuchs Endothelial Corneal Dystrophy )

#### 2.4.1.1.4 Family history

Thirteen participants in the study (3.8%) reported a family history of FECD. Eleven expansion positive patients self-reported a positive family history, of which 8 knew of at least one affected first degree relative, 2 reported 2 affected first degree relatives and 1 reported a maternal uncle with a known diagnosis of FECD (Table 4).

Repeat Expansion Status	Length of repeat expansion	Ethnicity	Gender	Affected family member(s) effected
Positive	97	Caucasian	M	Brother
Positive	103	Other	F	Son
Positive	92	Caucasian	F	Mother
Positive	70	Caucasian	F	Sister
Positive	81	Caucasian	F	Father
Positive	112	Caucasian	M	Mother
Positive	107	Caucasian	F	Mother, Sister, Nephew (affected sister's son)
Positive	96	Caucasian	M	Sister
Positive	95	Caucasian	F	Maternal aunt, maternal uncle
Positive	86	Caucasian	F	Mother
Positive	81	Caucasian	M	2 Brothers
Negative	15	Caucasian	F	Mother, Sister, Nephew
Negative	29	Caucasian	F	Father

Table 4: Table of family members reported to show symptoms of FECD within the MEH FECD study cohort. Of the 13 participants who reported a family member diagnosed with FECD, 84.6% were repeat expansion positive. In 72.7% of cases, the effected family member was a first degree relative.

#### 2.4.1.1.5 Age of Diagnosis

The age-of-diagnosis was available for 233/342 study participants. The average age at which FECD was diagnosed is 64.4 years; the range of diagnosis was between 23 years and 89 years of age. Eight subjects (3.43%) were diagnosed before the age of 40 years and were considered an early-onset variant

of the disease in keeping with the IC3D classification (Weiss, Moller et al. 2015) . Only 2 of the 8 early-onset patients were positive for the *CTG18.1* expansion. In the early-onset group, 2 patients (25%) also had keratoconus; one expansion positive and the other expansion negative.

The age at which patients reported the onset of visual symptoms (i.e. blurring of vision that improved through the day or blurring of vision/glare that was not related to other coexisting ocular pathology) was available for 243/342 patients. The majority of FECD patients (75.6%) were diagnosed following the onset of symptoms, but in the remainder the diagnosis was made as an incidental finding prior to patients reporting visual disturbance related to guttata (glare) or corneal oedema (blurring of vision).

#### 2.4.1.2 Surrogate markers for disease severity

To investigate the correlation between severity of corneal endothelial disease in FECD and the repeat expansion status of the patients, the following surrogate markers of disease severity were applied to the study participants:

##### 2.4.1.2.1 Age at the time of first corneal transplant surgery

Corneal transplant surgery is offered to patients when endothelial disease has progressed to a level that significantly effects visual acuity and impacts activities of daily living. Age of first corneal graft surgery was therefore applied as a surrogate marker of severity as it indicated a timepoint in the patient's life when corneal disease had reached a threshold that warranted surgical intervention.

##### a. Influence of *CTG18.1* repeat expansion status on the age at first corneal transplant surgery

Age of surgery data was available for 262 FECD patients: 198 expansion-positive and 64 expansion-negative. Analysis of the relationship between the dependent variable of age of first surgery and the independent, dichotomous categorical variable of expansion status by Mann-Whitney U analysis showed no statistically significant difference was between age of grafting and expansion status ( $U = 5900$ ,  $p = 0.408$ ). A Wilcoxon Signed Rank test was also performed to challenge the hypothesis that there is not shared underlying similarity between the repeat expansion positive and expansion negative FECD cohort as assumed by the Mann Whitney U test. The Wilcoxon W analysis also demonstrated an absence of a statistically significant relationship between age of surgery and expansion status ( $W = 7980$ ,  $p = 0.408$ )(Figure 4) (Appendix B, Table 4).

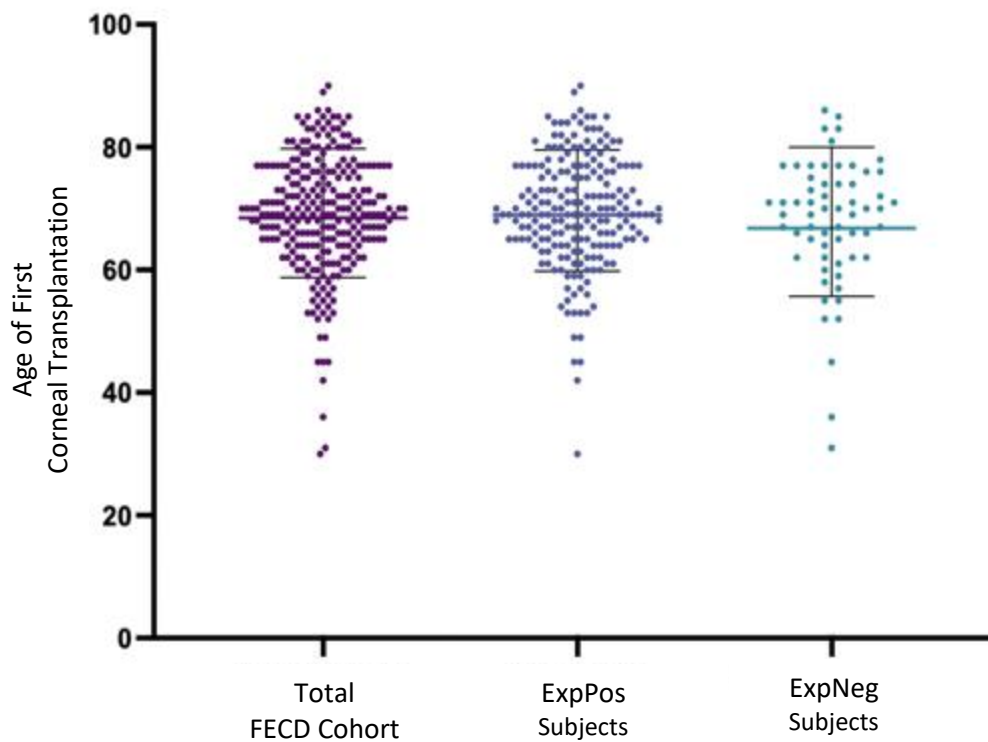


Figure 4: Bee swarm plot of age of first corneal transplantation within the MEH FECD cohort in accordance with expansion status. Age of surgery data was available for 262 FECD patients: 198 expansion-positive and 64 expansion-negative. Analysis of the relationship between the dependent variable of age of first surgery and the categorical variable of expansion status showed no statistically significant difference was between age of grafting and expansion status ( $U = 5900, p = 0.408$ ).

- b. Correlation between age at first corneal transplant surgery and *CTG18.1* repeat length within the expansion-positive cohort

To assess the correlation between disease severity and the length of the intronic repeat in 198 subjects, Spearman's rho analysis was applied to measure the strength and direction of association between the two variables. The results demonstrate a statistically significant, but weak negative correlation between expansion length and age of grafting, ( $r = -0.251, n=198, p=0.001$ )(Figure 5). This informs us that the longer the length of the triplet repeat the expansion, the younger the age of first corneal transplantation.

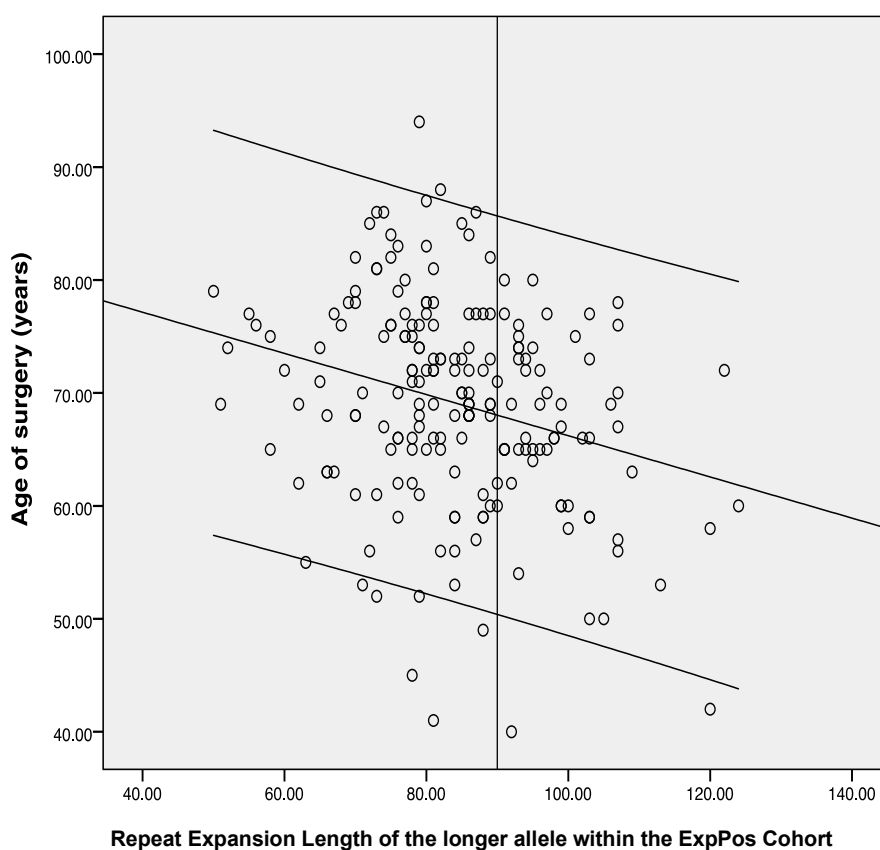


Figure 5: Correlation analysis of the relationship between age of first corneal transplant surgery and repeat expansion length in the Expansion Positive FECD cohort. Spearman's rho analysis demonstrates a weak but statistically significant, negative correlation between expansion length and age of grafting, ( $r = -0.251$ ,  $n=198$ ,  $p=0.001$ ). Therefore, the longer the repeat length the younger the age of first corneal transplantation.

c. Comparison of age at first corneal transplant surgery (endothelial keratoplasty) within the repeat expansion-positive cohort stratified to exclude prior cataract surgery

Cataract surgery can accelerate endothelial cell loss and it is a potential cause for corneal decompensation, particularly in patients with FECD (Seitzman, Gottsch et al. 2005). To exclude the confounding variable of secondary endothelial cell damage at the time of cataract surgery, patients who underwent cataract surgery prior to corneal transplantation were excluded from the analysis of the expansion positive cohort. In this stratified subgroup analysis of expansion positive FECD patients, there remains a weak negative correlation between expansion length and age of grafting, ( $r = -0.254$ ,  $n=112$ ,  $p=0.007$ ) (Appendix B, Table 5).



#### 2.4.1.2.2 Modified clinical grading score

Modified clinical grading (MCG) scores were applied retrospectively to 255 subjects based on analysis of clinical data available at the time of the first corneal graft surgery. The MCG score is assessed as an ordinal variable (i.e. the disease severity is analysed as ordered categorical data rather than a continuous variable) applying a Mann-Whitney U test. Adjusting for age of surgery, no statistically significant difference was noted between the disease severity graded by MGS between the repeat expansion positive and repeat expansion negative cohort ( $U = 5229$ ,  $p = 0.318$ ) (Appendix A, Table 6).

When analysing the repeat expansion positive cohort, ordinal regression was performed on the dependent variable of MCG score against the repeat expansion length, while accounting for age of first corneal graft. By doing so, it was possible to investigate the presence of a statistically significant relationship between repeat expansion length and MCG while eliminating the effect of the age of first corneal transplant. No statistically significant association between the MCG score and repeat expansion length was noted after accounting for age of first corneal transplant ( $p = 0.148$ ) (Appendix B, table 7).

#### 2.4.1.2.3 Central corneal thickness (CCT) at the time of first corneal graft surgery

Central corneal thickness data at the time of listing for first corneal transplant surgery was available for 172 patients. Linear regression modelling was performed to adjust for age of surgery in order to assess for the correlation between repeat expansion status and Central Corneal Thickness. Analysis of variance (ANOVA) found no association between the expansion status and CCT after accounting for the age at first grafting ( $p = 0.663$ ) (Appendix B, Table 8). Therefore, no statistically significant relationship was identified to denote a difference between the CCT at a given age at the time of surgery between the expansion positive and expansion negative cohorts.

## 2.5 Discussion

Analysis of the phenotypic characteristics of the 342 FECD patients in this study has ascertained clinical features that differentiate the repeat expansion positive (ExpPos) cohort from the expansion negative (ExpNeg) cohort. In terms of demographic data, the MEH FECD cohort was found to be predominantly Caucasian (88.3%). FECD patients of Caucasian origin were more likely to be expansion positive (92.1%) while the repeat expansion negative cohort was more ethnically diverse (24.7% non-Caucasian). Chi Square analysis of the categorical variables of ethnicity and expansion status showed a statistically significant association between ethnicity and expansion status, as Caucasian probands are statically more likely to be expansion positive while Black/Afro-Caribbean patients are more likely to be expansion negative (Chi square 34.7,  $p < 0.001$ ).

FECD was also noted to be more common in females (55%; 188/342), consistent with findings of previous publications (Krachmer, Purcell et al. 1978, Rosenblum, Stark et al. 1980, Wilson and Bourne 1988). Recent studies by Jurkunas *et al* have shown that, even in cases of differing underlying genetic mutations, female FECD patients display an increased endothelial cell susceptibility to oxidative stress (Miyajima, Melangath et al. 2020). In vivo FECD models have shown that UVA light causes impaired oestrogen metabolism in female patients that could confer an additional risk of FECD in genetically susceptible individuals (Liu, Miyajima et al. 2020). In this study we noted that male FECD patients were more likely to be expansion positive than female FECD patients. Our finding that males in the MEH FECD cohort were statistically more likely to be repeat-expansion positive (Chi square = 7.71,  $p < 0.005$ ) was comparable to the results published by Vasanth et al who reported a similar male preponderance in their expansion positive group (Vasanth, Eghrari et al. 2015).

Within the MEH FECD cohort, ocular co-morbidities were found in both the expansion-positive and expansion-negative groups; however, there were no statistically significant differences between the two groups. Glaucoma was the most common concomitant ocular disease in this study, with a prevalence of 7.9%. Population based prevalence studies of glaucoma in Caucasian patients above the age of 70 years have published values from 2.2% to 8.5% (Klein, Klein et al. 1992, Leske, Connell et al. 1994, Mitchell, Smith et al. 1996, Wensor, McCarty et al. 1998, Friedman, Jampel et al. 2006). The wide range of reported prevalence makes it difficult to draw comparisons with the prevalence of glaucoma in the MEH FECD cohort.

Although glaucoma and FECD may share a common mechanism of cellular dysfunction in the form of oxidative stress (Borderie, Baudrimont et al. 2000, Jurkunas, Bitar et al. 2010, Kimura, Namekata et al. 2017, Moazzeni, Mirrahimi et al. 2019), the exact relationship between the two conditions remains uncertain (Krachmer, Purcell et al. 1978, Ali, Whitson et al. 2011, Nagarsheth, Singh et al. 2012, Rice, Wright et al. 2014). A post hoc analysis of the FECD Genetics Multi-Centre Study cohort by Nagarsheth *et al* is the largest study to report a higher prevalence of glaucoma or ocular hypertension in patients with severe FECD versus controls (control subjects were matched according to age, gender, and ethnicity to FECD cases) (Nagarsheth, Singh et al. 2012). Although the overall incidence of glaucoma was 6.6% in FECD patients versus 6.0% in controls, further analysis by the Nagarsheth group showed that, after adjusting for age, in more severe FECD cases (defined as Krachmer grade 4 through 6) the prevalence rose to 11.2% for index cases and 8.5% for affected family members. The grading system applied retrospectively to the MEH FECD does not allow direct comparison to the findings of the Nagarsheth study in regards to the relationship between FECD severity and prevalence of glaucoma. The grading system utilized in our study indicates that 82.6% of glaucoma patients within the MEH cohort showed signs of corneal oedema at the time of enrollment, which could tentatively be classified as severe by the traditional Krachmer score (although number and confluence of guttata are not known). As 82.2% of the total MEH FECD cohort met these criteria of severity, no statistically significant relationship could be demonstrated between FECD grade and glaucoma in this study ( $\chi^2 = 0.196$ ,  $p=0.406$ ).

Although reports of a higher prevalence of glaucoma in both FECD patients and affected family members, would support a proposed genetic link between the two conditions (Krachmer, Purcell et al. 1978, Nagarsheth, Singh et al. 2012), a mechanical cause may underlie the relationship between the two diseases. Studies by Brunette et al (Brunette, Sherknies et al. 2011) and Shousha *et al* (Shousha, Perez et al. 2010) have shown that corneal oedema leads to progressive bowing of the posterior corneal curvature into the anterior chamber angle of patients with FECD. Both studies reported that as the oedema increases and spreads peripherally, the posterior surface of the cornea comes into closer contact with the anterior chamber angle, thus narrowing the drainage passage of aqueous leading to elevated intraocular pressure in severe FECD.

Keratoconus was another corneal disease noted as a dual pathology within this FECD cohort. Due to the small numbers of patients studied (n=3), no statistically significant association could be found between this corneal ectasia and FECD expansion status. However, it was interesting to note that the incidence of keratoconus within the MEH FECD cohort (0.9%) was higher than had been previously

published in the majority of reported populations, with the exception of the Maori (2.25%) and Western Australian population (1.2%) (Papali'i-Curtin, Cox et al. 2019, Chan, Chong et al. 2021) (Table 5) (Kennedy, Bourne et al. 1986, Pearson, Soneji et al. 2000). This finding is in keeping with reports of an association between the two conditions (Lipman, Rubenstein et al. 1990, Jurkunas and Azar 2006, Cremona, Ghosheh et al. 2009). To further investigate the association between keratoconus and FECD, I have carried out a separate study to investigate this dual pathology (Chapter 4).

Publication	Population [Diagnostic Criteria]	Prevalence
Kennedy <i>et al.</i> 1986 (Kennedy, Bourne et al. 1986)	Population based epidemiological study of Olmsted County, Minnesota [Scissors movement on retinoscopy and keratometry]	0.05%
Ihalainen <i>et al.</i> 1986 (Ihalainen 1986)	Clinical and epidemiological features of keratoconus (KC) were studied in a series comprising all the 212 KC patients treated at Oulu University Central Hospital from 1964 to 1984 [Diagnostic criteria not specified]	0.03%
Pearson <i>et al.</i> 2000 (Pearson, Soneji et al. 2000)	10-year retrospective review of hospital records of an ophthalmology department in the United Kingdom with a catchment population of approximately 900 000 (87% white, 11% Asian, 2% other) [Diagnostic criteria not specified]	Asian: 0.23% White: 0.06%
Godefrooij <i>et al.</i> 2017 (Godefrooij, de Wit et al. 2017)	Data was extracted from the largest health insurance provider in the Netherlands [Diagnostic criteria not specified]	0.27%
Bak-Nielsen <i>et al.</i> 2019 (Bak-Nielsen, Ramlau-Hansen et al. 2019)	All patients diagnosed with keratoconus in the National Danish Patient Register 1977-2015 [Diagnostic criteria not specified]	0.04 %
Papali'i-Curtin <i>et al.</i> 2019 (Papali'i-Curtin, Cox et al. 2019)	Population-based prospective cross-sectional study 1916 students with a mean age of 14.6 years from 20 schools in Wellington New Zealand [Videokeratography measurement of algorithm based (Belin/Ambrósio) enhanced ectasia display score of 1.88 or more]	0.52% overall 2.25% Maori participants.
Chan <i>et al.</i> 2021 (Chan, Chong et al. 2021)	1259 20 year old participants in a multigenerational, longitudinal cohort study based in Perth, Western Australia [Videokeratography measurement of algorithm based (Belin/Ambrósio) enhanced ectasia display score of 2.6 or more]	1.2%

Table 5: Summary of publications investigating the prevalence of Keratoconus in predominantly Caucasian populations. Both large scale epidemiological studies of national databases (Godefrooij, de Wit et al. 2017, Bak-Nielsen, Ramlau-Hansen et al. 2019) and hospital based studies of patient populations (Ihalainen 1986, Kennedy, Bourne et al. 1986, Pearson, Soneji et al. 2000) have shown a high degree of variation in the prevalence of keratoconus in the population (0.03% to 0.27%). Pearson *et al* and Papali'i-Curtin *et al* were able to show that ethnicity played an important role in the prevalence of this condition which was noted to be almost 4 times higher in Asian and Maori subjects compared to the Caucasian cohort of the study. The prevalence of 0.9% within the predominantly Caucasian MEH FECD cohort is therefore noted to be higher than previously reported in all but that of the Australian population (1.2%).

Although studies have reported that FECD is an inherited disease, displaying both complete and incomplete patterns of segregation, only 3.8% of participants in this cohort reported a family history (Magovern, Beauchamp et al. 1979, Sundin, Jun et al. 2006, Mootha, Gong et al. 2014, Saade, Xing et al. 2018). Of those who reported a positive family history, 84.6 % (n=11/13) were white and found to harbour the repeat expansion. This finding likely represents an ascertainment bias as 92.1% (265/342) of patients within the study were expansion-positive and Caucasian. To ensure that this data was not skewed by poor documentation in clinical notes, study participants were contacted directly to clarify if any relatives were known to have FECD or history of previous corneal transplant surgery. Within our FECD study population, the average age at which the condition was diagnosed was 64.4 years. It is therefore possible that patients of this age may not have known if their parents had also been diagnosed with FECD. As the treatment offered for corneal decompensation 20 years ago was penetrating keratoplasty, the threshold for intervention would have been higher and may explain to a degree why patients did not report older family members having undergone corneal transplantation. The low reporting of affected siblings however is an anomaly in this study and must be considered a limitation in regards to accuracy of retrospective data analysis and history taking. As reported by Elhalis *et al*, the indolent course of the disease in addition to the late onset of the dystrophy, results in failures both in recognizing the condition as well as in establishing full pedigrees of patients with FECD (Elhalis, Azizi et al. 2010).

In regards to the age of clinical presentation, 96.6% of this study cohort consisted of late-onset FECD (average age of diagnosis 64.4 years; range of 23- 89 years). The threshold age of 40 years was used as a cut-off to define early and late-onset disease (Weiss, Moller et al. 2008). Only 8 patients were diagnosed before the age of 40 years, the youngest at 23 years of age. Of the 8 early onset patients only 2 (25%) were repeat expansion-positive. One of the early onset patients was diagnosed with keratoconus first and FECD was an incidental finding based on the presence of central guttata. This patient remained asymptomatic in terms of diurnal variation with no signs of corneal oedema. Further analysis of the age at which patients reported visual symptoms rather than the age of diagnosis, showed that in 24.4% of patients the diagnosis was made as an incidental clinical finding before the onset of visual symptoms (glare, diurnal variation).

To assess the correlation between expansion status and disease progression, age of first corneal transplant, Modified Clinical Score (MCS) staging and central corneal thickness were used as surrogate markers of disease severity. There was no statistically significant difference in all three measures of severity when the FECD population was divided in a binary manner into expansion-positive and

expansion-negative cohorts. Studies by Soh *et al*, Vasanth *et al* and Eghrari *et al* have all reported increased disease severity in expansion-positive FECD patients harbouring the CTG18.1 mutation compared to those who were expansion negative. The absence of a difference in disease severity based on expansion status within the MEH FECD cohort compared to published data could be attributed to the following factors:

A. Bias in severity introduced by recruitment methodology

FECD patients within the MEH study were recruited at the time of listing for surgery or on the day of surgery. Only one of the 342 patients in this study had not undergone corneal transplantation. This is significantly higher than the Eghrari *et al* study in which only 18.5% of the cohort required transplantation. Additionally, as a tertiary referral centre it is possible that the MEH cohort of patients is biased towards a more severe disease phenotype, with patients being followed up at their local eye units and referred to MEH when surgery is indicated.

B. Discrepancy in grading of FECD severity

Studies by Vasanth *et al* and Soliman *et al* categorised post keratoplasty eyes as Krachmer Grade 6 in accordance with the original grading system that was developed in the era of penetrating keratoplasty (Krachmer, Purcell *et al*. 1978). However, application of Krachmer Grade 6 to patients who have undergone endothelial keratoplasty overestimates the level of disease severity. The introduction of endothelial keratoplasty as a surgical technique allows surgeons to intervene much earlier in the course of the disease and patients benefit from faster post-operative recovery (Anshu, Price *et al*. 2012). The threshold at which the risks of surgery (infection, suture loosening, graft rejection) are outweighed by the benefits is therefore much lower, leading to earlier intervention in FECD. On the basis of the MCS system applied in this study, 82.2% of FECD patients underwent corneal transplantation at Grade 2 and 3.

C. Error in defining the ExpNeg cohort as a single disease entity

In dividing the study cohort by the presence or absence of the CTG18.1 trinucleotide repeat expansion, an assumption is made that the expansion negative cohort consists of patients with a single underlying disease. However, the repeat expansion negative cohort remains an as yet undefined genetically heterogeneous population (Wieben, Aleff *et al*. 2018). The following chapter will aim to investigate the repeat expansion negative FECD cohort in greater detail to address this area of uncertainty.

Interestingly, when analysis the of the ExpPos FECD cohort separately, it was confirmed that a negative correlation exists between the length of the *CTG18.1* repeat expansion and age of corneal transplantation. Longer CTG18.1 expansion length was therefore associated with patients having to undergo corneal transplant surgery at a younger age. To date, Soliman *et al* are the only study that have analysed the impact of repeat expansion length on FECD severity. By adopting keratoplasty as a marker of severity in FECD, the study demonstrated a correlation between increased *CTG18.1* repeat length and earlier age of surgery (Soliman, Xing et al. 2015). However, certain caveats must be applied in analysing the results of their study. It was not stated if patients who had undergone cataract extraction and intraocular lens implantation prior to corneal decompensation were excluded from the analysis. In this study and that of Soh *et al*, it is recognised that cataract surgery accelerates endothelial cell loss in FECD and therefore the data was stratified to exclude patients who had lens surgery prior to keratoplasty (Seitzman, Gottsch et al. 2005, Soh, Peh Swee Lim et al. 2019). In the MEH repeat expansion positive cohort, the statistically significant correlation between longer repeat length and younger age of first corneal surgery was found to be consistent in the stratified cohort of expansion positive FECD.

Reported Correlation with Repeat Expansion Status	Number of subjects (p value)	Clinical Significance
Ethnicity	342 (p = 0.001)	<ul style="list-style-type: none"> <li>▪ Black/Afro-Caribbean patients were more likely to be expansion negative</li> <li>▪ White patients were more likely to be expansion positive</li> </ul>
Gender	342 (p = 0.005)	<ul style="list-style-type: none"> <li>▪ Male FECD patients are more likely to be repeat expansion positive female patients</li> </ul>
Age of first corneal transplantation in expansion positive subjects	198 (p=0.002)	<ul style="list-style-type: none"> <li>▪ The longer the length of the triplet repeat the expansion, the younger the age of first corneal transplantation</li> </ul>
Age of first corneal transplantation in expansion positive subjects stratified to exclude post cataract surgery patients	112 (p=0.007)	<ul style="list-style-type: none"> <li>▪ When the cohort of repeat expansion positive patients was stratified to exclude the confounding risk of cataract surgery in accelerating corneal decompensation, longer repeat expansion length was still noted to correlate with younger age of corneal graft surgery</li> </ul>

Table 6: Summary of FECD disease characteristics that were shown to correlate significantly with repeat expansion status or length. This study found that white male FECD patients were the most likely to harbour the repeat expansion. In repeat expansion positive patients, it was note that the longer the repeat expansion the younger the age of corneal transplant surgery, indicating more rapid disease progression with longer repeat length. This association remained statistically significant when the FECD cohort was stratified to exclude patients who had undergone cataract surgery prior, a known exacerbating cause of corneal decompensation.



## 2.6 Limitations of this study

One of the main challenges of assessing disease progression in FECD is defining an objective and repeatable measure of disease severity. In this study, visual acuity data could not be used as an independent measure of visual function as cataracts are a common cause of visual impairment in patients over the age of 60 years. It was therefore difficult to ascertain if a drop in visual acuity was due to opacification of the lens secondary to cataract formation or as result of the loss of corneal clarity secondary to progressive corneal oedema in FECD.

Central corneal thickness (CCT) data is another parameter by which to measure corneal endothelial function, as the thickness increases as the cornea decompensates (Mandell, Polse et al. 1989, Kopplin, Przepyszny et al. 2012). However, the reliability of this measure is compromised by the natural history of the disease which exhibits diurnal fluctuation in corneal oedema (Fritz, Grewing et al. 2019). Central corneal thickness is at its peak in the early part of the day and decreases in thickness as the day progresses. Due to the normal variation in central corneal thickness within the population, there exists an added difficulty in assessing disease progression based on CCT in patients unless a baseline value of corneal thickness is available (Brandt, Beiser et al. 2001).

Another potential measure of FECD progression is through quantifying of endothelial cells at the central cornea. Accurate and reproducible measurements are however difficult as the presence of oedema as well as guttate can cause poor image quality and difficulty in visualising endothelial cells. Automated specular microscopy analysis of endothelial cells is commonly utilised in clinical settings as a time efficient manner of obtaining cell count measures. However, automated analysis is known to significantly overestimates endothelial cell density in the presence of high polymegathism and larger cell size in FECD (Huang, Maram et al. 2018). It has also been shown that inter-examiner variability can differ by -17% to +14% cell/mm<sup>2</sup> depending on the instrument, introducing further difficulty in the interpretation of endothelial cell count as a measure of FECD progression (Cheung and Cho 2000, Nichols, Kosunick et al. 2003)

In this study, the retrospective application of the MCS score allowed subjective grading of disease severity at the time of corneal transplantation. However, this method of measuring disease severity created very broad parameters for each stage of the disease. The inability to define clear stages of FECD progression compromised the accurate staging clinical disease progression.

The retrospective nature of this study further highlighted the real-life clinical limitations of data collection and documentation in a busy NHS service. Clinical measures of corneal thickness and endothelial cell count are valuable in circumstances of clinical uncertainty to aid diagnosis. However, in cases of clear clinical signs on slitlamp examination, these ancillary tests were often not performed as these measures do not influence the decision to proceed with surgery. Instead, the effect of the disease on the quality of life and the patient's subjective symptoms in regards to limitations on activities of daily living influenced the clinical decision for surgical intervention. For this reason, corneal transplantation was taken an alternative surrogate marker for assessing disease severity in this study.

As we continue to investigate the genotype -phenotype correlation in repeat expansion mediated FECD, it is important that we draw on the lessons learned from similar studies in the field of neuropathology. Huntington's disease (HD) was the earliest expansion mediated disease in which a correlation was demonstrated between longer repeat length, earlier age of onset and death as well as higher grade of neuropathological staging (Vonsattel 2008). The Vonsattel grading system is widely used as a research tool for staging HD by measuring distinct topographic image changes within the brain as a marker of disease severity (Myers, Vonsattel et al. 1988). However, subsequent studies have shown that the application of this topographic staging criteria did not correlate to the actual clinical severity of disease, when assessing both cognitive and functional scores of HD patients just prior to death (Myers, Vonsattel et al. 1988, Rosenblatt, Abbott et al. 2003, Pillai, Hansen et al. 2012). It has therefore called into question the findings of studies that reported a clear relationship between repeat expansion length and disease severity based on this commonly applied grading system.

## 2.7 Conclusion

It is vital that we continue to investigate parameters by which to define the phenotypic characteristics of our FECD patient population. Studies such as this highlight the real life challenges of deep clinical phenotyping and help to guide the development of appropriate criteria by which to measure disease progression. By clearly defining genotype-phenotype correlations and understanding the natural history of the disease, we can begin to identify optimal treatment windows for new and emerging gene based FECD therapeutics. It is hoped that early intervention in patients identified to harbour the mutation could be delivered prior to the onset of characteristic disease features such as corneal guttae, loss of CECs and subsequent stromal oedema.

The findings of this study support the theory that CTG18.1 repeat expansion length does influence disease progression. This finding is in keeping with the proposed hypothesis that longer CTG18.1 repeat expansion cause increased accumulation of toxic RNA aggregates within the cell and greater somatic instability with increased repeat length. The resulting accelerated dysfunction of corneal endothelial cells could explain the earlier corneal decompensation reported in patients harbouring longer repeat expansions. It would therefore be advisable that therapies aimed at halting disease progression should be prioritised for patients with longer repeat length and administration at a younger age should be considered. Repeat length could also further guide our decision making in planning surgical intervention for patients with longer repeat length. If endothelial compromise is greater in those with longer repeat length, it is possible that endothelial cell loss following lens extraction surgery may be greater in those affected individuals. Further prospective studies will need to be carried out to improve our understanding of this disease phenotype and the relationship to the underlying genetic change.

ANALYSIS OF  
CTG18.1 EXPANSION NEGATIVE  
FUCHS CORNEAL ENDOTHELIAL DYSTROPHY  
COHORT

### 3.1 Introduction

The study of molecular pathology can be divided into two phases: Firstly, seeking to understand the effect of a genetic sequence change on the gene function and secondly to understand the effect of the genetic change on a person's phenotype (Strachan and Read 2019). The identification of the CTG18.1 intronic repeat expansion mutation as the predominant genetic cause of FECD has led to the recognition of interesting genotype-phenotype correlations, discussed in chapter one. It has also highlighted the differences between FECD patients who are positive for the intron repeat sequences and those who do not harbour the mutation. Nearly a quarter of patients diagnosed clinically as having FECD, may experience similar corneal dystrophy symptoms, but at a molecular level the underlying cause of their disease is different (Wieben, Aleff et al. 2014, Zarouchlioti, Sanchez-Pintado et al. 2018).

As we enter an era of personalised medical care that allows us to offer patients not only improved treatments, but clearer guidance in terms of prognosis based on their genetic code, it is imperative that we continue to investigate the underlying mutations and genotype-phenotype correlations of the almost one in four FECD patients in whom we are yet to understand the molecular basis of their disease. This chapter aims to understand the genotype-phenotype correlation of the FECD patients within the MEH FECD cohort who were found to be CTG18.1 repeat expansion-negative (ExpNeg).

## 3.2 Methods

From the overall cohort of CTG18.1 ExpNeg-patients, 78 patients were selected for whole exome sequencing on the basis of research funding availability. In addition to the original FECD cohort, a patient initially diagnosed as having another form of corneal endothelial cell dystrophy (Posterior polymorphous corneal dystrophy) was also included for whole exome sequencing in view of ambiguity in the diagnosis.

### 3.2.1 Whole Exome Sequencing (WES)

WES analysis was outsourced to Novogene where sequencing libraries were generated by SureSelect Human All Exome V6 kit (Agilent, USA). This exome design targets only coding regions from RefSeq, CCDS, GENCODE & UCSC Known Genes on which variant functional annotations were based. Libraries were sequenced on HiSeq4000 sequencer (Illumina). Raw sequencing data was returned in FATSQ format which provided both the nucleotide sequence as well as a corresponding quality score of the data.

#### ▪ 3.2.1.1 Alignment of read data and variant calling

Alignment of reads and variant calling was performed by Dr Nikolas Pontikos, resident bioinformatician at UCL. The process of variant calling involves the identification of single nucleotide polymorphisms (SNPs) and small insertions and deletion (indels) from next generation sequencing data.

#### ▪ 3.2.1.2 Variant Filtering of WES data

Variants were first filtered for those present in genes already known to be associated with FECD and for those reported to be associated with FECD in a recent GWAS by Afshari *et al.* (Table 1)(Afshari, Igo *et al.* 2017). The rare variants were filtered for a frequency of  $\leq 0.01$  in the 1000 Genome project, ESsp and UCLex datasets.

### 3.2.2 Pathogenicity Prediction Tools

#### ▪ 3.2.2.1 In silico prediction tools were utilised to enable mutational effect analysis:

##### a. Polymorphism Phenotyping V2 (PolyPhen2)

Polyphen2 (<http://genetics.bwh.harvard.edu/pph2/>) was utilised to predict the possible impact of amino acid substitution on the structure and function of a human protein. The program assigned a score from 0.0 to 1.0, with 0 representing a benign or tolerated change and 1 being deleterious to the protein based on physical and comparative considerations.

b. Sorting Intolerant from Tolerant (SIFT) Prediction

The SIFT algorithm (<https://sift.bii.a-star.edu.sg>) was applied to predict the effect of an amino acid substitution on the function of the polypeptide structure formed. The prediction is based on the degree of conservation of amino acid residues in sequence alignments derived from closely related sequences. The algorithm produces a score ranging from 0 to 1, with 0 representing a deleterious effect while 1 is well tolerated.

c. Splice Predictor Tools

SpliceAid2 ([http://193.206.120.249/splicing\\_tissue.html](http://193.206.120.249/splicing_tissue.html)) was utilised to predict the effect on a variant on splicing if it was predicted to occur in a position involved in mRNA splicing (Piva, Giulietti et al. 2012). Human Splice Site Finder version 3.1 (<http://www.umd.be/HSF3/>) was also applied to predict the effect of variants on splicing motifs (Desmet, Hamroun et al. 2009).

- 3.2.2.2 Variant Effect Predictor analysis was also performed through the Ensembl genome browser (<https://www.ensembl.org/index.html>). Ensembl provided the following information:
  - Genes and transcripts affected by the variants
  - The location of the variants : upstream of a transcript, in coding sequence, in non-coding RNA or in regulatory regions
  - Consequence of your variants on the protein sequence: stop gained, missense, stop lost or frameshift
  - Identifies known variants and associated minor allele frequencies (MAF) from the 1000 Genomes Project
  - Reconfirms SIFT and PolyPhen-2 scores
  
- 3.2.2.3 Online Mendelian Inheritance in Men (OMIM)  
OMIM (<https://www.omim.org/>) was used to identify existing genotype-phenotype correlations between genetic disorders and their clinical traits
  
- 3.2.2.4 BioEdit Alignment Editor  
ClustalW on the BioEdit sequence alignment editor (version 7.1.30) was used to align multiple protein sequences to identify gene sequences that were similar across species, thus indicating a level of amino acid conservation

### 3.2.3 Filtering strategy applied in investigating the CTG18.1 Expansion Negative Cohort

Whole exome analysis was carried out on the selected cohort of 77 CTG18.1 ExpNeg FECD probands and 1 additional candidate in whom the diagnosis of endothelial dystrophy was uncertain due to the unusual phenotype. WES analysis and sequencing was outsourced to Novogene, a commercial sequencing provider.

Raw sequence analysis was aligned and annotated courtesy of Dr Nicolas Pontikos (UCL resident bioinformatician). Variant filtration was then performed by Miss Amanda Sadan (PhD student) to exclude those with MAF >0.01 in the control dataset. The control datasets utilised in this process were the 1000 Genome project, ESP and UCLex. Variants were then filtered into 2 phases:

- Genes previously associated with FECD
- Genes found to have a significant association with FECD by a recent GWAS (Afshari, Igo et al. 2017)

Variants were then prioritised on the basis of functional impact, pathogenicity and frequency in the control data sets. Following filtration, the identified variants were validated by Sanger sequencing of amplified regions containing the variant. A schematic representation of the filtering strategy is shown below in Figure 1 along with the genes that were investigated detailed in Table 1.



Associated Gene or loci	Protein	OMIM	Most significantly associated SNP	Reference
Gene harbouring presumed Causative variant(s)				
<i>TCF4</i>	Transcription factor 4	613267	rs613872 rs784257	Baratz <i>et al.</i> 2010 Wieben <i>et al.</i> 2012 Afshari <i>et al.</i> 2017
<i>COL8A2</i>	Collagen Type VIII Alpha 2 Chain	136800	NA	Biswas <i>et al.</i> 2001
<i>COL8A1</i>	Collagen Type VIII Alpha 1 Chain	120251	NA	Hopfer <i>et al.</i> 2005
<i>SLC4A11</i>	Solute carrier family 4 (sodium borate cotransporter), member 11	613268	NA	Vithana <i>et al.</i> 2008
<i>ZEB1</i>	Zinc finger E box-binding homeobox 1	613270	NA	Mehta <i>et al.</i> 2008
<i>AGBL1</i>	ATP/GTP-binding protein-like 1	615523	NA	Riazuddin <i>et al.</i> 2013
<i>LOXHD1</i>	Lipoxygenase homology domain-containing 1	NA	NA	Riazuddin <i>et al.</i> 2012
Associated loci identified via Genome Wide Association Study				
<i>KANK4</i>	KN motif- and ankyrin repeat domain- containing protein 4	NA	rs79742895	Afshari <i>et al.</i> 2017
<i>LAMC1</i>	Laminin, gamma-1	NA	rs3768617	Afshari <i>et al.</i> 2017
<i>LINC00970/ATP1B1</i>	ATPase, Na <sup>+</sup> /K <sup>+</sup> transporting, beta-1 polypeptide	NA	rs1200114	Afshari <i>et al.</i> 2017

OMIM: online inheritance in man; GWAS: genome wide association study; SNP: single nucleotide polymorphism

Table 1 : Summary of genes and loci associated with Fuchs endothelial corneal dystrophy (FECD) [Adapted from Fautsch *et al.* 2021(Fautsch, Wieben *et al.* 2021)]. Genes previously associated with differing phenotypes of FECD were applied in a filtering strategy to identify potential candidate genes in the *TCF4* repeat expansion-negative cohort.

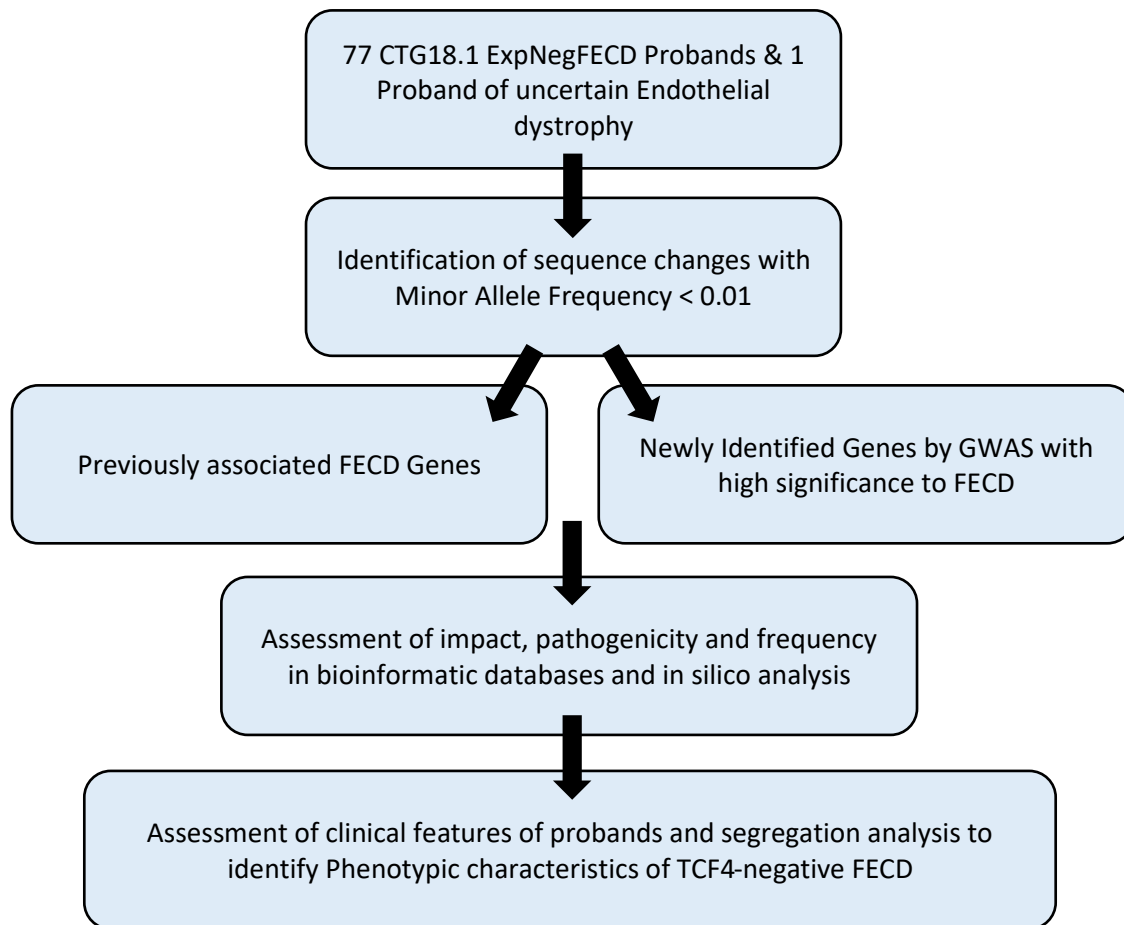


Figure 1: Whole exome sequencing (WES) filtering strategy employed by this study to identify potential FECD-associated variants and enable genotype-phenotype correlation analysis. The flow chart illustrates the process by which variants identified via WES were stratified to identify those already known to be associated with FECD as well as those known to have a highly significant association with FECD. The functional impact, pathogenicity and frequency of the identified variants was analysed and those that were noted to be more likely to be disease causing were prioritised for phenotype analysis.

The filtering strategy successfully identified 15 rare variants (MAF  $\leq 0.01$ ) in 14 CTG18.1 ExpNeg FECD subjects. Figure 2 shows the breakdown of the cohort in which variants of interest were identified within FECD-associated genes.

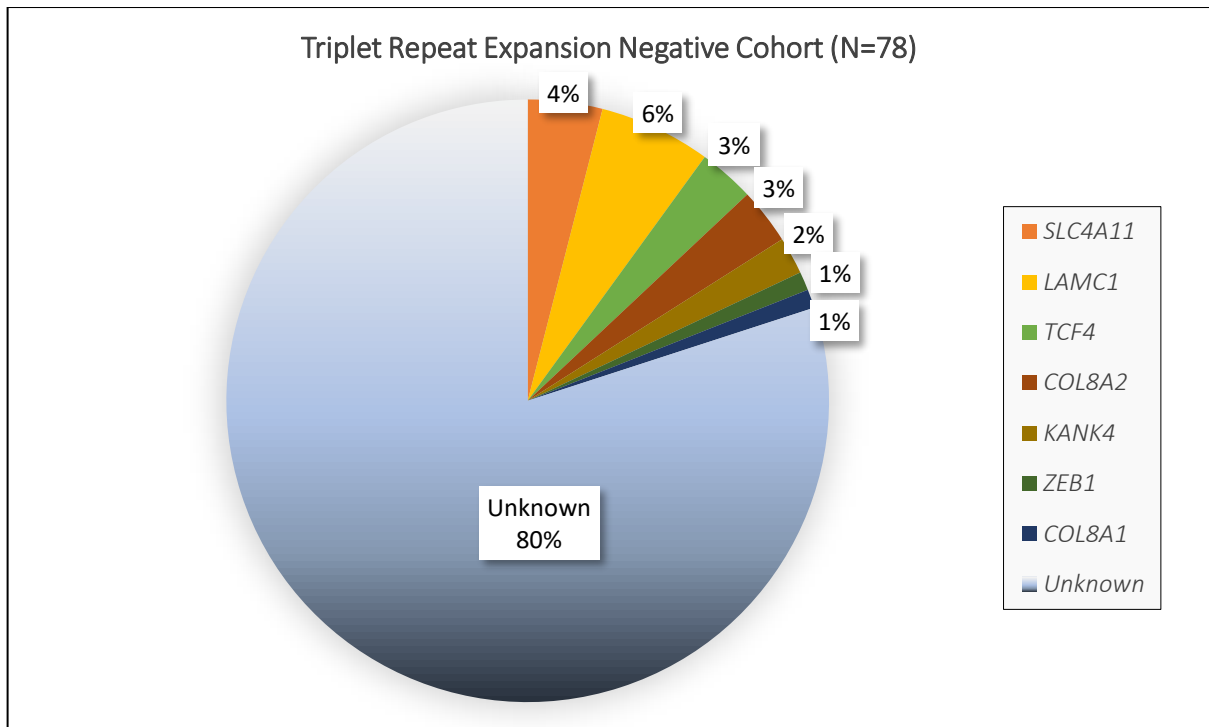


Figure 2: Pie chart depicting the percentage of the FECD repeat-expansion negative subjects investigated by Whole Exome Sequencing that were found to harbour rare variants in genes associated with FECD as well as genes reported in a genome wide association study (GWAS) as promising candidate genes. The filtering strategy successfully identified 15 rare variants (MAF  $\leq$  0.01) in 14 repeat expansion-negative subjects. The underlying genetic cause of disease in eighty percent of the subjects studied remains unresolved.

### 3.2.4 Patient Recruitment

For patients in whom rare variants were detected, family members were contacted to enable phenotyping and further segregation analysis. The study followed the tenets of the Declaration of Helsinki and was approved by Moorfields Eye Hospital Research Ethics Committee (09/H0724/25).

### 3.2.5 Phenotyping

#### 3.2.5.1 Clinical Data Collection

Retrospective review of clinical notes from subjects was supplemented wherever possible with prospective assessment to obtain: Snellen best-corrected visual acuity (BCVA), slit-lamp biomicroscopy assessment of the corneal changes and clinical history of disease symptoms as well as past ocular

history. The same prospective assessment of subjects' family members was also sought in all cases of identified variants.

#### 3.2.5.2 Imaging and structural assessment

Slit lamp camera images were obtained along with corneal topography (Pentacam, Oculus Optikgeräte GmbH, Wetzlar, Germany) and in-vivo confocal microscopy (IVCM, Heidelberg). Expert interpretation of the confocal images was provided by Mr Scott Hau (Lead corneal imaging specialist, Moorfield Eye Hospital).

#### 3.2.5.3 Pathology

When available, sections of corneal tissue removed at the time of endothelial keratoplasty were stained with haematoxylin and eosin prior to light microscopy evaluation by Consultant Ophthalmic Pathologist, Dr Caroline Thaug. Histological features attributed to FECD include thickened and laminated Descemet's membrane, excrescences from DM posteriorly in keeping with guttate, corneal stromal oedema resulting in loss of normal stromal architecture, epithelial bullae and blebs as well as reduced endothelial cells.

## RESULTS

3.3.1

EARLY-ONSET  
FUCHS ENDOTHELIAL CORNEAL DYSTROPHY  
AND  
COLLAGEN VIII

### 3.3.1.1 COL8A2

#### 3.3.1.1.1 Background

*COL8A2* encodes a non-fibrillar short chain collagen that forms a major component of Descemet's membrane. Collagen Type VIII is made up of 2 similar  $\alpha$  chains: the alpha 1 chain and the alpha 2 chain. In 2001, Biswas et al performed a genome wide search on three generations of a family that exhibited clinical features of early onset FECD. Linkage analysis highlighted the transmission of a critical 6-7cM region on the short arm of chromosome 1 (1p34.3-p32). It was recognised that the *COL8A2* gene localised to this area and was an ideal candidate gene for further investigation. A heterozygous missense mutation c.1364C>A, leading to the substitution of lysine for glutamine p.Q455K was identified in *COL8A2*. The mutation was found to co-segregate with the disease phenotype in 12 affected family members (Biswas, Munier et al. 2001). Probands in this family, in addition to two other pedigrees harbouring the identical mutation, all developed clinical features of FECD at an early age.

Intriguingly, Biswas et al also identified the same mutation in 2 affected individuals from an additional family who had undergone penetrating keratoplasty for a presumed diagnosis of Posterior Polymorphous Corneal Dystrophy (PPCD2; OMIM 609140). On this basis the authors concluded that the same missense variant could cause both early-onset FECD and PPCD. PPCD is a rare corneal endothelial dystrophy that normally exhibits an autosomal dominant inheritance pattern. The severity and phenotype of this particular endothelial dystrophy is highly variable and can present as early as the first decade of life. The underlying pathophysiological process in PPCD is the transition of corneal endothelial cells to an epithelial-like cell state, due to dysregulation epithelial to mesenchymal (EMT) governing transcription factors) (Liskova, Dudakova et al. 2018). These abnormal endothelial cells abnormally proliferate and multi-layer. Consequently, they are not able to deturgesce the cornea thus resulting in corneal oedema in more severe cases. Clinically the condition presents as an irregular posterior corneal surface and occasional opacities of variable size and shape clinically described as bands or geographic or vesicular lesions.

Two further robustly verified disease-associated *COL8A2* mutations have since been reported to co-segregate with autosomal dominant endothelial disease; c.1349T>G, p.(L450W) (Gottsch, Sundin et al. 2005, Liskova, Prescott et al. 2007, Eghrari, Riazuddin et al. 2016) and c.1370-1371CA>GT, p.(Q455V) (Mok, Kim et al. 2009). The p.Q450V, was identified by *Gottsch et al.* (Gottsch, Sundin et al. 2005) in 21 cases of FECD and one patient with PPCD. In the FECD cohort, the disease presented with an early-

onset and exhibited a unique phenotype. In contrast to late-onset FECD, patients with this mutation exhibited a fine, patchy distribution of guttata. On confocal specular microscopy, the guttata were mildly elevated and occurred within the endothelial cell body, as opposed to the more typical appearance of guttata at the endothelial cell junction. Descemet's membrane in these subjects did not demonstrate posterior excrescences characteristic of FECD, but showed 'buried' guttata that were covered by excess amorphous material. A peripheral distribution of oedema was also reported with anterior microcystic corneal changes. This distinct clinical phenotype was subsequently reported to be predictive of the p.Q450V mutation in a patient with no known family history of FECD (Eghrari, Riazuddin et al. 2016). Penetrating keratoplasty histology specimens demonstrated that DM from these patients was thicker than both control tissue and late-onset FECD. Descemet's membrane from these cases did not demonstrate posterior excrescences characteristic of FECD. It was hypothesized that guttata visualized on slit lamp examination of these patients occurred as a result of distortion of light passing through thickened DM (Gottsche, Zhang et al. 2005). Liskova *et al.* also reported a similar phenotype of atypical guttata central to the endothelial cell and the absence of DM excrescences on histology in a British family with the p.Q450W mutation (Liskova, Prescott et al. 2007). Of interest, one 10 year old patient with the p.Q450W mutation was noted on confocal microscopy by *Gottsche et al.* to exhibit an atypical phenotype which showed mulberry like focal excrescences across multiple corneal endothelial cells, a phenotype more characteristic of PPCD (Babu and Murthy 2007).

In 2009, *Mok et al.* observed the p.Q455V in the Korean FECD population and reported early-onset FECD patients identified to have the glutamine substitution of valine were observed to have a fine distribution of guttata in contrast to the late onset FECD (Mok, Kim et al. 2009).

In this section, I describe two patients with early-onset FECD who are positive for the p.Q455K mutation in *COL8A2*. I aim to describe the clinical phenotype of this mutation and to differentiate the features of this disease from late-onset FECD and PPCD.



### 3.3.1.1.2 Genotyping of COL8A2

Analysis of the genes already known to be associated with FECD in the CTG18.1 ExpNeg cohort identified a heterozygous missense variant, c.1363C>A, p.Q455K within the COL8A2 in two subjects:

- Proband COL-A
- Proband COL-B

The variant was not present in any of the control datasets. The two unrelated probands were identified to harbour the same heterozygous COL8A2 missense mutation, c.1363C>A, p.Q455K previously reported by Biswas et al (Biswas, Munier et al. 2001) (Figure 1).

#### a. In Silico Pathogenicity and conservation Assessments

The SIFT score was 0.35 which indicated that it was possible that the point substitution was deleterious to the protein function. The Polyphen2 predicted the variant to be tolerated with a score of 0.346.

Multiple Sequencing Alignment was performed and showed that the conservation of the amino acid glutamine at p.Q455 was highly conserved across 9 orthologues (Figure 3).

<i>Homo sapiens</i>	PGVAGALGQK	GDLGLPGQPG	LRGPSGIPGL	QGPAGPIGPQ	GLPGLKGEPG
<i>Pan troglodytes</i>	PGVAGALGQK	GDLGLPGQPG	LRGPSGIPGL	QGPAGPIGPQ	GLPGLKGEPG
<i>Pongo abelii</i>	PGVAGALGQK	GDLGLPGQPG	LRGPSGIPGL	QGPAGPIGPQ	GLPGLKGEPG
<i>Mus musculus</i>	PGVAGALGQK	GDLGLPGQPG	LRGPSGIPGL	QGPAGPIGPQ	GLPGLKGEPG
<i>Canis familiaris</i>	PGVAGALGQK	GDLGLPGQPG	LRGPSGIPGL	QGPAGPIGPQ	GLPGLKGEPG
<i>Sus scrofa</i>	PGVAGALGQK	GDLGLPGQPG	LRGPSGIPGL	QGPAGPIGPQ	GLPGLKGEPG
<i>Oryctolagus cuniculus</i>	PGVAGALGQK	GDLGLPGQPG	LRGPSGIPGL	QGPAGPIGPQ	GLPGLKGEPG
<i>Mesocricetus auratus</i>	PGVAGALGQK	GDLGLPGQPG	LRGPSGIPGL	QGPAGPIGPQ	GLPGLKGEPG
<i>Tursiops truncatus</i>	PGVAGALGQK	GDLGLPGQPG	LRGPSGIPGL	QGPTGPIGPQ	GLPGLKGEPG
<i>Ficedula albicollis</i>	PGLTGGPGPK	GDGGIPGQPG	LRGPSGIR--	-----	----LKGEPG

Figure 3: Multiple Sequencing Alignment showing conservation of amino acid residue p.Q455 COL8A2 across orthologues. The amino acid residue Q (Glutamine) is well conserved across 9 orthologues. The altered amino acid residue in c.1363C>A, p.Q455K is highlighted in red.

b. Molecular modelling

A three dimensional homology model of the Collagen VIII heterotrimer was developed on the basis of structural similarity to the published FLJ00201 protein (<https://www.ncbi.nlm.nih.gov/protein/BAB84955.2>). The model was built from the PDB “4auo-collagen” structure using the PHYRE2 software (Kelley and Sternberg,2009). The p.Q455K variant of the COL8A2 protein is predicted to cause a structural change in the trimer surface (Figure 4). The outward facing configuration of the structural abnormality is anticipated to disrupt the interaction with other collagen fibrils rather than affect the organisation of the trimer itself. The figure was drawn USING MacPymol.

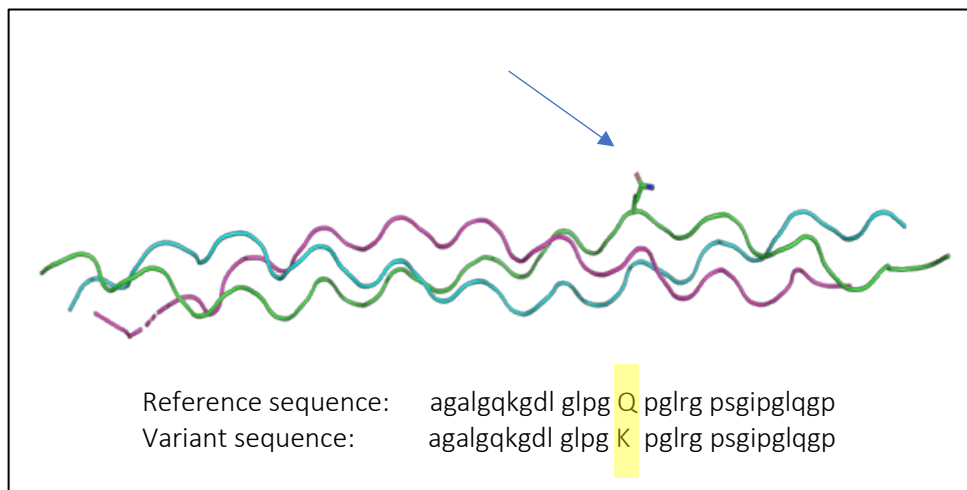


Figure 4: Molecular model of Collagen VIII mutant. A three-dimensional homology model of the Collagen VIII heterotrimer was model was built from the PDB “4auo-collagen” structure using the PHYRE2 software (Kelley and Sternberg,2009) and the figure was drawn using MacPymol software. The pink strand shown here represents the COL8A1 protein while the green and blue structures are two COL8A2 strands. The p.Q455K variant of the COL8A2 protein is predicted to cause a structural change in the trimer surface (highlighted by arrow).

### 3.3.1.1.3 Phenotypic Characteristics of two *COL8A2* Probands

Proband COL-A is a 51-year-old Caucasian female referred to Moorfields Eye Hospital at the age of 51 years for management of post penetrating keratoplasty astigmatism in her left eye. Corneal transplant surgery was performed at the age of 30 years for corneal decompensation secondary to Fuchs Endothelial Corneal Dystrophy (FECD). The initial diagnosis of FECD was made at the age of 20 years when the patient first began to see halos of light and noted blurring of vision in the left eye. The patient reported that the unoperated right eye developed similar visual symptoms in her mid-forties. The right eye was noted to have confluent central guttae but no oedema on slitlamp examination. The endothelial cell count in the right eye was 1600/mm<sup>2</sup> and the central corneal thickness was within normal limits at 552 µm. The left corneal graft was found to have a reduced endothelial cell count of 898/mm<sup>2</sup> but maintained a central corneal thickness of 546 µm.

At the time of presentation, the patient's best unaided Snellen visual acuity in the right eye was 6/9 and the left eye was 1/60 unaided. The vision in both eyes improved with refractive correction to 6/4 in the right eye (glasses) and 6/9 in the left eye (contact lens). Proband COL-A reported a positive family history as both her father (III:3) and paternal first cousin (IV:1) have been diagnosed with FECD. On optician review, her two sons aged 35 years (V:1) and 25 years (V:2) did not have signs of FECD and remained asymptomatic. Her paternal great grandmother (I:2) is also known to have lost her vision in both eyes at a young age but the underlying diagnosis is not known. Unfortunately, DNA from these individuals was not available for testing, however her unaffected mother was determined to be wildtype for the allele (Figure 5).

Proband COL-B is a 25-year-old Caucasian male of Polish decent who was referred to Moorfields Eye Hospital by his optician due to bilateral reduced vision secondary to FECD. The patient complained primarily of diplopia which was noted to be in worse in the daytime. The unaided Snellen visual acuity in the right eye was 6/36 improving to 6/24 with pinhole and 6/18 with no improvement on pinhole in the left eye. The right eye was known to be amblyopic. On slitlamp examination he was noted to have bilateral confluent granular changes across the posterior corneal surface. Confocal microscopy demonstrated guttata with polymegathism and polymorphism of the endothelial cells (Figure 8C). The right central corneal thickness was 705 µm and the endothelial cell count was 1221/mm<sup>2</sup>. The left eye was less severely affected with a central corneal thickness of 609µm and an endothelial cell count of 1249/mm<sup>2</sup>. It was interesting to note that in both eye endothelial dysfunction resulting in oedema

occurred despite maintaining a relatively high endothelial cell count. Following bilateral Descemet membrane endothelial keratoplasties (DMEK) the BCVA improved to 6/6 right eye and 6/6 left eye.

Proband Col-B's mother (individual I:1, 3X) developed bilateral corneal decompensation at the age of 24 years but had declined surgery. At 44 years of age her acuity was counting fingers in both eyes. DNA from other family members, including the affected mother, was not available to allow genotyping (Figure 6).

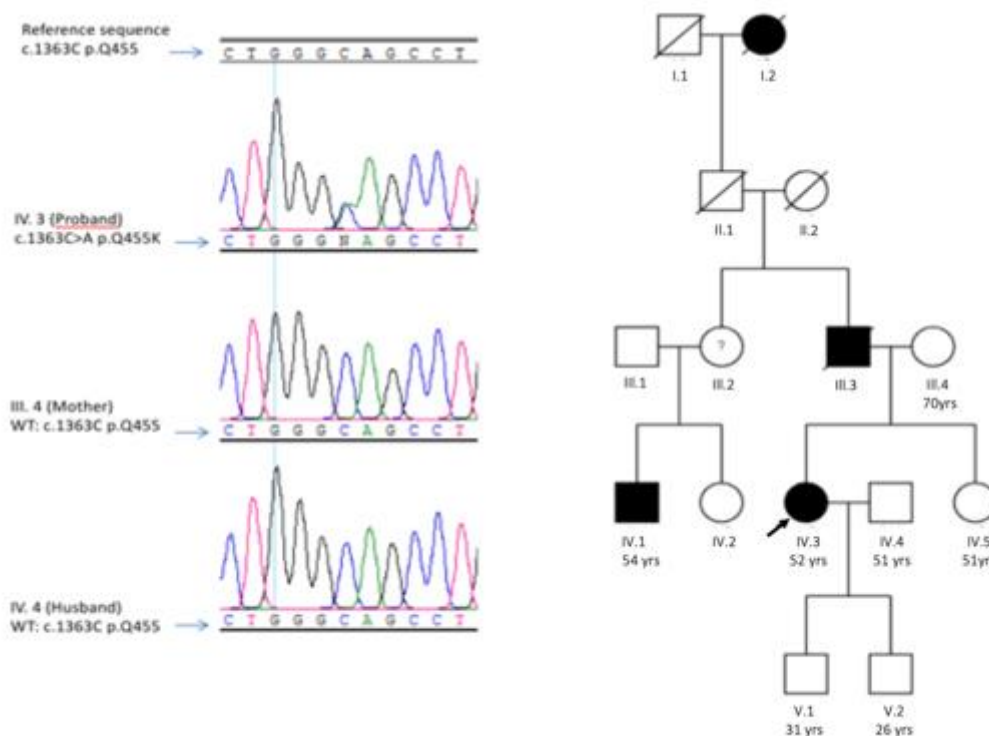


Figure 5: Pedigree of Proband COL-A (IV.3), a 51 year old Caucasian female who is heterozygous for the p.Q455K missense variant. The subject's father (III.3) and first cousin (IV.1) were also known to have developed corneal endothelial decompensation necessitating keratoplasty. The probands mother (III.4) and husband (IV.4) were both wild type for the mutation and did not exhibit features of corneal pathology. It was not possible to obtain blood samples from relatives of the proband.

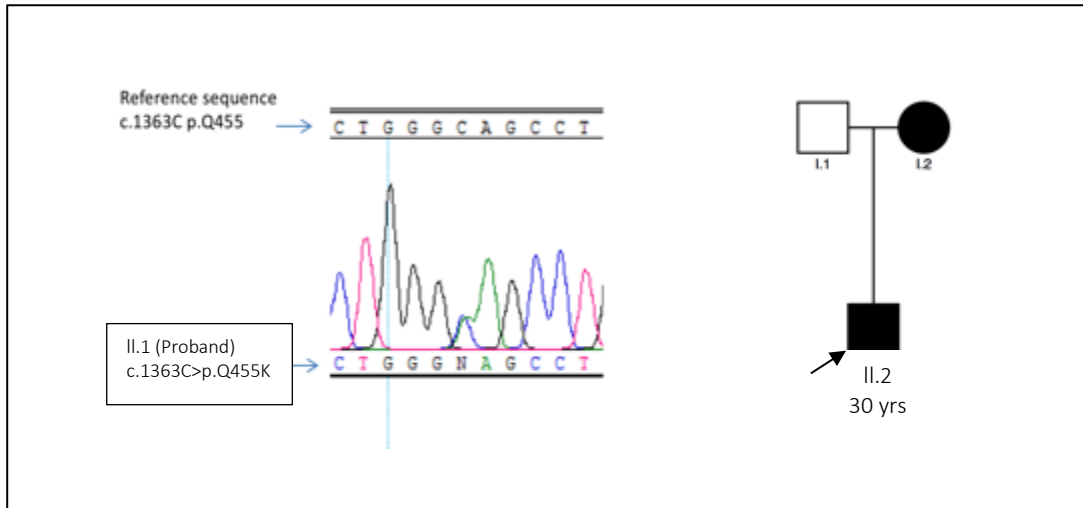


Figure 6: Pedigree of Proband COL-B (II.2), a 25 year old Caucasian male who is heterozygous for the p.Q455K missense variant. The subject's mother (I.2) was also known to have developed corneal endothelial decompensation in her twenties but declined the option of surgical intervention. It was not possible to obtain blood samples from relatives of the proband.

#### 3.3.1.1.4 Corneal Imaging and Histopathology

Slitlamp images of the Proband COL-A's right, unoperated eye revealed mild corneal haze with no associated stromal oedema to suggest endothelial decompensation. Retro-illumination imaging of the same eye demonstrated fine granular changes in Descemet's membrane that extended to the peripheral cornea. (Figure 7A). These changes can be observed more clearly on magnification of the peripheral cornea (Figure 7B).

Specular microscopy of Proband COL-A's right eye showed that in addition to generalised pleomorphism and polymegathism of the endothelial cells, fine low elevation guttata were found occurring central to the endothelial cell (Figure 8A).

Slitlamp and specular images were not available for Proband B. However, previously unpublished specular microscopy images of a 32 year old male reported by Liskova *et al.* be heterozygous for missense variant, c.1363C>A, p.Q455K demonstrate a similar pattern of elevation occurring central to the endothelial cell (Liskova, Prescott et al. 2007) (Figure 8B).

Confocal images for Proband COL-B confirmed the generalised pleomorphism and polymegathism of the endothelial cells. The cornea was also noted to show an atypical appearance of areas of hypo-reflectivity associated with occasional central hyper-reflectivity at the apical border of the endothelial cells (Figure 8C). The areas of hyper reflectivity could represent guttata buried within Descemet's membrane.

Histopathology was available for corneal samples obtained at the time of corneal transplant surgery from Proband B. Haematoxylin and eosin staining of these specimens showed bilateral nonspecific endothelial cell loss. The Descemet's membrane was not found to be thickened and there was a notable absence of guttata (Figure 9).

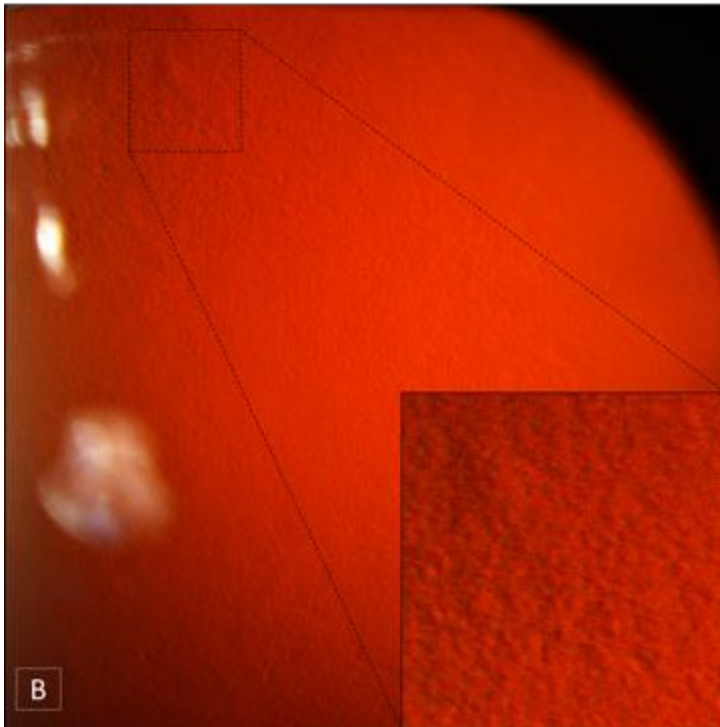
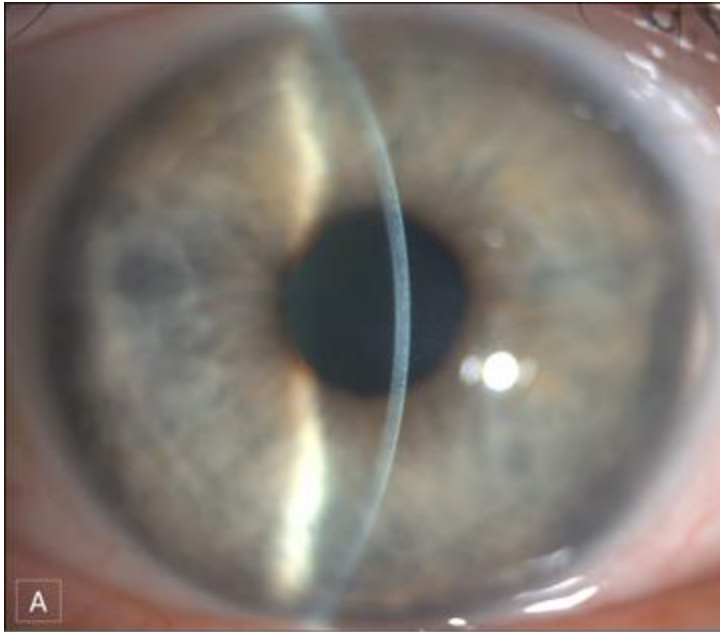


Figure 7: Slitlamp images of Proband A's unoperated right eye .

(A) Slit lamp image of Proband COL-A (51-year-old female) shows mild corneal haze with no stromal oedema to suggest endothelial decompensation. The subject does not report symptoms of diurnal variation in her vision.

(B) Retroillumination image of Proband COL-A demonstrates fine granular changes in Descemet's membrane that extend to the peripheral cornea. The inset image is a magnification of the fine, confluent changes observed in the DM

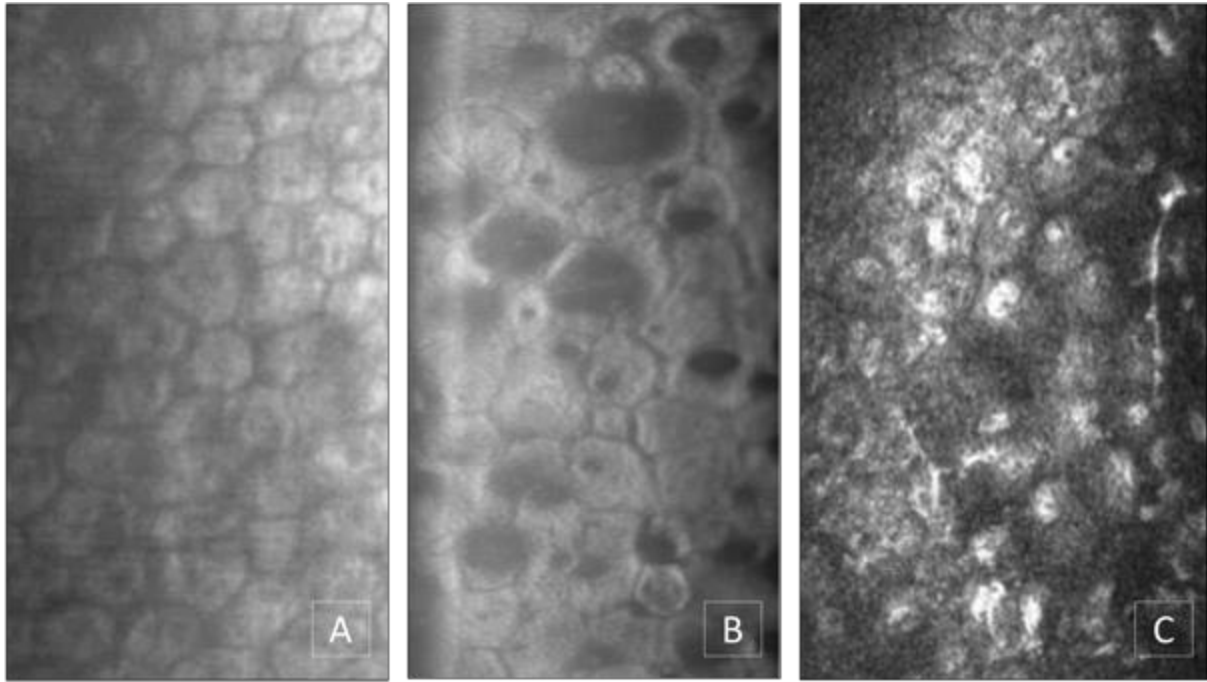


Figure 8: Corneal endothelial cell imaging of three subjects harbouring mutations in *COL8A2*.

(A) Specular microscopy image of Proband COL-A showing fine low elevation guttata occurring central to the endothelial cell. The patient harbours the heterozygous p.Q455K missense variant. She remains asymptomatic in this eye and there is no corneal oedema. The endothelial cell count in the right eye was 1600/mm<sup>2</sup> and the central corneal thickness was within normal limits at 552 µm

(B) Specular microscopy of the left eye of a 32 year old male subject heterozygous for the p.Q455V missense variant. The previously unpublished image is courtesy of Dr Petra Liskova shows large, guttata occurring central to the endothelial cell in the presence of significant endothelial polymegathism and polymorphism.

(C) In vivo confocal microscopy (IVCM) of Proband COL-B harbouring the heterozygous p.Q455K missense variant shows findings revealed generalised pleomorphism and polymegathism of the endothelial cells an atypical appearance of areas of hypo-reflectivity associated with occasional central hyper-reflectivity at the apex of the endothelial cells. The areas of hyper-reflectivity may correspond to buried guttata within Descemet's membrane



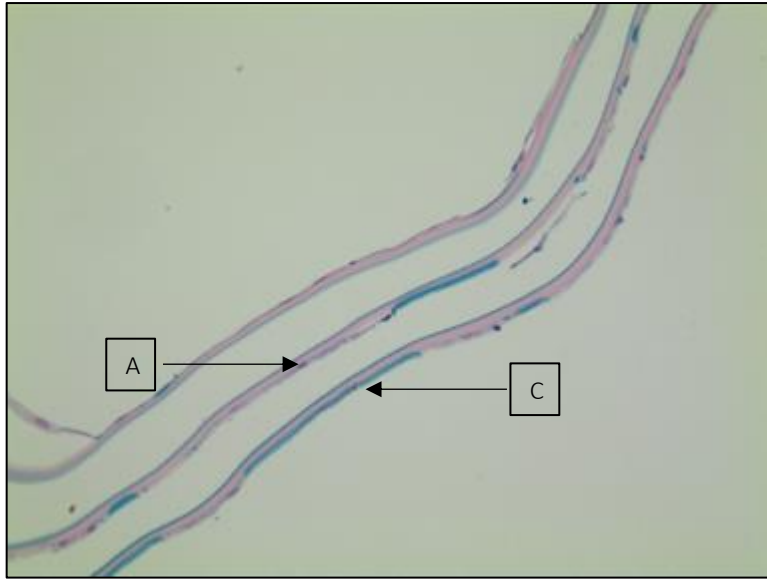


Figure 9: Magnified image of histology specimen obtained from Proband COL-B. The image shows a cross sectional view of a folded sheet of Descemet's membrane devoid of stroma.

A) Descemet's membrane was not noted to be thickened on this sample but no exophytic guttata were visualised on the posterior surface

C) Endothelial cells are noted to be present on the posterior surface but the cell population is found to be depleted.

### 3.3.1.1.5 Discussion

Here clinical features of two individuals with endothelial disease associated with a heterozygous missense mutation c.1363C>A, p.Q455K in the *COL8A2* gene, have been identified within the CTG18.1 ExpNeg cohort. Both probands described in this section, as well as their affected relatives, first developed visual symptoms in their early twenties. This relatively early-onset of disease compared to CTG18.1 repeat ExpPos FECD is a consistent feature in the majority of published individuals harbouring *COL8A2* mutations (Biswas, Munier et al. 2001, Gottsch, Sundin et al. 2005, Mok, Kim et al. 2009). The corneal changes are also reported to be markedly asymmetric, as was the case with proband B who maintained a Snellen visual acuity of 6/6 in one eye but required a penetrating keratoplasty in the contralateral eye 20 years previously (Magovern, Beauchamp et al. 1979, Liskova, Prescott et al. 2007).

Published findings of specular and confocal microscopy of patients carrying the *COL8A2* mutation identified areas with abnormal endothelial cell morphology with small refractile structures localizing within the boundaries of the endothelial cells (Gottsch, Zhang et al. 2005, Liskova, Prescott et al. 2007). In this study, specular images of Proband Col-A's right eye showed similar fine, low elevation refractile structures (presumed to be guttata) occurring central to the endothelial cell. One previous report also described large mulberry-like excrescences surrounded by small guttata in a patient with a p.L450W mutations in *COL8A2*.(Gottsch, Zhang et al. 2005). A survey of the specular images obtained in this study did not identify similar groupings of excrescences in our subjects

The confocal microscopy findings in late-onset FECD include areas of hyporeflectivity with an occasional central hyperreflective change (Chiou, Kaufman et al. 1999). *Gottsch et al.* reported that confocal specular microscopy detected single, low elevation guttata associated with individual cells in early-onset *COL8A2* disease as opposed to sharply raised guttae with high elevation and areas of coalescence in the late-onset FECD (Gottsch, Sundin et al. 2005). In *COL8A2*-associated dystrophy, the hyporeflective regions are comparatively fainter than seen in late-onset FECD and the hyperreflective lesions are positioned more eccentrically (Gottsch, Sundin et al. 2005). Confocal images from Proband COL-B demonstrated similar atypical areas of hyporeflectivity associated with the occasional finding of central hyper-reflectivity at the apex the endothelial cells. These appearances are similar to the 'epithelioid' cells reported in both irido-corneal endothelial syndrome (ICE) and posterior polymorphous corneal dystrophy (PPCD) (Chiou, Kaufman et al. 1999, Anderson, Badawi et al. 2001). It should be noted that neither vesicular nor band-like structures commonly associated with PPCD were observed in either of the patients in this study.

Three dimensional homology modelling of the Collagen VIII was performed and predicted that the mutation would lead to a structural change on the surface of the protein. The point mutation leads to an outward facing configuration of the structural abnormality which is anticipated to disrupt the interaction with other collagen fibrils rather than affect the organisation of the trimer itself. Type VIII collagen is a non-fibrillar short chain collagen molecule that is a heterodimer formed of  $\alpha 1(\text{VIII})$  and  $\alpha 2(\text{VIII})$  polypeptide subunits that are encoded by the *COL8A1* and *COL8A2* genes (Muragaki, Jacenko et al. 1991, Muragaki, Mattei et al. 1991, Ricard-Blum 2011). A change in the interaction between this major extracellular matrix component of endothelial basement membranes could feasibly alter both the structural and functional relationship between Descemet's membrane and the corneal endothelial cell layer thus resulting in the abnormal appearance of buried guttata occurring central to the endothelial cell (Muragaki, Mattei et al. 1991, Biswas, Munier et al. 2001).

On histology, previous studies have noted that Descemet membrane from individuals with *COL8A2*-associated disease is thicker than normal (Magovern, Beauchamp et al. 1979, Biswas, Munier et al. 2001, Gottsch, Zhang et al. 2005, Liskova, Prescott et al. 2007). Over time a fibrillar layer appears on the on the posterior aspect of Descemet's membrane and the shallow guttata are buried and appear as refractile bodies within Descemet's membrane (Zhang, Bell et al. 2006). Consistent with these previous reports, there was no histological evidence of elevated guttata on the two samples from Proband COL-B (Figure 9). Biswas *et al.* reported two patients with the p.Q455K mutation who had endothelial cell multilayering, intercellular desmosome attachments and surface cells with short microvilli consistent with epithelial-like metaplasia (Biswas, Munier et al. 2001). This led to a diagnosis of PPCD in the family, although these features have not been reported in other papers. It was noted that histological assessment of DM from Proband COL-B showed that it was not thickened. One reason for this could be the difference in surgical technique used to obtain the sample at the time of Descemet's membrane endothelial keratoplasty (DMEK). Published histological findings on *COL8A2* tissue have been performed on penetrating keratoplasty samples that allow imaging and staining of full thickness corneal samples. DMEK surgery employs a scoring and scraping technique to peel the membrane off the posterior aspect of the cornea. It is therefore possible that sheering of the layers could have occurred and that the sample does not consist of the complete Descemet's membrane. Eghrari *et al.* reported that Descemet's membrane was removed in strips when performing endothelial keratoplasty on a proband carrying the p.L450W mutation, and although histology confirmed an absence of guttata the DM thickness was not commented upon (Eghrari, Riazuddin et al. 2016).

In this thesis, I describe the occurrence of the heterozygous p.Q455K mutation in two unrelated probands affected by primary endothelial disease and provide a comprehensive summary of published *COL8A2*-associated phenotypes. Both subjects in this study displayed an early-onset of the corneal disease associated with an atypical corneal phenotype of guttata buried within Descemet's membrane. Characterisation of the clinical phenotype and a review of the previously published cases (Table 1), supports the hypothesis that mutations in *COL8A2* are associated with an early-onset primary endothelial dystrophy that is clinically distinct from both FECD and PPCD (Aldave, Han et al. 2013, Eghrari, Riazuddin et al. 2016).

The results reported here add support for the classification of the *COL8A2*-associated corneal dystrophy as a clinical entity distinct from both FECD and PPCD. Although corneal oedema secondary to endothelial dysfunction is the final common pathology for all primary corneal endothelial dystrophies, there are significant differences in disease severity and genetically distinct forms. Patients with *COL8A2* mutations represent a rare subgroup with an early-onset phenotype. Ongoing genomic investigations are anticipated to further define other genetically distinct and rare forms of corneal endothelial disease.

Study	COL8A2 Mutation	Subjects	Clinical examination	Histological Features	Confocal / Non-contact Specular Imaging
MaGovern <i>et al.</i> , 1979	c.1349T>G p.L450W	19 affected family members across three generations	Clinical data available for 20 eyes of 10 subjects (5 male, 5 Female). <ul style="list-style-type: none"> <li>Endothelial described as patchy, tightly packed and essentially central. DM described as irregularly thickened and of subtly silvery quality.</li> <li>9 cases described as bilateral. One case of unilateral disease necessitating corneal transplant surgery reported in a 28 year old female.</li> <li>In total 4 subjects underwent corneal transplant surgery.</li> </ul>	4 corneal specimens (3 full thickness, 1 full thickness corneal rim): <ul style="list-style-type: none"> <li>DM uniformly thickened with disrupted, pigment laden endothelial cells</li> <li>Deep to the endothelial cells lies a row of poorly formed, fine guttata like structures.</li> <li>Poorly differentiated guttata are covered by a filamentous basement membrane.</li> <li>"Invader cells" were noted to intrude between epithelium and Bowman's membrane</li> <li>Warts on thickened DM.</li> </ul>	Nil
Gottsch <i>et al.</i> , 2005	c.1349T>G p.L450W	Detailed genotyping of family	Fine, patchy distribution of guttae in contrast to patients with late-onset Fuchs endothelial corneal dystrophy	3 full thickness corneas: <ul style="list-style-type: none"> <li>All three demonstrated thicker than normal DM.</li> <li>Early stage specimen: shallow guttata visible.</li> <li>More advanced specimen: Thickened DM. Fibrous refractile bodies within DM. Posterior aspect devoid of guttata</li> <li>Severe disease specimen: Thickest DM of the three specimens. DM had pronounced posterior and interstitial laminations</li> </ul>	Confocal microscopy: Endothelial cells were associated with a single, low-elevation guttata, a pattern of high density that alternated with large areas devoid of guttae.
Gottsch <i>et al.</i> , 2005		previously reported	Corneal oedema noted in an early subepithelial, peripheral distribution in an affected 1.1-year-old male subject identified from the multigenerational family.		
Zhang <i>et al.</i> , 2006		Magovern <i>et al.</i> , 1979	Unrelated subject followed up from age 38 years for a decade showed progression from mild subepithelial and anterior stromal microcystic oedema to diffuse corneal oedema with peripheral bullae.		
Eghrari <i>et al.</i> , 2016		Clinical details of 1 unrelated 40 year old male in whom distinct clinical appearance was predictive of COL8A2 mutation			
Liskova <i>et al.</i> , 2007	c.1349T>G p.L450W	4 patients from 1 pedigree	Age of diagnosis 18 to 53 years. Slitlamp biomicroscopy findings described as similar to MaGovern <i>et al.</i>	Thickened DM without classic corneal guttata	No-contact specular microscopy shows endothelial pleomorphism and

		across three generations				corneal guttata in 55 year old asymptomatic subject
Biswas <i>et al.</i> 2001	c.1363C>A, p.Q455K	Pedigree 1: 12 affected subjects. Autosomal dominant inheritance pattern	Subjects diagnosed between age 21 – 48 years. Two subjects in the 3 <sup>rd</sup> decade described as to have grouped central corneal guttata. 5 of the 12 patients underwent keratoplasty	2 full thickness corneas from presumed PPCD: <ul style="list-style-type: none"> <li>Posterior collagenous layer (PCL) between the endothelium and a thickened DM1. The PCL was organized into a hexagonal matrix resembling that normally formed by type VIII collagen.</li> <li>Endothelial cell multilayering with desmosomal intercellular attachments and surface cells with short microvilli consistent with epithelial-like metaplasia of the endothelial cells.</li> </ul>	Confocal micrograph: guttae with morphology strikingly similar to those reported in the L450W-COL8A2 Gottsch et al 2005 Non-contact specular microscopy showed endothelial polymorphism and cornea guttata located both centrally and within the borders of endothelial cells	
		Pedigree 2: 20 affected subjects. Autosomal dominant inheritance pattern.	6 subjects diagnosed between 3 <sup>rd</sup> and 5 <sup>th</sup> decade 2 patients reported to have undergone keratoplasty in 3 <sup>rd</sup> and 6 <sup>th</sup> decade respectively. No phenotype data			
		Pedigree three: 2 patients described as PPCD	Bilateral grafts in 3 <sup>rd</sup> and 6 <sup>th</sup> decade respectively No phenotype data			
Mok <i>et al.</i> 2009	c.1370-1371CA>GT p.Q455V	12 patients from 6 pedigrees 2 unrelated FECD patients	Age of diagnosis 21-40 years All 14 patients revealed a fine distribution of guttata in contrast to patients with late onset FECD	Nil	Nil	Nil

Table 2: A summary of published phenotypic characteristics of subjects identified as harbouring disease-associated heterozygous missense variants within the *COL8A2* gene.

### 3.3.1.2 COL8A1

#### 3.3.1.2.1 Background

Having established that disease-associated variants in the *COL8A2* gene lead to a distinctive early-onset FECD phenotype, the *COL8A1* gene also represents an attractive potential candidate gene for patients with similar phenotypic presentations, given that both encode polypeptides that function as a heterodimer.

Knock-out mouse models of both the *Col8a1* and *Col8a2* genes have been shown to develop ocular anterior segment dysgenesis with no other major systemic abnormalities. In these animal models, the phenotype manifested as bilateral protruding, globoid corneas resembling keratoglobus. When frozen sections of the abnormal corneas were obtained, transmission electron microscopy revealed exceedingly thin Descemet's membrane, with an absence of the anterior banded layer that should have formed in-utero. Although the finding of thin DM is not in keeping with classic FECD, the immunohistochemical assessment confirmed more typical endothelial cell polymegathism and polymorphism (Hopfer, Fukai et al. 2005).

To date, only one study by Aldave *et al.* has investigated the possible association between *COL8A1* and *COL8A2* mutations with familial late-onset FECD (Aldave, Rayner et al. 2006). Although this study was not able to confirm any associations between mutations in *COL8A1* and FECD, the gene was not screened in early-onset FECD cohort. It would stand to reason that as the disease phenotype of the *COL8A2* mutations manifested in early life, variants in the *COL8A1* may be found within the early-onset subset of FECD.

### 3.3.1.2.2 Genotyping

A single unique non-synonymous variant, c.619A>T, p.I207F was identified in the *COL8A1* gene in proband COL-C.

#### a. In Silico Pathogenicity and conservation Assessments

The SIFT score was 0.1 which indicated that the point substitution was deleterious to the protein function. The Polyphen2 also predicted the variant was deleterious with a score of 0.9701.

Multiple Sequencing Alignment was performed and showed that the conservation of the amino acid alanine at p.I207 was highly conserved across 9 orthologues (Figure 10).

<i>Homo sapiens</i>	IGQKGEIGPM	GIPGPQGPPG	PHGLPGIGKP	GGPGLPGQPG	PKGDRGPKGL
<i>Pan troglodytes</i>	IGQKGEIGPM	GIPGPQGPPG	PHGLPGIGKP	GGPGLPGQPG	PKGDRGPKGL
<i>Pongo abelii</i>	IGQKGEIGPM	GIPGPQGPPG	PHGLPGIGKP	GGPGLPGQPG	PKGDRGPKGL
<i>Mus musculus</i>	IGPKGEIGPM	GIPGPQGPPG	PHGLPGIGKP	GGPGLPGQPG	AKGERGPKGP
<i>Canis familiaris</i>	IGPKGEIGPM	GIPGPQGPPG	PHGLPGIGKP	GGPGLPGQPG	AKGERGPKGP
<i>Sus scrofa</i>	IGPKGEIGPM	GIPGPQGPPG	PHGLPGIGKP	GGPGLPGQPG	AKGERGPKGP
<i>Oryctolagus cuniculus</i>	IGPKGEIGPM	GIPGPQGPPG	PHGLPGIGKP	GGPGLPGQPG	AKGDRGPKGP
<i>Mesocricetus auratus</i>	IGPKGEIGPM	GIPGPQGPPG	PHGLPGIGKP	GGPGLPGQPG	AKGERGPKGP
<i>Tursiops truncatus</i>	IGPKGEIGPM	GIPGPQGPP-	PHGLPGIGKP	G-PGLSG-PG	AKGERGPKGL
<i>Ficedula albicollis</i>	MGPKGEIGPM	GIPGPQGPPG	PHGLPGIGKA	GAPGLQGQPG	PKGEFGMKGP

Figure 10: Multiple Sequencing Alignment showing conservation of amino acid residue p.I207 *COL8A1* across orthologues. The amino acid residue I (Isoleucine) is well conserved across 9 orthologues. The altered amino acid residue in c.619A>T, p.I207F is highlighted in red.

#### b. Familial Segregation Analysis

Segregation analysis of the heterozygous c.619A>T, p.I207F *COL8A1* variant in proband COL-C showed that the variant did not segregate with the disease phenotype in the family. Both proband COL-C's affected siblings were shown to be wild type as was his affected father. The probands un-affected mother was shown to carry the same *COL8A1* heterozygous variant as the proband (Figure 2). The variant is therefore shown not to be the disease-causing mutation in this family pedigree.



### 3.3.1.2.3 Phenotyping

Proband COL-C is a Caucasian male subject diagnosed with early-onset FECD at the age of 31 years. At the time of diagnosis, slitlamp biomicroscopy revealed significant central corneal oedema with a central corneal thickness of 723 $\mu\text{m}$  and vision of 6/24 Snellen in the right eye. The left eye exhibited milder corneal decompensation with a thickness of 597 $\mu\text{m}$  and Snellen Best Corrected Visual Acuity (BCVA) of 6/9.

The subject had not undergone any previous ocular surgery leading up to the corneal endothelial transplantation to the right eye at the age of 32 years. It was noted intraoperatively that the Descemet's membrane in the eye was thicker and more adherent than normal. Corneal transplantation was performed on the left eye 6 months later.

At the time of enrolment in the study, proband COL-C was aware that his father had also recently been diagnosed with a corneal disease in Italy. His father (Figure 11, I.1) was diagnosed with FECD and concomitant cataract at the age of 56 years. He reported symptoms of diurnal variation in vision from the age of 50 years. His vision at the time of assessment was Snellen BCVA of 6/24 in the right eye and 6/18 in the left eye. On examination, both corneas had developed signs of corneal decompensation with the right eye measuring a central corneal thickness of 602  $\mu\text{m}$  and 583  $\mu\text{m}$  on the left. The endothelial cell count in the right eye was 697/ $\text{mm}^2$  and 866/ $\text{mm}^2$  in the left eye. Bilaterally, the appearance of confluent guttata appeared to be located within a thickened Descemet's membrane rather than as posterior excrescences from the membrane (Figure 12, 3A and 3B).

The proband's younger sister (Figure 11, II.1) was 30 years old at the time of assessment and showed early signs of FECD in the form of fine granular, confluent corneal guttata but no signs of corneal oedema (Figure 12, 3C). The central corneal thickness in the right eye was 545 $\mu\text{m}$  and 551 $\mu\text{m}$  in the left eye. The BCVA in both eyes was 6/5. The confluent nature of guttata that extended across the posterior corneal surface led to difficulty in specular imaging and quantification of corneal endothelial cells.

The proband's 38-year-old sister (Figure 11, II.3) showed early signs of corneal change in the form of fine, granular guttata noted to be more prominent in the peripheral cornea (Figure 13, 4A). Guttata were not evenly spread across the corneal surface and were found to be more prominent along the peripheral and inferior cornea. Sections of the cornea were noted to maintain a normal appearance

both on specular and confocal microscopy as shown in Figure 13, 4B and 4C. The less diffuse pattern of guttata in Proband COL-C's older sister and father allowed quantification of endothelial cells on specular microscopy: 3182/mm<sup>2</sup> in the right eye and 3527 /mm<sup>2</sup> in the left. Central corneal thickness in the right eye was 549µm and 559µm in the left eye.

The proband's 52-year-old mother and 38-year-old sister showed no signs of corneal disease on slitlamp examination and specular imaging.

#### 3.3.1.2.4 Corneal Imaging and Histology

##### a. Histology

Histology specimens of Descemet's membrane were obtained from Proband COL-C at the time of Descemet's Membrane Endothelial keratoplasty. On Haematoxylin and Eosin staining, prominent exophytic guttata were noted at the junction of endothelial cells (Figure 15). Although endothelial cells were present, the cell population was noted to be depleted. In addition, scattered lymphocytes were present on the posterior surface suggestive of a reactive inflammatory phenomenon of the endothelial layer. Subsequent reference lab PCR testing was found to be negative for Herpes simplex virus, Varicella Zoster Virus and Cytomegalovirus.

##### b. Confocal Imaging

*In vivo* confocal microscopy (IVCM) of Proband COL-C's siblings and father shared similar characteristics of generalised pleomorphism and polymegathism of the endothelial cells (Figure 5). The finding of dark round hypo-reflective regions with occasional central white reflex found on IVCM were typical of corneal guttae. Within the areas of hypo-reflectivity, there were occasional central hyper-reflectivity at the apex of the cells which was a more atypical finding. Aside from the pleomorphic endothelial cells, occasional hyper-reflective inflammatory cells were seen, particularly in Proband COL-C's father (Figure 14 A).

### 3.3.1.2.5 Discussion

Although the *COL8A1* gene is a potentially promising candidate gene in early-onset FECD, the findings of this study do not support that the c.619A>T, p.I207F variant was causative of disease in this proband and affected family members. In terms of phenotypic characteristics, the clinical presentation of the disease in this family displayed a variable age of onset. Although the proband displayed an early onset of the disease, both his sisters have yet to manifest symptoms of corneal decompensation despite showing signs of fine, granular corneal guttata. Even between the two siblings, CT who is 8 years younger than DT shows more advanced signs of corneal disease. Although the proband's father was diagnosed in the 5<sup>th</sup> decade of life, it remains possible that signs of endothelial disease may have been visible at an earlier age.

It was also interesting to note that similar to the finding of "buried guttata" in *COL8A2* mutations, the proband's father displayed coarse guttata that appeared to be located within the thickened Descemet's membrane, rather than the more typical posterior excrescences of the Descemet's membrane (Zhang, Bell et al. 2006). Histology samples obtained from IT however did not mirror these findings, as the guttata were noted to be the more typical focal protuberances on the posterior surface of Descemet's membrane.

A notable finding on histological assessment of the proband's Descemet's membrane as well as on *in vivo* confocal microscopy of his younger sister's cornea, was the presence of inflammatory cells within Descemet's membrane. No episodes of ocular inflammation were recorded in Proband COL-C's clinical history and his sister showed no other signs of inflammation at the time of assessment. These findings are in keeping with previous reports of *in vivo* confocal microscopy studies that revealed even in early FECD, density of inflammatory cells were significantly increased within the stroma compared to both normal corneas and pseudophakic bullous keratopathy (Aggarwal, Cavalcanti et al. 2018). Immunohistochemical studies have also identified the serum amyloid A1 within the corneal stromal cells of FECD patients, supporting a role for chronic inflammation in this dystrophy. Gene expression studies have similarly shown a significant expression level of genes involved in helper T-cell activation, signalling and neuro inflammation in both CTG18.1 ExpPos and ExpNeg FECD (Chu, Hu et al. 2020). Although it is possible that the oxidative stress pathway involved in endothelial cell death and apoptosis could lead to a subclinical inflammatory reaction in FECD, further study is required to understand the mechanism of immune activation in this dystrophy (Jurkunas 2018).

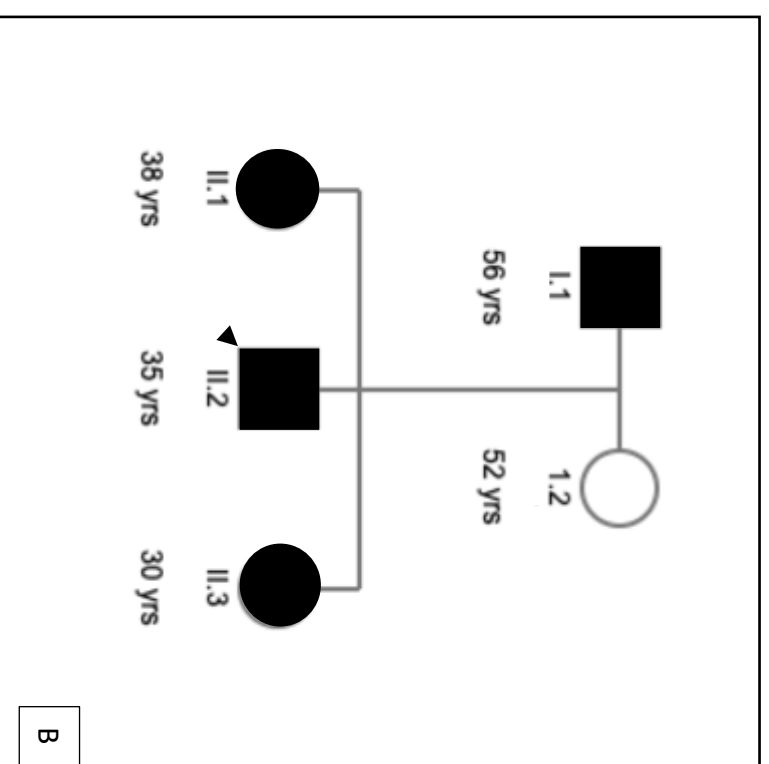
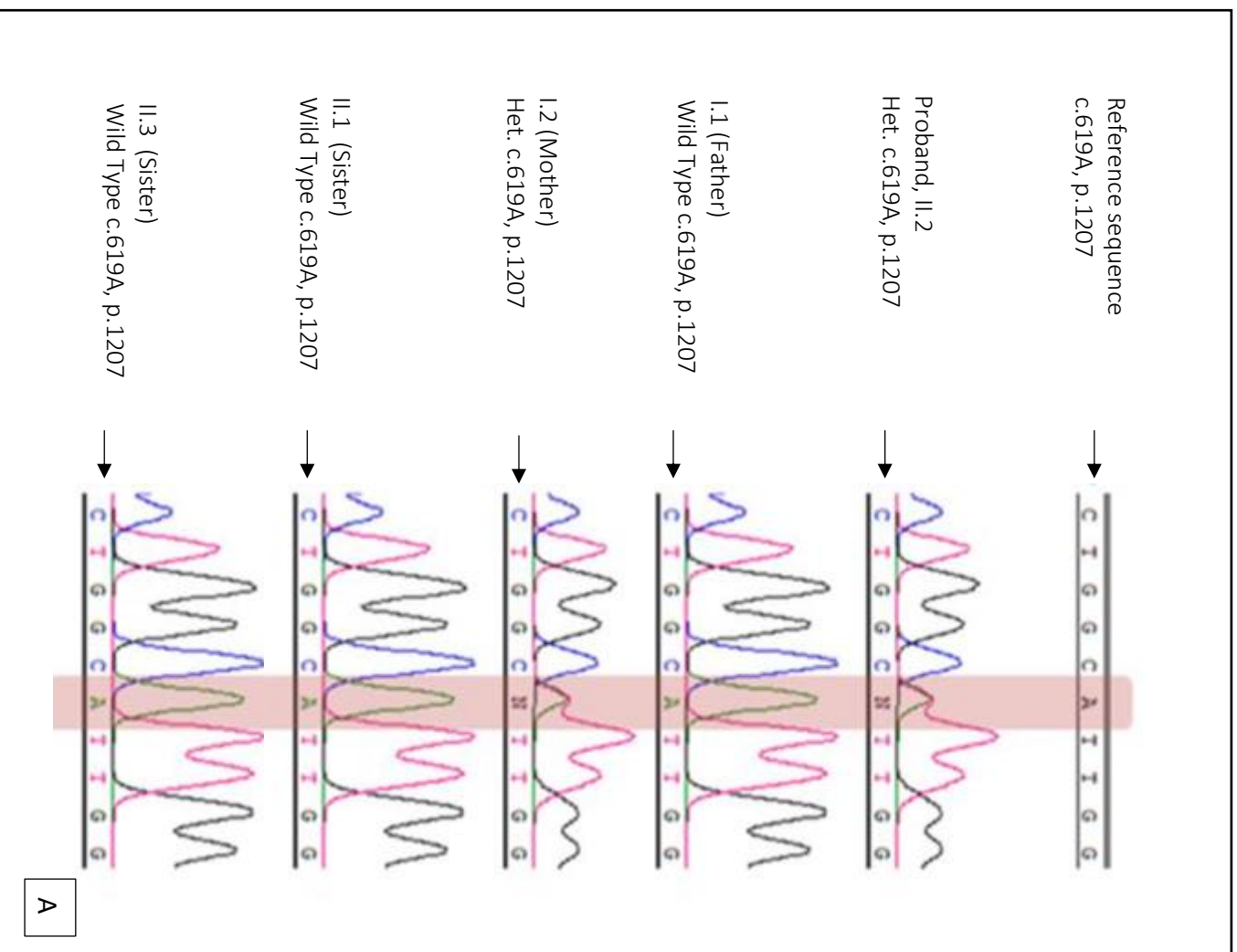


Figure 11: Familial Segregation of unique COL8A1 variant in Proband COL-C.

**A.** Sanger sequencing chromatogram (courtesy of Miss Amanda Sadan) confirms the presence of the heterozygous variant in proband COL-C and his unaffected mother while his affected father (I.1) and affected sisters (II.1, II.3) were found to be wildtype (the variant is highlighted in red).

**B.** The family pedigree for proband COL-C shows the affected father (I.1) and the affected sisters (II.1,II.3)

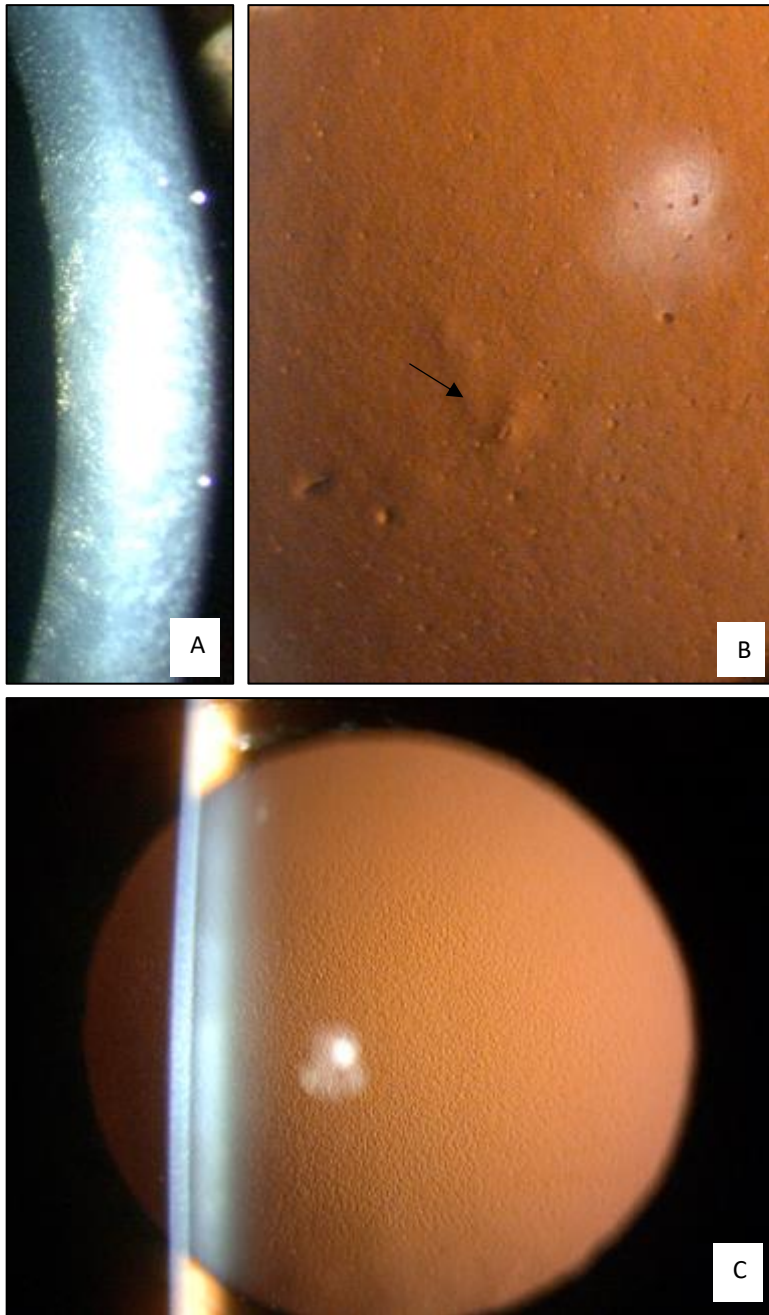


Figure 12: Slitlamp biomicroscopy images of first-degree relatives of proband COL-C affected by FECD.  
**(A)** Slit-beam illumination of Proband COL-C's 56-year-old father, shows stromal oedema, confluent guttata and thickened Descemet's membrane.  
**(B)** A magnified image on retroillumination of the proband's father's central cornea shows the atypical nature of the coarse guttata that appeared to be located within a thickened Descemet's membrane rather than as posterior excrescences.  
**(C)** A retroillumination slitlamp image of the proband's 30-year-old sister, who shows signs of fine, granular guttata distributed across the cornea in the absence of stromal oedema.

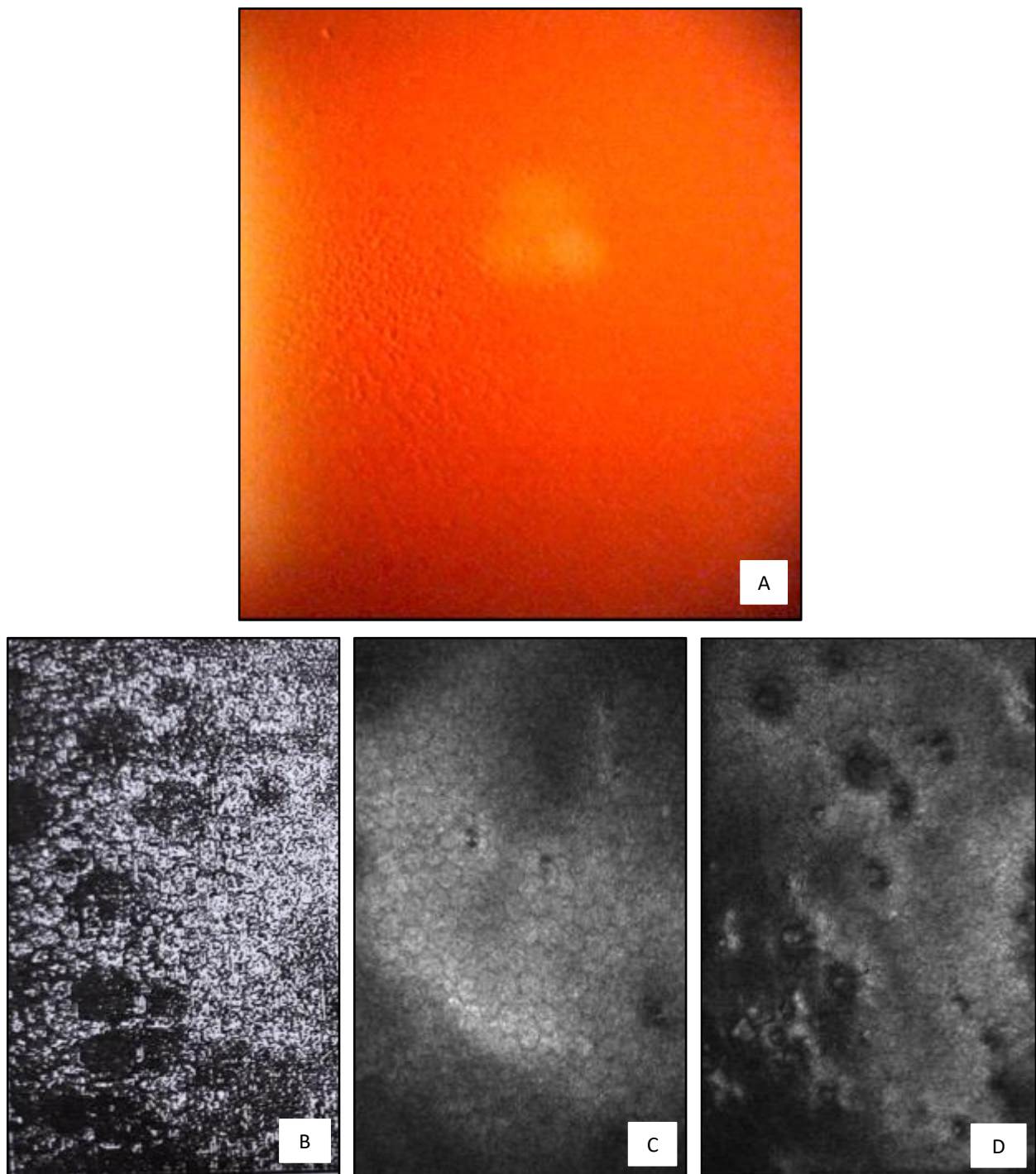


Figure 13: Imaging of Proband COL-C's 38-year-old sister

**(A)** Retroillumination of the cornea shows the appearance of guttata that were noted to be more prominent on the peripheral cornea compared to the central cornea.

**(B)** Specular microscopy imaging shows large well defined corneal guttata surrounded by endothelial cells that retain normal morphology and density. The endothelial cell count in this eye was maintained at 3182/mm<sup>2</sup>

**(C)** Confocal imaging confirms the normal appearance of endothelial cells with only a small number of small guttata visualised

**(D)** Confocal imaging of the peripheral cornea out width the central 4 mm shows the presence of larger more defined guttata in the presence of normal endothelial cell structure and density

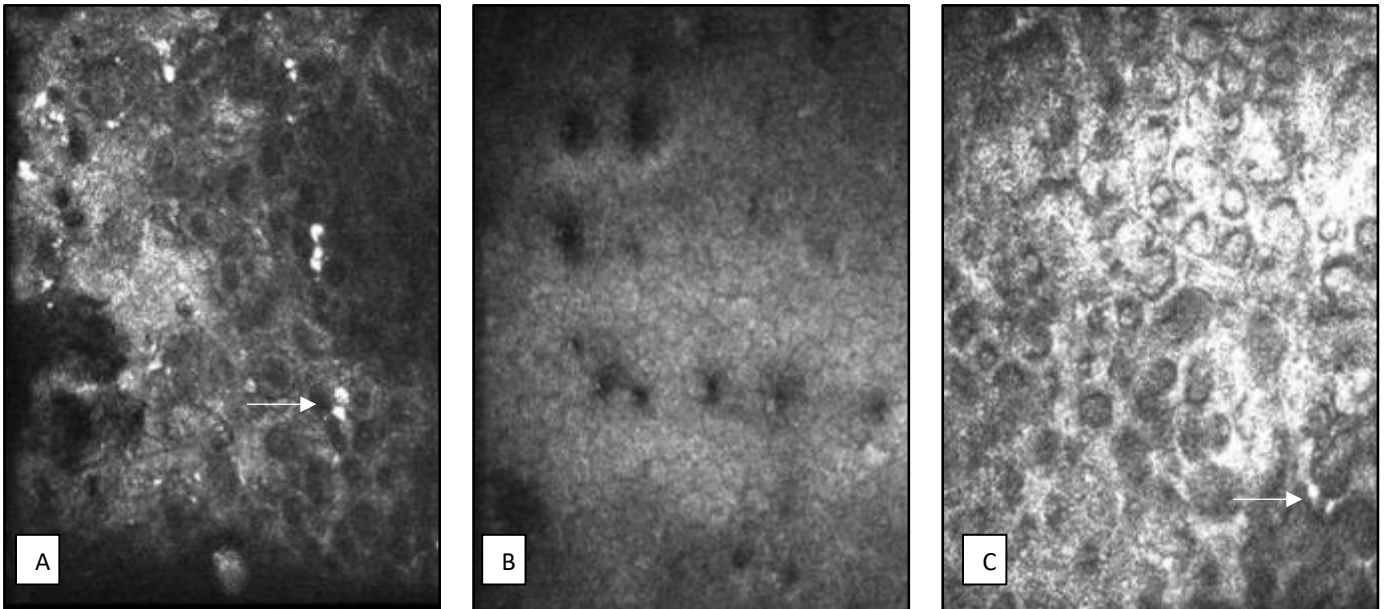


Figure 14: Confocal images of Proband IT 1639's affected siblings and father.

- (A) Proband COL-C's 30-year-old younger sister shows endothelial cell polymegathism and polymorphism in the presence of multiple large guttata noted to occur within the endothelial cell border. The arrow shows well defined hyperreflective point occurring at the level of the corneal endothelium that are in keeping with inflammatory cells
- (B) Proband COL-C's 30-year-old elder sibling shows preservation of endothelial cell structure and an endothelial cell density within normal limits. Guttata are shown noted but are occurring mainly at the endothelial cell junction. No inflammatory cells were noted in any sections of the scan.
- (C) Proband COL-C's 56-year-old father's scans show markedly abnormal endothelial cells with marked polymegathism and polymorphism. Although less marked than the finding in the probands sister (A), inflammatory cells were found occurring at the endothelial cell layer.

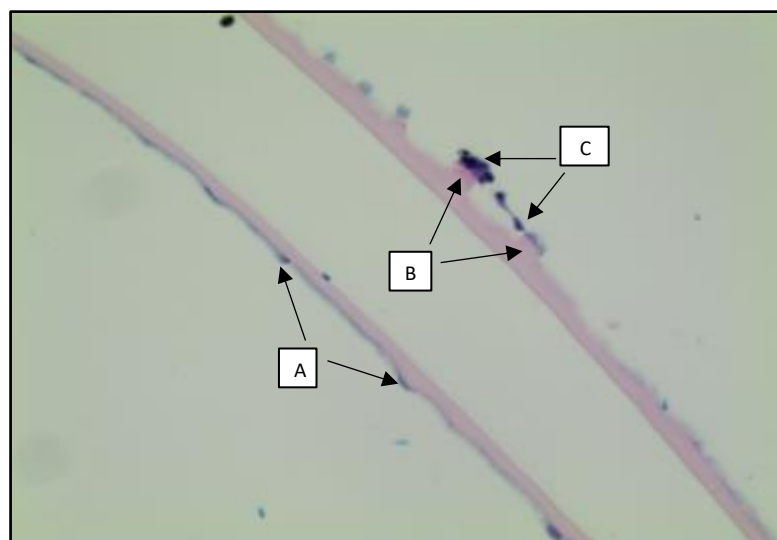


Figure 15: Descemet's membrane and endothelial cell layer removed at the time of partial thickness endothelial keratoplasty from Proband COL-C stained with haematoxylin and eosin, viewed at a magnification of x40. The arrows highlight the following histological features of the tissue viewed on cross section: (A)Exophytic guttata, (B)Inflammatory lymphocytes and (C)Scanty endothelial cells. No marked thickening of Descemet's membrane was noted on the pathological specimen

## Genes Previously Associated with FECD



### 3.3.2.1 *SLC4A11*

#### 3.3.2.1.1 Background

The SLC4A11 protein is made up of a cytoplasmic domain and a membrane domain that localizes to the basolateral surface of the corneal endothelial cell. The transmembrane structure of the protein facilitates its function as a co-transporter within the endothelial cell fluid pump. It has been shown to function as a Na<sup>+</sup> independent H<sup>+</sup>(OH<sup>-</sup>) Na<sup>+</sup>/OH<sup>-</sup> transporter, NH<sub>3</sub> transporter, Na<sup>+</sup>/OH<sup>-</sup> co-transporter and allows H<sub>2</sub>O movement across the cell (Malhotra, Loganathan et al. 2019).

*SLC4A11* mutations are hypothesized to cause corneal decompensation by two different pathways:

a. Impaired solute transport

SLC4A11 mutant proteins fail to fold in the correct orientation and the misfolded proteins are then recognised as abnormal and retained by the endoplasmic reticulum. Retention of the protein then leads to intracellular degradation (Kumar, Bhattacharjee et al. 2007, Vithana, Morgan et al. 2008, Riazuddin, Vithana et al. 2010). Abnormal proteins that do manage to localise to the cell membrane remain unable to function normally in maintaining endothelial cell detergence (Malhotra, Loganathan et al. 2019). A combination of compromise in function as well as impaired protein localisation to the endothelial cell surface are therefore thought to contribute to the impaired transmembrane water flux in FECD (Vilas, Loganathan et al. 2013).

b. Impaired endothelial cell adhesion

Structural analysis of SLC4A11 has shown that the extracellular loop 3 of the protein is located within the cytosolic domain and plays a functional role both in dimerisation of SLC4A11 molecules as well as a possible anchoring mechanism between endothelial cells and Descemet's membrane (Malhotra, Jung et al. 2020). Specifically, it has been shown that SLC4A11-EL3 regulation is closely linked to *COL8A1* and *COL8A2* expression, another gene product known to be associated with FECD (Biswas, Munier et al. 2001, Gottsch, Sundin et al. 2005, Liskova, Prescott et al. 2007, Malhotra, Jung et al. 2020).

Identification of rare variants within the *SLC4A11* gene and understanding the position of the variant within the complex structural domain of the protein are therefore of great interest in understanding the mechanism of dysfunction in FECD.

### 3.3.2.1.2 Genotyping

WES analysis identified 3 nonsynonymous heterozygous variants in the *SLC4A11* gene in 3 individuals: SLC-A, SLC-B and SLC-C (Table 3).

Patient Identifier	Nucleotide change Within <i>SLC4A11</i>	Amino Acid change	In Silico Pathogenicity Assessment (PolyPhen2 /SIFT)	Control Datasets			Implications of findings
				UCL ex	ESP Control Dataset	1000 Genome Project Dataset	
SLC-A	c.937G>C	p.V313L	0/0.56	NA	NA	NA	Non-synonymous, well tolerated
SLC-B	c.931G>A	p.G311S	0/0.25	NA	0.000077	NA	Non-synonymous, well tolerated
SLC-C	c.245G>T	p.R82L	0.998/1	0.000148	0.000077	0.0005	Non-synonymous, tolerated by SIFT but deleterious by PolyPhen2

Table 3: Three heterozygous variants in *SLC4A11* were identified through whole exome sequencing. The PolyPhen2 and the SIFT score for the three nonsynonymous variants were not indicative of a disease-causing mutation.

#### a. In silico pathogenicity assessment and multiple sequencing alignment

The variant p.V313L was a unique change that did not appear in all three control datasets. The amino acid Valine was not found to be well conserved across orthologues and in silico analysis predicted that the substitution for Leucine would be well tolerated.

The variant p.G311S was only found in the ESP control data set with a MAF of 0.000077. The amino acid Glycine was not highly conserved across orthologues and both the SIFT score (0.25) and the PolyPhen2 score (0) predicted the change to Serine would be well tolerated.

The substitution of Arginine for Leucine at position 82 was found to have a MAF of 0.000148 in the UCLex control database, 0.0005 in the 1000 Genome control dataset and 0.000148 in the UCLex control dataset. Arginine was shown to be well conserved across orthologues and although the SIFT score of 1

suggested that the variant was benign, the PolyPhen2 score of 0.998 indicates a potentially deleterious change (Figure16).

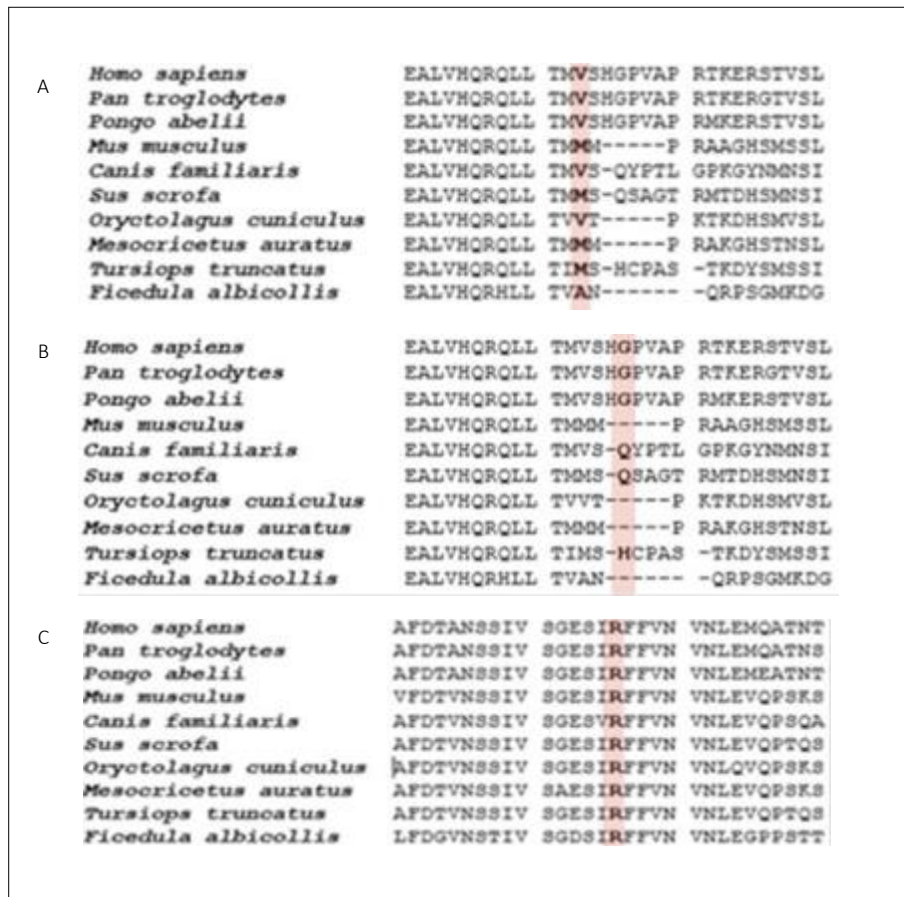


Figure 16: Multiple Sequencing Alignment showing conservation of amino acid across orthologues corresponding to 3 nonsynonymous heterozygous variants in the SLC4A11 gene in 3 individuals.

The position of altered amino acids is highlighted in red across orthologues

- A. Amino acid residue p.V313 was not highly conserved multiple species suggesting the variant c.937G>C, p. V313L could be tolerated
- B. Amino acid residue p.G311 in multiple species demonstrates that the affected residue is not highly conserved across orthologues and the heterozygous mutation c.931G>A, p.G311S may therefore be tolerated
- C. Amino acid residue p.R82 is shown to be well conserved across 9 orthologues suggesting that the change reported in c.245G>T, p.R82L would not be well tolerated.

b. Molecular modelling of *SLC4A11*

A three-dimensional homology model of the SLC4A11 protein dimer (Figure 17) was built from the PDB structure c5jho using PHYRE2 software (Kelley and Sternberg,2009) and MacPymol software. The variant p.R82L (c.245G>T) was noted to occur inside the  $\beta$ -sheets of the protein structure while the p.G311S (c.931G>A) and p.V313L (c.937G>C) variants occur in a loop near the dimer interface. The changes occurring at the interface could potentially disrupt the structure of the SLC4A11 dimer.

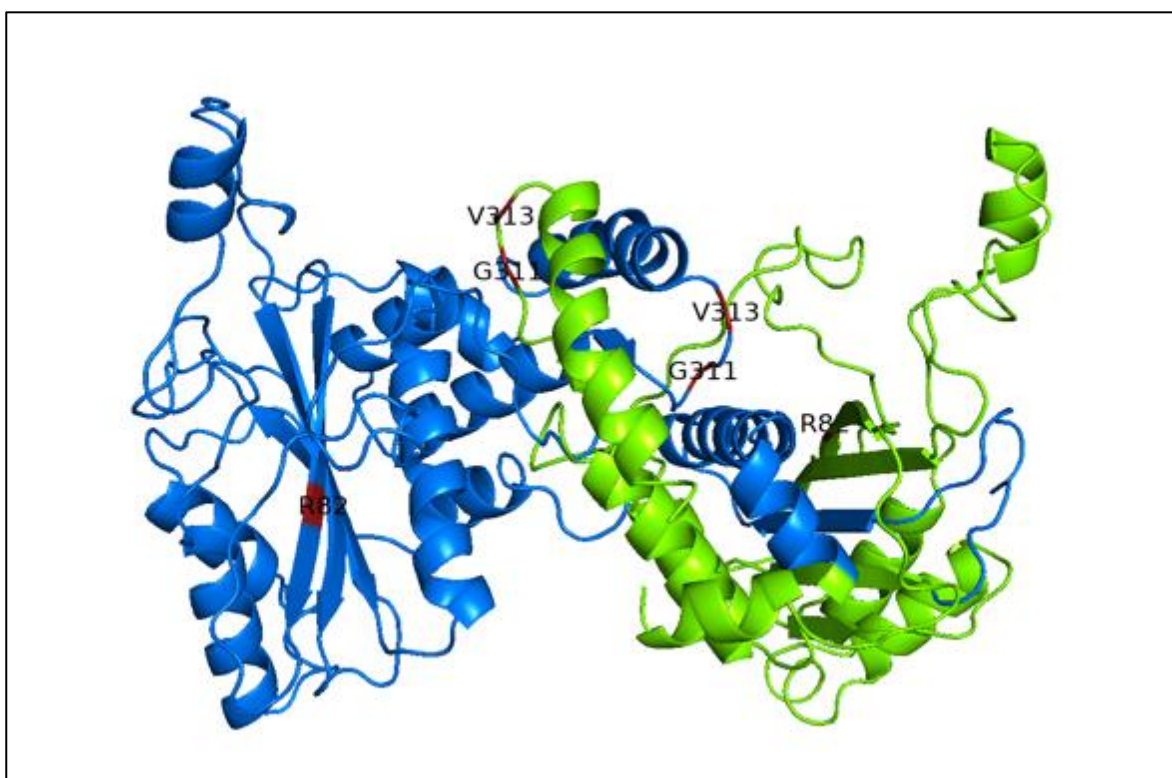


Figure 17: Molecular model of SLC4A11 protein homodimer.

The figure shows a three-dimensional homology model of the SLC4A11 dimerised protein based on PDB 5jho. The ribbon structures in the figure represent  $\alpha$ -helices and the thicker arrows represent  $\beta$ -sheets. The three amino acids that were identified to have undergone non-synonymous point substitutions in this study [p.R82L (c.245G>T), p.G311S (c.931G>A) and p.V313L (c.937G>C)] are highlighted in red.

### 3.3.2.1.3 Phenotyping

A non-synonymous heterozygous *SLC4A11* variant c.937G>C, p.V313L was identified in SLC-A, an Afro-Caribbean female subject who was first diagnosed with FECD at the age of 36 years (early-onset). She reported that symptoms began with diurnal variation in both eyes 10 years before at the age of 26 years. At the time of diagnosis, the BCVA was 6/12 in both eyes and slitlamp biomicroscopy of the cornea identified confluent central guttata and mild stromal oedema in both eyes. The patient was reviewed over a ten-year period by which time both corneas were noted to have progressed to more severe corneal oedema and the patient reported that diurnal variation in vision was affecting her ability to work. Her vision remained BCVA 6/12 in both eyes. Imaging of endothelial cells and endothelial cell count were not available for this subject. Combined endothelial keratoplasty and cataract extraction with intraocular lens insertion were performed on both eyes at the age of 45 years. She did not report a positive family history.

SLC-B is an 80-year-old Asian Indian female who presented with late-onset FECD. The patient remained asymptomatic of diurnal variation in both eyes until the point of undergoing right cataract extraction by phacoemulsification with intraocular lens implantation. Corneal decompensation occurred only after cataract surgery at the age of 76 years. She was referred to MEH for the purpose of undergoing right endothelial keratoplasty surgery which was performed at the age of 77 years. Retrospective review of the medical notes showed that despite the presence of central guttata on slitlamp biomicroscopy, clinically the left cornea showed no signs of corneal oedema to indicate endothelial decompensation. The patient was therefore referred back to her local eye unit for future left cataract surgery as she was not assessed as requiring corneal transplant surgery to that eye. The proband reported no family history of the disease and additional family members were unavailable to perform segregation analysis of the *SLC4A11* variant.

SLC-C is a 77-year-old Caucasian female patient who was diagnosed with late-onset FECD at the age of 64 years. Her vision was BCVA 6/9 in both eyes at the time of diagnosis and had not undergone any previous ocular surgery. Symptoms of diurnal variation and glare started at the age of 69 years after having undergone left cataract extraction and intraocular lens implantation. She underwent corneal transplant surgery to the left eye within the same year. The right cornea shows signs of guttata and corneal oedema, but the patient had opted not to undergo further surgery to that eye.

Familial segregation analysis showed that the proband SLC-C's unaffected husband is wildtype while the variant segregates in both the affected son (II.1, 52 years) and unaffected daughter (II.2, 43

years)(Figure 18). It is possible that as the disease presented as late on set in SLC-C, that future follow up of the daughter may reveal clinical signs of FECD in later life.

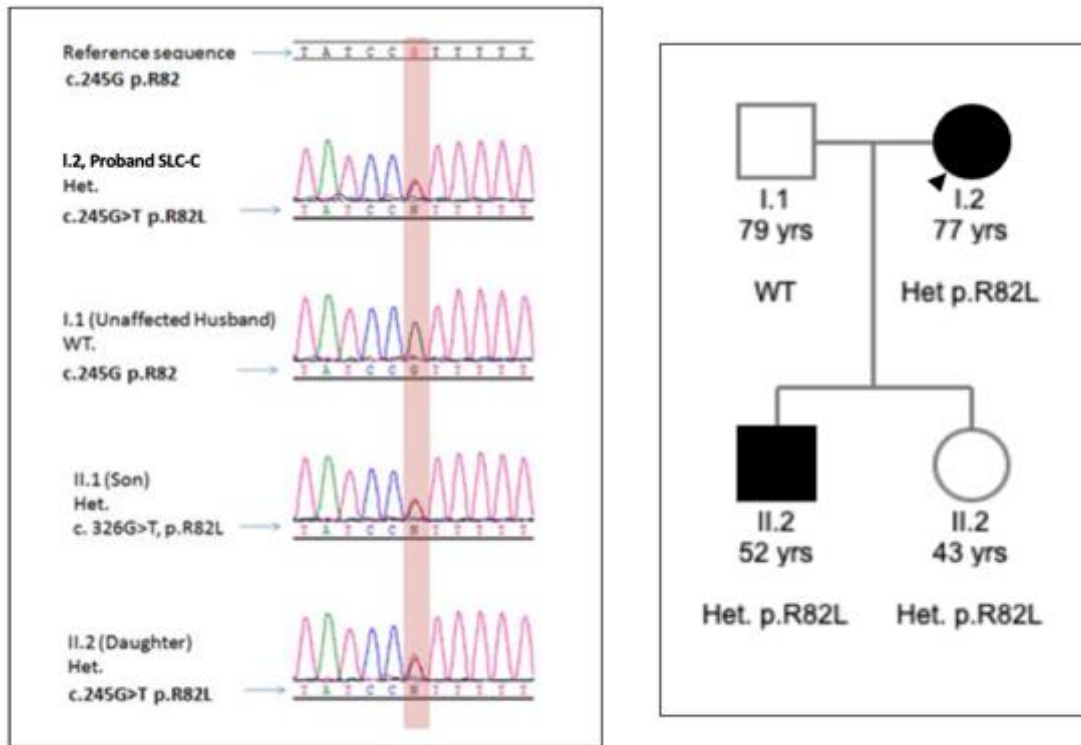


Figure 18: Sanger sequencing chromatogram and familial pedigree of proband SLC-C. The chromatogram of the same region the non-synonymous heterozygous variant c.245G>T identified in Proband SLC-C as well as her affected daughter, unaffected son and husband are shown here. Both children are shown to have inherited the variant form the proband as her husband is shown to be wild type.

#### 3.3.2.1.4 Discussion

The 3 patients in whom non-synonymous variants were noted in the SLC4A11 gene developed the signs and symptoms of the disease at different timepoints in their life. While SLC-A could be classified as early-onset FECD, SLC-B and SLC-C did not develop symptoms of corneal decompensation until later life. Proband SLC-A reached the threshold of requiring corneal transplant surgery in both eyes by the age of 45 years. In the case of both SLC-B and SLC-C however, corneal decompensation only occurred following cataract surgery in one eye, while the contralateral eye that had not undergone surgery showed no signs of oedema on slitlamp biomicroscopy. Unfortunately, due to the retrospective nature of data collection in these cases, no imaging of the cornea was available to examine the phenotype of guttata and oedema in more detail in both cases.

In all three of our study subjects, the amino acid substitution occurred within the cytoplasmic domain of SLC4A11 (1-374). It has been hypothesized that mutations occurring within the cytoplasmic domain structure may lead to greater misfolding thus making the abnormal protein an easier target for endoplasmic reticular retention. However, Alka *et al.* 2019 noted that in the majority of FECD cases with *SLC4A11* mutations, cell surface trafficking was not impaired. Another mechanism of endothelial cell dysfunction that has been postulated by Loganathan *et al.* is a failure of the cytoplasmic domain to interact with the membrane domain to allow substrate translocation (Loganathan, Schneider *et al.* 2016).

Two of the variants identified in this study, p.G311S and p.V313L are located within 3 base pairs of each other and were found to be poorly conserved across orthologues along with *in silico* pathogenicity scores that predict the variants to be benign. To more conclusively determine if these non-synonymous variants are rare polymorphisms rather than mutations causing repeat ExpNeg FECD, further segregation analysis and phenotyping would need to be performed within the extended families of the affected probands. Likewise, *in vitro* characterisation of these variants and their effect on SLC4A11 trafficking and function also warrants further investigation.

### 3.3.2.2 ZEB1

#### 3.3.2.2.1 Background

Mutations in *ZEB1* were first identified to be causative in the endothelial corneal dystrophy Posterior Polymorphous Corneal Dystrophy 3 (PPCD3)(Krafchak, Pawar et al. 2005, Aldave, Yellore et al. 2007, Liskova, Filipec et al. 2010). Following the identification of heterozygous frameshift, nonsense mutations were in PPCD3, heterozygous missense and nonsense mutation were subsequently found in late-onset FECD (Table 4).

Publication	Population	<i>ZEB1</i> Variations predicted to be deleterious
Gupta <i>et al</i> 2015 (Gupta, Kumawat et al. 2015)	82 late-onset FED patients from Northern India	p.Glu733Lye p.Leu947stop
Mehta <i>et al</i> 2008 (Mehta, Vithana et al. 2008)	74 late onset FECD patients of Chinese ethnicity from Singapore	p.Asn696Ser
Lechner et al 2013 (Lechner, Dash et al. 2013)	1 multigenerational Caucasian family: variant segregates in late-onset FECD proband and 2 children with keratoconus	p. Gln640His
Bhavna <i>et al</i> 2018 (Rao, Ansar et al. 2018)	52 late-onset and 5 early-onset FECD cases of Indian origin	p.Q841P
Riazuddin <i>et al</i> 2010 (Riazuddin, Zaghoul et al. 2010)	192 unrelated late onset FECD Caucasian patients	p.N78T p.Q810P p.Q840P p.A905G
	1 multigenerational family Familial segregation analysis: Mutation was present in 7/12 affected family members	p.Q840P

Table 4: Summary of associated ZEB1 variants reported in late and early onset FECD. To date 5 publications have identified variants in ZEB1 that were predicted to be deleterious. While the majority of these cases were reported as isolated cases, in 2 multigenerational families the variant was noted only to partially segregate with FECD suggesting that the mutation may be sufficient but not necessary for pathogenesis.



### 3.3.2.2.2 Genotyping

A non-synonymous heterozygous variant c.635C>T, p.T212M was identified within the *ZEB1* gene. The variant was not present in the 1000 genome project control data set or the UCLex control data set and has a MAF 0.000077 in the ESP control data set.

#### a. In Silico Pathogenicity and Conservation Assessment

The variant was found to have a SIFT score of 0 and PolyPhen2 score of 0.996, predicting it to be deleterious. This amino acid was seen to be well conserved across a diverse range of orthologues were aligned (Figure 19).

<i>Homo sapiens</i>	TQLERHMTSH	KSGRDQRHVT	QSGGNRKFKC
<i>Pan troglodytes</i>	TQLDRHMTSH	KSGRDPRHVT	QSSGNRKFKC
<i>Pongo abelii</i>	TQLERHMTSH	KSGRDQRHVT	QSGCNRKFKC
<i>Mus musculus</i>	TQLERHMTSH	KSGREQRHVT	QSGGNRKFKC
<i>Canis familiaris</i>	TQLERHMTSH	KSGREQRHVT	QSGGNRKFKC
<i>Sus scrofa</i>	TQLERHMTSH	KSGRDQRHVT	QSGGNRKFKC
<i>Oryctolagus cuniculus</i>	TQLERHMTSH	KSGRDQRHVT	QSGCNRKFKC
<i>Mesocricetus auratus</i>	TQLERHMTSH	KSGRDQRHVT	QSGCNRKFKC
<i>Tursiops truncatus</i>	TQLERHMTSH	KSGRDQRHVT	QSGGNRKFKC
<i>Ficedula albicollis</i>	TQLERHMTSH	KSGRDQRHVT	QSGGNRKFKC

Figure 19: Multiple Sequencing Alignment showing conservation of amino acid residue p.T212 in *ZEB1* across orthologues. The amino acid residue T(Threonine) is well conserved across 9 orthologues. The altered amino acid residue is highlighted in red.

### 3.3.2.2.3 Phenotyping

Proband SLC-B who harbours the *ZEB1* mutation above was also found to harbour the non-synonymous heterozygous variant c.931G>A, p.G311S in the *SLC4A11* gene. Please refer to section 3.3.2.1.3.

### 3.3.2.2.4 Discussion

The variant in *ZEB1* identified in Proband SLC-B altered the amino acid threonine to methionine at position 212, a position found to be highly conserved. The change was also predicted to be deleterious by SIFT and Polyphen2, suggesting that the variant may be causative for late-onset FECD in this proband.

Interestingly, this proband was also identified as having a nonsynonymous heterozygous variant c.931G>A, p.G311S in the *SLC4A11* gene. However, in silico analysis showed that the variant was unlikely to be detrimental in the poorly conserved amino acid position. It is therefore more likely that the disease-causing variant in this proband is nonsynonymous change occurring in the *ZEB1* gene.

Unfortunately, segregation analysis could not be performed due to lack of available familial samples to explore this hypothesis further. Riazuddin *et al.* are the only study to show segregation of a *ZEB1* mutation (p.Q840P) across a multigenerational family effected by late onset FECD. Although 12 members of the family exhibited the phenotype of late onset FECD, only 7 were found to harbour the same heterozygous *ZEB1* mutation. The study concluded this allele to be sufficient but not necessary for pathogenesis. The same study went on to perform a genome-wide scan that identified an additional late-onset FCD locus on chromosome 9p (9p22.1-p24.1 haplotype). They found that in family members who carried the variant within *ZEB1* in combination the haplotype on chromosome 9p, the FECD manifestation was more severe than those who carried only one pathogenic allele.

It is possible that similar to the findings of Riazuddin *et al.*, the presence of a variant in *SLC4A11* could cause genetic interaction that influenced the expression of the disease phenotype seen in Proband SLC-B. Variants that contribute to complex conditions such as FECD may have a subtle effect on the cellular environment in isolation and depend on the presence of other variants to create a change in phenotype.

GWAS ASSOCIATED  
FECD GENES

### 3.3.3.1 *LAMC1*

#### 3.3.3.1.1 Background

The GWAS by Afshari *et al.* and found that the rs3768617 within the *LAMC1* gene to be the most significantly associated SNP within this region and went on to show that it conferred a greater risk of disease in women compared to men (odd ratio= 1.52 in women, 1.16 in men). Interestingly, a recent study has since identified one potential disease-associated variant in the *LAMC1*; a heterozygous c.1468C>T p.R490W (Ensembl transcript: ENST00000258341)(Wieben, Aleff et al. 2018). The identified variant was observed in a single CTG18.1 repeat expansion-negative FECD patient. It is tempting to hypothesise that this variant could be causal for FECD, however, without replication of similar findings in additional unrelated FECD patients it is not possible to confirm this association.

#### 3.3.3.1.2 Genotyping

Five probands were found to harbour rare single nucleotide variants in the *LAMC1* gene (Table 1). Of the variants that were found, two were synonymous changes, thus considered most likely to be benign: c.C1836T, p.G612G and c.A4152G, p.A1384A.

The variant c.G4303A, p.A1435T is a non-synonymous variant with an MAF score of 0.000461 in the ESP control dataset, 0.0018 in the 1000 genome project dataset and 0.000847 in the UCLex dataset. Although the affected amino acid residue was found to be well conserved across orthologues, the PolyPhen2 score was 0 and the SIFT score 0.45 (Table 5). The in silico analysis assessment therefore indicated that the variant would be benign and well tolerated.

Both the remaining two variants, c.G1240A, p.G414S and c.G2701A, p.V901M were predicted to be deleterious. The non-synonymous heterozygous variant c.G1240A was not found in any of the control datasets and is a unique change. The Sift score of 0 and the PolyPhen2 score of 0.993 both predict that the resulting amino acid substitution from glycine to serine could be deleterious. The affected amino acid was found to be well conserved across orthologues (Figure 20). The other deleterious non-synonymous variant c.G2701A (SIFT score 0.05, PolyPhen2 score 0.921) was confirmed as a rare variant in both the ESP control dataset and the 1000 Genome project dataset while absent from the UCLex Dataset. Protein alignment confirmed that the amino acid was also well conserved across orthologues.

Patient Identifier	Nucleotide change Within LAMC1	Amino Acid change	In Silico Pathogenicity Assessment (PolyPhen2/SIFT)	Control Datasets			Implications of findings
				UCL ex	ESP Control Dataset	1000 Genome Project Dataset	
LAM-A	c.G4303A	p.A1435T	0/0.45	0.000847	0.000461	0.0018	Non-synonymous, benign, well tolerated,
<b>LAM-B</b>	<b>c.G1240A</b>	<b>p.G414S</b>	<b>0.999/0</b>	<b>0</b>	<b>NA</b>	<b>NA</b>	<b>Non-synonymous, potentially deleterious,</b>
LAM-C	c.A4152G	p.A1384A	NA/NA	0	NA	NA	Synonymous heterozygous variant
<b>LAM-D</b>	<b>c.G2701A</b>	<b>p.V901M</b>	<b>0.921/0.05</b>	<b>0</b>	<b>0.000308</b>	<b>0.0009</b>	<b>Non-synonymous, potentially deleterious</b>
LAM-E	c.C1836T	p.G612G	NA/NA	0	NA	NA	Synonymous heterozygous variant

Table 5: Identification of rare variants in LAMC1 within the CTG18.1 ExPNeq cohort. Of the five rare single nucleotide variants that were found, two were synonymous changes (c.C1836T and c.A4152G) that were assessed to be benign. The variant c.G4303A is a non-synonymous variant but in silico pathogenicity tools predicted that this change would also be well tolerated and not contributing to the pathogenesis of FECD. The remaining two variants, c.G1240A and c.G2701A, were predicted to be deleterious (highlighted in bold). It was also noted that c.G1240A is a unique variant that was not present in any of the control datasets.

A	<i>Homo sapiens</i>	ATEAKNKAHE	AERIASAVQK	NATSTKAEAE
	<i>Pan troglodytes</i>	ATEAKNKAHE	AERIASAVQK	NATSTKAEAE
	<i>Pongo abelii</i>	ATEAKNKAHE	AERIASAVQK	NATSTKAEAE
	<i>Mus musculus</i>	ATEAKNKAHE	AERIASAVQK	NATSTKAEAE
	<i>Canis familiaris</i>	ATEAKNKAHE	AERIASAVQK	NATSTKAEAE
	<i>Sus scrofa</i>	ATEAKNKAHE	AERIASAVQK	NATSTKAEAE
	<i>Oryctolagus cuniculus</i>	ATEAKLKAHE	AERIASAVQK	NATSTKAEAE
	<i>Mesocricetus auratus</i>	ATEAKNKAHE	AERIASAVQK	NATSTKAEAE
	<i>Tursiops truncatus</i>	ATEAKNKAHE	AERIASAVQK	NATSTKAEAE
	<i>Ficedula albicollis</i>	AREAKARADD	AEKIASSVQK	SAAATRAEAD
B	<i>Homo sapiens</i>	CSPVGSLSLSTQ	CDSYGRCSCK	PGVMGDKCDR
	<i>Pan troglodytes</i>	CSPVGSLSLSTQ	CDSYGRCSCK	PGVMGDKCDR
	<i>Pongo abelii</i>	CSPVGSLSLSTQ	CDSYGRCSCK	PGVMGDKCDR
	<i>Mus musculus</i>	CSPVGSLSLSTQ	CDSYGRCSCK	PGVMGDKCDR
	<i>Canis familiaris</i>	CSPVGSLSLSTQ	CDSYGRCSCK	PGVMGDKCDR
	<i>Sus scrofa</i>	CSPVGSLSLSTQ	CDSYGRCSCK	PGVMGDKCDR
	<i>Oryctolagus cuniculus</i>	-----	-----	-----
	<i>Mesocricetus auratus</i>	CSPVGSLSLSTQ	CDSYGRCSCK	PGVMGDKCDR
	<i>Tursiops truncatus</i>	CSPVGSLSLSTQ	CDSYGRCSCK	PGVMGDKCDR
	<i>Ficedula albicollis</i>	CNPFVGSLSLSTQ	CDSYQQCSCK	PGVMGDKCDR
C	<i>Homo sapiens</i>	GTMKQQSSCN	FVTGQCECLP	HVTGQDCGAC
	<i>Pan troglodytes</i>	GTMKQQSSCN	FVTGQCECLP	HVTGRDCGAC
	<i>Pongo abelii</i>	GTVKQQSSCN	FVTGQCECLP	HVTGRDCGAC
	<i>Mus musculus</i>	GTVQQQSSCN	FVTGQCCCLP	HVSGRDCGTC
	<i>Canis familiaris</i>	GTVKQQSSCN	FVTGQCECLP	HVTGRDCGAC
	<i>Sus scrofa</i>	GTVKQQSSCN	FVTGQCECLP	HVTGRDCGAC
	<i>Oryctolagus cuniculus</i>	GTLRQQGGCN	FVTGQCACL	HVAGRDCGAC
	<i>Mesocricetus auratus</i>	GTVQQQSSCN	FVTGQCECLP	HVSGRDCGAC
	<i>Tursiops truncatus</i>	GTVKQQSSCN	FVTGQCECLP	HVTGRDCGAC
	<i>Ficedula albicollis</i>	GTVNQQTICN	QVTGQCECLS	HVTGRDCSAC

Figure 20: Multiple Sequencing Alignment showing conservation of amino acid across orthologues corresponding to 3 nonsynonymous heterozygous variants in the *LAMC1* gene in 3 individuals. The position of altered amino acids is highlighted in red across orthologues.

a. Amino acid residue p.A1435 is shown to be well conserved across orthologues indicating the variant c.4303G>A, p.A1435T would not be tolerated in proband LAM-A

b. The amino acid residue p.G414 is shown to be well conserved across orthologues suggesting the heterozygous c.1240G>A, p.G414S variant in proband LAM-B would not be well tolerated

c. Amino acid residue p.V901 is shown to be well conserved across 8 of 9 orthologues suggesting that the change c.2701G>A, p.V901M reported LAM-D not be well tolerated.

### 3.3.3.1.3 Phenotyping

Two subjects were assessed as harbouring potentially disease associated non-synonymous variants in the *LAMC1* gene:

- a) Proband LAM-B is a white Caucasian female with late onset FECD who underwent combined endothelial keratoplasty and cataract extraction surgery to the right eye at the age of 68 years. The same procedure was performed for the treatment of corneal decompensation and cataract in the left eye within 2 years. It was not possible to provide an age of onset or diagnosis from review of the notes and in speaking with the patient. She reports no family history of ocular disease. Unfortunately, retrospective review of the notes and imaging data did not allow for further phenotyping of this case
- b) Proband LAM-D was a Black African male, diagnosed with late onset FECD. The patient has unfortunately passed away at the time of this study. He was originally diagnosed elsewhere and referred to Moorfields Eye Hospital following failure of a corneal graft performed elsewhere. No FECD phenotyping data was available for this patient.

The 3 remaining probands harbouring variants in the *LAMC1* gene were assessed as well tolerated genetic changes that were unlikely to be disease causing:

- a) Proband LAM-C was also found to harbour the variant c.1363C>A, p.Q455K in *COL8A2* in addition to the synonymous variant in *LAMC1*. Detailed phenotyping is provided in section 3.3.1.1.3.
- b) Proband LAM-A (non-synonymous heterozygous variant, c.4303G>A) is a white Caucasian female who was diagnosed with FECD at the age of 68 years. After undergoing cataract surgery to the left eye, it was noted that the signs of corneal decompensation were more advanced in the right eye that had yet to undergo any surgery. Combined cataract surgery and endothelial keratoplasty was performed on her right eye at the age of 72 years. The left eye cornea did not require keratoplasty for another 6 years.
- c) Proband LAM-E is a white Caucasian male diagnosed with late onset FECD at the age of 65 years. The onset of diurnal variation in vision in the right eye occurred a year later only after undergoing cataract surgery. The central corneal thickness was 586  $\mu\text{m}$  in the right eye and 549  $\mu\text{m}$  in the left eye. He underwent keratoplasty to the right eye at the age of 67 years followed by combined endothelial keratoplasty and cataract extraction in the left eye at the age of 68 years. Blood

samples for genotyping were available from 2 of the probands unaffected brother and one unaffected son (Figure 21). Although both family members were able to provide blood samples via their local GP, they were not able to attend for phenotyping. The probands brother who also harboured the same variant did not report any visual symptoms and was not informed of the existence of any corneal changes at his last opticians review.

#### 3.3.3.1.4 Discussion

Three of the five patients harbouring variants in *LAMC1* were female, in keeping with the female preponderance reported by Afshari et al (Afshari, Igo et al. 2017). Of the five rare single nucleotide variants that were found, two were synonymous changes (c.C1836T and c.A4152G) that were assessed to be benign. Proband LAM-C who harbours the synonymous variant c.A4152G, is also known to carry a variant in the *COL8A2* gene which is believed to be the underlying cause of FECD. Familial segregation analysis of proband LAM-E further confirmed that the variant c.C1836T was unlikely to be disease causing as it was present in the patient's 65-year-old brother who was asymptomatic of FECD. The variant c.G4303A is a non-synonymous variant but in silico pathogenicity tools predicted that this change would also be well tolerated and not contributing to the pathogenesis of late onset FECD in Proband LAM-A, despite being highly conserved.

The remaining two variants, c.G1240A (a unique variant that was not present in any of the control dataset) and c.G2701A, were predicted to be deleterious. Unfortunately, DNA samples were not available for the either patient to enable segregation analysis to be performed to further investigate the potential pathogenicity of either variant.



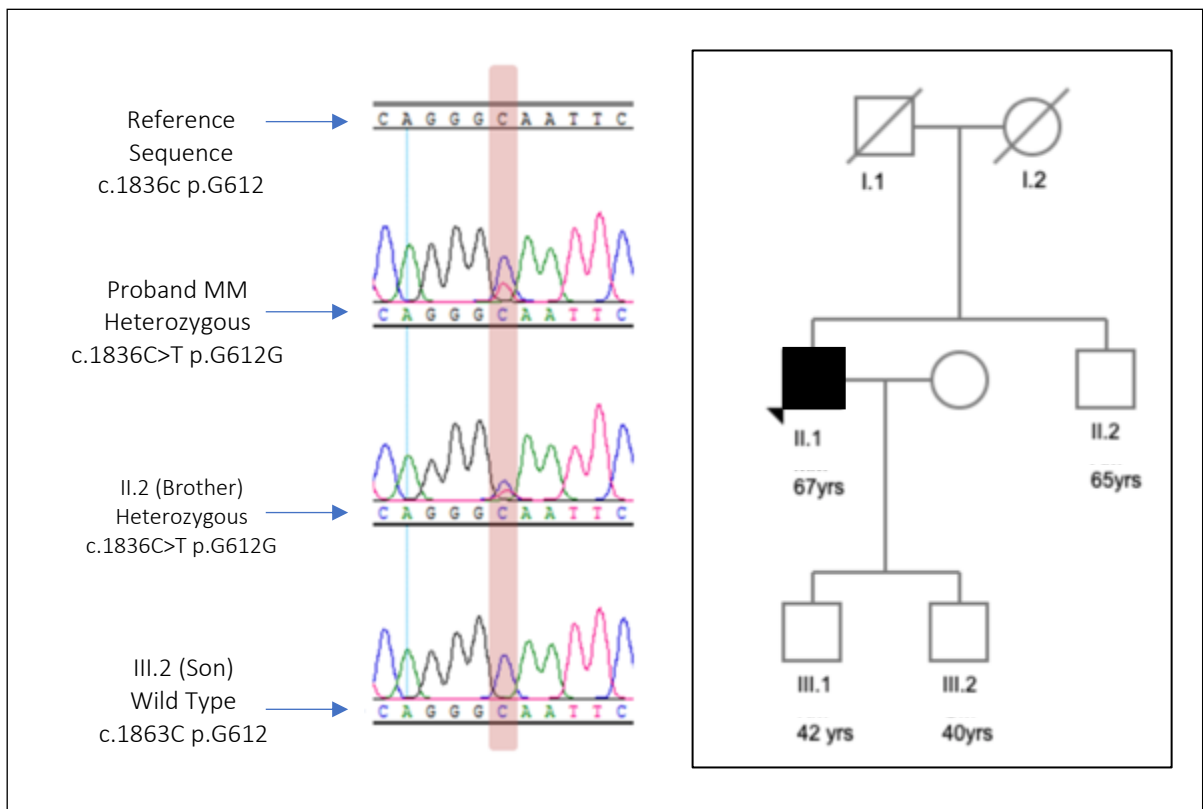


Figure 21: Identification and segregation analysis of the rare LAMC1 variant c.1836C>T. Sanger sequence chromatogram (courtesy of Miss A Sadan) confirms the presence of the c.1836C>T variant in the effected Proband LAM-E as well as the 65-year-old unaffected brother (II.2). The proband's son (III.2) was shown to be wild type and reported no signs of FECD. These finding suggests that this synonymous variant is not causative of FECD in this family.

### 3.3.3.2 *KANK4*

#### 3.3.3.2.1 Background

*KANK4* encodes KN motif and ankyrin repeat-containing protein 4, a protein that is believed to play a role in actin polymerization (Chen, Sun et al. 2018). It has been hypothesized that this protein may contribute to both cell-cell contact and tissue integrity, similar to the role of *KANK1*, 2 and 3 proteins (Chen, Sun et al. 2018). *KANK1* has been shown to inhibit cell spreading and migration, and knockdown of the gene resulted in enhanced cell migration (Kakinuma, Roy et al. 2008, Roy, Kakinuma et al. 2009). It is possible that *KANK4* mutations may influence normal endothelial cell migration that should occur as a compensatory mechanism following CEC loss.

Recessive mutations in *KANK4* have been associated with kidney nephrotic syndrome (Gee, Zhang et al. 2015). Within the renal filtration system, the *KANK4* mutations are believed to affect the epithelial cells (podocytes) that contributes to ultrafiltration, a form of fluid homeostasis within the glomerulus. The podocytes also perform a secondary role in secreting and maintaining the glomerular basement membrane (Bowman's capsule). It has been suggested that the altered expression of the *KANK4* protein can lead to abnormalities of the cell cytoskeletal structure which manifests as a change in podocyte cell structure and disorganization of the glomerular basement membrane. As podocyte cells share common physiological functions of corneal endothelial cells, it is plausible that *KANK4* dysfunction could also lead to the abnormal fluid pump mechanism and changes in Descemet's membrane observed in FECD.

#### 3.3.3.2.2 Genotyping

Proband KAN-A was found to have a heterozygous non-synonymous variant, c.1762G>A, p.A588T, in the *KANK4* gene. The variant was not present in the ESP or 1000 genome control data set and had a MAF 0.000164 in the UCLex control data set. Predicted pathogenicity scores were 0.07 from Polyphen2 and 0.981509 from SIFT suggesting the variant is benign. The altered amino acid is well conserved across numerous species when orthologues were aligned (Figure 3A).

Proband KAN-B harboured a unique non-synonymous heterozygous variant, c.797G>A, p.D266G, was identified within the *KANK4* gene. Polyphen2 predicted a pathogenicity score of 0.12 for the variant suggesting it to be benign, however, SIFT score the variant 0.01621 indicating the variant to be

deleterious. The amino acid residue was seen to be conserved to some extent across a diverse range of species when orthologues were aligned (Figure 22,B).

A	<i>Homo sapiens</i>	EQWNCLEHGY	PELASAIKQP	ASKLSSIQSQ
	<i>Pan troglodytes</i>	EQWNCLEHGY	PELASAIKQP	ASKLSSIQSQ
	<i>Pongo abelii</i>	EQWNCLEHGY	PELASAIKQP	ASKLSSIQSQ
	<i>Mus musculus</i>	EQWNCLEHGY	PELASAIKQP	ASKLSSIQSQ
	<i>Canis familiaris</i>	EQWSCLEHGY	PELASAIKQP	ASKLSSIQSQ
	<i>Sus scrofa</i>	EQWSCLEHGY	PELARAIAKQP	ASKLSSIQSQ
	<i>Oryctolagus cuniculus</i>	EQWNCLEHGY	PELASAIKQP	ASKLSSIQSQ
	<i>Mesocricetus auratus</i>	EQWNCLEHGY	PELASAIKQP	ASKLSSIQSQ
	<i>Tursiops truncatus</i>	EQWLCLEHGY	PELASAIKQP	ASKLSSIQSQ
	<i>Ficedula albicollis</i>	EQWSCLEHGY	PELAHAIAKQP	ASKLSSIQSQ
B	<i>Homo sapiens</i>	PFSFQNVLVV	LEDKEDEHNA	REAEVLFT-P
	<i>Pan troglodytes</i>	PFSFQNALVV	LEDKEDEHNA	REAEVLFT-P
	<i>Pongo abelii</i>	PFSFQNALVV	LEDKEDEHKA	REAEVVFT-P
	<i>Mus musculus</i>	SSAVQSVPM	LEEVEIEHHM	REAEVLFT-P
	<i>Canis familiaris</i>	PFFSQDALVV	LEDEEDEPKT	REAEVVVS-P
	<i>Sus scrofa</i>	LFSPPNVLVV	LEDAEEQHEG	GEAEAGVTTS
	<i>Oryctolagus cuniculus</i>	PSSFFMALVV	LEDAED--KT	RDADTVFT-P
	<i>Mesocricetus auratus</i>	PSSVQNVPIV	LEGVEIQHQV	RNAEVLFT-S
	<i>Tursiops truncatus</i>	PFSS---LVV	LEDAEDQQES	RQAEVAVTTP
	<i>Ficedula albicollis</i>	PWLNQQLQVV	ME-----SGG	EEGDAAEMGG

Figure 22: Multiple Sequencing Alignment showing conservation of amino acid across orthologues corresponding to 2 nonsynonymous heterozygous variants in the *KANK4* gene in 2 individuals.

The position of altered amino acids is highlighted in red across orthologues.

- A. Conservation of amino acid residue p.A588 is shown to be well conserved across orthologues and therefore the variant c.1762G>A, p.A588T is not likely to well tolerated
- B. Conservation of amino acid residue p.D266 in conserved in 6 of the 9 orthologues, suggesting that the variant c.797G>A, p.D266G may be tolerated

### 3.3.3.2.3 Phenotyping

Proband KAN-A is a Caucasian female who first reported symptoms of diurnal variation and glare secondary to mild corneal decompensation at the age of 65 years. The disease was noted to be symmetrical (MCS score 2) and she had no history of previous ocular surgery. The vision was Snellen Best Corrected Visual Acuity of 6/12+3 at that time. The following year she underwent bilateral cataract extraction and intraocular lens implantation surgery which improved the vision to 6/9. The mild central corneal oedema was noted to be the reason for not achieving 6/6 vision. The option of corneal transplantation was discussed with the patient, but she opted not to have surgery at that time as she was happy with the level of vision achieved.

Six years later at the age of 72 years, the left corneal decompensation had worsened, and the patients underwent endothelial keratoplasty to that affected eye. The right eye deteriorated slowly over the next 3 years at which point corneal transplant surgery was performed to the contralateral eye as well.

Proband KAN-B is a white Caucasian female who was diagnosed with FECD at the age of 61 years. Retrospective review of the notes showed that the disease was noted to be symmetrical with signs of mild central corneal oedema as well as early cataracts in both eyes. The patient underwent combined endothelial keratoplasty and cataract extraction with intraocular lens implantation first to the right eye at 61 years of age and subsequently to the left eye within a year.

Neither Proband KAN-A nor Proband KAN-B reported a positive family history and no family members were amenable to undergoing clinical examination and segregation analysis of the *KANK4* variant.

### 3.3.3.2.4 Discussion

It is not possible to confirm the role of the *KANK4* variants identified in this study as causative of FECD. It should be noted that the variants found in this study were only partially conserved across orthologues and the change was predicted to be well tolerated by SIFT and PolyPhen2. Recent studies have demonstrated that proteins containing ankyrin-repeats do not recognize specific sequences, and instead interacting residues are discontinuously dispersed into the whole molecules of both the ankyrin repeat protein and its partner (Li, Mahajan et al. 2006). This adds a further complexity to the process of assessing the impact of a single nucleotide variant on the overall function of the protein. Future functional analysis and familial segregation studies are required to clarify the role of this gene in FECD.

### 3.4 Conclusion

The findings of this study support the understanding of the extensive genetic heterogeneity of Fuchs Endothelial Corneal Dystrophy (FECD). Although corneal oedema secondary to endothelial dysfunction is the final common pathological outcome for all patients clinically diagnosed as FECD, at the molecular level the basis for their disease may vary considerably. Ongoing genomic investigations are needed to genetically define other distinct and rare forms of corneal endothelial disease. There remains a significant proportion of the Repeat Expansion Negative cohort of FECD that remains genetically undefined. The scope of investigation of this study this cohort has focused on variants already known to be associated with FECD as well as those known to have a highly significant association with FECD. As research funding availability arises, further genome wide sequencing of the unresolved section of the ExpNeg cohort will be carried out with the aim of identifying variants of interest.

Similar to the findings of the Westminster Health Forum, this study highlights one of the greatest challenges that the NHS faces in preparing for this paradigm shift in patient care: fragmented data collection and poor quality of patient data input. In busy present day clinical settings, where the only treatment available to patients is surgical intervention, the routine need for nuanced and detailed phenotyping of individuals presenting with FECD simply does not arise. However, as clinicians, it is imperative that we change our practice to align with the advances that continue to be made in the field of genomic medicine. As genomic databases such as Online Mendelian Inheritance in Man and HapMap continue to thrive alongside advance in personalised medicine, so too should clinicians work toward developing unified phenotypic databases that would allow us to define the natural history, prognosis and targeted treatment for each specific disease subtype.

As a result of my experience of this study, I have begun to develop a Corneal Genetics clinic to support the ongoing corneal genomics research at the UCL Institute of Ophthalmology. By improving the quality and quantity of clinical data collection on the natural history of corneal dystrophies, standardising imaging and corneal structural analysis as well as investigating families of affected individuals, the goal of our team is to develop a consolidated genotype-phenotype database to understand specific features of corneal dystrophies and guide our evaluation of an individual's targeted treatment in the future.

## Chapter 4

# Investigating the Dual Presentation of Fuchs Endothelial Corneal Dystrophy and Keratoconus

## 4.1 Background

Keratoconus (KC, OMIM 14830) is a non-inflammatory corneal ectasia that leads to progressive thinning of the corneal stroma and subsequent steepening of the corneal curvature (Rabinowitz 1998, Davidson, Hayes et al. 2014, Gordon-Shaag, Millodot et al. 2015). The resulting change in shape of the corneal refractive surface causes an increase in irregular astigmatism, progressive myopia and associated visual loss. At the early stage of the ectasia, refractive correction can be achieved with glasses and often improved further by contact lenses. However, with progressive thinning of the cornea, the structural integrity is compromised further and focal areas of elevation and weakness occur.

Keratoconus is a disease that presents mainly in the younger population and exhibits a male preponderance. Fuchs endothelial corneal dystrophy conversely is a disease of later life with a higher incidence among women. FECD is also more commonly seen in the Caucasian population while the prevalence of The estimated incidence of KC is between 3.3-13.3 per 100000 in White European population and 19.6-25 per 100000 in South Asians, whilst the prevalence has been predicted to be 55-57 and 229 per 100000 in these two ethnic groups, respectively (Pearson, Soneji et al. 2000, Georgiou, Funnell et al. 2004, Godefrooij, de Wit et al. 2017).

Unlike keratoconus which can rarely present unilaterally, FECD is a bilateral disease albeit with sometimes varying degrees of severity between each eye (Ferdin, Nguyen et al. 2019).

In patients with keratoconus, a more objective approach to defining disease progression has been adopted as the introduction of new treatment modalities such as corneal cross linking created the need to identify the optimal therapeutic window in the natural history of the disease. Scheimpflug imaging scans of keratoconic eyes allow clinicians to assess and compare tomographical and refractive 3-dimensional measurements of the cornea at separate time points. This allows the monitoring of keratoconus progression by defined and objective parameters. A protocol is implemented at MEH to define progression based on the Scheimpflug imaging parameters and to allow a more standardized approach to (Appendix D).

In addition to assessing progression of ectasia by these parameters, in cases where the diagnosis of keratoconus is uncertain, the profile of both the anterior cornea (anterior float) and posterior corneal (back float) are taken in consideration. Although the anterior profile of the cornea may retain a relatively normal shape, ectasia are often found to manifest first as abnormal elevations of the posterior corneal curvature. These posterior changes can persist even in the presence of stromal oedema and

believe the existence of a subclinical ectasia. Careful evaluation of these various corneal measures is therefore important in ascertaining the diagnosis of keratoconus in combination with FECD.

The dual presentation of FECD and Keratoconus in patients is a rare but recognised clinical entity (Lipman, Rubenstein et al. 1990, Jurkunas and Azar 2006, Salouti, Nowroozzadeh et al. 2010, Kaushik, Jain et al. 2015)(Table 1). As noted in Chapter 2 (Section 2.5 Discussion) , within the sample of 342 patients in the MEH FECD study, the incidence of keratoconus was higher than previously reported in comparative population studies (0.9% versus 0.03%- 1.2%; average 0.31% ). This finding highlighted the need for a more detailed study of this subset of patients who present with both forms of corneal pathology.

The first reports of concurrent FECD and keratoconus in the literature were in the 1990s (Lipman, Rubenstein et al. 1990, Orlin, Raber et al. 1990). To date there are 13 publications identifying this combined pathology, consisting mainly of case reports and case series, with Cremona *et al* and Parker *et al* publishing largest studies of the condition (Cremona, Ghosheh et al. 2009, Parker, Birbal et al. 2019). A summary of the literature to date is provided in Table 1. Across these publications patients were diagnosed at various stages of the disease, from early presentation of visual loss to incidental late findings at the time of assessment for cataract surgery. Orlin *et al* present the only known case of the combined pathology occurring in the paediatric population, while all other cases are reported in patients over the age of 30 years (Orlin, Raber et al. 1990). A meta-analysis of the published data by Mylona *et al* noted that of the total 69 cases, there exists a slight female preponderance of 56.5% (39/69) although this was not statistically significant (Mylona, Tsinopoulos et al. 2020). However, it should be noted that in their analysis, Mylona *et al* included publications by Darlington *et al*, Martone *et al* and Alexandrakis *et al*, that do not fulfil the criteria for the diagnosis of combined keratoconus and FECD on the basis that the first 2 case studies reported unilateral guttata while the third case describes the development of guttata on corneal graft tissue following graft surgery in keratoconus patients (Alexandrakis, Filatov et al. 2000, Darlington, Mannis et al. 2001, Martone, Tommasi et al. 2007). Correcting for this, the female preponderance is reduced to 52.9% (36/68).

It was not possible to ascertain from the literature the interval between the two diagnoses within this patient population. Further to this, there is no published data examining the prevalence of the concurrent presentation of KC and FECD. Cremona *et al* analysed retrospective data over a 10-year period of patients diagnosed with corneal dystrophies at the Wills Eye Hospital, Pennsylvania, United States. Their study of 51 keratoconus patients with other concomitant corneal dystrophies showed that the most common dual pathology was FECD (27/51 cases, 52.9%) (Cremona, Ghosheh et al. 2009).



This finding is in keeping with FECD being the most common corneal dystrophy and does not in itself prove a shared causal link between the two conditions (Vedana, Villarreal et al. 2016). Although some reports speculate that a shared genetic cause may underlie the pathophysiology of both conditions, no definitive genetic link between the two has been established. However, a recent high powered keratoconus genome wide association study has identified two distinct loci, encompassing *PIDD1/SLC25A22* (rs7117921,  $p = 1.09 \times 10^{-26}$ ) and *ATP1B1* (rs1200108,  $p = 4.52 \times 10^{-10}$ ), that had previously also been demonstrated to confer susceptibility to FECD by an independent GWAS (Afshari, Igo et al. 2017, Hardcastle, Liskova et al. 2021). It is yet to be determined if these signals of association are driven by distinct or common variants. However, it is tempting to speculate that variants at these loci could confer shared suitability for both diseases.

Mazzotta *et al* report a single case of a 55 year old subject presenting with clinical symptoms of FECD and keratoconus as well as epithelial basement membrane dystrophy who was shown to harbour a heterozygous variant in exon 7 (c.1920G>T; p.Gln640His) of the *ZEB1* gene. The variant was believed to be disease causing based on previous reported findings by Lechner *et al* identifying mutations in *ZEB1* in individuals who presented with isolated FECD and keratoconus, suggesting a possible shared mechanism of disease (Lechner, Dash et al. 2013, Mazzotta, Traversi et al. 2014). However, given the lack of segregation analysis reported by both studies it remains plausible that the *ZEB1* variant only underlies FECD and not KC in these probands.

In cases of combined KC and FECD, penetrating keratoplasty has been the treatment modality of choice as it replaces both the ectatic epithelial and stromal layers as well as the thickened basement membrane and compromised endothelial layer. However, the published literature further demonstrates a shift in surgical management of this patient population away from full thickness corneal transplantation towards partial thickness posterior endothelial keratoplasty in cases where endothelial decompensation was the primary cause of visual loss (Jurkunas and Azar 2006, Vira, Abugo et al. 2014, Price and Price 2017). In adapting posterior lamellar surgery in a subset of the KCFECD population, it is important to consider the implications of residual irregular astigmatisms in the patient population and the implications to post-operative visual rehabilitation.

Author	Year	N	Gender M:F	Findings
Lipman et al. (Lipman, Rubenstein et al. 1990)	1990	1	0:1	Familial component as FECD was noted in three female generations and keratoconus in both male and female relatives across 2 generations  Criteria of clinical diagnosis not provided. Histological specimen obtained at time of PK showed features of epithelial thickening , dimpling of Bowman's membrane , guttata and thickened Descemet's Membrane
Orlin et al. (Orlin, Raber et al. 1990)	1990	5	2:3	To report clinical findings of 5 patients with combined KF+FECD including histopathology of 2 corneas following penetrating keratoplasty  Reports the only case in the literature of a child (15 years old) showing signs of both pathology
Jurukunas et al. (Jurkunas and Azar 2006)	2006	8	3:5	Normalisation of corneal pachymetry was shown to occur in a subset of patients, potentially masking disease severity recommends the routine use of preoperative corneal topography and specular microscopy in such case  Diagnostic criteria: KC diagnosed on topographic finding of inferior steepening and FECD based on presence of guttae on slit-lamp examination and reduced cell counts with pleomorphism and polymegathism on specular microscopy
Cremona et al. (Cremona, Ghosheh et al. 2009)	2009	27	9:16	FECD was shown to be the most common concomitant corneal dystrophy in patients with keratoconus at the Will Eye Institute (27/51 cases, 52.9%)  Diagnostic criteria: KC diagnosed on topographic findings of localized steepening, Slitlamp and pachymetric assessment of corneal thickness. FECD based on slit-lamp findings of guttata and specular microscopy confirmation of guttae, pleomorphism and polymegathism.
Salouti et al. (Salouti, Nowroozadeh et al. 2010)	2010	2	0:2	Clinical description of 2 cases of bilateral KC+FECD  KC diagnosed on topographic finding of inferior steepening and FECD based on presence of guttae on slit-lamp examination and reduced cell counts with pleomorphism and polymegathism on specular microscopy
Vira et al. (Vira, Abugo et al. 2014)	2014	4	2:2	Reports the viability of DSEK surgery in KC+FECD Specifies that the procedure should be attempted in patient who have yet to develop apical scarring secondary to KC  KC diagnosed on topographic finding of inferior steepening and FECD based on presence of guttae on slit-lamp examination
Mazzotta et al. (Mazzotta, Traversi et al. 2014)	2014	1	1:0	Reports the finding of a potential mutation in the <i>ZEB1</i> gene as the underlying cause of the dual pathology  As no comprehensive segregation data was provided, it is not possible to conclude that both phenotypes are attributed to this single variant.

				KC diagnosed on topographic finding of inferior steepening and FECD based on presence of guttae on confocal laser scanning microscopy
Kaushik et al. (Kaushik, Jain et al. 2015)	2015	1	0:1	Case report highlighting the challenge of intraocular lens selection in this patient population and the need to anticipate the implication of a hyperopic shift should future corneal endothelial graft be required  KC diagnosed on topographic finding of inferior steepening and FECD based on presence of guttae on slit-lamp examination
Cooper et al.	2017	1	1:0	Reports the viability of DMEK+IOL surgery in KC+FECD  KC diagnosed on topographic finding of inferior steepening and FECD based on presence of guttae on slit-lamp examination
Gupta et al. (Gupta, Kinderyte et al. 2017)	2017	1	1:0	Report surgical outcomes in a case of DMEK+IOL, highlight an unexpected refractive outcome due to the normalization of corneal topography  KC diagnosed on topographic finding of inferior steepening and FECD based on presence of guttae on confocal laser scanning microscopy
Parker et al. (Parker, Birbal et al. 2019)	2019	10	8:2	To report on sixteen eyes of 10 patients with comorbid KC and Fuchs endothelial corneal dystrophy (FECD) underwent uncomplicated Descemet membrane endothelial keratoplasty (DMEK)  Challenges the concept that breaks in Descemet's membrane lead to hydrops in patients with keratoconus as even complete removal of this layer during DMEK surgery did not lead to hydrops.  Diagnostic criteria of KC and FECD not provided.
McKelvie et al (Wang and McKelvie 2020)	2020	1	0:1	Highlights diagnostic monitoring and treatment challenges of dual pathology as well as viability of DMEK as a treatment  Reports atypical late-onset progressive KC in a patient over the age of 40 years  KC diagnosed on topographic finding of inferior steepening and FECD based on presence of guttae on slit-lamp examination and reduced cell counts with pleomorphism and polymegathism on specular microscopy

Table 1: Literature review of combined cases of Keratoconus and FECD. The table summarises the 66 reported cases to date of patients presenting with both KC and FECD from 1990 to present day. The findings suggest a slight female preponderance of 52.9% (36/68). Orlin *et al* present the only known case of the combined pathology occurring in the paediatric population, while all other cases are reported in patients over the age of 30 years. Studies that discuss surgical treatment highlight the viability of partial thickness

endothelial keratoplasty in this patient population, while Parker *et al* further query the existing pathophysiological finding of hydrops in keratoconus based on their intraoperative experience of DMEK in this population.

## 4.2 Aims

The hallmark thinning of the cornea in KC can be masked by the progressive oedema seen in FECD, creating a diagnostic challenge to ophthalmologists. Further to this, the diametrically opposed approach to surgical management of these two diseases introduces further uncertainty in the choice of corneal transplant technique adopted to provide maximal visual rehabilitation while minimising risk to the patient. It is therefore important to recognise that both conditions can co-exist and highlight the clinical appearance of the cornea when both pathologies manifest simultaneously.

I aim to identify cases of combined FECD and keratoconus in the MEH patient population and to document the pattern of first clinical presentation and the natural progression of the disease. In addition, I will report the outcomes of corneal endothelial graft surgery within this cohort so as to understand the potential challenges in the diagnosis and treatment of this group of patients.

Genotyping studies were performed on this sample of patients with combined FECD and KC to determine if CTG18.1 expansion underlies the clinical features of FECD seen in this cohort.

### 4.3 Methods

MEH patients diagnosed with both KC and FECD were identified by first performing a data search of the electronic patient record system for the terms “ Fuchs”, “Keratoconus” and “Ectasia”. The identified patient records were then searched individually to confirm the presence of verified diagnosis of both diseases in 17 individuals (32 eyes). FECD was defined as confluent central corneal guttata on slit lamp biomicroscopy. Keratoconus was diagnosed on clinical examination as well as topographic evidence of ectasia (stromal thinning, irregular astigmatism).

Slitlamp biomicroscopy findings, corneal topography and sequential central corneal thickness (CCT) were obtained for the 17 subjects. Surgical interventions and clinical reasoning for surgical decisions were also recorded along with surgical outcomes.

Genotyping was performed on 11 patients to determine CTG18.1 repeat expansion status (Appendix A). Written informed consent was received from all participants who provided blood for this study. Genomic DNA was extracted from whole blood using conventional methodologies.

#### 4.4 Results

A total of 17 adult patients were identified as having a diagnosis of combined FECD and keratoconus (Table 2). The cohort consisted of 8 male and 11 female patients. In all but one patient, keratoconus was diagnosed bilaterally. In the single case of unilateral KC, the contralateral eye was considered a keratoconus suspect as signs of ectasia were only noted on the posterior profile of the cornea.

Most patients who presented were White (n=9, 52.9%) with the remaining population comprised of 6 Black patients (35.3%) and 2 (11.8%) South Asian patients. Of the 17 patients, 5 patients were diagnosed with keratoconus first, 3 were initially diagnosed with FECD and in 4 patients both pathologies were recognised at first presentation. The average age of patients first diagnosed with KC was 37.8 years (ranges: 26 – 46 years) while the average age of patients first diagnosed with FECD was 50.3 years (range: 38-69 years). No statistically significant difference was noted between the age of diagnosis of the second corneal pathology between patients diagnosed with FECD first versus those diagnosed with KC first [t-test: p= 0.8176 (CI: -20.76 -25.25)]. Five patients were referred from other hospitals and the sequence of diagnosis could not be ascertained. Sixteen of the seventeen patients were followed up for an average period of 48 months (range of follow up: 6-91 months). One patient did not attend further appointments following the first assessment and diagnosis. As 3 patients had undergone corneal transplant surgery prior to referral to MEH and one patient was listed for keratoplasty on the first visit, local follow up data was available for 28 eyes in this cohort.

In patients where FECD was diagnosed first (3 patients), the time to KC diagnosis was on average 1.3 years. The diagnosis of keratoconus was made as a result of routine Scheimpflug imaging scans in 2 cases and the third patient was noted to show signs of the ectasia on pre-assessment for cataract surgery. When KC was the primary diagnosis, FECD was diagnosed on average 9 years later based on slitlamp findings of central guttata and 3 of the 5 also exhibited signs of central stromal corneal oedema. Specular microscopy was performed in 8 eyes but endothelial cell count (ECC) could not be obtained in 3 eyes due to the severity of FECD. Mean ECC was  $1769.6 \pm 723.08/\text{mm}^2$  and none of the analysed eyes had undergone corneal transplantation. Specular images of corneal endothelium revealed abnormal mosaic pattern with dark areas and prominent edges compatible with corneal guttata. Pleomorphism and polymegathism were also present.

Ambiguity in diagnosis occurred in one case, as guttae were mistaken for Krukenberg spindles in keeping with the known diagnosis of pigmentary glaucoma, causing a delay in the initial diagnosis of FECD by 2 years. "Pseudo" guttata were also considered as a potential differential in this population of KC patients in whom some patients achieved Best Corrected Visual Acuity with rigid contact lenses.

Contact lens related hypoxia can lead to the appearance of guttata on Descemet's Membrane, but similar to guttata seen in inflammation this finding is transient and improves when contact lens wear is reduced (Moshirfar, H et al. 2019).

Of the 28 eyes of 16 patients studied, 9 showed an increase in central corneal thickness suggestive of corneal decompensation secondary to FECD, while 17 eyes showed thinning of the central cornea in keeping with KC progression. It was interesting to note that in 6 patients (37.5%), while one eye showed signs of thinning the contralateral eye showed signs of increased corneal thickness (Table 3).

In addition to the diagnosis of the two corneal pathologies, eight patients in this cohort were also noted to have other ocular co-morbidities: 5 cases of glaucoma, 1 age related macular degeneration and 1 patient was diagnosed with floppy eyelid syndrome. Of the five cases of glaucoma, two were noted to have normal tension glaucoma, one case of pigmentary glaucoma, one primary open angle glaucoma and one developed secondary glaucoma following corneal graft surgery as a result of topical steroid drops (Table 2). One patient had Ehler-Danlos syndrome, a condition known to be associated with KC but not FECD (Ihalainen 1986).

#### 4.4.1 Genetic Analysis

Blood samples were obtained from 11 patients in this cohort to allow genotyping for the CTG18.1 repeat expansion (Table 2). Six patients were positive for the repeat (defined as harbouring at least one allele with  $\geq 50$  CTG repeats). Of the 11 patients genotyped, disease onset and diagnosis data were available for 9 patients. The average age of FECD diagnosis in the expansion positive patients was 56.75 years compared to 46.8 years in the expansion negative individuals. This difference was statistically significant, (Chi square  $p=0.0434$ ).

The expansion positive cohort was predominantly White (5/6) while the majority of the expansion negative sample was non-White (4/5). No statistically significant association was found between the ethnicity and expansion status (Chi square  $p=0.36$ ). The 5 (71.3%) of the male patients were found to harbour the repeat compared to one (25%) of the 4 female patients. Although this result is in keeping with the finding within the larger FECD cohort that men are more likely to harbour the repeat expansion ( $p<0.005$ ) (Chapter 2, section 2.4.1.1.2), the finding within the dual pathology cohort was not found to be statistically significant (Chi square  $p=0.14$ ).



Patient ID	Gender	Ethnicity	Expansion Status (Allele Length)	Age of FECD diagnosis	Age of KC Diagnosis	Interval Between KC and FECD Diagnosis (years)	Surgical Intervention (Age of surgery)		Other Ocular Co-Morbidities
							Right	Left	
KF 1	M	White	Positive (18, 70)	61	43	18	NR	NR	Normal Tension Glaucoma
KF 2	F	Black	N/A	55	30	25	NR	NR	Normal Tension Glaucoma
KF 3	F	Asian	N/A	50	N/A	N/A	none	PK (49)	None
KF 4	F	Black	Negative (12, 18)	34	26	8	NR	NR	None
KF 5	M	Black	Negative (15, 28)	38	39	-1	DSAEK (46)	NR	Pigmentary Glaucoma
KF 6	M	White	Positive (12, 83)	69	71	-2	NR	NR	Age related macular degeneration
KF 7	F	Black	N/A	35	35	0	CXL (39)	NR	None
KF 8	M	White	N/A	44	45 (unilateral)	-1	DMEK+Phaco +IOL (54)	PK (48)	None
KF 9	F	White	N/A	N/A	N/A	N/A	PK (68)	NR	Floppy eyelid syndrome
KF 10	F	Black	Negative (15, 18)	58	58	0	NR	NR	None
KF 11	M	Asian	Positive (12,125)	51	46	5	NR	NR	None
KF 12	F	Black	Negative (16, 16)	54	54	0	DSAEK+Phaco + IOL (57)	DMEK + Phaco + IOL (56)	None
KF 13	M	White	Positive (18, 85)	N/A	69	N/A	DMEK (69)	PK (61)	Primary Open angle Glaucoma
KF 14	F	White	Positive (18, 90)	N/A	N/A	N/A	PK (34)	NR	Secondary glaucoma (steroid response)
KF 15	F	White	N/A	34	34	0	CXL (38)	CXL (38)	None
KF 16	M	White	Positive (18, 85)	46	44	2	NR	NR	None
KF 17	M	White	Negative (12, 27)	50	50	0	PK + Phaco +IOL (52)	NR	None

Table 2: Tabulation of demographic data, CTG18.1 repeat expansion status, surgical intervention and other ocular co-morbidities within the KC FECD patient population. The average age of patients first diagnosed with KC was 37.8 years (ranges: 26 – 46 years) while the average age of patients first diagnosed with FECD was 50.3 years (range: 38-69 years). The data shows that the population is predominantly White with a slight female preponderance. Repeat expansion status data was available for 11 of the 17 patients. A greater proportion of male patients harboured the mutation but the association between gender and expansion status in the dual pathology cohort was not found to be statistically significant ( $p=0.14$ ). No statistically significant association was noted between the ethnicity and expansion status (Chi square  $p=0.36$ ). The average age of FECD diagnosis in the expansion positive patients was 56.75 years compared to 46.8 years in the expansion negative individuals. This difference was statistically significant, (Chi square  $p=0.0434$ ). Co-pathology noted in this patient population included 5 patients diagnosed with glaucoma, 1 case of age related macular degeneration and 1 case of floppy eyelid syndrome. Fourteen eyes in this study required surgical intervention in the form of corneal transplantation ( $n=11$ ) and cross linking ( $n=3$ ).

Patient ID	Period of Follow Up Right Eye (months)	Period of Follow Up Left Eye (months)	Right Eye Progression				Left Eye at Progression			
			CCT ( $\mu\text{m}$ )	K1 (D)	K2 (D)	Kmax (D)	CCT ( $\mu\text{m}$ )	K1 (D)	K2 (D)	Kmax (D)
KF 1	84	84	↓90	↓0.1	↑0.3	↑5.0	↑28	↑1.3	↓1.1	↑12.5
KF 2	96	96	↓25	↑7.8	↑4.0	↑14.5	↓3	↑1.9	↑0.1	↑1.1
KF 3	25	-	↓10	↑0.8	↑0.3	↑0.5	-	-	-	-
KF 4	42	42	↑18	↑0.7	↑2.9	↑1.7	↓35	↑0.1	↑0.8	↑0.4
KF 5	91	91	↑94	↓3.9	↓3.2	↓3.6	↓1	↑0.9	↑1.8	↑1.3
KF 6	-	-	-	-	-	-	-	-	-	-
KF 7	51	51	↓23	↑0.7	↑0.3	↑0.5	↑30	↓0.5	↓0.8	↓0.7
KF 8	60	14	↓24	↑0.1	↓0.2	↓0.1	↓34	↓1.5	↑0.8	↓0.4
KF 9	-	66	-	-	-	-	-	↑4.6	↑0.7	↑2.8
KF 10	53	53	↓15	↓0.3	↓0.6	↓0.4	↓9	↓1.2	↓1.1	↓1.1
KF 11	57	57	↑9	↑4.0	↑1.0	↑2.6	↑13	↑4.7	↑1.6	↑3.2
KF 12	19	7	↓2	↑0.2	↓0.1	↑0.1	↓15	↑0.5	↑1.2	↑0.8
KF 13	3	-	-	-	-	-	-	-	-	-
KF 14	-	21	-	-	-	-	↑4	↑0.5	↓0.6	0
KF 15	6	6	↑6	↑0.1	↑1.1	↑0.5	↓17	↓0.1	↑0.3	↑0.1
KF 16	17	17	↓5	↓0.8	↓1.6	↓1.2	↓1	↓2.0	↓1.4	↓1.7
KF 17	11	11	↓11	↑0.2	↓0.2	↑0.1	↑5	↓0.9	↑0.1	↓0.5

Table 3: Follow up and progression data of KCFED patients documenting changes in corneal curvature and central corneal thickness. Follow up data was available for 28 eyes of 16 patients within this cohort. The follow up period ranged from 3 to 96 months (average 44 months) and covered the period from first attendance at Moorfields Eye Hospital/diagnosis to the last available follow up review or to the point of surgical intervention. Nine eyes (32.1%) were noted to show an increase in central corneal thickness from baseline scans, suggestive of corneal decompensation secondary to FECD, while 17 eyes (60.7%) showed thinning of the central cornea in keeping with progressive ectasia. It was interesting to note that in 6 patients (37.5%), while one eye showed signs of thinning the contralateral eye showed signs of increased corneal thickness demonstrating that disease progression can show intraindividual asymmetry.

#### 4.4.2 Surgical Intervention

Of the 34 eyes in the 17 patients studied, 14 required surgery due to disease progression. Six eyes were treated with penetrating keratoplasty (PK), with one case performed as a combined procedure to allow removal of cataract and insertion of an intraocular lens. Of the 6 cases, 3 of the transplants were performed at other hospitals prior to referral to MEH. The average age at which patients underwent PK was 58 years (range 34 to 68 years).

Five eyes were treated for corneal decompensation by undergoing posterior lamellar endothelial transplantation. Specifically, 3 eyes underwent DMEK surgery (2 combined with cataract extraction and intraocular lens implantation) and 2 eyes were treated by DSAEK surgery (1 combined with cataract extraction and intraocular lens implantation). The average age for DMEK was 59.7 years (range 54-69 years) and the average age of DSAEK was 51 years (46 and 57 years).

Patients who underwent surgical intervention are discussed in greater detail as case studies in the following section.

##### 4.4.2.1 Case studies

###### A. Case report KF13

KF13 is a white male who was first diagnosed with keratoconus in his mid-thirties. The condition was noted bilaterally but was more advanced in the left eye for which he underwent a combined full thickness penetrating keratoplasty, cataract extraction and intraocular lens implantation at his local hospital at the age of 61 years. He was referred to Moorfields Eye Hospital a year after surgery for treatment of advanced normal tension glaucoma in both eyes. A right trabeculectomy was performed when he was 65 years old. It was noted at that time that the right eye, which has undergone cataract extraction at the age of 62 years, showed signs of corneal decompensation secondary to FECD.

KF13 was then referred to the corneal service at the age of 69 years with a right best corrected Snellen visual acuity of 6/18 ph 6/12 and Hand Movements vision in the left eye. The poor vision in the left eye was the result of optic nerve damage secondary to glaucoma, as confirmed by the presence of a relative afferent pupillary defect. The visual acuity in the right eye was attributed in part to central corneal oedema visible on slitlamp examination as well corneal structural changes in keeping with ectasia. The Scheimpflug tomography scan of the right eye showed an area of inferior steepening on the anterior curvature with milder corresponding changes on the posterior float, indicative of an ectasia. The thinnest point of the cornea was off axis and displaced inferotemporally. However, due

to the presence of corneal oedema, it was noted that even at the thinnest point the cornea maintained a thickness of 540 $\mu$ m and the central cornea was slightly thickened at 578 $\mu$ m (Figure 1). The changes in corneal curvature resulted in irregular astigmatism of 1.5D.

Genotyping was performed and further confirmed the clinical diagnosis of FECD by identifying a homozygous *TCF4* intron expansion, 85 repeats in length.

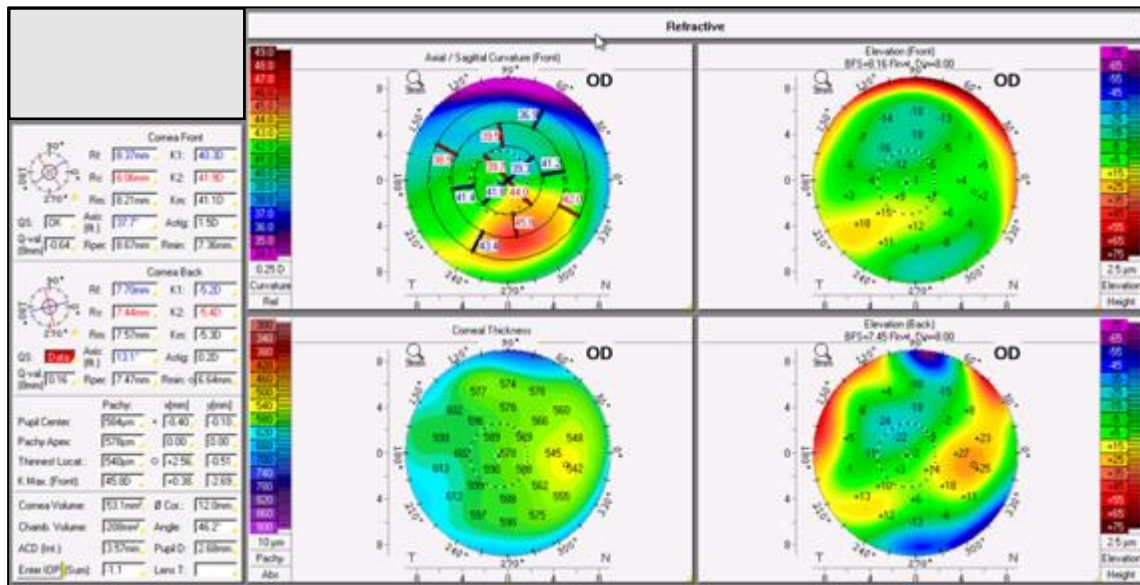


Figure 1. Pre-operative Scheimpflug corneal tomography (Pentacam) scan of KF13's right eye at the age of 69 years. The pentacam scan shows an area of inferior steepening on the anterior curvature float with milder corresponding changes of the posterior float, indicative of an ectasia. The thinnest point of the cornea is off axis and displaced intertemporally. The thinnest point of the cornea is 540  $\mu$ m and the central cornea is 578 $\mu$ m.

Clinical evaluation of the corneal changes suggested that oedema was the main cause of visual loss and KF13 was listed for DMEK surgery to the right eye. Following uncomplicated graft surgery, the post-operative best spectacle corrected visual acuity in the right eye improved to Snellen 6/7.6 and was maintained over a 2 year follow up period. Scheimpflug corneal tomography (Pentacam), performed 25 months following surgery are more evident of corneal ectasia with a prominent area of inferior corneal steepening on both the anterior and posterior float. Resolution of the oedema lead to a reduction in central corneal thickness to 452 $\mu$ m (Figure 2).

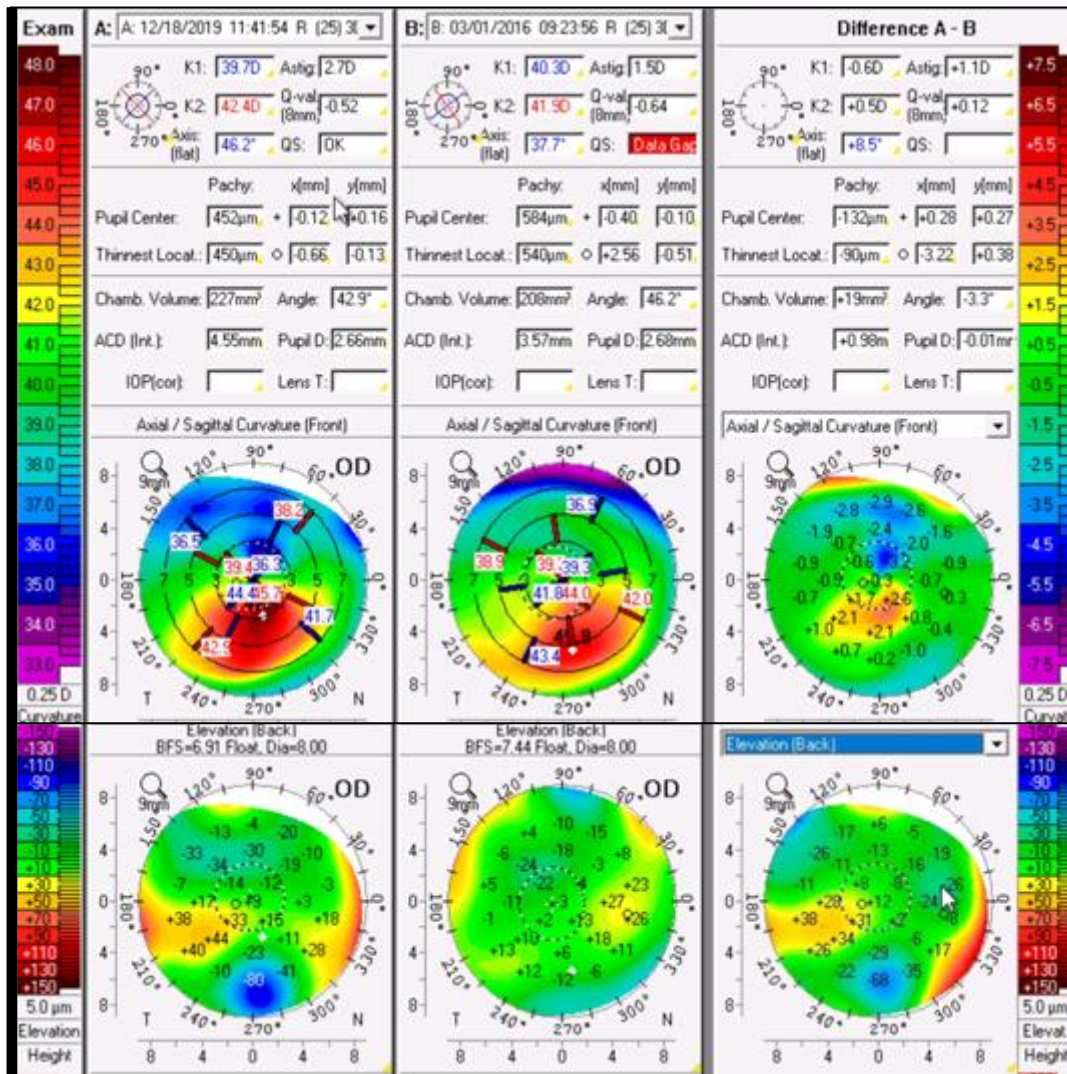


Figure 2: Comparative Scheimpflug corneal tomography (Pentacam) scans performed 25 months following Right DMEK surgery in subject KF13. Resolution of corneal oedema from 584µm to 452µm has created a more evident area of corneal ectasia with a prominent area of inferior corneal steepening on the anterior float and posterior elevation shows a maximal increase of 67µm. The corneal astigmatism increased by 1.1D but the post-operative best corrected spectacle visual acuity in the right eye improved to Snellen 6/7.6

B. Case report KF12

KF12 is a Black African female who was referred at the age of 54 years by her optician as a keratoconus suspect. The best spectacle corrected Snellen visual acuity was 6/9 in the right eye and 6/12 in the left eye on first assessment. The left eye was noted on presentation to show irregular astigmatism (K1 37.9D, K2 46.9D) and an area of greatest elevation noted inferiorly (Kmax 54.0D) (Figure 3 B). The ectasia was most prominent inferotemporally on both the anterior and posterior elevation profiles. The

central corneal thickness was 474 $\mu$ m and the thinnest area was 460 $\mu$ m. Although the irregular astigmatism and area of maximal elevation was less pronounced in the right eye (K1 39.3D, K2 41.7D, Kmax 42.5D), an area of inferotemporal elevation in keeping with keratoconus was noted on the posterior elevation scan (Figure 3 A). The central corneal thickness was 469 $\mu$ m and the thinnest area was 462 $\mu$ m.

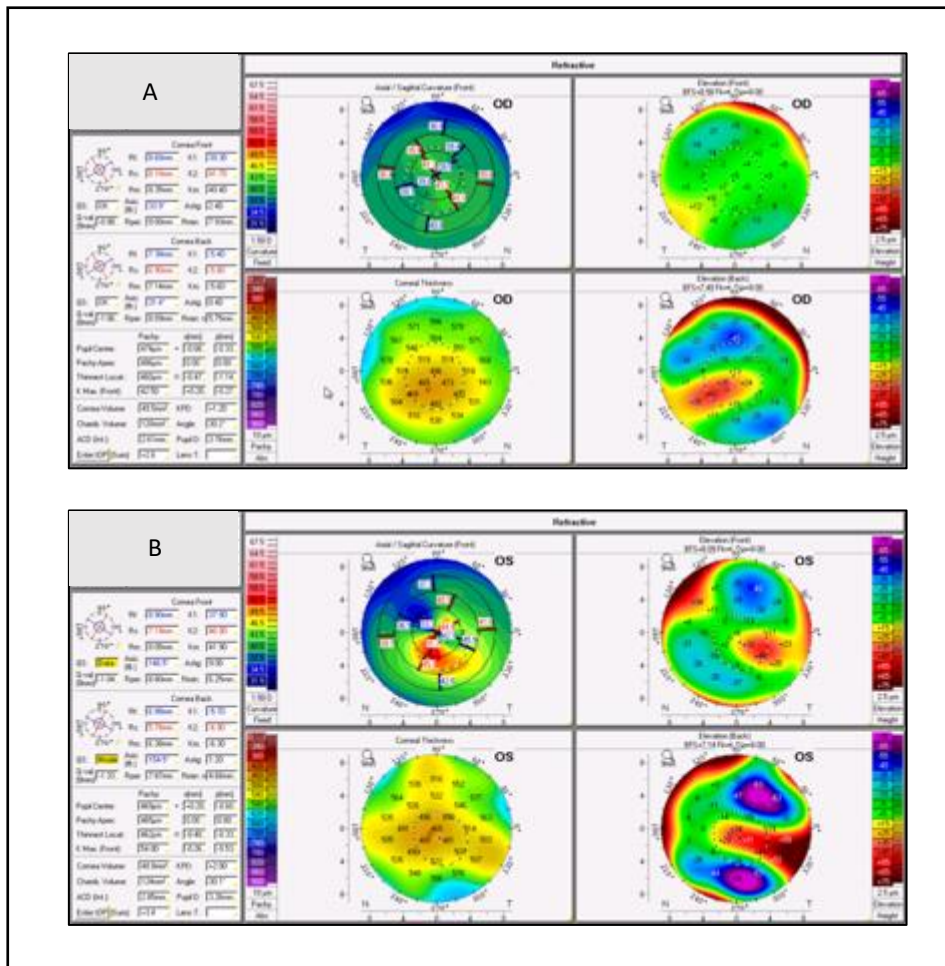


Figure 3. Scheimpflug corneal tomography (Pentacam) scans obtained from KF12 on presentation at the age of 52 years. A: Pentacam scans of the right eye show an area of inferotemporal elevation in keeping with keratoconus. There is a corresponding corneal thinning and irregular astigmatism in the right eye. B: Both the anterior and posterior float of the left eye show an area of greatest elevation inferotemporally. There a greater degree of corneal astigmatism in the left eye than the right.

At the time of presentation, central guttata and mild stromal oedema were noted bilaterally leading to the diagnosis of FECD. The patient reported diurnal fluctuation in vision, mainly in the left eye, with the vision also effected by the presence of a cataract. KF13 was offered left DMEK surgery in

combination with cataract extraction and intraocular lens implant to address both the cataract and corneal decompensation secondary to FECD.

Following the left DMEK surgery in the left eye at age 55 years, the visual acuity improved but resolution of corneal oedema lead to greater prominence of corneal ectasia. The central corneal thickness 5 months post-transplant dropped to 381 $\mu$ m with the thinnest local area of 371 $\mu$ m (Figure 4). The post-operative best corrected spectacle visual acuity in the left eye was 6/9.

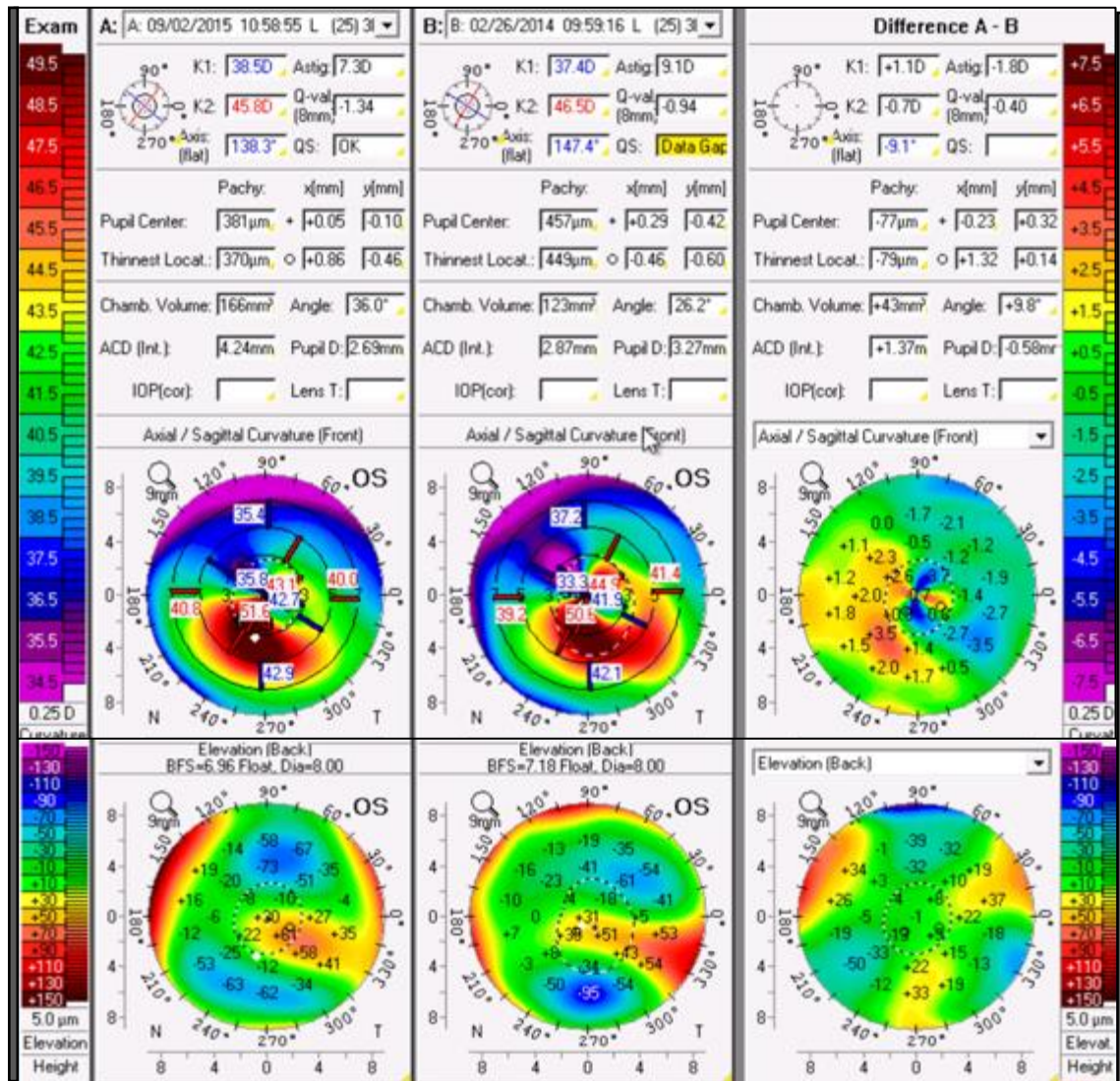


Figure 4. Scheimpflug corneal tomography (Pentacam) obtained from KF12 following left DMEK surgery. Resolution of corneal oedema lead to a central corneal thickness of 381 $\mu$ m with a thinnest area measuring 370 $\mu$ m located inferotemporally, -0.59mm from the apex. With the resolution of stromal oedema, a greater normalisation of the corneal thickness spatial profile was noted. Despite the residual irregular astigmatism, the patient achieved 6/9 Best Corrected Spectacle Visual Acuity in the left eye.



Over a 2 year period of monitoring, the right eye showed signs of early cataract and it was felt to be the main contributing factor to the decline of best corrected Snellen visual acuity of 6/15. Cataract surgery was performed but required a secondary phacolytic and vitrectomy to remove lens fragments from the posterior chamber. Post lens extraction surgery the right eye remained aphakic and further progression of central corneal oedema was noted (CCT 476 $\mu$ m).

In view of both the previous post-operative increase in ectasia that was noted following left DMEK surgery as well as the aphakic state of the right eye, DSAEK surgery combined with intraocular lens implantation was performed to address endothelial decompensation in the right eye.

Resolution of corneal oedema following right DSAEK surgery did not reveal significant underlying corneal ectasia. The corneal graft (shown in figure 5A) comprised a lamellae of stromal tissue in addition to Descemet's membrane and endothelial cells, thus adding approximately 100 $\mu$ m of tissue to the posterior corneal surface. It should be noted, however, that overall irregularity of the corneal curvature on the anterior sagittal section was more prominent following the surgery leading to an increase in astigmatism from 2.4D at presentation to 4.0D post operatively. The best corrected spectacle visual acuity in the left eye following surgery was 6/9. Over a further 14 months of follow up, both eyes remained stable with no progression of ectasia.

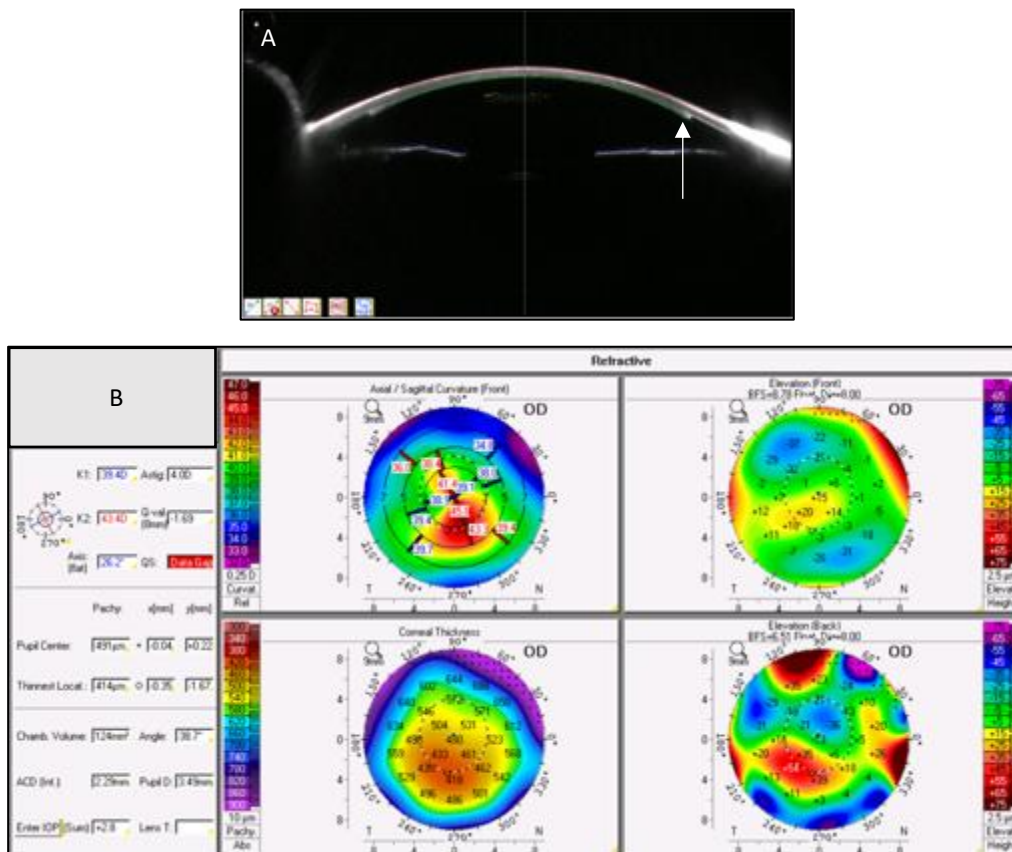


Figure 5: Scheimpflug corneal tomography (Pentacam) of KF12 following right corneal transplant surgery (DSAEK) surgery and intraocular lens implantation. A. In a cross-sectional image, the DSAEK graft is shown to be fully attached to the posterior surface of the cornea and was noted to be 100µm thick. B: The presence of an additional lamellae of transplanted stromal tissue on posterior corneal provides additional corneal thickness to the right cornea allowing a central corneal thickness of 491µm and thinnest area of 414µm despite clinical resolution of corneal oedema. Note however that the irregular corneal astigmatism of the anterior sagittal section is more prominent in the presence of an area of elevation seen inferonasally.

C. Case Report KF8

KF8 is a white male who was first diagnosed with FECD at the age of 44 years based on the finding of corneal guttata and oedema visualised on slit lamp biomicroscopy. An incidental finding of bilateral irregular astigmatism associated with corneal thinning on Pentacam scans lead to the diagnosis of keratoconus the following year. At the time of diagnosis, the left the central corneal thickness was 523 $\mu$ m with the thinnest area of 504 $\mu$ m corresponding to an inferotemporal area of ectasia (Figure 6). Pentacam scans measured irregular astigmatism of 4.3D, with corneal curvature measures of K1 45.1D and K2 49.4D. Due to the irregular astigmatism of the corneal surface secondary to keratoconus, the best corrected Snellen visual acuity of 6/9 in the left eye was achieved in rigid gas permeable contact lenses.

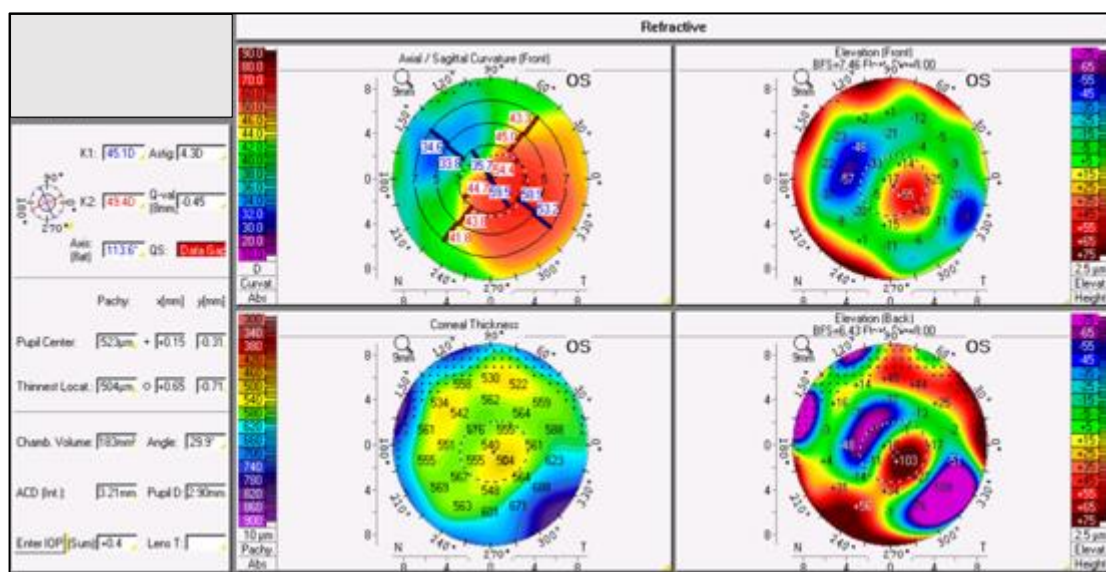


Figure 6: Left eye Scheimpflug corneal tomography (Pentacam) of KF8, a 44 year old white Caucasian male taken at the time of diagnosis. Pentacam scans of the left eye show an area of inferotemporal elevation in keeping with keratoconus. There is a corresponding area corneal thinning of 504  $\mu$ m seen in the area of greatest elevation.

In the right eye, the Pentacam scan showed an area of inferotemporal elevation on the sagittal curvature scan with a corresponding area of elevation seen on the posterior float to support the diagnosis of ectasia (Figure 7). The central corneal thickness in the right eye was 586 $\mu$ m with the thinnest point of the cornea measuring 558 $\mu$ m. The irregular corneal astigmatism was 1.7D, with corneal curvature measures of K1 41.8D and K2 42.6D. The best corrected Snellen visual acuity achieved in hard contact lenses in the right eye was 6/6 unaided.

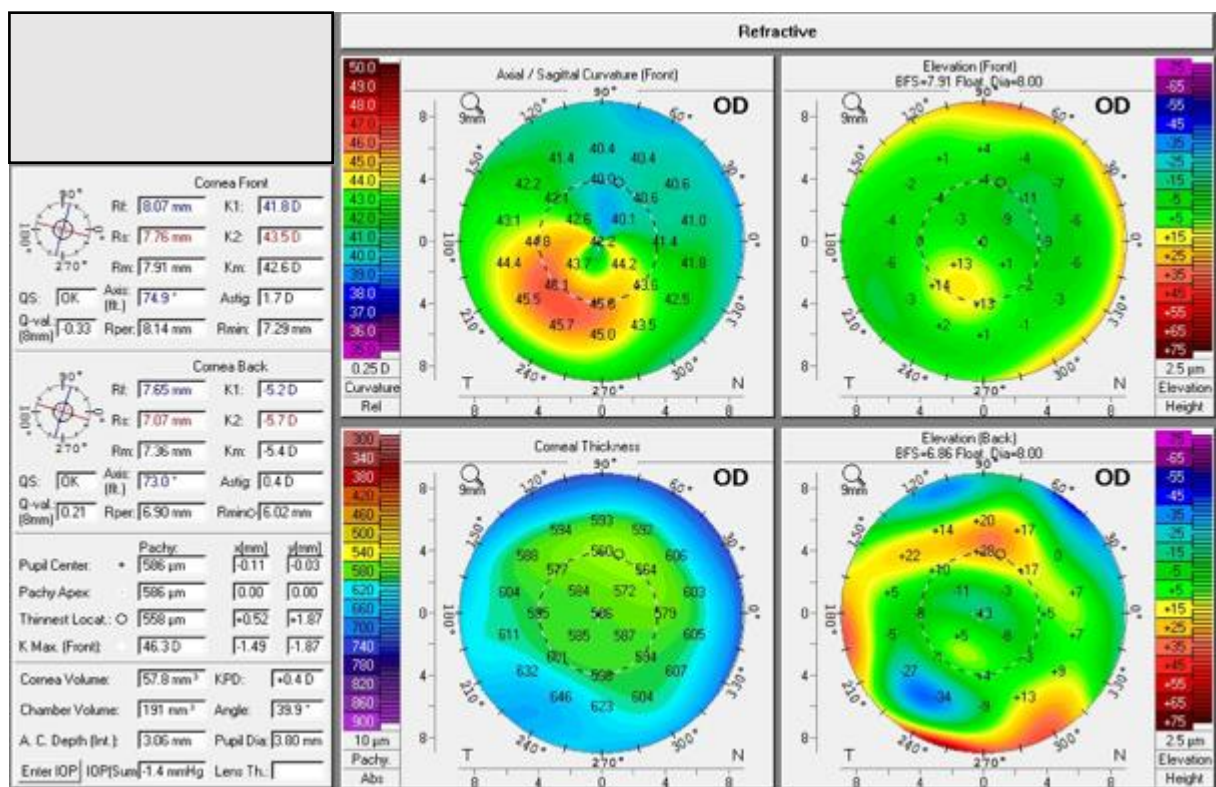


Figure 7: The right Scheimpflug corneal tomography (Pentacam) of KF8, a 44 year old white Caucasian male taken at the time of diagnosis. The scan shows an area of inferotemporal elevation on the sagittal curvature scan that was suggestive of keratoconus supported a milder area of corresponding posterior elevation to support the diagnosis of ectasia. The central corneal thickness was 586μm with the thinnest point of the cornea measuring 558μm. The corneal astigmatism was 1.7D on average with K reading of K1 41.8D and K2 42.6D.

At the time of diagnosis KF8 had become increasingly intolerant of rigid gas permeable and opted to pursue surgical intervention. A left penetrating keratoplasty was performed to treat the combined features of irregular astigmatism and endothelial disease.

Over a period of 7 years follow up, KF8 noted increasing diurnal fluctuation in the right vision which was attributed to oedema secondary to FECD. Due to the increased central corneal thickness and less advanced ectasia of the right eye cornea, he was listed for right DMEK surgery combined with cataract extraction and intraocular lens implantation Figure 8A. Following right endothelial transplantation, the central corneal thickness reduced from 611μm to 485μm and the corneal astigmatism normalised from 4.3D to 1.2D. The posterior float of the cornea did not show significant areas of elevation post-surgery

(Figure 8B). Unaided visual acuity in the right eye improved to Snellen 6/7.5, in keeping with the refractive intraocular lens selection for emmetropia (-0.58D).

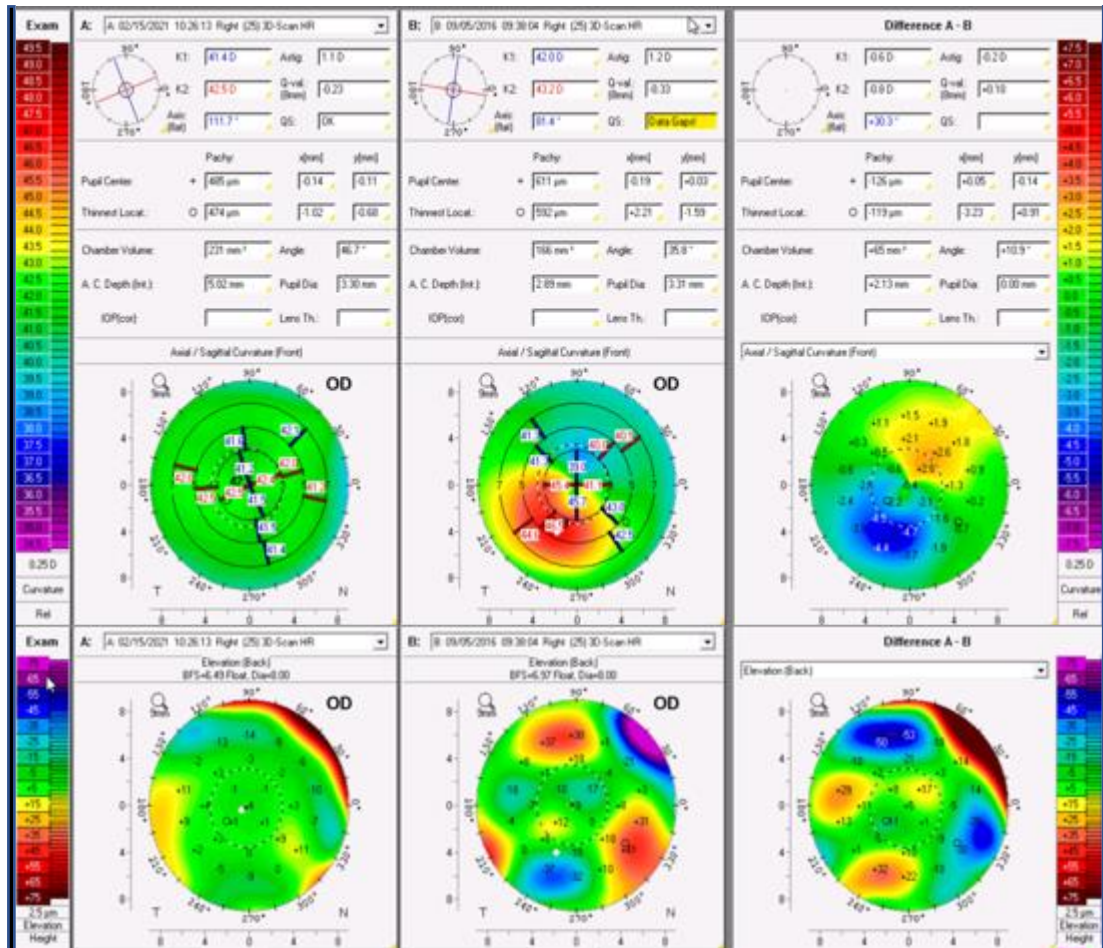


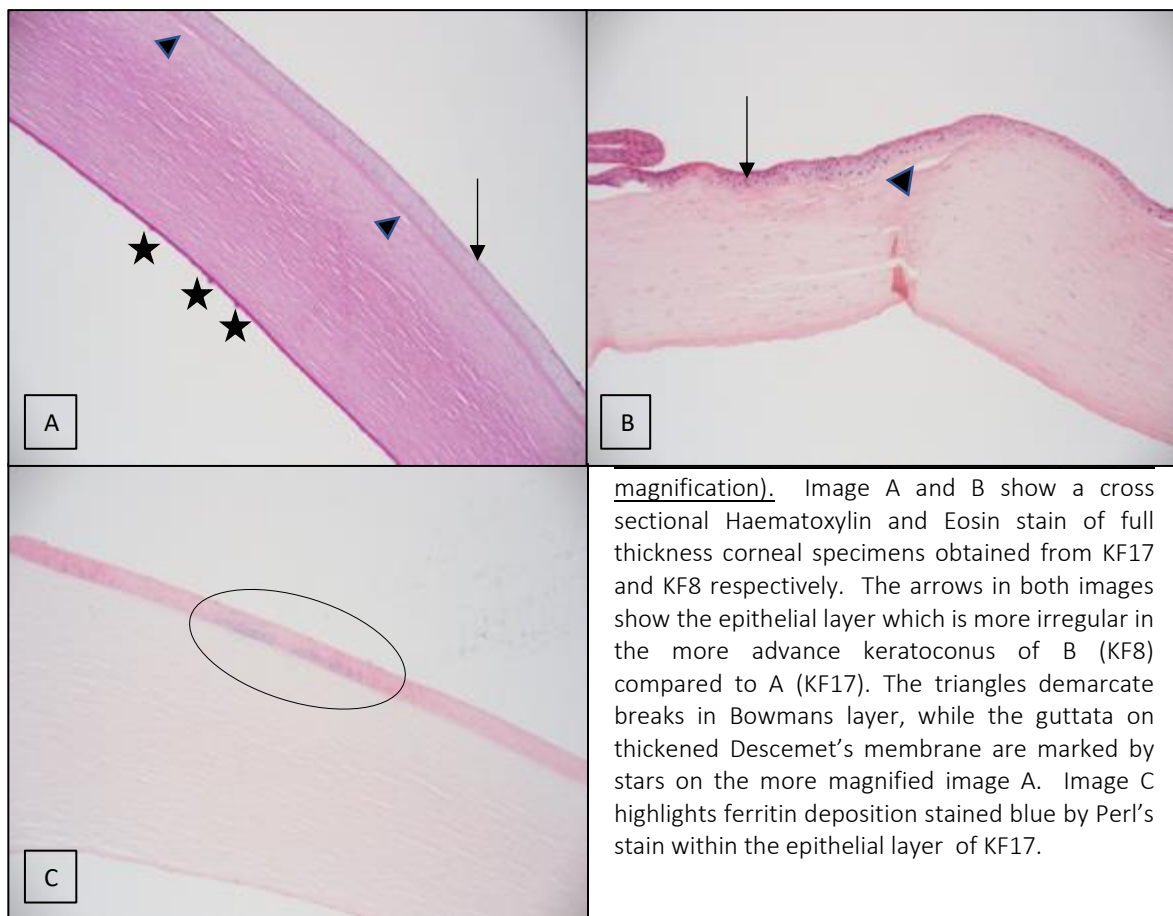
Figure 8: Scheimpflug corneal tomography (Pentacam) of KF8's right cornea pre and post DMEK surgery. KF8's right eye at the age of 51 years showed thickening secondary to corneal oedema along with irregular astigmatism with an area of inferotemporal steepening. Clinically it was assessed that the predominant pathology leading to visual loss in this eye was corneal oedema and cataract which lead to the decision to proceed with right DMEK surgery, cataract extraction and intraocular lens implantation. Following surgery, the scans show resolution of corneal oedema leaving a residual central corneal thickness of 485μm with the thinnest point measuring 474μm. Despite the reduction in corneal thickness, the corneal shape as shown on corneal tomography sections shows a decrease in irregular astigmatism compared to preoperative scans.

#### 4.4.3 Histopathology

Following full thickness corneal transplant surgery to KF8, KF14 and KF17, the excised corneal buttons were sent for histological assessment. While the epithelial thickness from KF17 was noted to be of fairly regular thickness, that of KF14 and KF8 was found to be thin and irregular. This is in keeping with the clinical assessment of KF17 showing signs of less advanced keratoconus with a Kmax of 43.4D compared to more advanced changes in corneal curvature seen in KF14 and KF8 with Kmax readings of 47.2D and 60.8D respectively.

In all cases breaks were noted in Bowman's layer in keeping with keratoconus. Additionally, all specimen exhibited thickened basement membrane displaying exophytic guttata along with depletion of endothelial cells, supporting the diagnosis of FECD.

Perls' staining was performed on specimens from KF14 and KF17 which confirmed the presence of ferrous deposition in the peripheral epithelium expected in keratoconus.



## 4.5 Discussion

This study of 17 MEH patients with co-existing keratoconus and FECD highlights the clinical challenges in both the diagnosis and management of this patient population. Although 23.5% (n=4) of the cohort was diagnosed with both diseases at the time of presentation, in the majority of cases dual pathology was only recognised after a period of monitoring. As keratoconus typically present in early life while FECD commonly presents after the 4<sup>th</sup> decade, the average age of KC diagnosis was 37.8 years while first diagnosis of FECD occurred on average at 50.3 years. This was further reflected in the period between diagnosis, as patients first diagnosed with KC were noted to have signs of FECD on average 9 years later, while the recognition of underlying ectasia in FECD patients occurred on average within 1.3 years.

Interestingly, only 9 of the 28 eyes (32.14% ) diagnosed with both conditions were noted to show an increase in central corneal thickness secondary to corneal endothelial decompensation. In the majority of cases (n= 9, 52.9%), progressive thinning of the cornea secondary to ectasia was the more prominent pathological feature. However, the disease process was not symmetrical between the two eyes, as noted in the case of 6 patients in whom one eye exhibited an increase in corneal thickness while the contralateral eye thinned due to ectasia. This finding is relevant when counselling patients in regards to the natural history of their disease, as different surgical techniques may need to be considered for each eye. This was illustrated in the case report of patient KF8 who required a full thickness corneal transplant in the left eye with more advanced keratoconus, but achieved excellent visual rehabilitation of the right eye following DMEK surgery which solely addressed the effects of FECD.

The average age of the 17 patients in this study was 55.5 years, with follow up data available for only two patients below the age of 40 years. A longer follow up period may be required to appreciate the effect of endothelial decompensation within this patient population.

Although genotyping data from this cohort was limited, the CTG18.1 expansion status was again noted to be more common amongst white patients (83.3%, n=5,) compared to non-white (25%,n=1) and also occurred more frequently in men (71.3%, n=7) versus women (25%, n=1). These findings are in keeping with that of the larger FECD population studied in Chapter 2 (Results section: 3.1.1.1, 3.1.1.2). Although the average age of FECD diagnosis among the repeat expansion negative patients was 8.2 years younger than the repeat expansion positive cohort, the finding is not of statistical significance due to the limited number of samples. Overall within this population, KC on average diagnosed later and FECD earlier due to the masking of disease created by the presence of the dual pathology.

As discussed in Chapter 2, there exists an overlap between the underlying disease processes that occur in both FECD and KC. This is also supported by the overlapping risk loci (*PIDD1/SLC25A22* and *ATP1B1*) that have been identified for both conditions independently (Afshari, Igo et al. 2017, Hardcastle, Liskova et al. 2021). While the identification of the CTG18.1 repeat expansion in the majority of FECD patients has allowed greater insight into the disease mechanism underlying this dystrophy, keratoconus remains a genetically heterogeneous disease associated with a number of genetic risk loci and environmental risk factors that are yet to be fully understood (Davidson, Hayes et al. 2014, Galvis, Sherwin et al. 2015, Gordon-Shaag, Millodot et al. 2015, Hardcastle, Liskova et al. 2021). The *TCF4* gene had not been previously associated with keratoconus in Genome Wide Association Studies that applied central corneal thickness as a marker ectasia (Li, Bykhovskaya et al. 2012, Lu, Vitart et al. 2013, Hardcastle, Liskova et al. 2021). However recent studies have suggested that Corneal Hysteresis (CH) and Corneal Resistance Factor (CRF) allow more sensitive measures of corneal changes in keratoconus and could therefore be applied in identifying genes associated with keratoconus more accurately (Luce 2005, Ortiz, Pinero et al. 2007, Fontes, Ambrosio et al. 2010). A GWAS performed by Khawaja et al. applied CH and CRF as a marker of keratoconus and found a significant association with a locus near *TCF4* (Khawaja, Rojas Lopez et al. 2019). This finding in itself does not show that the *TCF4* gene directly underlies the pathogenesis of keratoconus, but does highlight that possibility that the gene plays a common role in altering corneal biomechanics in both KC and FECD.

Salouti *et al.* have previously postulated that the shared embryological origin of both corneal stroma and endothelium from neural crest cells could be an indication of dysregulation of terminal differentiation of these cells that leads to the development of both diseases (Salouti, Nowroozzadeh et al. 2010). However, this hypothesis has not been verified and no shared abnormality of an embryogenesis pathway has been identified in this patient population.

As both KC and FECD are not uncommon in the UK population, it is probable that both conditions could manifest together purely by chance and not as a result of a shared pathological pathway. As FECD occurs predominantly in a white population, in order to ascertain if the prevalence of the combined condition was occurring at a higher frequency that would be expected by chance alone, prevalence data of keratoconus within a predominantly white population would be required to allow a comparative assessment. However as shown in Table X, the range of reported prevalence in the literature ranges from 0.03- 1.2%. Assessment of prevalence of keratoconus is further complicated by the absence of a consensus regarding diagnostic criteria which leads to the application of varying indices in defining the condition (Gomes, Tan et al. 2015). It is therefore not possible to definitively conclude if the occurrence



of combined keratoconus and FECD is more than would be expected of two randomly occurring diseases.

Although the occurrence of this dual pathology may be rare, the clinical significance of recognising this condition remains high due to the implications to surgical management of these patients. The measurement of central corneal thickness has been used for assessing corneal decompensation and the need for surgical intervention in patients with FECD (Jurkunas and Azar 2006). However, in cases of combined keratoconus with FECD, false normalisation of the corneal thickness necessitates a greater reliance on clinical judgement to determine the predominant cause of visual dysfunction.

While corneal tomography is an established imaging modality for diagnosing forme fruste KC and documenting ectatic progression, more recently Scheimpflug imaging has been recommended as a useful tool to detect subclinical corneal oedema in FECD (Sun, Wacker et al. 2019). Three specific tomographic features of FECD corneas with oedema were described by Sun et al., including: loss of parallel isopachs, displacement of the thinnest point of the cornea, and focal posterior corneal depression. While the documentation of these signs could be useful for early detection of sub-clinical corneal oedema in FECD, its utility might be limited in eyes with co-occurrence of KC as some of these tomographic features could also be observed in ectatic cornea.

In this study, surgical decision making was mainly guided by slit lamp evaluation of corneal oedema, scheimpflug imaging and assessment of corneal curvature in addition to the patients best corrected visual acuity in the 4<sup>th</sup> decade of life. As corneal decompensation secondary to FECD normally occurs in later life, it was conceivable that correction of endothelial decompensation alone could restore vision to the level attained prior to the onset of corneal oedema.

While penetrating keratoplasty was once the surgery of choice to address both stromal ectasia and the endothelial dysfunction, this case series highlights the utility of both DMEK and DSAEK surgery in the management of this patient population. Since 2014, 6 cases of DSEK and 2 cases of DMEK have been published in the literature for the management of cases of combined FECD and KC where corneal decompensation was the dominant pathological process. Similar to the cases reported in this study, endothelial transplantation was shown to provide good visual rehabilitation. However, in two of the three cases in this series (KF 12, KF 13) the irregular corneal astigmatism measurement was shown to increase following resolution of oedema as the ectasia became more prominent. This change has not previously been reported in the literature. Although none of the cases reported an increase in

prominence of ectasia post operatively, it was interesting to note that similar to KF12's right eye, two cases of DSEK reported by Vira et al demonstrated increased corneal thickness following attachment of the additional lamellae of stromal tissue (Vira, Abugo et al. 2014). In all three cases the pre-operative central corneal thickness was noted to be below 500  $\mu\text{m}$  despite the presence of stromal oedema . In cases such as these, DSEK offers the benefit of the added lamellar stromal layer that provides structural integrity over the thinner DMEK graft and is a safer option to avoid exacerbation of features of ectasia postoperatively.

Jurukunas *et al* have also highlighted that in a case of combined DMEK and cataract extraction with intraocular lens implantation, the normalisation of the corneal topography lead to difficulty in predicting the refractive outcome as shown by an unanticipated postoperative refractive error of +3.75D in their patient (Gupta, Kinderyte et al. 2017). The unpredictability of the post-transplant corneal curvature in this patient population necessitates adequate patient counselling to ensure patients are aware that further refractive correction will be required post-surgery. Within this cohort of combined KCFECD, patients were found to achieve good spectacle corrected visual acuity and were satisfied with the postoperative outcomes. It should also be noted that due to the asymmetry of the combined disease process, patients should be counselled appropriately in regards to the possible treatment modalities. The case of patient KF8 shows that variations in disease severity between each eye may require different surgical interventions that carry distinct risks and postoperative rehabilitation.

In addition to the impact on surgical decision making, the presence of this dual pathology could also impact a clinician's ability to diagnose other comorbidities. Within this study, 7 patients were noted to have further pathology which included glaucoma, age related macular degeneration and floppy eyelid syndrome. Of these, glaucoma accounted for 29.4% (5/17), with normal tension glaucoma (NTG) making up 40% (n=2) of those cases. This incidence of NTG is in keeping with the published literature but is interesting in that the diagnosis was made in two individuals below the age of 60 years. NTG is more common in patients over the age of 60 years and in those of Asian ancestry unlike the 2 patients in this study (white male, black female) (Killer and Pircher 2018). In both cases, intraocular pressure measurements fluctuated and the diagnosis was made on the basis of optic disc changes noted over a period of monitoring. It should be considered that as changes in corneal oedema and hysteresis are known to influence intraocular pressure measurements, inaccuracies in the assessment of eye pressure within this patient population are likely to occur (Deol, Taylor et al. 2015). Although the patient sample in this cohort is too small to draw definitive conclusions, optic disc assessment should ideally be

performed on a regular basis in addition of intraocular pressure measurement to avoid missing signs of glaucoma in these patients.

Publication	Age (Years)/ Gender	Treatment	Pre Op BCVA	Post Op BCVA	Change in mean keratometry (Preop, Post Op)	Change in CCT/ $\mu$ m (Preop, Post Op)	Complications
MEH KCFECD Cohort	69 M	DMEK	6/18	6/7.6	↓0.6D (2.7,1.5)	↓132 (584,452)	
	51M	DMEK +IOL	6/9	6/7.5	↑0.6D (42.0D, 42.6D)	↓ 126 (611,485)	
	55 F	DMEK +IOL	6/18	6/9	↓0.1D (41.9D,41.8D)	↓77 (457, 381)	
	57 F	DSEK	6/15	6/12	↑2.0D (41.4D,43.4D)	↑15 (476, 491)	PCR,CMO
Jurkunas 2017 (Gupta, Kinderyte et al. 2017)		DMEK +IOL	6/12	6/6	↓4.5D (50.8D, 46.3D)	↓ 138 (615, 477)	Refractive surprise of +3.75D
Cooper 2016	63 M	DMEK	6/15	6/7.5	↓ 0.7D (49.0D, 48.3D)	↓ 75 (558,483)	-
Vira 2014 (Vira, Abugo et al. 2014)	41 F	DSEK	6/9	6/7.5	↓2.6 D (52.5D, 49.9D)	↓ 62 (610, 548)	Graft dislocation rate of 16.67%
	41 F	DSEK	6/12	6/12	↓5.8D (56.0D, 50.2D)	↓ n/a (662,-)	
	70 M	DSEK	6/24	6/6	↓1.0D (44.0D, 42.9D)	↓ 14 (640, 626)	
	70 M	DSEK	6/18	6/7.5	↓0.9D (43.2D, 42.3D)	↓ 21 (696,675)	
	75 M	DSEK	6/18	6/12	↓4.0D (48.6D,44.6D)	↑42 (485,527)	
	63 F	DSEK	6/18	6/7.5	↓0.5D (44.2D, 43.8D)	↑84 (541,625)	

◆ PCR: posterior capsule rupture, CMO: Cystoid Macular Oedema, DMEK: Descemet's Membrane Endothelial Keratoplasty, DSEK: Descemet's Stripping Endothelial Keratoplasty

Table 4: Summary of surgical outcomes following both DMEK and DSEK surgery in patients with combined keratoconus and FECD. This study reports an additional 4 cases to the 8 published cases of partial thickness endothelial keratoplasty (DMEK and DSEK) in KCFECD patients in whom corneal decompensation was the predominant cause of visual decline. In two of the MEH cases it was noted that corneal curvature was more irregular following surgery, with an increase in anterior corneal curvature following a case of DMEK and DSEK. In cases of resolution of oedema leading to flattening of the corneal surface, Jurukunas *et al* further highlighted the potential refractive of a hyperopic outcome if the procedure is combined with cataract surgery and intraocular lens implantation. In all reposted cases, BCVA was shown to improve following both DMEK and DSEK surgery.

#### **4.6 Limitations of this study**

The main limitation of this study is the small number of patients identified as exhibiting signs of both corneal pathologies. Meaningful statistical analysis of the data obtained in regards to patients demographics is therefore not possible from this retrospective case series. Mining of letters from the electronic database further limits the patients identified to those with detailed correspondence documenting both diagnoses. It is possible that if patient letters were stored as PDF documents on the legacy database or did not have an adequate summary of their diagnosis within the correspondence could have been missed by this search.

The limited scope of the data search further hinders assessment of the prevalence of the dual pathology within the MEH patient population as a whole. Without a larger database of diagnosis attributed to patients attending the corneal service it is not possible to compare the prevalence of keratoconus combined with FECD to the prevalence of each condition independently.

The limited number of blood samples obtained for genotyping was a further limitation of this study and did not allow for meaningful assessment of the correlation between disease phenotype and expansion status. A question of interest in the assessment of this cohort would have been the natural history of repeat expansion positive FECD compared to expansion negative FECD in the presence of keratoconus. It would be of clinical interest to determine if the rate of corneal decompensation differed between the two groups as this could further inform the clinicians choice of surgical intervention.

#### **4.7 Conclusion**

In summary, it is vital that clinicians are aware of the rare but complex presentation of keratoconus and FECD as a dual pathology. The cases reported here in addition to the published literature highlights the importance of detailed clinical assessment of disease progression in order to determine the best surgical treatment in this patient population. A greater understanding of treatment options and potential complications will serve to improve our ability to counsel this population and provide informed and personalised patient care.

PHASE I CLINICAL TRIAL  
TO INVESTIGATE AN  
ANTISENSE OLIGONUCLEOTIDE-BASED THERAPY  
FOR  
FUCHS ENDOTHELIAL CORNEAL DYSTROPHY

## 5.1 Ocular Gene Based Therapies

As a greater understanding of the genetics and molecular pathogenesis of FECD develops, the focus of treatment can begin to shift from alleviating symptoms to targeting the genetic changes and/or the downstream molecular signatures that underlie this dystrophy. The last 25 years has born witness to significant achievements in the development of clinically applicable, targeted gene based treatments of ocular disease (Figure 1)(Lee, Wang et al. 2019).

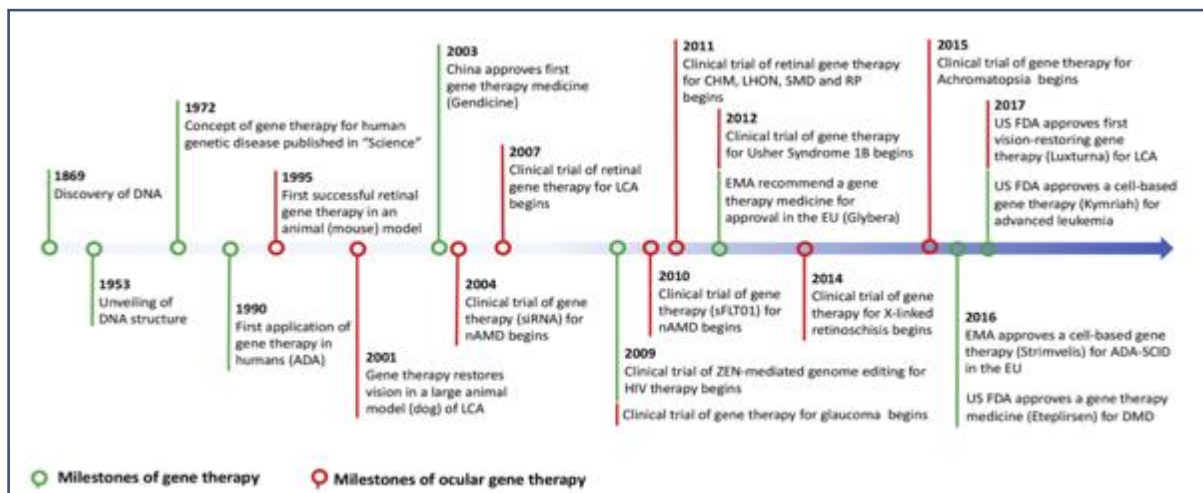


Figure 1: Timeline of milestones in ocular gene therapy (Figure obtained from Lee, Wang *et al.* 2019) ADA: adenosine deaminase deficiency, nAMD: neovascular age-related macular degeneration, CHM: choroideremia, DMD: Duchenne muscular dystrophy, EMA: European Medicines Agency, FDA: food and drug administration, HIV: human immunodeficiency virus, LCA:

The eye is often cited as an ideal target for gene based therapy, for the following reasons (Petit, Khanna et al. 2016):

- The blood-retinal and blood-aqueous barrier affords the eye an immune privileged state. In addition to protecting ocular structures from the body's immune systemic immune response, these barrier layers prevent the leakage of gene based therapies into the systemic circulation
- The relatively small size of the eye requires lower doses of both the therapeutic gene as well as the delivery modality compared to systemic drug administration

- Direct visualisation of ocular structures allows us to evaluate both the efficacy and potential side effect profile of new therapies through a variety of non-invasive methods including confocal microscopy, electroretinography and optical coherence tomography.
- The fellow non-treated eye allows for an ideal intraindividual control in clinical trials of new treatment modalities

However, despite successes in the field of inherited retinal disease, to date no gene therapy targeting inherited corneal disease has transitioned to clinical trials in human subjects (Xue and MaLaren 2020). The aim of this chapter is to highlight the ongoing and future work involved in transitioning a targeted gene based therapy for FECD to a Phase I Clinical Trial (Figure 2).

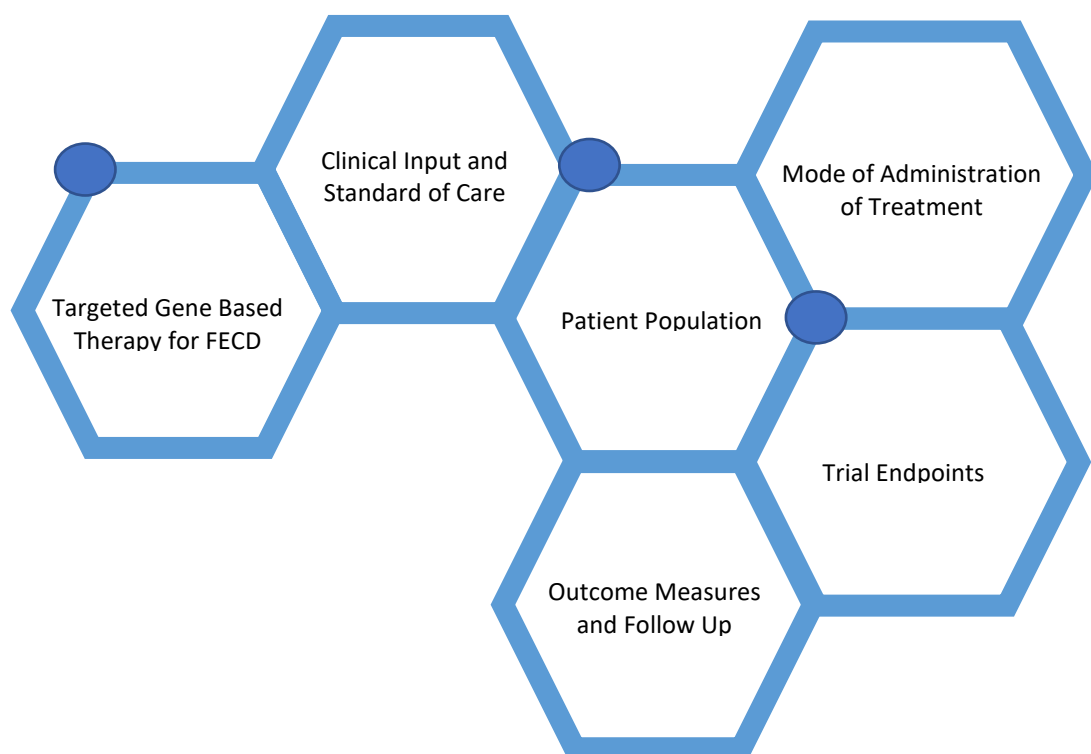


Figure 2: Schematic representation of factors that were evaluated in the design of a Phase I clinical trial for the treatment of Expansion Positive Fuchs Endothelial Corneal Dystrophy with a targeted gene based therapy.

## 5.2 Developing a novel gene based therapy for FECD

### 5.2.1 Background

The earliest gene therapies were developed with the aim of compensating for loss-of-function mutations by introducing a copy of the normal gene to the cells in which the deficiency causes disease (Chung, Lee et al. 2009). This can be achieved through the application of viral vectors that rely on the ability of viruses to invade living cells and deliver their own genetic material into the host (Anguela and High 2019). Viral vectors developed as vehicles for gene therapy are rendered incapable of replicating in order to allow controlled delivery of recombinant nucleic acids.

Another approach to gene therapy is by suppressing gain-of-function mutations that lead to formation of toxic RNA and/or protein products. Oligonucleotide based treatments are one such modality that are developed with the aim of creating rationally designed nucleic acid chains to bind specific disease-causing RNA sequences, thus directly modulating toxic gene expression or function (Juliano 2016). The 3 main forms of oligonucleotide based therapies are summarised in Figure 3 (Mehta, Deeksha et al. 2019, Roberts, Langer et al. 2020):

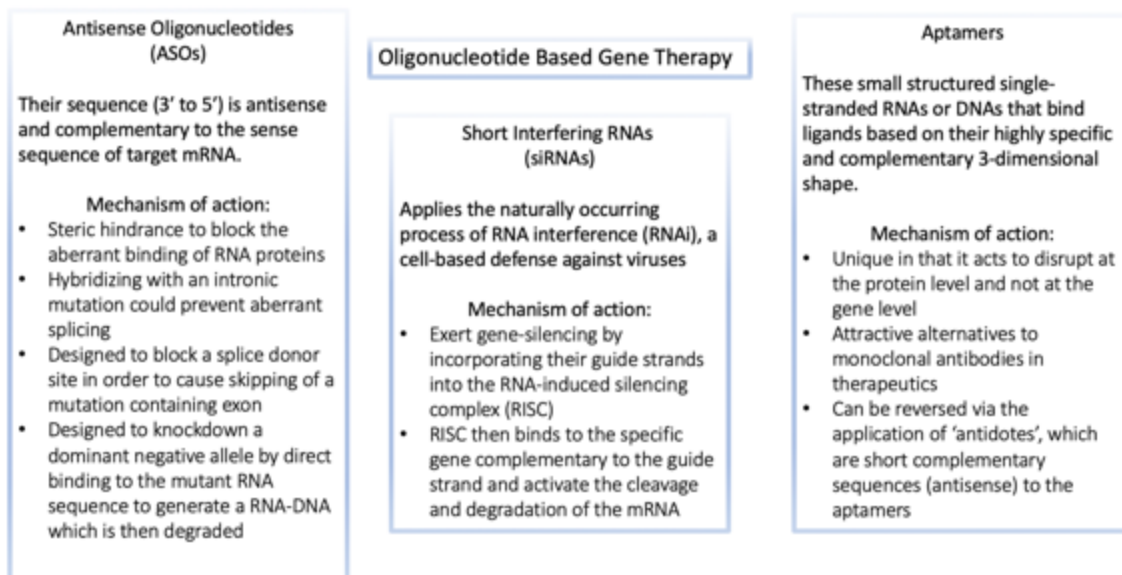


Figure 3: Oligonucleotide Based Gene Therapy. The figure summarises 3 common oligonucleotide based gene therapy platforms that carry potential therapeutic application by altering gene expression of an affected individual.



Of these oligonucleotides based treatments, antisense oligonucleotides (ASOs) have been the first to make the transition to ophthalmic clinical practice. Synthetic ASOs are single stranded oligonucleotides, generally 12-30 nucleotides in length, designed to bind a specific sequence of target mRNA in a complementary manner (Mehta, Deeksha et al. 2019). ASO binding is able to exert its function by exerting a knockdown effect on the disease-causing RNA, causing an alteration of splicing pattern or blocking aberrant binding of RNA proteins via steric hindrance (Bennett 2019) (Xue and MacLaren 2020). The first ocular application of ASO therapy was in the form of Fomivirsen, an ASO designed to treat cytomegalovirus (CMV) retinitis that was approved by for use in human in 1998 (Mulamba, Hu et al. 1998). Fomivirsen was administered via intravitreal injection and provided proof-of-concept that ASO pharmacokinetics maintained functionality when delivered via this route.

In a collaborative effort between the Institute of Ophthalmology (UCL), Moorfields Eye Hospital and ProQR Therapeutics, the feasibility of designing an ASO aimed at targeting *TCF4* CTG18.1 derived transcripts was investigated with the aim of reversing the pathologic changes observed in repeat expansion positive FECD. In 2018, this led to the successful development of a potentially transformative gene based therapy for FECD that demonstrated reversal of toxic gain-of-function changes in *in vitro* models of the disease (Zarouchlioti, Sanchez-Pintado et al. 2018).

### 5.2.2 Developing an ASO to Treat Repeat Expansion Positive FECD

In repeat expansion mediated FECD, the expanded CTG18.1 trinucleotide repeats are transcribed into abnormally long RNA chains that are prone to toxic aggregation. Accumulation of these aggregates within the cell nucleus leads to the formation of characteristic RNA foci that exert toxicity by sequestering RNA binding proteins. These RNA binding proteins, including splicing factor muscleblind-like (MBNL) proteins, are sequestered in ribonucleoprotein structures known as RNA foci (Sznajder, Thomas et al. 2018). Depletion of freely circulating splicing factors results in a wide-spread changes in pre-mRNA splicing regulation which disrupts normal endothelial cell homeostasis (Zarouchlioti, Sanchez-Pintado et al. 2018).

In order to reverse the toxic gain-of-function induced by the *TCF4* CTG18.1 expansion, we studied the feasibility of an antisense oligonucleotide (ASO) designed to target the trinucleotide repeat RNA transcripts with the aim of preventing formation of foci. Our hypothesis is that by preventing foci formation, the pool of splicing factors could be restored which then leads to normalisation of RNA splicing patterns (Zarouchlioti, Sanchez-Pintado et al. 2018).

To enable the development of an in vitro model of FECD, a primary corneal endothelial cell culture (CEC) was developed by *Zarouchlioti et al.* from endothelial cells obtained from repeat expansion positive FECD patients at the time of corneal transplant surgery (Peh, Chng et al. 2015, Zarouchlioti, Sanchez-Pintado et al. 2018). DM and endothelial cells removed at the time of routine DMEK surgery were transported to the lab within 24 hours of surgery. Endothelial cells were then dislodged from DM to allow seeding and promote proliferation in order to develop a robust cell line for experimentation. These cultured cell colonies were shown to harbour RNA foci formed from the repeat expansion that lead to sequestration of mRNA splicing factors muscleblind-like splicing regulator 1 (MBNL1), muscleblind-like splicing regulator 2 (MBNL2) and nuclear mitotic apparatus protein 1 (NUMA1) (Figure 4). The corneal endothelial cell (CEC) model displayed similar downstream dysregulation of abnormal endothelial cell physiology observed in FECD and therefore represented a valid in vitro model of FECD disease.

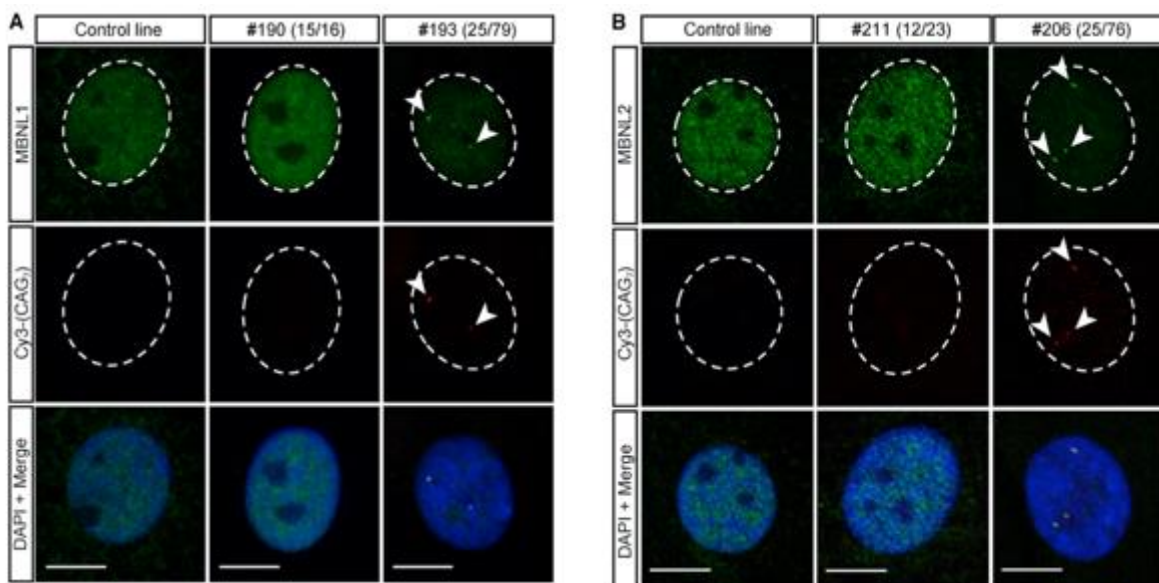


Figure 4 mRNA splicing factors MBNL1 and MBNL2 are sequestered to RNA foci of corneal endothelial cells derived from FECD patients [Image obtained from Zarouchlioti et al. 2018]: The image above shows corneal endothelial cells from a healthy control subject, repeat expansion negative subject (#211) and a *CTG18.1* repeat expansion positive subject (#206). The RNA foci are shown to be present in the repeat expansion positive cells as shown in red and highlighted by arrows when labeled with a Cy3-(CAG)<sub>7</sub> FISH probe and DAPI is used to stain nuclei. Similarly, staining of MBNL1 and 2 are highlighted in green with corresponding arrows. The merged image confirms co-localization of the MBNL proteins and RNA foci as shown in the bottom row of both panels. These images confirm the recruitment of mRNA splicing

factor to CUG-specific nuclear RNA foci in expansion-positive CECs (Zarouchlioti, Sanchez-Pintado et al. 2018).

In order to test the therapeutic potential of the ASO designed to target the CTG18.1 intron, Zarouchlioti *et al.* transfected the CEC model with an antisense oligonucleotide (AON) developed to target the CTG18.1 intron repeat. Following transfection, it was noted that sequestration of splicing factors (MBNL1, MBNL2, NUMA1) within RNA foci was significantly decreased (Figure 5). Redistribution of splicing factors then lead to the normalisation of RNA splicing patterns within CECs (Zarouchlioti, Sanchez-Pintado et al. 2018).

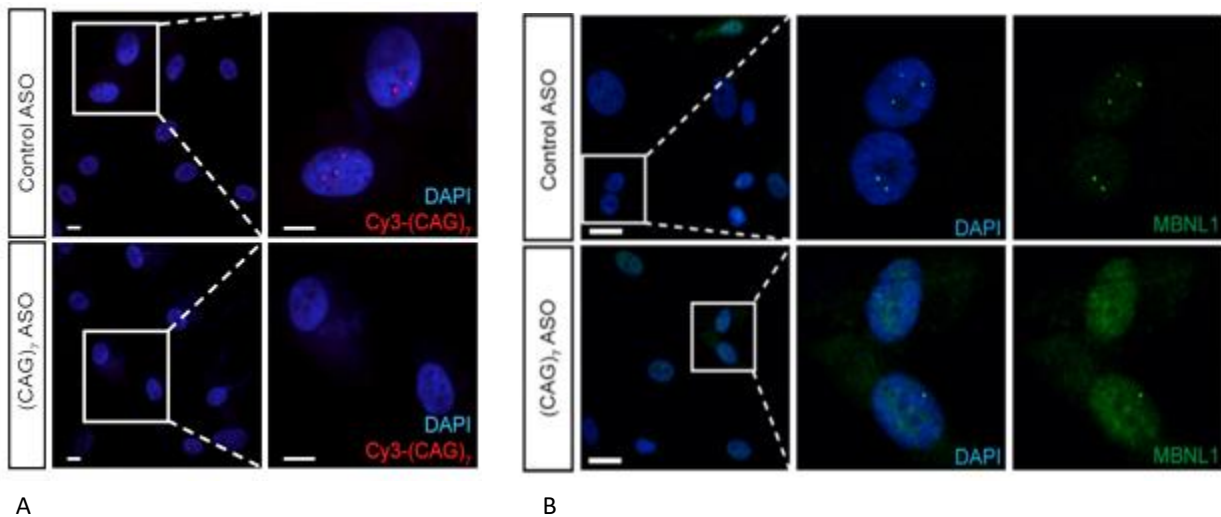


Figure 5: ASO-Mediated treatment of cultured corneal endothelial cells (CECs) significantly reduces foci number and rescues MBNL1 nuclear localization [Image obtained from Zarouchlioti *et al.* 2018]. The images shown here are of CECs 24 hours following treatment with a control ASO and a (CAG)<sub>7</sub> ASO designed to bind to the CUG repeat expansion. In both images the cell nucleus has undergone staining with DAPI while the RNA foci seen in image A have been labeled with a Cy3-(CAG)<sub>7</sub> FISH probe that appears red while image B shows MBNL1 Fish probe labelling with a fluorescent green probe. The row on top shows treatment of the cell lines with a control ASO while the bottom row shows cell lines treated with the (CAG)<sub>7</sub> study ASO designed to bind specifically to the CUG RNA expansion. In all cases CECs were treated with 200 nM (CAG)<sub>7</sub> or control ASO for 24 hr

- A) Treatment with the (CAG)<sub>7</sub> ASO shows a reduction in the number of visible RNA foci within the FECD corneal endothelial cells compared to the control line in which foci remain visible.
- B) Treatment of repeat expansion positive FECD corneal endothelial cells were further shown to reduce sequestration of the RNA splicing factor MBNL1 within RNA foci, with reduction of MBNL1 puncta and the changes in MBNL1 localization when cells were treated with the (CAG)<sub>7</sub> ASO.

To further assess the viability of the ASO in the treatment of FECD in vivo, commercial mouse models were used to study the effectiveness and accessibility of the gene based therapy. Intravitreal (IVT) injection of the ASO resulted in uptake within the mouse corneal endothelium in both a dose and time dependent manner. It was also shown that a higher uptake of the ASO between day 2 and 14 following IVT was achieved when compared to topical administration (Zarouchlioti, Sanchez-Pintado et al. 2018).

By restoring normal cell transcription activity, we aim to apply the ASO as a treatment to prevent or slow corneal degeneration in patients with ExpPos FECD. To this end, a first-in-human clinical trial will assess the therapeutic potential of this gene based therapy in subjects with genetically confirmed ExpPos FECD by evaluating the safety and tolerability of the ASO.

### 5.3 Potential pathways for the delivery of ASO gene therapy to the corneal endothelium

A key factor in the development of a gene-based therapy targeting the corneal endothelium lies in identifying an effective and safe route by which to deliver the treatment. The ideal delivery model would allow the therapeutic agent to reach the corneal endothelium with minimal damage to the surrounding tissue, illicit no immune response and cause minimal discomfort to the patient. Administration of any therapeutic agent to the eye must be able to overcome both anatomical and physiological challenges posed by the static barriers formed by the physical structures of the eye, as well as dynamic barriers created by ocular surface tear dilution, aqueous turnover with the anterior chamber, clearance through tissue blood flow via the choroid and conjunctiva in addition to lymphatic clearance (Gaudana, Ananthula et al. 2010). To date, the two most common routes for delivery of therapeutic agents to the eye are topical administration of drops or ointment to the ocular surface and intravitreal injection directly into the posterior chamber of the eye.

The corneal epithelium creates the main barrier to transgene delivery via topical administration. The existence of epithelial cell tight junctions as well as the hydrophobic state of this layer creates a barrier against pathogens invading the eye. Although paracellular pathways exist that could transport hydrophilic molecules across the epithelium, this is only applicable to small molecules. Macromolecules such as ASOs are therefore not able to cross an intact corneal epithelial layer (Juliano 2016).

Minimally invasive techniques for delivering therapeutic agents directly to the corneal endothelium remain in the early stages of development and have not as yet been tested in human subjects (Mohan, Tovey et al. 2012). Table 1 details the pros and cons of new techniques currently being assessed in animal models that could produce new avenues for delivery of gene based therapies to patients in the future.

At present, the most reliable method by which to deliver targeted treatment to intraocular structures remains physical introduction of the therapeutic agent via sharp needle or surgical techniques. Injecting directly into the anterior chamber of the eye to deliver the agent into the aqueous humour is a potential mode of delivery, but does present challenges. In addition to the limited anterior chamber space posing greater risk of intraoperative complication during the process of injecting (trauma to the cornea, iris or anterior lens capsule), raised pressure within the anterior chamber can result in efflux of the injected agent as well as discomfort for the patient. If only a small volume of fluid can be safely injected into the anterior chamber this presents potential difficulties in to achieving a therapeutic concentration of the agent with one administration. Subconjunctival injections would allow a less

invasive, more comfortable method of delivering high volumes of a therapeutic agent. However, issues with targeting the corneal endothelium arise as the subconjunctival space is not contained within the blood ocular barrier.

Through the development of treatment for retinal pathology, intravitreal drug delivery remains a tried and tested route for intraocular gene based therapy. Although it is a more invasive route of delivery, intravitreal injection allows direct intraocular dosing and achieves sustained drug levels (Avery, Bakri et al. 2014). Intravitreal injection via the pars plana approach allows dosing into the vitreous humor and subsequent percolation of the therapeutic agent to both the posterior pole structures as well as the anterior chamber, including the corneal endothelium. Intravitreal injection of antiviral medication has been shown to be effective in the treatment of patients with refractory corneal endotheliitis (Yu, Peng et al. 2020). The intravitreal route of delivery used in these studies was shown to achieve effective and sustained concentrations of medication within the aqueous humor and allowed targeting of the endothelium.

Although the concept of injecting a drug aimed at the cornea into the posterior chamber may seem counterintuitive, it offers the following benefits:

1. The safety profile of intravitreal injection is proven and is a commonly performed method of ocular drug delivery (Avery, Bakri et al. 2014)
2. The larger volume of the posterior chamber of the eye allows delivery of a higher volume and dose of the therapeutic agent
3. Vitreous humor turnover is slower than that of aqueous within the anterior chamber, thus creating a slow release mechanism of drug distribution and potentially slower clearance rate of the drug (Del Amo, Rimpela et al. 2017).
4. The risk of physical damage to ocular structures is less when injecting into the posterior chamber of the eye than the anterior chamber as it allows more space for sharp needle access (Johnson, Hollands et al. 2010, Fagan and Al-Qureshi 2013, Falavarjani and Nguyen 2013, Orozco-Hernandez, Ortega-Larrocea et al. 2014)

It is important to consider that ASO delivery via intravitreal route to the posterior chamber could have the potential to induce off-target effects. By injecting into the posterior chamber, off-target binding may occur as a consequence of complementary binding between the ASO and unintended RNA that share a similar sequence to the target RNA within non-corneal ocular tissue (Yoshida, Naito et al. 2019)

(Lindow, Vornlocher et al. 2012). In order to minimise this risk, in silico analysis utilising human RNA databases to rule out other potential intraocular off-target sites. Never the less, the design of the Phase I trial will take into consideration the possibility of such side effects as well as potential non-sequence specific effects of ASO chemistry within the posterior chamber such as vitreous opacities, lenticular opacities and cystic retinal changes as highlighted in the ASO treatment trial of *CEP290* (Cideciyan, Jacobson et al. 2019).

Carrier	Mechanism of Action	Advantages	Disadvantages
<p><b>Nanocarriers</b> (Liaw, Chang et al. 2001, Barreleiro, May et al. 2003, Gardlik, Palfly et al. 2005, Tong, Chang et al. 2007)</p>	<p>Carrier molecules developed within the range of the paracellular pore diameter are fused with gene plasmids to allow carriage of the gene across the epithelial layer.</p> <p>Allow cell penetration via a variety of pathways including phagocytosis, macro-pinocytosis and endocytosis.</p>	<ul style="list-style-type: none"> <li>▪ Allows passage of gene therapy to the corneal stroma</li> <li>▪ PEO-PPO-PEO copolymer nanoparticle delivery systems are FDA approved for ocular drug delivery</li> <li>▪ Penetration of corneal endothelial cells by polyamidoamine (PAMAM) dendrimer nanoparticles has been demonstrated in rabbit and human corneas in ex vivo culture</li> </ul>	<ul style="list-style-type: none"> <li>▪ Requires the use of permeation enhancers such as EDTA to overcome the tight junction as endocytosis contributes to the transport pathway</li> <li>▪ Topical delivery has not been proven to result in endothelial cell penetration</li> </ul>
<p><b>Iontophoresis</b> (Hughes and Maurice 1984, Sarraf and Lee 1994, Berdugo, Valamanesh et al. 2003)</p>	<p>Implementation of an electric field to enhance delivery of a charged ionic compound across a cell membrane</p>	<ul style="list-style-type: none"> <li>▪ Able to aide transport of charged macromolecules</li> <li>▪ Enhanced drug delivery by this mechanism has been shown in human subjects</li> <li>▪ In vivo animal studies have been successful in delivering antisense oligonucleotides to all layers of rat eyes</li> </ul>	<ul style="list-style-type: none"> <li>▪ Can result in corneal epithelial or conjunctival oedema</li> <li>▪ Decreased corneal endothelial cell counts which may be due to applying high current densities to small ocular surface</li> <li>▪ Effect on compromised FECD endothelial cells has not been reported</li> </ul>
<p><b>Electro-permeabilization</b> (Zhou and Dean 2007, Hao, Li et al. 2009, He, Pipparelli et al. 2010)</p>	<p>Administration of high intensity electrical pulses leads to the formation of transient pores within the cell membrane</p>	<ul style="list-style-type: none"> <li>▪ Enables passage of large DNA constructs</li> <li>▪ In vivo testing on murine corneal epithelium and keratocytes confirmed gene delivery without signs of inflammation, oedema or inflammation</li> <li>▪ Ex vivo studies on human corneal endothelium showed successful</li> </ul>	<ul style="list-style-type: none"> <li>▪ Only low levels of gene delivery were accomplished</li> <li>▪ Increasing electrical pulse intensity and duration enhanced gene transfer but damages corneal tissue secondary to irreversible cell membrane damage</li> </ul>



		<p>gene transport into the cell nucleus with low cell death and no changes to tight junction integrity</p>	
<p><b>Ultrasound mediated gene transfer</b> (Sonoda, Tachibana et al. 2006)</p>	<p>Delivery of ultrasound energy in combination with the presence of microbubbles had been shown to enhance uptake of gene therapies into rabbit corneal epithelial cells</p>	<ul style="list-style-type: none"> <li>▪ Allows focused gene transfer to specific areas of corneal stroma</li> <li>▪ No immediate damage was noted to occur to the cornea or surrounding structures following</li> </ul>	<ul style="list-style-type: none"> <li>▪ Has not as yet been shown to penetrate to the depth of the endothelial layer</li> </ul>
<p><b>Biobalistic gene transfer</b> (Tanelian, Barry et al. 1997, Shiratshi, Converse et al. 1998)</p>	<p>Particle mediated delivery system that transfacts cell by physically breaching the cell wall utilising low pressure helium pulses</p>	<ul style="list-style-type: none"> <li>▪ Gene expression was detected within epithelial cells at day 2 and day 4</li> </ul>	<ul style="list-style-type: none"> <li>▪ Restricted to epithelial cells</li> <li>▪ Level of discomfort in human subjects is yet to be assessed</li> <li>▪ Documented to cause damage to corneal epithelium and stroma as well as inflammation</li> </ul>

Table 1: Emerging techniques in the field of ocular drug delivery. In order to overcome the natural physical and physiological protective barriers of the eye, various modalities are being investigated to aid intraocular drug delivery. However, to date no published techniques have been shown to effectively penetrate to the depth of the corneal endothelial layer without adverse effects to the surrounding tissue.

## 5.4 Understanding the FECD Patient Population

### 5.4.1 Patient Engagement

In order to ascertain that both patient and research priorities aligned in the design of a first in human gene therapy trial, a Patient and Public Involvement (PPI) event was organized with the aim of understanding the FECD patients' perspective and concerns. It was important that patients understood that a Phase I trial would be aimed principally at identifying adverse reactions and would not be expected to improve the progression of their disease. As such, trial participants would not be expected to gain any direct benefit as the treatment would be administered prior to planned DMEK surgery. The session was attended by myself, Dr Alice Davidson (Chief Scientist leading the MEH FECD study) and two members of the Moorfield's patient engagement team. Issues of interest were presented by the clinical and research teams to a group of eight FECD patients who has previously undergone corneal transplantation (DMEK).

The following information relevant to trial development was ascertained from this sample of patients:

- Subjects were unanimously willing to be subjects in a trial that would not benefit them personally but could potentially help other FECD patients in the future
- Although subjects stated that they would prefer a topical treatment, they were not averse to intravitreal drug administration
- Subjects preferred the option of a preventative treatment over having to undergo a surgical procedure as many felt the period of declining vision that lead to surgery was very stressful
- All patients within this cohort felt they would have benefitted from a genetic test to confirm their diagnosis of FECD prior to the onset of symptoms if the option had been available to them

### 5.4.2 Evaluating Patient Burden in Trial Participation

In engaging directly with patients, we recognised that it was vital that patient-experience was prioritised to ensure no unnecessary burden was placed on subjects over the course of the trial. The participants' comfort was paramount in guiding decisions regarding selection of outcome measures, number of clinical visits and number of interventions. In discussions between the clinicians leading the investigations, scientists from the Institute of Ophthalmology, representatives of the biotechnology company (ProQR Therapeutics) and the Moorfields Eye Hospital Research and Ethics Committee, the following issues were considered when planning the sequence of trial visits:

- The burden on patients was minimised in terms of number of follow ups and intensity of investigation at each visit
- Subjects participation in the trial would not lead to delay in performing corneal transplantation
- Principal investigators would be adequately supported by both the research and clinical teams to ensure open lines of communication were available to trial subjects should any queries arise
- The financial burden on participants was minimised by ensuring ethically appropriate financial reimbursement is provided for trial related expenses

It was recognised that prioritising these factors was not only essential to allow accrual of trial participants but also to minimise drop out over the trial period.

#### 5.4.3 Assessing the potential recruitment base of MEH FECD patients

It is planned that 10 ExpPos FECD subjects with signs of corneal decompensation will be recruited to participate in this study. The sample size is not based on power calculations but is an empirical number that is considered adequate to fulfil the objectives of the study.

Based upon the data gained from the study of 342 patients in the MEH FECD cohort, the following data has been ascertained about the patient population:

- Between 2014 and 2018: 342 FECD patients aged  $\geq 18$  were recruited for genotyping (85 subjects per year)
- Genotyping confirmed that 265/342 (77.5%) patients were ExpPos
- Assessment of disease progression leading to need for surgical intervention:
  - >80% were documented to have significant disease warranting surgery in both eyes at time of first review
  - Disease asymmetry was mainly noted in eyes referred following cataract surgery from other centres. Second eye surgery was therefore performed as combined cataract extraction and endothelial keratoplasty
  - A sampling of the first 100 study patients indicated that 24% underwent bilateral DMEK +IOL
- A sampling of the 100 patients first recruited shows bilateral VA of  $\leq 6/12$  as 51%

- 20.8% were noted to have ocular comorbidities which may pose a risk for participation in the clinical trial or may influence the results
- In assessing patients as showing clinical signs of early stage versus late stage:
  - 214/342 showed signs of corneal decompensation not advanced enough to cause bullae
  - 49/342 had mild oedema with diurnal variation

From this data it was ascertained that approximately 2 FECD patients per month attending MEH would meet the recruitment criteria detailed in Appendix E.

## 5.5 Considerations when choosing trial outcome measures

When designing a clinical trial for an ASO based therapy targeting the corneal endothelium, one of the challenges that remains to be addressed is the manner in which to reliably assess the efficacy of these new treatments. In order to interpret the findings of gene based clinical trials, it is important that we establish a clear understanding of the relationship between the outcome measures and both disease severity as well as disease progression. Without establishing clear parameters by which to measure the impact of the treatment on the patient's disease, we will struggle to define the appropriate therapeutic treatment window for our FECD cohort.

Although clinical application of corneal gene therapy remains in its infancy, 3 ASOs treating inherited retinal diseases (CEP290-associated Leber congenital amaurosis, RHO-associated autosomal dominant retinitis pigmentosa and c.2299deG mutation in Usher syndrome type 2) are currently active in the US National clinical Trials Database alone (ClinicalTrials.gov. NIH US National Library of Medicine. Available at: <https://clinicaltrials.gov/>. Accessed November 20, 2020)(Xue and MacLaren 2020). The rapid advances in retinal disease therapies lead to the development of the Monaciano Consortium, a panel of inherited retinal disease experts working together to develop recommendations addressing existing difficulties in gene therapy trial design. The priorities identified by the consortium are as relevant to the field of corneal gene therapy as they are to inherited retinal disease (Thompson, Iannaccone et al. 2020):

- The measurement of treatment outcome has been identified as an area requiring priority review in order to improve the robustness of clinical interventional trials
- Investigators have been tasked with developing appropriate outcome measures for each disease as defined by changes in both structure and function.
- It is vital that adequate testing measures should be balanced with the patient experience so as not to place an unreasonable burden on the patient.
- In addition to standardization of testing protocols and data analysis, the reproducibility and reliability of tests should also be pre-defined

To date the, the various modalities applied to both the structural and functional measures of corneal endothelial disease have not produced a defined staging criterion for FECD. In clinical practice, slit lamp imaging of corneal guttata and clinical oedema has sufficed in guiding surgical treatment choices (Patel 2019). In order to assess the viability of ancillary tests of corneal anatomy and function, endothelial cell quantification and morphology as well as objective measures of visual function complemented by

the subject's own assessment of visual impairment, several outcome measures have been selected to characterise FECD in this study. Although not all the parameters measured would be expected to change following the administration of the ASO in this study, evaluation of the viability of these assessments will guide planning for future Phase II trials where disease progression will need to be measured.

The following are considered serious adverse events, based on the route of administration and based on what is known from the safety profile of other AONs (Mulamba, Hu et al. 1998, Cideciyan, Jacobson et al. 2019):

- Confirmed diagnosis of endophthalmitis
- Retinal detachment
- Persistent (i.e., assessed at 2 successive visits) decrease from baseline in BCVA, defined as a loss in BCVA  $\geq 15$  or more letters ( $\geq 3$  lines)
- Significant changes in ophthalmic examination findings, such as:
  - A persistent increase from baseline in IOP  $\geq 10$  mmHg (observed at 2 successive visits) or an absolute IOP value  $\geq 30$  mmHg, despite appropriate treatment
  - Intraocular inflammation of anterior chamber cells or vitreous cells, defined as:  $\geq 2$  grade increase from baseline in anterior chamber cell score; OR  $\geq 2$  grade increase from baseline in vitreous cells
  - A  $\geq 2$  grade increase from baseline in lens opacity according to the AREDS lens grading system
  - Decrease or increase  $\geq 40$   $\mu\text{m}$  in foveal thickness from a baseline measurable SD- OCT as confirmed by the masked central reading centre
  - Confirmed CME in the opinion of the Investigator

In order to detect adverse events and to assess the viability of testing modalities within this patient population, the following outcome measures have been selected for this trial:

#### 5.5.1 Objective assessment of visual function

Although an improvement in visual function is not an expected outcome of a Phase 1 clinical trial, assessment of visual function remains of vital in order to detect adverse events following treatment.

##### a. Best corrected visual acuity (BCVA)

BCVA will be measured using Early Treatment Diabetic Retinopathy Study (ETDRS) chart for both eyes. Each eye should be tested at 4 metres initially. Manual refraction will be performed at each study visit.

If the patient cannot read any letters on the ETDRS chart at 1 metre, then their ability to count fingers, detect hand movements or light perception should be measured.

##### b. Contrast sensitivity

Although visual acuity assessment by the ETDRS chart provides a reliable assessment of visual function, patients may have impaired contrast sensitivity despite normal visual acuity. Contrast sensitivity is a measure of a patient's ability to distinguish shades of grey. Contrast sensitivity affects many aspects of vision such as motion detection, visual field, pattern recognition and dark adaptation (Richman, Spaeth et al. 2013). In order to measure a subject's contrast sensitivity, a contrast sensitivity chart that gradually changes the shade or boldness of similar sized optotypes will be utilised. This will allow and evaluation of visual function by assessing the subject's ability to detect the difference in luminance between an object and its background (Ginsburg 2003, Richman, Spaeth et al. 2013).

##### c. Microperimetry

Microperimetry is used to test retinal function within the macular area. The assessment allows measurement of retinal sensitivity to light across specific locations across the retina. Each patient should be re-tested on the same machine, if possible. Microperimetry is largely an automated test, but tester input is required in setting up the machine and monitoring of test performance.

d. Full-field stimulus threshold (FST) and Full-field electroretinogram (ERG)

Electrophysiological assessment of the retina is useful in establishing the level of any abnormality (e.g. photoreceptor/RPE or inner retina) and also the extent, in terms of macular and or/peripheral dysfunction. The standard electrophysiological tests that are performed include the electro-oculogram (EOG), a full-field electroretinogram (ERG) and pattern ERG (PERG). There are established protocols for each of these assessments, defined by the International Society for Clinical Electrophysiology of Vision (REF).

5.5.2 Anatomical Assessment of Outcome Measure

a. Slitlamp Biomicroscopy and Intraocular Pressure Measurement

At screening, the main aim of slit lamp biomicroscopy is to confirm the presence of clinically significant corneal oedema and to allow grading of corneal guttae in accordance with a modified Krachmer scale. As the application of this scale can be subjective, interobserver variability will be minimised by limiting the number of clinical assessors (Eghrari, Mumtaz et al. 2017). Further ocular examination detailed below will be carried out to rule out any further ocular pathology at baseline and to recognise pathology that may occur following ASO administration :

Anatomical Feature	Characteristics
Pupil	-noting the size/shape tested in the room light used to measure BCVA - direct reaction to light -presence/absence of afferent pupillary defect
External adnexa	-presence of lid erythema or other abnormalities -evaluation of lashes and lacrimal apparatus;
Conjunctiva (bulbar and palpebral)	-presence of hyperaemia, pterygium, chemosis, conjunctivitis
Cornea	-Evaluation of epithelium, stroma and endothelium, including presence of oedema, guttae -Identification of gutta performed on retroillumination post dilation
Anterior Chamber	Quantification of anterior chamber activity in accordance with the Standardization of Uveitis Nomenclature (SUN) Working Group grading scheme for anterior chamber flare
Goldmann Applanation Tonometry	Measurement of intraocular pressure



Iris	Document presence of synechiae, abnormal pigmentation, areas of atrophy
Lens	Lens opacity grading according to the Age-Related Eye Disease Study (AREDS) Clinical Lens Grading System (ARLNS)
Posterior Segment/Fundus Examination	Assessment of vitreous body, retina (macula and peripheral retina), choroid and optic nerve

b. Imaging of the Anterior Segment and Posterior Segment

As the ASO will be administered via an intravitreal route, assessment of post dosing side effects requires detailed examination of both the anterior and posterior segment of the eye. The proposed investigations and the parameters measures are detailed below:

Imaging Modality	Parameters Measured
Slit-lamp retroillumination image post dilation	- Quantification and distribution of guttata within the central 8mm of the cornea
Specular Microscopy	- Quantification of central endothelial cell count before and after ASO administration
Scheimpflug tomography	- Corneal thickness mapping  - Tomographic changes in posterior elevation including the maximal point of depression on the posterior elevation map  - Monitoring of changes in symmetry of central isopachs  - Monitoring changes in the displacement of the thinnest point of the cornea
Anterior segment optical coherence tomography (AS-OCT)	- High resolution imaging of layers of the cornea to allow detection of changes in corneal structure due to changes in distribution of oedema, stromal opacification or changes Descemet's membrane such as thickening or irregularity
Spectral domain optical coherence tomography of the retina and nerve fiber layer (SD-OCT)	- objective clinical assessment of progressive retinal changes including monitoring of retinal thickness and macula oedema  - monitoring for decreased nerve fibre layer thickness measurements

### 5.5.3 Assessment of Bioavailability

In order to establish bioavailability of the ASO to the endothelium following administration, Descemet's membrane and endothelial cells will be removed at the time of planned DMEK surgery within 2 weeks of treatment. Digital droplet PCR will be performed to quantify levels of aberrant splicing of MBNL1 and MBNL2 between treated and untreated eyes will be carried out on the endothelial cell layer in order to identify foci and splice factors as well as to establish fraction of absorption as well as distribution of the ASO within the central 8mm of endothelial cells.

Serum blood samples will also be obtained to assess for potential leakage of the ASO into systemic circulation,

### 5.5.4 Patient Reported Outcomes Measure

The Visual Function and Corneal Health Status (V-FUCHS) is a standardized and validated questionnaire developed to allow patient-reported quantification of visual disability (Wacker, Baratz et al. 2018). The questionnaire has been tested in both a North American and German FECD patient populations where it demonstrated both valid and reliable assessment of visual disability (Grewing, Fritz et al. 2020).

All ophthalmic examinations and endpoints may be reviewed by external experts, in order to provide an independent assessment of the corneal/retinal structure or visual function throughout the clinical study.

## 5.6 Study Design

In designing a single dose exploratory Phase I Study of a new gene based treatment for ExpPos FECD, it was vital that the standard of care was maintained in the treatment of the trial participants. The study is therefore based on routine clinical practice at Moorfields Eye Hospital for the treatment of FECD patients eligible for DMEK, with or without combined cataract extraction with intraocular lens implantation (phaco+IOL) in both eyes. To assess the safety profile of the ASO, additional safety follow-ups and assessments were added for the purpose of this study.

### Screening Visits

Study participant screening should be conducted at least 6 weeks prior to performing DMEK +/- phaco+IOL to Eye 1.

Prior to or at the Screening visit, a blood sample for *TCF4* repeat expansion analysis will be obtained to ascertain that the participant does harbour the CTG18.1 repeat expansion.

Patient eligibility will be confirmed first with less intensive clinical assessments (slit lamp biomicroscopy, Pentacam scan, endothelial cell count and anterior segment OCT as per routine Moorfields clinical work up of FECD patients) and more intensive assessments shall be conducted after eligibility by all other criteria have been confirmed at the first screening visit.

Determination of the first eye to undergo surgery will be at the discretion of the Primary Investigator.

### Surgical and Dosing Visits

Each participant will go through the following two parts in this study:

#### *Part A: Without study drug administration:*

Part A of the study starts once DMEK +/- phaco+IOL of Eye 1 has been scheduled and the eligibility of the participant has been confirmed during the Screening visit (to be conducted  $\leq$  6 weeks prior to LRS/DMEK of Eye 1).

At the time of DMEK +/- phaco+IOL of Eye 1, Descemet's membrane and corneal endothelium will be collected for molecular biomarker assessments. Data generated during this period will serve as intra-participant control for data generated in Part B. A recovery period of at least 1 month will be observed post-surgery of Eye 1 to monitor for safety events prior to scheduling the DMEK for Eye 2. Depending

on the recovery period necessary post-surgery of Eye 1, as well as the availability of cornea transplant material, DMEK of Eye 2 will take place approximately 1 - 6 months after surgery of Eye 1.

*Part B: With study drug administration:*

Part B of the study starts once DMEK +/- phaco+IOL in Eye 2 can be scheduled and eligibility of the participant for Part B has been confirmed. At least 4 weeks prior to the scheduled DMEK +/- phaco+IOL in Eye 2, the participant will receive a single dose of the study ASO administered intravitreally in Eye 2. Following DMEK +/- phaco+IOL in Eye 2 Descemet's membrane and corneal endothelium will be collected for molecular biomarker assessments.

(The complete schedule and sequence of visits and assessment is provided in Appendix F)

The open label design proposed in this study and the use of the study participants contralateral eye as a control will allow an intraindividual baseline to assess safety and tolerability in addition to assessing change in corneal endothelium molecular biomarker data following ASO administration.

The study has been designed with the aim of achieving the following objectives:

Primary:

To evaluate safety and tolerability of an antisense oligonucleotide administered by IVT injection

Secondary:

- 1) To assess the effect(s) of an antisense oligonucleotide on molecular biomarker(s) in the corneal endothelium
- 2) To evaluate the pharmacokinetics of an antisense oligonucleotide (serum levels)
- 3) To explore potential clinical endpoints for use in future studies

Recruitment to the clinical trial based on this framework (Fuchs Focus PQ-504a-001, ClinicalTrials.gov Identifier: NCT05052554) opened on 22 of September 2021. On completion of this this Phase I trial, we hope to demonstrate that ASO mediated treatment of FECD is safe, well tolerated and successfully targets the corneal endothelium following intravitreal investigation. The experience gained from this trial will guide future planning of a Phase II clinical trial to allow assessment of the viability of this ASO in preventing progression of FECD when administered earlier in the course of the disease.

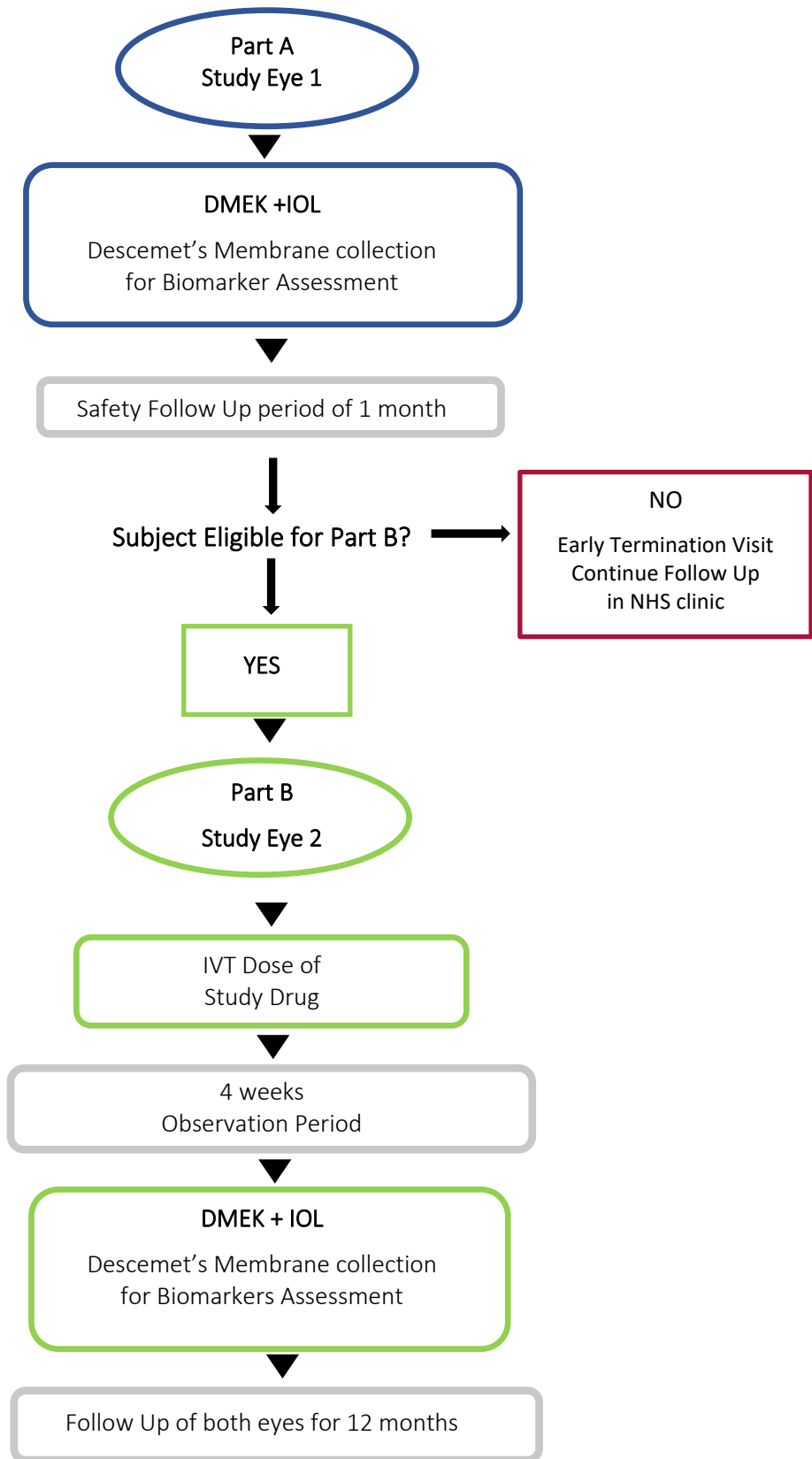


Figure 6: Planned patient treatment pathway over the period of enrolment in a Phase I Clinical Trial.

# CONCLUSION

This study enhances our understanding of Fuchs Endothelial Corneal Dystrophy (FECD) genetic heterogeneity and highlights that although corneal oedema secondary to endothelial dysfunction is the final common pathological outcome for patients clinically diagnosed as FECD, at the molecular level the basis for their disease may vary considerably.

Through detailed evaluation of phenotypic characteristics of patients harbouring different mutations, this study highlights clinically significant variations in disease onset, severity and progression within genetically defined subgroups of FECD. These findings not only contribute to an evolving understanding of this common sight threatening disease but also signals the need for a shift in clinical perspective when evaluating patients with FECD. This study contributes to the development of a personalised genetic medical model that informs FECD patients in regards to disease prognosis and potential new treatments. By clearly defining genotype-phenotype correlations and understanding the natural history of the disease, we can begin to identify optimal treatment windows for new and emerging gene-based FECD therapeutics.

Ongoing genomic investigations are needed to genetically define other distinct and rare forms of corneal endothelial disease and improve our ability to deliver innovative new gene based therapies to our patient population.

## References

(1993). "A novel gene containing a trinucleotide repeat that is expanded and unstable on Huntington's disease chromosomes. The Huntington's Disease Collaborative Research Group." Cell 72(6): 971-983.

Adamis, A. P., V. Filatov, B. J. Tripathi and R. C. Tripathi (1993). "Fuchs' endothelial dystrophy of the cornea." Surv Ophthalmol 38(2): 149-168.

Afshari, N. A., R. P. Igo, Jr., N. J. Morris, D. Stambolian, S. Sharma, V. L. Pulagam, S. Dunn, J. F. Stamler, B. J. Truitt, J. Rimmner, A. Kuot, C. R. Croasdale, X. Qin, K. P. Burdon, S. A. Riazuddin, R. Mills, S. Klebe, M. A. Minear, J. Zhao, E. Balajonda, G. O. Rosenwasser, K. H. Baratz, V. V. Mootha, S. V. Patel, S. G. Gregory, J. E. Bailey-Wilson, M. O. Price, F. W. Price, Jr., J. E. Craig, J. H. Fingert, J. D. Gottsch, A. J. Aldave, G. K. Klintworth, J. H. Lass, Y. J. Li and S. K. Iyengar (2017). "Genome-wide association study identifies three novel loci in Fuchs endothelial corneal dystrophy." Nat Commun 8: 14898.

Afshari, N. A., A. B. Pittard, A. Siddiqui and G. K. Klintworth (2006). "Clinical study of Fuchs corneal endothelial dystrophy leading to penetrating keratoplasty: a 30-year experience." Arch Ophthalmol 124(6): 777-780.

Aggarwal, S., B. M. Cavalcanti, L. Regali, A. Cruzat, M. Trinidad, C. Williams, U. V. Jurkunas and P. Hamrah (2018). "In Vivo Confocal Microscopy Shows Alterations in Nerve Density and Dendritiform Cell Density in Fuchs' Endothelial Corneal Dystrophy." Am J Ophthalmol 196: 136-144.

Agre, P. (1998). "Aquaporin null phenotypes: the importance of classical physiology." Proc Natl Acad Sci U S A 95(16): 9061-9063.

Aldave, A. J., J. Han and R. F. Frausto (2013). "Genetics of the corneal endothelial dystrophies: an evidence-based review." Clin Genet 84(2): 109-119.

Aldave, A. J., S. A. Rayner, A. K. Salem, G. L. Yoo, B. T. Kim, M. Saeedian, B. Sonmez and V. S. Yellore (2006). "No pathogenic mutations identified in the COL8A1 and COL8A2 genes in familial Fuchs corneal dystrophy." Invest Ophthalmol Vis Sci 47(9): 3787-3790.

Aldave, A. J., V. S. Yellore, F. Yu, N. Bourla, B. Sonmez, A. K. Salem, S. A. Rayner, K. M. Sampat, C. M. Krafchak and J. E. Richards (2007). "Posterior polymorphous corneal dystrophy is associated with TCF8 gene mutations and abdominal hernia." Am J Med Genet A 143A(21): 2549-2556.

Alexandrakis, G., V. Filatov and A. P. Adamis (2000). "Denovo development of corneal guttae and Fuchs' dystrophy in corneal grafts." CLAO J 26(1): 44-46.

Ali, Z. K., J. T. Whitson, V. V. Mootha, S. R. Witherspoon, J. A. Joseph, A. M. Joseph, L. S. Hynan and H. D. Cavanagh (2011). "Glaucoma in patients with corneal endothelial dystrophy." Eye Contact Lens 37(6): 332-336.



Amin, S. R., K. H. Baratz, J. W. McLaren and S. V. Patel (2014). "Corneal abnormalities early in the course of Fuchs' endothelial dystrophy." Ophthalmology 121(12): 2325-2333.

Anderson, N. J., D. Y. Badawi, H. E. Grossniklaus and R. D. Stulting (2001). "Posterior polymorphous membranous dystrophy with overlapping features of iridocorneal endothelial syndrome." Arch Ophthalmol 119(4): 624-625.

Andrew, S. E., Y. P. Goldberg, B. Kremer, H. Telenius, J. Theilmann, S. Adam, E. Starr, F. Squitieri, B. Lin, M. A. Kalchman and et al. (1993). "The relationship between trinucleotide (CAG) repeat length and clinical features of Huntington's disease." Nat Genet 4(4): 398-403.  
Anguela, X. M. and K. A. High (2019). "Entering the Modern Era of Gene Therapy." Annu Rev Med 70: 273-288.

Anshu, A., M. O. Price, D. T. Tan and F. W. Price, Jr. (2012). "Endothelial keratoplasty: a revolution in evolution." Surv Ophthalmol 57(3): 236-252.

Anthony Griffiths, J. D., Catherine Peichel, David A. Wassarman (2020). Introduction to Genetic Analysis (International Edition), Macmillan.

Avery, R. L., S. J. Bakri, M. S. Blumenkranz, A. J. Brucker, E. T. Cunningham, Jr., D. J. D'Amico, P. U. Dugel, H. W. Flynn, Jr., K. B. Freund, J. A. Haller, J. M. Jumper, J. M. Liebmann, C. A. McCannel, W. F. Mieler, C. N. Ta and G. A. Williams (2014). "Intravitreal injection technique and monitoring: updated guidelines of an expert panel." Retina 34 Suppl 12: S1-S18.

Babu, K. and K. R. Murthy (2007). "In vivo confocal microscopy in different types of posterior polymorphous dystrophy." Indian J Ophthalmol 55(5): 376-378.

Bak-Nielsen, S., C. H. Ramlau-Hansen, A. Ivarsen, O. Plana-Ripoll and J. Hjortdal (2019). "Incidence and prevalence of keratoconus in Denmark - an update." Acta Ophthalmol 97(8): 752-755.

Baratz, K. H., N. Tosakulwong, E. Ryu, W. L. Brown, K. Branham, W. Chen, K. D. Tran, K. E. Schmid-Kubista, J. R. Heckenlively, A. Swaroop, G. Abecasis, K. R. Bailey and A. O. Edwards (2010). "E2-2 protein and Fuchs's corneal dystrophy." N Engl J Med 363(11): 1016-1024.  
Barreleiro, P. C., R. P. May and B. Lindman (2003). "Mechanism of formation of DNA-cationic vesicle complexes." Faraday Discuss 122: 191-201; discussion 269-182.

Bennett, C. F. (2019). "Therapeutic Antisense Oligonucleotides Are Coming of Age." Annu Rev Med 70: 307-321.

Berdugo, M., F. Valamanesh, C. Andrieu, C. Klein, D. Benezra, Y. Courtois and F. Behar-Cohen (2003). "Delivery of antisense oligonucleotide to the cornea by iontophoresis." Antisense Nucleic Acid Drug Dev 13(2): 107-114.

Biswas, S., F. L. Munier, J. Yardley, N. Hart-Holden, R. Perveen, P. Cousin, J. E. Sutphin, B. Noble, M. Batterbury, C. Kielty, A. Hackett, R. Bonshek, A. Ridgway, D. McLeod, V. C. Sheffield, E. M. Stone, D. F. Schorderet and G. C. Black (2001). "Missense mutations in

COL8A2, the gene encoding the alpha2 chain of type VIII collagen, cause two forms of corneal endothelial dystrophy." Hum Mol Genet 10(21): 2415-2423.

Bonanno, J. A. (2012). "Molecular mechanisms underlying the corneal endothelial pump." Exp Eye Res 95(1): 2-7.

Borderie, V. M., M. Baudrimont, A. Vallee, T. L. Ereau, F. Gray and L. Laroche (2000). "Corneal endothelial cell apoptosis in patients with Fuchs' dystrophy." Invest Ophthalmol Vis Sci 41(9): 2501-2505.

Bourassa, S., W. J. Benjamin and R. L. Boltz (1991). "Effect of humidity on the deswelling function of the human cornea." Curr Eye Res 10(6): 493-500.

Bourne, W. M. (2003). "Biology of the corneal endothelium in health and disease." Eye (Lond) 17(8): 912-918.

Bourne, W. M., D. H. Johnson and R. J. Campbell (1982). "The ultrastructure of Descemet's membrane. III. Fuchs' dystrophy." Arch Ophthalmol 100(12): 1952-1955.

Bourne, W. M., L. R. Nelson and D. O. Hodge (1997). "Central corneal endothelial cell changes over a ten-year period." Invest Ophthalmol Vis Sci 38(3): 779-782.

Brandt, J. D., J. A. Beiser, M. A. Kass and M. O. Gordon (2001). "Central corneal thickness in the Ocular Hypertension Treatment Study (OHTS)." Ophthalmology 108(10): 1779-1788.

Brunette, I., D. Sherknies, M. A. Terry, M. Chagnon, J. L. Bourges and J. Meunier (2011). "3-D characterization of the corneal shape in Fuchs dystrophy and pseudophakic keratopathy." Invest Ophthalmol Vis Sci 52(1): 206-214.

Cano, A. and F. Portillo (2010). "An emerging role for class I bHLH E2-2 proteins in EMT regulation and tumor progression." Cell Adh Migr 4(1): 56-60.

Chan, E., E. W. Chong, G. Lingham, L. J. Stevenson, P. G. Sanfilippo, A. W. Hewitt, D. A. Mackey and S. Yazar (2021). "Prevalence of Keratoconus Based on Scheimpflug Imaging: The Raine Study." Ophthalmology 128(4): 515-521.

Chen, N. P., Z. Sun and R. Fassler (2018). "The Kank family proteins in adhesion dynamics." Curr Opin Cell Biol 54: 130-136.

Cheung, S. W. and P. Cho (2000). "Endothelial cells analysis with the TOPCON specular microscope SP-2000P and IMAGEnet system." Curr Eye Res 21(4): 788-798.

Chiou, A. G., S. C. Kaufman, R. W. Beuerman, T. Ohta, H. Soliman and H. E. Kaufman (1999). "Confocal microscopy in cornea guttata and Fuchs' endothelial dystrophy." Br J Ophthalmol 83(2): 185-189.

Chu, Y., J. Hu, H. Liang, M. Kanchwala, C. Xing, W. Beebe, C. B. Bowman, X. Gong, D. R. Corey and V. V. Mootha (2020). "Analyzing pre-symptomatic tissue to gain insights into the molecular and mechanistic origins of late-onset degenerative trinucleotide repeat disease." Nucleic Acids Res 48(12): 6740-6758.

Chung, D. C., V. Lee and A. M. Maguire (2009). "Recent advances in ocular gene therapy." Curr Opin Ophthalmol 20(5): 377-381.

Cideciyan, A. V., S. G. Jacobson, A. V. Drack, A. C. Ho, J. Charng, A. V. Garafalo, A. J. Roman, A. Sumaroka, I. C. Han, M. D. Hochstedler, W. L. Pfeifer, E. H. Sohn, M. Tanel, M. R. Schwartz, P. Biasutto, W. Wit, M. E. Cheetham, P. Adamson, D. M. Rodman, G. Platenburg, M. D. Tome, I. Balikova, F. Nerinckx, J. Zaeytijd, C. Van Cauwenbergh, B. P. Leroy and S. R. Russell (2019). "Effect of an intravitreal antisense oligonucleotide on vision in Leber congenital amaurosis due to a photoreceptor cilium defect." Nat Med 25(2): 225-228.

Crawford, K. M., S. A. Ernst, R. F. Meyer and D. K. MacCallum (1995). "NaK-ATPase pump sites in cultured bovine corneal endothelium of varying cell density at confluence." Invest Ophthalmol Vis Sci 36(7): 1317-1326.

Cremona, F. A., F. R. Ghosheh, C. J. Rapuano, R. C. Eagle, Jr., K. M. Hammersmith, P. R. Laibson, B. D. Ayres and E. J. Cohen (2009). "Keratoconus associated with other corneal dystrophies." Cornea 28(2): 127-135.

Cristol, S. M., H. F. Edelhauser and M. J. Lynn (1992). "A comparison of corneal stromal edema induced from the anterior or the posterior surface." Refract Corneal Surg 8(3): 224-229.

Cross, H. E., A. E. Maumenee and S. J. Cantolino (1971). "Inheritance of Fuchs' endothelial dystrophy." Arch Ophthalmol 85(3): 268-272.

Darlington, J. K., M. J. Mannis and W. A. Segal (2001). "Anterior keratoconus associated with unilateral cornea guttata." Cornea 20(8): 881-884.

Davidson, A. E., S. Hayes, A. J. Hardcastle and S. J. Tuft (2014). "The pathogenesis of keratoconus." Eye (Lond) 28(2): 189-195.

de Oliveira, R. C. and S. E. Wilson (2020). "Descemet's membrane development, structure, function and regeneration." Exp Eye Res 197: 108090.

Del Amo, E. M., A. K. Rimpela, E. Heikkinen, O. K. Kari, E. Ramsay, T. Lajunen, M. Schmitt, L. Pelkonen, M. Bhattacharya, D. Richardson, A. Subrizi, T. Turunen, M. Reinisalo, J. Itkonen, E. Toropainen, M. Casteleijn, H. Kidron, M. Antopolsky, K. S. Vellonen, M. Ruponen and A. Urtti (2017). "Pharmacokinetic aspects of retinal drug delivery." Prog Retin Eye Res 57: 134-185.

Deol, M., D. A. Taylor and N. M. Radcliffe (2015). "Corneal hysteresis and its relevance to glaucoma." Curr Opin Ophthalmol 26(2): 96-102.

Desmet, F. O., D. Hamroun, M. Lalande, G. Collod-Beroud, M. Claustres and C. Beroud (2009). "Human Splicing Finder: an online bioinformatics tool to predict splicing signals." Nucleic Acids Res 37(9): e67.

Du, H., M. S. Cline, R. J. Osborne, D. L. Tuttle, T. A. Clark, J. P. Donohue, M. P. Hall, L. Shiue, M. S. Swanson, C. A. Thornton and M. Ares, Jr. (2010). "Aberrant alternative splicing and extracellular matrix gene expression in mouse models of myotonic dystrophy." Nat Struct Mol Biol 17(2): 187-193.

Du, J., R. A. Aleff, E. Soragni, K. Kalari, J. Nie, X. Tang, J. Davila, J. P. Kocher, S. V. Patel, J. M. Gottesfeld, K. H. Baratz and E. D. Wieben (2015). "RNA toxicity and missplicing in the common eye disease fuchs endothelial corneal dystrophy." J Biol Chem 290(10): 5979-5990.

Duan, R., S. Sharma, Q. Xia, K. Garber and P. Jin (2014). "Towards understanding RNA-mediated neurological disorders." J Genet Genomics 41(9): 473-484.

Duyao, M., C. Ambrose, R. Myers, A. Novelletto, F. Persichetti, M. Frontali, S. Folstein, C. Ross, M. Franz, M. Abbott and et al. (1993). "Trinucleotide repeat length instability and age of onset in Huntington's disease." Nat Genet 4(4): 387-392.

Eger, A., K. Aigner, S. Sonderegger, B. Dampier, S. Oehler, M. Schreiber, G. Berx, A. Cano, H. Beug and R. Foisner (2005). "DeltaEF1 is a transcriptional repressor of E-cadherin and regulates epithelial plasticity in breast cancer cells." Oncogene 24(14): 2375-2385.

Eghrari, A. O., B. S. Garrett, A. A. Mumtaz, A. E. Edalati, D. N. Meadows, E. J. McGlumphy, B. W. Iliff and J. D. Gottsch (2015). "Retroillumination Photography Analysis Enhances Clinical Definition of Severe Fuchs Corneal Dystrophy." Cornea 34(12): 1623-1626.

Eghrari, A. O., E. J. McGlumphy, B. W. Iliff, J. Wang, D. Emmert, S. A. Riazuddin, N. Katsanis and J. D. Gottsch (2012). "Prevalence and severity of fuchs corneal dystrophy in Tangier Island." Am J Ophthalmol 153(6): 1067-1072.

Eghrari, A. O., A. A. Mumtaz, B. Garrett, M. Rezaei, M. S. Akhavan, S. A. Riazuddin and J. D. Gottsch (2017). "Automated Retroillumination Photography Analysis for Objective Assessment of Fuchs Corneal Dystrophy." Cornea 36(1): 44-47.

Eghrari, A. O., S. A. Riazuddin and J. D. Gottsch (2016). "Distinct Clinical Phenotype of Corneal Dystrophy Predicts the p.(Leu450Trp) Substitution in COL8A2." Cornea 35(5): 587-591.

Eghrari, A. O., S. Vahedi, N. A. Afshari, S. A. Riazuddin and J. D. Gottsch (2017). "CTG18.1 Expansion in TCF4 Among African Americans With Fuchs' Corneal Dystrophy." Invest Ophthalmol Vis Sci 58(14): 6046-6049.

Eghrari, A. O., S. Vasanth, B. C. Gapsis, H. Bison, U. Jurkunas, S. A. Riazuddin and J. D. Gottsch (2018). "Identification of a Novel TCF4 Isoform in the Human Corneal Endothelium." Cornea 37(7): 899-903.

- Eghrari, A. O., S. Vasanth, J. Wang, F. Vahedi, S. A. Riazuddin and J. D. Gottsch (2017). "CTG18.1 Expansion in TCF4 Increases Likelihood of Transplantation in Fuchs Corneal Dystrophy." Cornea 36(1): 40-43.
- Elhalis, H., B. Azizi and U. V. Jurkunas (2010). "Fuchs endothelial corneal dystrophy." Ocul Surf 8(4): 173-184.
- Fagan, X. J. and S. Al-Qureshi (2013). "Intravitreal injections: a review of the evidence for best practice." Clin Exp Ophthalmol 41(5): 500-507.
- Falavarjani, K. G. and Q. D. Nguyen (2013). "Adverse events and complications associated with intravitreal injection of anti-VEGF agents: a review of literature." Eye (Lond) 27(7): 787-794.
- Fares, U., A. M. Otri, M. A. Al-Aqaba and H. S. Dua (2012). "Correlation of central and peripheral corneal thickness in healthy corneas." Cont Lens Anterior Eye 35(1): 39-45.
- Fautsch, M. P., E. D. Wieben, K. H. Baratz, N. Bhattacharyya, A. N. Sadan, N. J. Hafford-Tear, S. J. Tuft and A. E. Davidson (2021). "TCF4-mediated Fuchs endothelial corneal dystrophy: Insights into a common trinucleotide repeat-associated disease." Prog Retin Eye Res 81: 100883.
- Ferdi, A. C., V. Nguyen, D. M. Gore, B. D. Allan, J. J. Rozema and S. L. Watson (2019). "Keratoconus Natural Progression: A Systematic Review and Meta-analysis of 11 529 Eyes." Ophthalmology 126(7): 935-945.
- Fischbarg, J. and J. J. Lim (1974). "Role of cations, anions and carbonic anhydrase in fluid transport across rabbit corneal endothelium." J Physiol 241(3): 647-675.
- Foja, S., M. Luther, K. Hoffmann, A. Rupperecht and C. Gruenauer-Kloevekorn (2017). "CTG18.1 repeat expansion may reduce TCF4 gene expression in corneal endothelial cells of German patients with Fuchs' dystrophy." Graefes Arch Clin Exp Ophthalmol.
- Fontes, B. M., R. Ambrosio, Jr., D. Jardim, G. C. Velarde and W. Nose (2010). "Corneal biomechanical metrics and anterior segment parameters in mild keratoconus." Ophthalmology 117(4): 673-679.
- Friedman, D. S., H. D. Jampel, B. Munoz and S. K. West (2006). "The prevalence of open-angle glaucoma among blacks and whites 73 years and older: the Salisbury Eye Evaluation Glaucoma Study." Arch Ophthalmol 124(11): 1625-1630.
- Fritz, M., V. Grewing, P. Maier, T. Lapp, D. Bohringer, T. Reinhard and K. Wacker (2019). "Diurnal Variation in Corneal Edema in Fuchs Endothelial Corneal Dystrophy." Am J Ophthalmol 207: 351-355.
- Furtado, S., O. Suchowersky, B. Rewcastle, L. Graham, M. L. Klimek and A. Garber (1996). "Relationship between trinucleotide repeats and neuropathological changes in Huntington's disease." Ann Neurol 39(1): 132-136.

Gain, P., R. Jullienne, Z. He, M. Aldossary, S. Acquart, F. Cognasse and G. Thuret (2016). "Global Survey of Corneal Transplantation and Eye Banking." JAMA Ophthalmol 134(2): 167-173.

Galvis, V., T. Sherwin, A. Tello, J. Merayo, R. Barrera and A. Acera (2015). "Keratoconus: an inflammatory disorder?" Eye (Lond) 29(7): 843-859.

Gambato, C., E. Longhin, A. G. Catania, D. Lazzarini, R. Parrozzani and E. Midena (2015). "Aging and corneal layers: an in vivo corneal confocal microscopy study." Graefes Arch Clin Exp Ophthalmol 253(2): 267-275.

Gardlik, R., R. Palffy, J. Hodossy, J. Lukacs, J. Turna and P. Celec (2005). "Vectors and delivery systems in gene therapy." Med Sci Monit 11(4): RA110-121.

Gaudana, R., H. K. Ananthula, A. Parenky and A. K. Mitra (2010). "Ocular drug delivery." AAPS J 12(3): 348-360.

Gee, H. Y., F. Zhang, S. Ashraf, S. Kohl, C. E. Sadowski, V. Vega-Warner, W. Zhou, S. Lovric, H. Fang, M. Nettleton, J. Y. Zhu, J. Hoefele, L. T. Weber, L. Podracka, A. Boor, H. Fehrenbach, J. W. Innis, J. Washburn, S. Levy, R. P. Lifton, E. A. Otto, Z. Han and F. Hildebrandt (2015). "KANK deficiency leads to podocyte dysfunction and nephrotic syndrome." J Clin Invest 125(6): 2375-2384.

Georgiou, T., C. L. Funnell, A. Cassels-Brown and R. O'Connor (2004). "Influence of ethnic origin on the incidence of keratoconus and associated atopic disease in Asians and white patients." Eye (Lond) 18(4): 379-383.

Ginsburg, A. P. (2003). "Contrast sensitivity and functional vision." Int Ophthalmol Clin 43(2): 5-15.

Godefrooij, D. A., G. A. de Wit, C. S. Uiterwaal, S. M. Imhof and R. P. Wisse (2017). "Age-specific Incidence and Prevalence of Keratoconus: A Nationwide Registration Study." Am J Ophthalmol 175: 169-172.

Gomes, J. A., D. Tan, C. J. Rapuano, M. W. Belin, R. Ambrosio, Jr., J. L. Guell, F. Malecaze, K. Nishida, V. S. Sangwan, K. Group of Panelists for the Global Delphi Panel of and D. Ectatic (2015). "Global consensus on keratoconus and ectatic diseases." Cornea 34(4): 359-369.

Gordon-Shaag, A., M. Millodot, E. Shneor and Y. Liu (2015). "The genetic and environmental factors for keratoconus." Biomed Res Int 2015: 795738.

Gottsch, J. D., A. L. Bowers, E. H. Margulies, G. D. Seitzman, S. W. Kim, S. Saha, A. S. Jun, W. J. Stark and S. H. Liu (2003). "Serial analysis of gene expression in the corneal endothelium of Fuchs' dystrophy." Invest Ophthalmol Vis Sci 44(2): 594-599.

Gottsch, J. D., O. H. Sundin, S. H. Liu, A. S. Jun, K. W. Broman, W. J. Stark, E. C. Vito, A. K. Narang, J. M. Thompson and M. Magovern (2005). "Inheritance of a novel COL8A2 mutation

defines a distinct early-onset subtype of fuchs corneal dystrophy." Invest Ophthalmol Vis Sci 46(6): 1934-1939.

Gottsch, J. D., C. Zhang, O. H. Sundin, W. R. Bell, W. J. Stark and W. R. Green (2005). "Fuchs corneal dystrophy: aberrant collagen distribution in an L450W mutant of the COL8A2 gene." Invest Ophthalmol Vis Sci 46(12): 4504-4511.

Green, E. D., J. D. Watson and F. S. Collins (2015). "Human Genome Project: Twenty-five years of big biology." Nature 526(7571): 29-31.

Greenhill, N. S., B. M. Ruger, Q. Hasan and P. F. Davis (2000). "The alpha1(VIII) and alpha2(VIII) collagen chains form two distinct homotrimeric proteins in vivo." Matrix Biol 19(1): 19-28.

Grewing, V., M. Fritz, C. Muller, D. Bohringer, T. Reinhard, S. V. Patel and K. Wacker (2020). "[The German version of the Visual Function and Corneal Health Status (VFUCHS): a Fuchs dystrophy-specific visual disability instrument]." Ophthalmologe 117(2): 140-146.

Grillet, N., M. Schwander, M. S. Hildebrand, A. Sczaniecka, A. Kolatkar, J. Velasco, J. A. Webster, K. Kahrizi, H. Najmabadi, W. J. Kimberling, D. Stephan, M. Bahlo, T. Wiltshire, L. M. Tarantino, P. Kuhn, R. J. Smith and U. Muller (2009). "Mutations in LOXHD1, an evolutionarily conserved stereociliary protein, disrupt hair cell function in mice and cause progressive hearing loss in humans." Am J Hum Genet 85(3): 328-337.

Groger, N., H. Frohlich, H. Maier, A. Olbrich, S. Kostin, T. Braun and T. Boettger (2010). "SLC4A11 prevents osmotic imbalance leading to corneal endothelial dystrophy, deafness, and polyuria." J Biol Chem 285(19): 14467-14474.

Groh, W. J., M. R. Groh, C. Shen, D. G. Monckton, C. L. Bodkin and R. M. Pascuzzi (2011). "Survival and CTG repeat expansion in adults with myotonic dystrophy type 1." Muscle Nerve 43(5): 648-651.

Gupta, R., R. Kinderyte, D. S. Jacobs and U. V. Jurkunas (2017). "Elimination of Anterior Corneal Steepening With Descemet Membrane Endothelial Keratoplasty in a Patient With Fuchs Dystrophy and Keratoconus: Implications for IOL Calculation." Cornea 36(10): 1260-1262.

Gupta, R., B. L. Kumawat, P. Paliwal, R. Tandon, N. Sharma, S. Sen, S. Kashyap, T. C. Nag, R. B. Vajpayee and A. Sharma (2015). "Association of ZEB1 and TCF4 rs613872 changes with late onset Fuchs endothelial corneal dystrophy in patients from northern India." Mol Vis 21: 1252-1260.

Gusella, J. F., N. S. Wexler, P. M. Conneally, S. L. Naylor, M. A. Anderson, R. E. Tanzi, P. C. Watkins, K. Ottina, M. R. Wallace, A. Y. Sakaguchi and et al. (1983). "A polymorphic DNA marker genetically linked to Huntington's disease." Nature 306(5940): 234-238.

Haiman, C. A. and D. O. Stram (2008). "Utilizing HapMap and tagging SNPs." Methods Mol Med 141: 37-54.

Han, S. B., H. P. Ang, R. Poh, S. S. Chaurasia, G. Peh, J. Liu, D. T. Tan, E. N. Vithana and J. S. Mehta (2013). "Mice with a targeted disruption of Slc4a11 model the progressive corneal changes of congenital hereditary endothelial dystrophy." Invest Ophthalmol Vis Sci 54(9): 6179-6189.

Hannan, A. J. (2018). "Tandem repeats mediating genetic plasticity in health and disease." Nat Rev Genet 19(5): 286-298.

Hao, J., S. K. Li, C. Y. Liu and W. W. Kao (2009). "Electrically assisted delivery of macromolecules into the corneal epithelium." Exp Eye Res 89(6): 934-941.

Hardcastle, A. J., P. Liskova, Y. Bykhovskaya, B. J. McComish, A. E. Davidson, C. F. Inglehearn, X. Li, H. Choquet, M. Habeeb, S. E. M. Lucas, S. Sahebjada, N. Pontikos, K. E. R. Lopez, A. P. Khawaja, M. Ali, L. Dudakova, P. Skalicka, B. T. H. Van Dooren, A. J. M. Geerards, C. W. Haudum, V. L. Faro, A. Tenen, M. J. Simcoe, K. Patasova, D. Yarrand, J. Yin, S. Siddiqui, A. Rice, L. A. Farraj, Y. I. Chen, J. S. Rahi, R. M. Krauss, E. Theusch, J. C. Charlesworth, L. Szczotka-Flynn, C. Toomes, M. A. Meester-Smoor, A. J. Richardson, P. A. Mitchell, K. D. Taylor, R. B. Melles, A. J. Aldave, R. A. Mills, K. Cao, E. Chan, M. D. Daniell, J. J. Wang, J. I. Rotter, A. W. Hewitt, S. MacGregor, C. C. W. Klaver, W. D. Ramdas, J. E. Craig, S. K. Iyengar, D. O'Brart, E. Jorgenson, P. N. Baird, Y. S. Rabinowitz, K. P. Burdon, C. J. Hammond, S. J. Tuft and P. G. Hysi (2021). "A multi-ethnic genome-wide association study implicates collagen matrix integrity and cell differentiation pathways in keratoconus." Commun Biol 4(1): 266.

He, Z., A. Pipparelli, C. Manissolle, S. Acquart, O. Garraud, P. Gain and G. Thuret (2010). "Ex vivo gene electrotransfer to the endothelium of organ cultured human corneas." Ophthalmic Res 43(1): 43-55.

Helmholtz, H. v. and J. P. C. Southall (1924). "Helmholtz's treatise on physiological optics. Vol. 1 Vol. 1."

Hidayat, A. A. and G. C. Cockerham (2006). "Epithelial metaplasia of the corneal endothelium in Fuchs endothelial dystrophy." Cornea 25(8): 956-959.

Higa, A., H. Sakai, S. Sawaguchi, A. Iwase, A. Tomidokoro, S. Amano and M. Araie (2011).

"Prevalence of and risk factors for cornea guttata in a population-based study in a southwestern island of Japan: the Kumejima study." Arch Ophthalmol 129(3): 332-336.

Hollingsworth, J., I. Perez-Gomez, H. A. Mutalib and N. Efron (2001). "A population study of the normal cornea using an in vivo, slit-scanning confocal microscope." Optom Vis Sci 78(10): 706-711.

Hopfer, U., N. Fukai, H. Hopfer, G. Wolf, N. Joyce, E. Li and B. R. Olsen (2005). "Targeted disruption of Col8a1 and Col8a2 genes in mice leads to anterior segment abnormalities in the eye." FASEB J 19(10): 1232-1244.

Huang, J., J. Maram, T. C. Tepelus, C. Modak, K. Marion, S. R. Sadda, V. Chopra and O. L. Lee (2018). "Comparison of manual & automated analysis methods for corneal endothelial cell density measurements by specular microscopy." J Optom 11(3): 182-191.



Hughes, L. and D. M. Maurice (1984). "A fresh look at iontophoresis." Arch Ophthalmol 102(12): 1825-1829.

Ihalainen, A. (1986). "Clinical and epidemiological features of keratoconus genetic and external factors in the pathogenesis of the disease." Acta Ophthalmol Suppl 178: 1-64.

Ihanamaki, T., L. J. Pelliniemi and E. Vuorio (2004). "Collagens and collagen-related matrix components in the human and mouse eye." Prog Retin Eye Res 23(4): 403-434.

International Human Genome Sequencing, C. (2004). "Finishing the euchromatic sequence of the human genome." Nature 431(7011): 931-945.

Iwamoto, T. and A. G. DeVoe (1971). "Electron microscopic studies on Fuchs' combined dystrophy. I. Posterior portion of the cornea." Invest Ophthalmol 10(1): 9-28.

Jaspert, A., R. Fahsold, H. Grehl and D. Claus (1995). "Myotonic dystrophy: correlation of clinical symptoms with the size of the CTG trinucleotide repeat." J Neurol 242(2): 99-104.

Johnson, D., H. Hollands, S. Hollands and S. Sharma (2010). "Incidence and characteristics of acute intraocular inflammation after intravitreal injection of bevacizumab: a retrospective cohort study." Can J Ophthalmol 45(3): 239-242.

Joyce, N. C. (2003). "Proliferative capacity of the corneal endothelium." Prog Retin Eye Res 22(3): 359-389.

Joyce, N. C., D. L. Harris and D. M. Mello (2002). "Mechanisms of mitotic inhibition in corneal endothelium: contact inhibition and TGF-beta2." Invest Ophthalmol Vis Sci 43(7): 2152-2159.

Joyce, N. C., C. C. Zhu and D. L. Harris (2009). "Relationship among oxidative stress, DNA damage, and proliferative capacity in human corneal endothelium." Invest Ophthalmol Vis Sci 50(5): 2116-2122.

Juliano, R. L. (2016). "The delivery of therapeutic oligonucleotides." Nucleic Acids Res 44(14): 6518-6548.

Jun, A. S., H. Meng, N. Ramanan, M. Matthaei, S. Chakravarti, R. Bonshek, G. C. Black, R. Grebe and M. Kimos (2012). "An alpha 2 collagen VIII transgenic knock-in mouse model of Fuchs endothelial corneal dystrophy shows early endothelial cell unfolded protein response and apoptosis." Hum Mol Genet 21(2): 384-393.

Jurkunas, U. and D. T. Azar (2006). "Potential complications of ocular surgery in patients with coexistent keratoconus and Fuchs' endothelial dystrophy." Ophthalmology 113(12): 2187-2197.

Jurkunas, U. V. (2018). "Fuchs Endothelial Corneal Dystrophy Through the Prism of Oxidative Stress." Cornea 37 Suppl 1: S50-S54.

Jurkunas, U. V., M. S. Bitar, T. Funaki and B. Azizi (2010). "Evidence of oxidative stress in the pathogenesis of fuchs endothelial corneal dystrophy." Am J Pathol 177(5): 2278-2289.

Kakinuma, N., B. C. Roy, Y. Zhu, Y. Wang and R. Kiyama (2008). "Kank regulates RhoA-dependent formation of actin stress fibers and cell migration via 14-3-3 in PI3K-Akt signaling." J Cell Biol 181(3): 537-549.

Kakinuma, N., Y. Zhu, Y. Wang, B. C. Roy and R. Kiyama (2009). "Kank proteins: structure, functions and diseases." Cell Mol Life Sci 66(16): 2651-2659.

Kao, W. W. and C. Y. Liu (2002). "Roles of lumican and keratocan on corneal transparency." Glycoconj J 19(4-5): 275-285.

Kaushik, J., A. K. Jain, V. K. Jain and P. Chakma (2015). "Phacoemulsification in a rare case of keratoconus with Fuch's endothelial corneal dystrophy." Int J Ophthalmol 8(6): 1253-1254.

Kennedy, R. H., W. M. Bourne and J. A. Dyer (1986). "A 48-year clinical and epidemiologic study of keratoconus." Am J Ophthalmol 101(3): 267-273.

Kenney, M. C., S. R. Atilano, N. Zorapapel, B. Holguin, R. N. Gaster and A. V. Ljubimov (2004). "Altered expression of aquaporins in bullous keratopathy and Fuchs' dystrophy corneas." J Histochem Cytochem 52(10): 1341-1350.

Khawaja, A. P., K. E. Rojas Lopez, A. J. Hardcastle, C. J. Hammond, P. Liskova, A. E. Davidson, D. M. Gore, N. J. Hafford Tear, N. Pontikos, S. Hayat, N. Wareham, K. T. Khaw, S. J. Tuft, P. J. Foster and P. G. Hysi (2019). "Genetic Variants Associated With Corneal Biomechanical Properties and Potentially Conferring Susceptibility to Keratoconus in a Genome-Wide Association Study." JAMA Ophthalmol 137(9): 1005-1012.

Killer, H. E. and A. Pircher (2018). "Normal tension glaucoma: review of current understanding and mechanisms of the pathogenesis." Eye (Lond) 32(5): 924-930.

Kimura, A., K. Namekata, X. Guo, T. Noro, C. Harada and T. Harada (2017). "Targeting Oxidative Stress for Treatment of Glaucoma and Optic Neuritis." Oxid Med Cell Longev 2017: 2817252.

Kitagawa, K., M. Kojima, H. Sasaki, Y. B. Shui, S. J. Chew, H. M. Cheng, M. Ono, Y. Morikawa and K. Sasaki (2002). "Prevalence of primary cornea guttata and morphology of corneal endothelium in aging Japanese and Singaporean subjects." Ophthalmic Res 34(3): 135-138.

Klein, B. E., R. Klein, W. E. Sponsel, T. Franke, L. B. Cantor, J. Martone and M. J. Menage (1992). "Prevalence of glaucoma. The Beaver Dam Eye Study." Ophthalmology 99(10): 1499-1504.

Kopplin, L. J., K. Przepyszny, B. Schmotzer, K. Rudo, D. C. Babineau, S. V. Patel, D. D. Verdier, U. Jurkunas, S. K. Iyengar, J. H. Lass and G. Fuchs' Endothelial Corneal Dystrophy Genetics Multi-Center Study (2012). "Relationship of Fuchs endothelial corneal dystrophy severity to central corneal thickness." Arch Ophthalmol 130(4): 433-439.

Krachmer, J. H., J. J. Purcell, Jr., C. W. Young and K. D. Bucher (1978). "Corneal endothelial dystrophy. A study of 64 families." Arch Ophthalmol 96(11): 2036-2039.

Krafchak, C. M., H. Pawar, S. E. Moroi, A. Sugar, P. R. Lichter, D. A. Mackey, S. Mian, T. Nairus, V. Elnor, M. T. Schteingart, C. A. Downs, T. G. Kijek, J. M. Johnson, E. H. Trager, F. W. Rozsa, M. N. Mandal, M. P. Epstein, D. Vollrath, R. Ayyagari, M. Boehnke and J. E. Richards (2005). "Mutations in TCF8 cause posterior polymorphous corneal dystrophy and ectopic expression of COL4A3 by corneal endothelial cells." Am J Hum Genet 77(5): 694-708.

Lechner, J., D. P. Dash, D. Muszynska, M. Hosseini, F. Segev, S. George, D. G. Frazer, J. E. Moore, S. B. Kaye, T. Young, D. A. Simpson, A. J. Churchill, E. Heon and C. E. Willoughby (2013). "Mutational spectrum of the ZEB1 gene in corneal dystrophies supports a genotype-phenotype correlation." Invest Ophthalmol Vis Sci 54(5): 3215-3223.

Lee, J. H., J. H. Wang, J. Chen, F. Li, T. L. Edwards, A. W. Hewitt and G. S. Liu (2019). "Gene therapy for visual loss: Opportunities and concerns." Prog Retin Eye Res 68: 31-53.

Leejee H. Suh, M. V. E., Albert S. Jun (2008). Chapter 1  
Fuchs Endothelial Dystrophy: Pathogenesis and Management, Springer, Berlin, Heidelberg.

Leske, M. C., A. M. Connell, A. P. Schachat and L. Hyman (1994). "The Barbados Eye Study. Prevalence of open angle glaucoma." Arch Ophthalmol 112(6): 821-829.

Leung, B. K., J. A. Bonanno and C. J. Radke (2011). "Oxygen-deficient metabolism and corneal edema." Prog Retin Eye Res 30(6): 471-492.

Levy, S. G., J. Moss, H. Sawada, P. J. Dopping-Hepenstal and A. C. McCartney (1996). "The composition of wide-spaced collagen in normal and diseased Descemet's membrane." Curr Eye Res 15(1): 45-52.

Li, J., A. Mahajan and M. D. Tsai (2006). "Ankyrin repeat: a unique motif mediating protein-protein interactions." Biochemistry 45(51): 15168-15178.

Li, Q. J., M. F. Ashraf, D. F. Shen, W. R. Green, W. J. Stark, C. C. Chan and T. P. O'Brien (2001). "The role of apoptosis in the pathogenesis of Fuchs endothelial dystrophy of the cornea." Arch Ophthalmol 119(11): 1597-1604.

Li, X., Y. Bykhovskaya, T. Haritunians, D. Siscovick, A. Aldave, L. Szczotka-Flynn, S. K. Iyengar, J. I. Rotter, K. D. Taylor and Y. S. Rabinowitz (2012). "A genome-wide association study identifies a potential novel gene locus for keratoconus, one of the commonest causes for corneal transplantation in developed countries." Hum Mol Genet 21(2): 421-429.

Li, Y., J. Yang, S. Li, J. Zhang, J. Zheng, W. Hou, H. Zhao, Y. Guo, X. Liu, K. Dou, Z. Situ and L. Yao (2011). "N-myc downstream-regulated gene 2, a novel estrogen-targeted gene, is involved in the regulation of Na<sup>+</sup>/K<sup>+</sup>-ATPase." J Biol Chem 286(37): 32289-32299.

Liaw, J., S. F. Chang and F. C. Hsiao (2001). "In vivo gene delivery into ocular tissues by eye drops of poly(ethylene oxide)-poly(propylene oxide)-poly(ethylene oxide) (PEO-PPO-PEO) polymeric micelles." Gene Ther 8(13): 999-1004.

- Lindow, M., H. P. Vornlocher, D. Riley, D. J. Kornbrust, J. Burchard, L. O. Whiteley, J. Kamens, J. D. Thompson, S. Nochur, H. Younis, S. Bartz, J. Parry, N. Ferrari, S. P. Henry and A. A. Levin (2012). "Assessing unintended hybridization-induced biological effects of oligonucleotides." Nat Biotechnol 30(10): 920-923.
- Lipman, R. M., J. B. Rubenstein and E. Torczynski (1990). "Keratoconus and Fuchs' corneal endothelial dystrophy in a patient and her family." Arch Ophthalmol 108(7): 993-994.
- Liskova, P., L. Dudakova, C. J. Evans, K. E. Rojas Lopez, N. Pontikos, D. Athanasiou, H. Jama, J. Sach, P. Skalicka, V. Stranecky, S. Kmoch, C. Thaug, M. Filipiec, M. E. Cheetham, A. E. Davidson, S. J. Tuft and A. J. Hardcastle (2018). "Ectopic GRHL2 Expression Due to Non-coding Mutations Promotes Cell State Transition and Causes Posterior Polymorphous Corneal Dystrophy 4." Am J Hum Genet 102(3): 447-459.
- Liskova, P., M. Filipiec, S. Merjava, K. Jirsova and S. J. Tuft (2010). "Variable ocular phenotypes of posterior polymorphous corneal dystrophy caused by mutations in the ZEB1 gene." Ophthalmic Genet 31(4): 230-234.
- Liskova, P., Q. Prescott, S. S. Bhattacharya and S. J. Tuft (2007). "British family with early-onset Fuchs' endothelial corneal dystrophy associated with p.L450W mutation in the COL8A2 gene." Br J Ophthalmol 91(12): 1717-1718.
- Liu, C., T. Miyajima, G. Melangath, T. Miyai, S. Vasanth, N. Deshpande, V. Kumar, S. Ong Tone, R. Gupta, S. Zhu, D. Vojnovic, Y. Chen, E. G. Rogan, B. Mondal, M. Zahid and U. V. Jurkunas (2020). "Ultraviolet A light induces DNA damage and estrogen-DNA adducts in Fuchs endothelial corneal dystrophy causing females to be more affected." Proc Natl Acad Sci U S A 117(1): 573-583.
- Loganathan, S. K., H. P. Schneider, P. E. Morgan, J. W. Deitmer and J. R. Casey (2016). "Functional assessment of SLC4A11, an integral membrane protein mutated in corneal dystrophies." Am J Physiol Cell Physiol 311(5): C735-C748.
- Lopez, I. A., M. I. Rosenblatt, C. Kim, G. C. Galbraith, S. M. Jones, L. Kao, D. Newman, W. Liu, S. Yeh, A. Pushkin, N. Abuladze and I. Kurtz (2009). "Slc4a11 gene disruption in mice: cellular targets of sensorineuronal abnormalities." J Biol Chem 284(39): 26882-26896.
- Lorenzetti, D. W., M. H. Uotila, N. Parikh and H. E. Kaufman (1967). "Central cornea guttata. Incidence in the general population." Am J Ophthalmol 64(6): 1155-1158.
- Louttit, M. D., L. J. Kopplin, R. P. Igo, Jr., J. R. Fondran, A. Tagliaferri, D. Bardenstein, A. J. Aldave, C. R. Croasdale, M. O. Price, G. O. Rosenwasser, J. H. Lass, S. K. Iyengar and F. G. M.-C. S. Group (2012). "A multicenter study to map genes for Fuchs endothelial corneal dystrophy: baseline characteristics and heritability." Cornea 31(1): 26-35.
- Lu, Y., V. Vitart, K. P. Burdon, C. C. Khor, Y. Bykhovskaya, A. Mirshahi, A. W. Hewitt, D. Koehn, P. G. Hysi, W. D. Ramdas, T. Zeller, E. N. Vithana, B. K. Cornes, W. T. Tay, E. S. Tai, C. Y. Cheng, J. Liu, J. N. Foo, S. M. Saw, G. Thorleifsson, K. Stefansson, D. P. Dimasi, R. A. Mills, J. Mountain,

W. Ang, R. Hoehn, V. J. Verhoeven, F. Grus, R. Wolfs, R. Castagne, K. J. Lackner, H. Springelkamp, J. Yang, F. Jonasson, D. Y. Leung, L. J. Chen, C. C. Tham, I. Rudan, Z. Vataavuk, C. Hayward, J. Gibson, A. J. Cree, A. MacLeod, S. Ennis, O. Polasek, H. Campbell, J. F. Wilson, A. C. Viswanathan, B. Fleck, X. Li, D. Siscovick, K. D. Taylor, J. I. Rotter, S. Yazar, M. Ulmer, J. Li, B. L. Yaspan, A. B. Ozel, J. E. Richards, S. E. Moroi, J. L. Haines, J. H. Kang, L. R. Pasquale, R. R. Allingham, A. Ashley-Koch, N. Consortium, P. Mitchell, J. J. Wang, A. F. Wright, C. Pennell, T. D. Spector, T. L. Young, C. C. Klaver, N. G. Martin, G. W. Montgomery, M. G. Anderson, T. Aung, C. E. Willoughby, J. L. Wiggs, C. P. Pang, U. Thorsteinsdottir, A. J. Lotery, C. J. Hammond, C. M. van Duijn, M. A. Hauser, Y. S. Rabinowitz, N. Pfeiffer, D. A. Mackey, J. E. Craig, S. Macgregor and T. Y. Wong (2013). "Genome-wide association analyses identify multiple loci associated with central corneal thickness and keratoconus." Nat Genet 45(2): 155-163.

Luce, D. A. (2005). "Determining in vivo biomechanical properties of the cornea with an ocular response analyzer." J Cataract Refract Surg 31(1): 156-162.

Macnamara, E., G. W. Sams, K. Smith, J. Ambati, N. Singh and B. K. Ambati (2004). "Aquaporin-1 expression is decreased in human and mouse corneal endothelial dysfunction." Mol Vis 10: 51-56.

Magovern, M., G. R. Beauchamp, J. W. McTigue, B. S. Fine and R. C. Baumiller (1979). "Inheritance of Fuchs' combined dystrophy." Ophthalmology 86(10): 1897-1923.

Malhotra, D., M. Jung, C. Fecher-Trost, M. Lovatt, G. S. L. Peh, S. Noskov, J. S. Mehta, R. Zimmermann and J. R. Casey (2020). "Defective cell adhesion function of solute transporter, SLC4A11, in endothelial corneal dystrophies." Hum Mol Genet 29(1): 97-116.

Malhotra, D., S. K. Loganathan, A. M. Chiu, C. M. Lukowski and J. R. Casey (2019). "Human Corneal Expression of SLC4A11, a Gene Mutated in Endothelial Corneal Dystrophies." Sci Rep 9(1): 9681.

Mandell, R. B. and I. Fatt (1965). "Thinning of the human cornea on awakening." Nature 208(5007): 292-293.

Mandell, R. B., K. A. Polse, R. J. Brand, D. Vastine, D. Demartini and R. Flom (1989). "Corneal hydration control in Fuchs' dystrophy." Invest Ophthalmol Vis Sci 30(5): 845-852.

Mantelli, F., J. Mauris and P. Argueso (2013). "The ocular surface epithelial barrier and other mechanisms of mucosal protection: from allergy to infectious diseases." Curr Opin Allergy Clin Immunol 13(5): 563-568.

Martone, G., C. Tommasi, C. Traversi, A. Balestrazzi, E. Berni, E. Nuti and G. M. Tosi (2007). "Unilateral corneal endothelial dystrophy and anterior keratoconus." Eur J Ophthalmol 17(3): 430-432.

Maurice, D. M. (1972). "The location of the fluid pump in the cornea." J Physiol 221(1): 43-54.

Mazzotta, C., C. Traversi, F. Raiskup, C. L. Rizzo and A. Renieri (2014). "First identification of a triple corneal dystrophy association: keratoconus, epithelial basement membrane corneal dystrophy and fuchs' endothelial corneal dystrophy." Case Rep Ophthalmol 5(3): 281-288.

McLaren, J. W., L. A. Bachman, K. M. Kane and S. V. Patel (2014). "Objective assessment of the corneal endothelium in Fuchs' endothelial dystrophy." Invest Ophthalmol Vis Sci 55(2): 1184-1190.

Meek, K. M. and C. Boote (2004). "The organization of collagen in the corneal stroma." Exp Eye Res 78(3): 503-512.

Mehta, J. S., E. N. Vithana, D. T. Tan, V. H. Yong, G. H. Yam, R. W. Law, W. G. Chong, C. P. Pang and T. Aung (2008). "Analysis of the posterior polymorphous corneal dystrophy 3 gene, TCF8, in late-onset Fuchs endothelial corneal dystrophy." Invest Ophthalmol Vis Sci 49(1): 184-188.

Mehta, M., Deeksha, D. Tewari, G. Gupta, R. Awasthi, H. Singh, P. Pandey, D. K. Chellappan, R. Wadhwa, T. Collet, P. M. Hansbro, S. R. Kumar, L. Thangavelu, P. Negi, K. Dua and S. Satija (2019). "Oligonucleotide therapy: An emerging focus area for drug delivery in chronic inflammatory respiratory diseases." Chem Biol Interact 308: 206-215.

Meng, H., M. Matthaei, N. Ramanan, R. Grebe, S. Chakravarti, C. L. Speck, M. Kimos, N. Vij, C. G. Eberhart and A. S. Jun (2013). "L450W and Q455K Col8a2 knock-in mouse models of Fuchs endothelial corneal dystrophy show distinct phenotypes and evidence for altered autophagy." Invest Ophthalmol Vis Sci 54(3): 1887-1897.

Michels, R. G., K. R. Kenyon and A. E. Maumence (1972). "Retrocorneal fibrous membrane." Invest Ophthalmol 11(10): 822-831.

Mitchell, P., W. Smith, K. Attebo and P. R. Healey (1996). "Prevalence of open-angle glaucoma in Australia. The Blue Mountains Eye Study." Ophthalmology 103(10): 1661-1669.

Miyajima, T., G. Melangath, S. Zhu, N. Deshpande, S. Vasanth, B. Mondal, V. Kumar, Y. Chen, M. O. Price, F. W. Price, Jr., E. G. Rogan, M. Zahid and U. V. Jurkunas (2020). "Loss of NQO1 generates genotoxic estrogen-DNA adducts in Fuchs Endothelial Corneal Dystrophy." Free Radic Biol Med 147: 69-79.

Moazzeni, H., M. Mirrahimi, A. Moghadam, A. Banaei-Esfahani, S. Yazdani and E. Elahi (2019). "Identification of genes involved in glaucoma pathogenesis using combined network analysis and empirical studies." Hum Mol Genet 28(21): 3637-3663.

Mohan, R. R., J. C. Tovey, A. Sharma and A. Tandon (2012). "Gene therapy in the cornea: 2005--present." Prog Retin Eye Res 31(1): 43-64.

Mok, J. W., H. S. Kim and C. K. Joo (2009). "Q455V mutation in COL8A2 is associated with Fuchs' corneal dystrophy in Korean patients." Eye (Lond) 23(4): 895-903.

Mootha, V. V., X. Gong, H. C. Ku and C. Xing (2014). "Association and familial segregation of CTG18.1 trinucleotide repeat expansion of TCF4 gene in Fuchs' endothelial corneal dystrophy." Invest Ophthalmol Vis Sci 55(1): 33-42.

Moshirfar, M., Y. L. H, U. Vaidyanathan, N. S. A, C. H. G, R. B. J, B. H. M, B. R. D, N. M. M and C. H. P (2019). "Diagnosis and Management of Pseudoguttata: A Literature Review." Med Hypothesis Discov Innov Ophthalmol 8(3): 156-162.

Mulamba, G. B., A. Hu, R. F. Azad, K. P. Anderson and D. M. Coen (1998). "Human cytomegalovirus mutant with sequence-dependent resistance to the phosphorothioate oligonucleotide fomivirsen (ISIS 2922)." Antimicrob Agents Chemother 42(4): 971-973.

Muragaki, Y., O. Jacenko, S. Apte, M. G. Mattei, Y. Ninomiya and B. R. Olsen (1991). "The alpha 2(VIII) collagen gene. A novel member of the short chain collagen family located on the human chromosome 1." J Biol Chem 266(12): 7721-7727.

Muragaki, Y., M. G. Mattei, N. Yamaguchi, B. R. Olsen and Y. Ninomiya (1991). "The complete primary structure of the human alpha 1 (VIII) chain and assignment of its gene (COL8A1) to chromosome 3." Eur J Biochem 197(3): 615-622.

Murphy, C., J. Alvarado and R. Juster (1984). "Prenatal and postnatal growth of the human Descemet's membrane." Invest Ophthalmol Vis Sci 25(12): 1402-1415.

Myers, R. H., J. P. Vonsattel, T. J. Stevens, L. A. Cupples, E. P. Richardson, J. B. Martin and E. D. Bird (1988). "Clinical and neuropathologic assessment of severity in Huntington's disease." Neurology 38(3): 341-347.

Mylona, I., I. Tsinopoulos and N. Ziakas (2020). "Comorbidity of Keratoconus and Fuchs' Corneal Endothelial Dystrophy: A Review of the Literature." Ophthalmic Res 63(4): 369-374.

Nagaki, Y., S. Hayasaka, K. Kitagawa and S. Yamamoto (1996). "Primary cornea guttata in Japanese patients with cataract: specular microscopic observations." Jpn J Ophthalmol 40(4): 520-525.

Nagarsheth, M., A. Singh, B. Schmotzer, D. C. Babineau, J. Sugar, W. B. Lee, S. K. Iyengar, J. H. Lass and G. Fuchs' Genetics Multi-Center Study (2012). "Relationship Between Fuchs Endothelial Corneal Dystrophy Severity and Glaucoma and/or Ocular Hypertension." Arch Ophthalmol 130(11): 1384-1388.

Nakano, M., N. Okumura, H. Nakagawa, N. Koizumi, Y. Ikeda, M. Ueno, K. Yoshii, H. Adachi, R. A. Aleff, M. L. Butz, W. E. Highsmith, K. Tashiro, E. D. Wieben, S. Kinoshita and K. H. Baratz (2015). "Trinucleotide Repeat Expansion in the TCF4 Gene in Fuchs' Endothelial Corneal Dystrophy in Japanese." Invest Ophthalmol Vis Sci 56(8): 4865-4869.

Nanda, G. G., B. Padhy, S. Samal, S. Das and D. P. Alone (2014). "Genetic association of TCF4 intronic polymorphisms, CTG18.1 and rs17089887, with Fuchs' endothelial corneal dystrophy in an Indian population." Invest Ophthalmol Vis Sci 55(11): 7674-7680.

Nichols, J. J., G. M. Kosunick and M. A. Bullimore (2003). "Reliability of corneal thickness and endothelial cell density measures." J Refract Surg 19(3): 344-352.

Orlin, S. E., I. M. Raber, R. C. Eagle, Jr. and H. G. Scheie (1990). "Keratoconus associated with corneal endothelial dystrophy." Cornea 9(4): 299-304.

Orozco-Hernandez, A., X. Ortega-Larrocea, G. Sanchez-Bermudez, G. Garcia-Aguirre, V. M. Canton and R. Velez-Montoya (2014). "Acute sterile endophthalmitis following intravitreal bevacizumab: case series." Clin Ophthalmol 8: 1793-1799.

Ortiz, D., D. Pinero, M. H. Shabayek, F. Arnalich-Montiel and J. L. Alio (2007). "Corneal biomechanical properties in normal, post-laser in situ keratomileusis, and keratoconic eyes." J Cataract Refract Surg 33(8): 1371-1375.

Overend, G., C. Legare, J. Mathieu, L. Bouchard, C. Gagnon and D. G. Monckton (2019). "Allele length of the DMPK CTG repeat is a predictor of progressive myotonic dystrophy type 1 phenotypes." Hum Mol Genet 28(13): 2245-2254.

Papali'i-Curtin, A. T., R. Cox, T. Ma, L. Woods, A. Covello and R. C. Hall (2019). "Keratoconus Prevalence Among High School Students in New Zealand." Cornea 38(11): 1382-1389.

Parker, J., R. S. Birbal, K. van Dijk, S. Oellerich, I. Dapena and G. R. J. Melles (2019). "Are Descemet Membrane Ruptures the Root Cause of Corneal Hydrops in Keratoconic Eyes?" Am J Ophthalmol 205: 204-205.

Parker, J. S., R. S. Birbal, K. van Dijk, S. Oellerich, I. Dapena and G. R. J. Melles (2019). "Are Descemet Membrane Ruptures the Root Cause of Corneal Hydrops in Keratoconic Eyes?" Am J Ophthalmol 205: 147-152.

Patel, S. V. (2019). "Towards Clinical Trials in Fuchs Endothelial Corneal Dystrophy: Classification and Outcome Measures-The Bowman Club Lecture 2019." BMJ Open Ophthalmol 4(1): e000321.

Pearson, A. R., B. Soneji, N. Sarvananthan and J. H. Sandford-Smith (2000). "Does ethnic origin influence the incidence or severity of keratoconus?" Eye (Lond) 14 ( Pt 4): 625-628.

Peh, G. S., Z. Chng, H. P. Ang, T. Y. Cheng, K. Adnan, X. Y. Seah, B. L. George, K. P. Toh, D. T. Tan, G. H. Yam, A. Colman and J. S. Mehta (2015). "Propagation of human corneal endothelial cells: a novel dual media approach." Cell Transplant 24(2): 287-304.

Petersen, B. S., B. Fredrich, M. P. Hoepfner, D. Ellinghaus and A. Franke (2017). "Opportunities and challenges of whole-genome and -exome sequencing." BMC Genet 18(1): 14.

Petit, L., H. Khanna and C. Punzo (2016). "Advances in Gene Therapy for Diseases of the Eye." Hum Gene Ther 27(8): 563-579.

Pillai, J. A., L. A. Hansen, E. Masliah, J. L. Goldstein, S. D. Edland and J. Corey-Bloom (2012). "Clinical severity of Huntington's disease does not always correlate with neuropathologic stage." Mov Disord 27(9): 1099-1103.



- Piva, F., M. Giulietti, A. B. Burini and G. Principato (2012). "SpliceAid 2: a database of human splicing factors expression data and RNA target motifs." Hum Mutat 33(1): 81-85.
- Price, F. W., Jr. and M. O. Price (2017). "Combined Cataract/DSEK/DMEK: Changing Expectations." Asia Pac J Ophthalmol (Phila) 6(4): 388-392.
- Rabinowitz, Y. S. (1998). "Keratoconus." Surv Ophthalmol 42(4): 297-319.
- Ramprasad, V. L., N. D. Ebenezer, T. Aung, R. Rajagopal, V. H. Yong, S. J. Tuft, D. Viswanathan, M. F. El-Ashry, P. Liskova, D. T. Tan, S. S. Bhattacharya, G. Kumaramanickavel and E. N. Vithana (2007). "Novel SLC4A11 mutations in patients with recessive congenital hereditary endothelial dystrophy (CHED2). Mutation in brief #958. Online." Hum Mutat 28(5): 522-523.
- Rao, B. S., S. Ansar, T. Arokiasamy, R. R. Sudhir, V. Umashankar, R. Rajagopal and N. Soumittra (2018). "Analysis of candidate genes ZEB1 and LOXHD1 in late-onset Fuchs' endothelial corneal dystrophy in an Indian cohort." Ophthalmic Genet 39(4): 443-449.
- Rao, B. S., A. Tharigopala, S. R. Rachapalli, R. Rajagopal and N. Soumittra (2017). "Association of polymorphisms in the intron of TCF4 gene to late-onset Fuchs endothelial corneal dystrophy: An Indian cohort study." Indian J Ophthalmol 65(10): 931-935.
- Rao, G. N., L. E. Lohman and J. V. Aquavella (1982). "Cell size-shape relationships in corneal endothelium." Invest Ophthalmol Vis Sci 22(2): 271-274.
- Read, S. a. (2019). Human Molecular Genetics, CRC Press
- Repp, D. J., D. O. Hodge, K. H. Baratz, J. W. McLaren and S. V. Patel (2013). "Fuchs' endothelial corneal dystrophy: subjective grading versus objective grading based on the central-to-peripheral thickness ratio." Ophthalmology 120(4): 687-694.
- Reuter, J. A., D. V. Spacek and M. P. Snyder (2015). "High-throughput sequencing technologies." Mol Cell 58(4): 586-597.
- Riazuddin, S. A., D. S. Parker, E. J. McGlumphy, E. C. Oh, B. W. Iliff, T. Schmedt, U. Jurkunas, R. Schleif, N. Katsanis and J. D. Gottsch (2012). "Mutations in LOXHD1, a recessive-deafness locus, cause dominant late-onset Fuchs corneal dystrophy." Am J Hum Genet 90(3): 533-539.
- Riazuddin, S. A., N. A. Zaghoul, A. Al-Saif, L. Davey, B. H. Diplas, D. N. Meadows, A. O. Eghrari, M. A. Minear, Y. J. Li, G. K. Klintworth, N. Afshari, S. G. Gregory, J. D. Gottsch and N. Katsanis (2010). "Missense mutations in TCF8 cause late-onset Fuchs corneal dystrophy and interact with FCD4 on chromosome 9p." Am J Hum Genet 86(1): 45-53.
- Ricard-Blum, S. (2011). "The collagen family." Cold Spring Harb Perspect Biol 3(1): a004978.
- Rice, G. D., K. Wright and S. M. Silverstein (2014). "A retrospective study of the association between Fuchs' endothelial dystrophy and glaucoma." Clin Ophthalmol 8: 2155-2159.

Richman, J., G. L. Spaeth and B. Wirostko (2013). "Contrast sensitivity basics and a critique of currently available tests." J Cataract Refract Surg 39(7): 1100-1106.

Riley, M. (1985). "Pump and leak in regulation of fluid transport in rabbit cornea." Curr Eye Res 4(4): 371-376.

Riley, M. V., B. S. Winkler, C. A. Czajkowski and M. I. Peters (1995). "The roles of bicarbonate and CO<sub>2</sub> in transendothelial fluid movement and control of corneal thickness." Invest Ophthalmol Vis Sci 36(1): 103-112.

Roberts, T. C., R. Langer and M. J. A. Wood (2020). "Advances in oligonucleotide drug delivery." Nat Rev Drug Discov 19(10): 673-694.

Rong, Z., J. Hu, D. R. Corey and V. V. Mootha (2019). "Quantitative Studies of Muscleblind Proteins and Their Interaction With TCF4 RNA Foci Support Involvement in the Mechanism of Fuchs' Dystrophy." Invest Ophthalmol Vis Sci 60(12): 3980-3991.

Roos, W. P. and B. Kaina (2013). "DNA damage-induced cell death: from specific DNA lesions to the DNA damage response and apoptosis." Cancer Lett 332(2): 237-248.

Rosenblatt, A., M. H. Abbott, L. M. Gourley, J. C. Troncoso, R. L. Margolis, J. Brandt and C. A. Ross (2003). "Predictors of neuropathological severity in 100 patients with Huntington's disease." Ann Neurol 54(4): 488-493.

Rosenblum, P., W. J. Stark, I. H. Maumenee, L. W. Hirst and A. E. Maumenee (1980). "Hereditary Fuchs' Dystrophy." Am J Ophthalmol 90(4): 455-462.

Roy, B. C., N. Kakinuma and R. Kiyama (2009). "Kank attenuates actin remodeling by preventing interaction between IRSp53 and Rac1." J Cell Biol 184(2): 253-267.

Roy, O., V. B. Leclerc, J. M. Bourget, M. Theriault and S. Proulx (2015). "Understanding the process of corneal endothelial morphological change in vitro." Invest Ophthalmol Vis Sci 56(2): 1228-1237.

Saade, J. S., C. Xing, X. Gong, Z. Zhou and V. V. Mootha (2018). "Instability of TCF4 Triplet Repeat Expansion With Parent-Child Transmission in Fuchs' Endothelial Corneal Dystrophy." Invest Ophthalmol Vis Sci 59(10): 4065-4070.

Saikia, P., C. S. Medeiros, S. Thangavadivel and S. E. Wilson (2018). "Basement membranes in the cornea and other organs that commonly develop fibrosis." Cell Tissue Res 374(3): 439-453.

Salouti, R., M. H. Nowroozzadeh, M. Zamani and M. Ghoreyshi (2010). "Combined anterior keratoconus and Fuchs' endothelial dystrophy: a report of two cases." Clin Exp Optom 93(4): 268-270.

Sarkar, S., B. C. Roy, N. Hatano, T. Aoyagi, K. Gohji and R. Kiyama (2002). "A novel ankyrin repeat-containing gene (Kank) located at 9p24 is a growth suppressor of renal cell carcinoma." J Biol Chem 277(39): 36585-36591.

Sarraf, D. and D. A. Lee (1994). "The role of iontophoresis in ocular drug delivery." J Ocul Pharmacol 10(1): 69-81.

Seitzman, G. D. (2005). "Cataract surgery in Fuchs' dystrophy." Curr Opin Ophthalmol 16(4): 241-245.

Seitzman, G. D., J. D. Gottsch and W. J. Stark (2005). "Cataract surgery in patients with Fuchs' corneal dystrophy: expanding recommendations for cataract surgery without simultaneous keratoplasty." Ophthalmology 112(3): 441-446.

Shiraishi, A., R. L. Converse, C. Y. Liu, F. Zhou, C. W. Kao and W. W. Kao (1998). "Identification of the cornea-specific keratin 12 promoter by in vivo particle-mediated gene transfer." Invest Ophthalmol Vis Sci 39(13): 2554-2561.

Shousha, M. A., V. L. Perez, J. Wang, T. Ide, S. Jiao, Q. Chen, V. Chang, N. Buchser, S. R. Dubovy, W. Feuer and S. H. Yoo (2010). "Use of ultra-high-resolution optical coherence tomography to detect in vivo characteristics of Descemet's membrane in Fuchs' dystrophy." Ophthalmology 117(6): 1220-1227.

Sim, N. L., P. Kumar, J. Hu, S. Henikoff, G. Schneider and P. C. Ng (2012). "SIFT web server: predicting effects of amino acid substitutions on proteins." Nucleic Acids Res 40(Web Server issue): W452-457.

Sobrado, V. R., G. Moreno-Bueno, E. Cubillo, L. J. Holt, M. A. Nieto, F. Portillo and A. Cano (2009). "The class I bHLH factors E2-2A and E2-2B regulate EMT." J Cell Sci 122(Pt 7): 1014-1024.

Soh, Y. Q., G. Peh Swee Lim, H. M. Htoon, X. Gong, V. V. Mootha, E. N. Vithana, V. Kocaba and J. S. Mehta (2019). "Trinucleotide repeat expansion length as a predictor of the clinical progression of Fuchs' Endothelial Corneal Dystrophy." PLoS One 14(1): e0210996.

Soliman, A. Z., C. Xing, S. H. Radwan, X. Gong and V. V. Mootha (2015). "Correlation of Severity of Fuchs Endothelial Corneal Dystrophy With Triplet Repeat Expansion in TCF4." JAMA Ophthalmol 133(12): 1386-1391.

Sonoda, S., K. Tachibana, E. Uchino, A. Okubo, M. Yamamoto, K. Sakoda, T. Hisatomi, K. H. Sonoda, Y. Negishi, Y. Izumi, S. Takao and T. Sakamoto (2006). "Gene transfer to corneal epithelium and keratocytes mediated by ultrasound with microbubbles." Invest Ophthalmol Vis Sci 47(2): 558-564.

Soragni, E., L. Petrosyan, T. A. Rinkoski, E. D. Wieben, K. H. Baratz, M. P. Fautsch and J. M. Gottesfeld (2018). "Repeat-Associated Non-ATG (RAN) Translation in Fuchs' Endothelial Corneal Dystrophy." Invest Ophthalmol Vis Sci 59(5): 1888-1896.

Sun, S. Y., K. Wacker, K. H. Baratz and S. V. Patel (2019). "Determining Subclinical Edema in Fuchs Endothelial Corneal Dystrophy: Revised Classification using Scheimpflug Tomography for Preoperative Assessment." Ophthalmology 126(2): 195-204.

Sundin, O. H., A. S. Jun, K. W. Broman, S. H. Liu, S. E. Sheehan, E. C. Vito, W. J. Stark and J. D. Gottsch (2006). "Linkage of late-onset Fuchs corneal dystrophy to a novel locus at 13pTel-13q12.13." Invest Ophthalmol Vis Sci 47(1): 140-145.

Syed, Z. A., J. A. Tran and U. V. Jurkunas (2017). "Peripheral Endothelial Cell Count Is a Predictor of Disease Severity in Advanced Fuchs Endothelial Corneal Dystrophy." Cornea 36(10): 1166-1171.

Sznajder, L. J., J. D. Thomas, E. M. Carrell, T. Reid, K. N. McFarland, J. D. Cleary, R. Oliveira, C. A. Nutter, K. Bhatt, K. Sobczak, T. Ashizawa, C. A. Thornton, L. P. W. Ranum and M. S. Swanson (2018). "Intron retention induced by microsatellite expansions as a disease biomarker." Proc Natl Acad Sci U S A 115(16): 4234-4239.

Tam, V., N. Patel, M. Turcotte, Y. Bosse, G. Pare and D. Meyre (2019). "Benefits and limitations of genome-wide association studies." Nat Rev Genet 20(8): 467-484.

Tanelian, D. L., M. A. Barry, S. A. Johnston, T. Le and G. Smith (1997). "Controlled gene gun delivery and expression of DNA within the cornea." Biotechniques 23(3): 484-488.

Thoft, R. A. and J. Friend (1983). "The X, Y, Z hypothesis of corneal epithelial maintenance." Invest Ophthalmol Vis Sci 24(10): 1442-1443.

Thompson, D. A., A. Iannaccone, R. R. Ali, V. Y. Arshavsky, I. Audo, J. W. B. Bainbridge, C. G. Besirli, D. G. Birch, K. E. Branham, A. V. Cideciyan, S. P. Daiger, D. Dalkara, J. L. Duncan, A. T. Fahim, J. G. Flannery, R. Gattagna, J. R. Heckenlively, E. Heon, K. T. Jayasundera, N. W. Khan, H. Klassen, B. P. Leroy, R. S. Molday, D. C. Musch, M. E. Pennesi, S. M. Petersen-Jones, E. A. Pierce, R. C. Rao, T. A. Reh, J. A. Sahel, D. Sharon, P. A. Sieving, E. Strettoi, P. Yang, D. N. Zacks and C. Monaciano (2020). "Advancing Clinical Trials for Inherited Retinal Diseases: Recommendations from the Second Monaciano Symposium." Transl Vis Sci Technol 9(7): 2.

Tong, Y. C., S. F. Chang, C. Y. Liu, W. W. Kao, C. H. Huang and J. Liaw (2007). "Eye drop delivery of nano-polymeric micelle formulated genes with cornea-specific promoters." J Gene Med 9(11): 956-966.

Torricelli, A. A., V. Singh, M. R. Santhiago and S. E. Wilson (2013). "The corneal epithelial basement membrane: structure, function, and disease." Invest Ophthalmol Vis Sci 54(9): 6390-6400.

van der Meulen, I. J., S. V. Patel, R. Lapid-Gortzak, C. P. Nieuwendaal, J. W. McLaren and T. J. van den Berg (2011). "Quality of vision in patients with fuchs endothelial dystrophy and after descemet stripping endothelial keratoplasty." Arch Ophthalmol 129(12): 1537-1542.

- Vasanth, S., A. O. Eghrari, B. C. Gapsis, J. Wang, N. F. Haller, W. J. Stark, N. Katsanis, S. A. Riazuddin and J. D. Gottsch (2015). "Expansion of CTG18.1 Trinucleotide Repeat in TCF4 Is a Potent Driver of Fuchs' Corneal Dystrophy." Invest Ophthalmol Vis Sci 56(8): 4531-4536.
- Vedana, G., G. Villarreal, Jr. and A. S. Jun (2016). "Fuchs endothelial corneal dystrophy: current perspectives." Clin Ophthalmol 10: 321-330.
- Vilas, G. L., S. K. Loganathan, J. Liu, A. K. Riau, J. D. Young, J. S. Mehta, E. N. Vithana and J. R. Casey (2013). "Transmembrane water-flux through SLC4A11: a route defective in genetic corneal diseases." Hum Mol Genet 22(22): 4579-4590.
- Vilas, G. L., P. E. Morgan, S. K. Loganathan, A. Quon and J. R. Casey (2011). "A biochemical framework for SLC4A11, the plasma membrane protein defective in corneal dystrophies." Biochemistry 50(12): 2157-2169.
- Vira, S., U. Abugo, C. Y. Shih, I. J. Udell, B. Sperling, S. B. Hannush, S. Basti and C. S. Bouchard (2014). "Descemet stripping endothelial keratoplasty for the treatment of combined fuchs corneal endothelial dystrophy and keratoconus." Cornea 33(1): 1-5.
- Vithana, E. N., P. Morgan, P. Sundaresan, N. D. Ebenezer, D. T. Tan, M. D. Mohamed, S. Anand, K. O. Khine, D. Venkataraman, V. H. Yong, M. Salto-Tellez, A. Venkatraman, K. Guo, B. Hemadevi, M. Srinivasan, V. Prajna, M. Khine, J. R. Casey, C. F. Inglehearn and T. Aung (2006). "Mutations in sodium-borate cotransporter SLC4A11 cause recessive congenital hereditary endothelial dystrophy (CHED2)." Nat Genet 38(7): 755-757.
- Vithana, E. N., P. E. Morgan, V. Ramprasad, D. T. Tan, V. H. Yong, D. Venkataraman, A. Venkatraman, G. H. Yam, S. Nagasamy, R. W. Law, R. Rajagopal, C. P. Pang, G. Kumaramanickevel, J. R. Casey and T. Aung (2008). "SLC4A11 mutations in Fuchs endothelial corneal dystrophy." Hum Mol Genet 17(5): 656-666.
- Vonsattel, J. K., C.; Amaya, MDP (2008). Neuropathology of Huntington's disease. Handbook of Clinical Neurology. C. L. Duyckaerts, I., editors. 89: p. 599-617.
- Wacker, K., K. H. Baratz, W. M. Bourne and S. V. Patel (2018). "Patient-Reported Visual Disability in Fuchs' Endothelial Corneal Dystrophy Measured by the Visual Function and Corneal Health Status Instrument." Ophthalmology.
- Wacker, K., K. H. Baratz, W. M. Bourne and S. V. Patel (2018). "Patient-Reported Visual Disability in Fuchs' Endothelial Corneal Dystrophy Measured by the Visual Function and Corneal Health Status Instrument." Ophthalmology 125(12): 1854-1861.
- Wacker, K., J. W. McLaren, S. R. Amin, K. H. Baratz and S. V. Patel (2015). "Corneal High-Order Aberrations and Backscatter in Fuchs' Endothelial Corneal Dystrophy." Ophthalmology 122(8): 1645-1652.
- Wang, J., L. Kong, G. Gao and J. Luo (2013). "A brief introduction to web-based genome browsers." Brief Bioinform 14(2): 131-143.

Wang, N. and J. McKelvie (2020). "Coincident keratoconus and Fuchs' endothelial dystrophy: Dual dystrophies mask progression." Indian J Ophthalmol 68(12): 3074-3076.

Waring, G. O., 3rd, W. M. Bourne, H. F. Edelhauser and K. R. Kenyon (1982). "The corneal endothelium. Normal and pathologic structure and function." Ophthalmology 89(6): 531-590.

Weiss, J. S., H. U. Moller, A. J. Aldave, B. Seitz, C. Bredrup, T. Kivela, F. L. Munier, C. J. Rapuano, K. K. Nischal, E. K. Kim, J. Sutphin, M. Busin, A. Labbe, K. R. Kenyon, S. Kinoshita and W. Lisch (2015). "IC3D classification of corneal dystrophies--edition 2." Cornea 34(2): 117-159

Weiss, J. S., H. U. Moller, W. Lisch, S. Kinoshita, A. J. Aldave, M. W. Belin, T. Kivela, M. Busin, F. L. Munier, B. Seitz, J. Sutphin, C. Bredrup, M. J. Mannis, C. J. Rapuano, G. Van Rij, E. K. Kim and G. K. Klintworth (2008). "The IC3D classification of the corneal dystrophies." Cornea 27 Suppl 2: S1-83.

Wensor, M. D., C. A. McCarty, Y. L. Stanislavsky, P. M. Livingston and H. R. Taylor (1998). "The prevalence of glaucoma in the Melbourne Visual Impairment Project." Ophthalmology 105(4): 733-739.

West-Mays, J. A. and D. J. Dwivedi (2006). "The keratocyte: corneal stromal cell with variable repair phenotypes." Int J Biochem Cell Biol 38(10): 1625-1631.

Wieben, E. D., R. A. Aleff, B. W. Eckloff, E. J. Atkinson, S. Baheti, S. Middha, W. L. Brown, S. V. Patel, J. P. Kocher and K. H. Baratz (2014). "Comprehensive assessment of genetic variants within TCF4 in Fuchs' endothelial corneal dystrophy." Invest Ophthalmol Vis Sci 55(9): 6101-6107.

Wieben, E. D., R. A. Aleff, X. Tang, K. R. Kalari, L. J. Maguire, S. V. Patel, K. H. Baratz and M. P. Fautsch (2018). "Gene expression in the corneal endothelium of Fuchs endothelial corneal dystrophy patients with and without expansion of a trinucleotide repeat in TCF4." PLoS One 13(7): e0200005.

Wieben, E. D., R. A. Aleff, N. Tosakulwong, M. L. Butz, W. E. Highsmith, A. O. Edwards and K. H. Baratz (2012). "A common trinucleotide repeat expansion within the transcription factor 4 (TCF4, E2-2) gene predicts Fuchs corneal dystrophy." PLoS One 7(11): e49083.

Wilson, S. E. (2020). "Bowman's layer in the cornea- structure and function and regeneration." Exp Eye Res 195: 108033.

Wilson, S. E. and W. M. Bourne (1988). "Fuchs' dystrophy." Cornea 7(1): 2-18.

Wilson, S. E. and J. W. Hong (2000). "Bowman's layer structure and function: critical or dispensable to corneal function? A hypothesis." Cornea 19(4): 417-420.

Winkler, B. S., M. V. Riley, M. I. Peters and F. J. Williams (1992). "Chloride is required for fluid transport by the rabbit corneal endothelium." Am J Physiol 262(5 Pt 1): C1167-1174.

- Winkler, N. S., M. Milone, J. M. Martinez-Thompson, H. Raja, R. A. Aleff, S. V. Patel, M. P. Fautsch, E. D. Wieben and K. H. Baratz (2018). "Fuchs' Endothelial Corneal Dystrophy in Patients With Myotonic Dystrophy, Type 1." Invest Ophthalmol Vis Sci 59(7): 3053-3057.
- Xiang, Z. (2006). "Advances in homology protein structure modeling." Curr Protein Pept Sci 7(3): 217-227.
- Xing, C., X. Gong, I. Hussain, C. C. Khor, D. T. Tan, T. Aung, J. S. Mehta, E. N. Vithana and V. V. Mootha (2014). "Transethnic replication of association of CTG18.1 repeat expansion of TCF4 gene with Fuchs' corneal dystrophy in Chinese implies common causal variant." Invest Ophthalmol Vis Sci 55(11): 7073-7078.
- Xuan, M., S. Wang, X. Liu, Y. He, Y. Li and Y. Zhang (2016). "Proteins of the corneal stroma: importance in visual function." Cell Tissue Res 364(1): 9-16.
- Xue, K. and R. E. MacLaren (2020). "Antisense oligonucleotide therapeutics in clinical trials for the treatment of inherited retinal diseases." Expert Opin Investig Drugs 29(10): 1163-1170.
- Yohe, S. and B. Thyagarajan (2017). "Review of Clinical Next-Generation Sequencing." Arch Pathol Lab Med 141(11): 1544-1557.
- Yoshida, T., Y. Naito, H. Yasuhara, K. Sasaki, H. Kawaji, J. Kawai, M. Naito, H. Okuda, S. Obika and T. Inoue (2019). "Evaluation of off-target effects of gapmer antisense oligonucleotides using human cells." Genes Cells 24(12): 827-835.
- Yu, T., R. M. Peng, G. G. Xiao, L. N. Feng and J. Hong (2020). "Clinical Evaluation of Intravitreal Injection of Ganciclovir in Refractory Corneal Endotheliitis." Ocul Immunol Inflamm 28(2): 270-280.
- Zarouchlioti, C., B. Sanchez-Pintado, N. J. Hafford Tear, P. Klein, P. Liskova, K. Dulla, M. Semo, A. A. Vugler, K. Muthusamy, L. Dudakova, H. J. Levis, P. Skalicka, P. Hysi, M. E. Cheetham, S. J. Tuft, P. Adamson, A. J. Hardcastle and A. E. Davidson (2018). "Antisense Therapy for a Common Corneal Dystrophy Ameliorates TCF4 Repeat Expansion-Mediated Toxicity." Am J Hum Genet 102(4): 528-539.
- Zhang, C., W. R. Bell, O. H. Sundin, Z. De La Cruz, W. J. Stark, W. R. Green and J. D. Gottsch (2006). "Immunohistochemistry and electron microscopy of early-onset fuchs corneal dystrophy in three cases with the same L450W COL8A2 mutation." Trans Am Ophthalmol Soc 104: 85-97.
- Zhang, W., D. G. Ogando, E. T. Kim, M. J. Choi, H. Li, J. M. Tenessen and J. A. Bonanno (2017). "Conditionally Immortal Slc4a11<sup>-/-</sup> Mouse Corneal Endothelial Cell Line Recapitulates Disrupted Glutaminolysis Seen in Slc4a11<sup>-/-</sup> Mouse Model." Invest Ophthalmol Vis Sci 58(9): 3723-3731.
- Zhou, R. and D. A. Dean (2007). "Gene transfer of interleukin 10 to the murine cornea using electroporation." Exp Biol Med (Maywood) 232(3): 362-369.

Zoega, G. M., A. Fujisawa, H. Sasaki, A. Kubota, K. Sasaki, K. Kitagawa and F. Jonasson (2006). "Prevalence and risk factors for cornea guttata in the Reykjavik Eye Study." Ophthalmology 113(4): 565-569.

Zu, T., B. Gibbens, N. S. Doty, M. Gomes-Pereira, A. Huguet, M. D. Stone, J. Margolis, M. Peterson, T. W. Markowski, M. A. Ingram, Z. Nan, C. Forster, W. C. Low, B. Schoser, N. V. Somia, H. B. Clark, S. Schmechel, P. B. Bitterman, G. Gourdon, M. S. Swanson, M. Moseley and L. P. Ranum (2011). "Non-ATG-initiated translation directed by microsatellite expansions." Proc Natl Acad Sci U S A 108(1): 260-265.

Zu, T., A. Pattamatta and L. P. W. Ranum (2018). "Repeat-Associated Non-ATG Translation in Neurological Diseases." Cold Spring Harb Perspect Biol 10(12).



## APPENDIX

### A Genotyping for TCF4 CTG18.1 Repeat Expansion

Whole blood DNA extraction and storage

DNA was extracted within 2 weeks of blood sample collection. DNA extraction was performed by experienced laboratory technicians using Qiagen Genra Puregene Blood kit (Qiagen). Following extraction, DNA samples were stored at 4°C for immediate use or at -20°C for long term storage.

Short Tandem Repeat (STR) analysis

PCR was performed to amplify the *TCF4* polymorphic repeat (CTG18.1). The reagents in table # below were combined to create a master mix in a multiple of the number of samples to be analysed:

Reaction Component	GoTaq G2 colourless Master Mix (2x)	TCF4_repeat forward primer * (10µM)	TCF4_repeat reverse primer** (10µM)	ddH2O	Total volume
Volume	6.25 µL	0.5µL	0.5µL	4.25µL	11.5µL
Final concentration	1x	0.4 µM	0.4 µM	NA	NA

\* Forward primer that is 5'Fam conjugated to enable sizing of products via capillary electrophoresis:

5'-CAGATGAGTTTGGTGTAAGAT-3'

\*\* Reverse primer: 5'-ACAAGCAGAAAGGGGGCTGCAA-3'

Table 3: PCR reaction components and volume for STR analysis of CTG18.1 repeat

To each 100µL PCR tube, 12µL of the master mix was added along with 0.5µL of DNA sample. 2 control reactions were performed in parallel:

1. No-template-control in which DNA was omitted and replaced with an equivalent of ddH2O to allow detection of nucleotide contaminants in the reaction.
2. Positive control in which a previously sequenced DNA sample was used to confirm primer binding.

PCR was performed with an initial denaturation step of 95°C for 5 minutes followed by 35 cycles of: 92°C for 30 seconds to denature, 56°C for 30 seconds to anneal template then 72°C for 90 seconds to enable template extension. A final extension step of 72°C for 5 minutes was used.

#### Agarose gel electrophoresis

A 2% agarose gel mould was constructed by combining 7.5µL SafeView (NBS biologicals) (0.5mg/ml ethidium bromide), 150mL of 1X Tris-acetate-EDTA (TAE) buffer (Severn Biotech Ltd) and 3g of agarose powder (Bioline). 4µL of PCR product was combined with 1µL of loading dye (New England Biolabs). The 5µL sample was then placed into individual wells. 5µL DNA ladder (Purple 2-Log ladder) ( New England Biolabs) was also run for PCR product sizing. PCR products were visualised and compared against the DNA ladder in the ImageLab imaging system (BioRad). An assessment of the bands was made to confirm the presence of amplified PCR product.

#### DNA analysis via capillary electrophoresis.

To prepare the samples for electrophoresis, Rox500 Ladder and Formamide was first combined in a 1:50 ratio. 9.9µL of the Ladder and Formamide solution was the added to 1.1µL of amplified DNA in a PCR tube. The DNA was then denatured at 95°C for 5 minutes. Each 11µL denatured sample was then placed into a PCR plate prior to submission to an experienced technician to undergo capillary electrophoresis separation of the sample. Product separation was performed on the ABI 3730 Electrophoresis 96 capillary DNA analyser (Applied Biosystems). The data analysis was then performed using GeneMarker software (SoftGenetics).

B Statistical Analysis Chapter 2.0

Ethnicity versus Expansion Status Cross tabulation					
			Expansion50		Total
			Repeat Expansion Negative	Repeat Expansion Positive	
Ethnicity	Caucasian	Count	58	244	302
		Expected Count	68.0	234.0	302.0
		% within Ethnicity	19.2%	80.8%	100.0%
		Adjusted Residual	-4.0	4.0**	
	Black/Afro-Caribbean	Count	12	4	16
		Expected Count	3.6	12.4	16.0
		% within Ethnicity	75.0%	25.0%	100.0%
		Adjusted Residual	5.1**	-5.1	
	Asian	Count	6	6	12
		Expected Count	2.7	9.3	12.0
		% within Ethnicity	50.0%	50.0%	100.0%
		Adjusted Residual	2.3	-2.3	
	Other	Count	0	8	8
		Expected Count	1.8	6.2	8.0
		% within Ethnicity	0.0%	100.0%	100.0%
		Adjusted Residual	-1.5	1.5	
	Chinese	Count	1	3	4
		Expected Count	0.9	3.1	4.0
		% within Ethnicity	25.0%	75.0%	100.0%
		Adjusted Residual	0.1	-0.1	
Total	Count	77	265	342	
	Expected Count	77.0	265.0	342.0	
	% within Ethnicity	22.5%	77.5%	100.0%	

(a)

Chi-Square Tests for the association of Ethnicity with Expansion Status				
	Value	df	Asymptotic Significance (2-sided)	Exact Sig. (2-sided)
Pearson Chi-Square	34.695 <sup>a</sup>	4	.000	.000
Likelihood Ratio	30.210	4	.000	.000
Fisher's Exact Test	28.689			.000
N of Valid Cases	342			

(b)

Table 1: Crosstabulation analysis was performed to ascertain the relationship between subject ethnicity versus the expansion status. Table (a) shows the distribution of patients and the difference between the expected and actual frequencies of the subjects based on ethnicity and expansion status. An adjusted residual >2.5 was found in the Black/Afro-Caribbean and Caucasian populations as highlighted by \*\*. Table (b) shows Chi Square analysis of the categorical variables of ethnicity and expansion status showed a statistically significant association between ethnicity and expansion status, as Caucasian probands are more likely to be expansion positive while Black/Afro-Caribbean patients are more likely to be expansion negative (Chi square 34.7,  $p < 0.001$ ). Due to the small frequencies of variables, a Fisher exact test was performed to ensure the accuracy of results. A statistically significant association between ethnicity and expansion status was found ( $p=0.001$ ). Adjusted residuals were used to determine variables were contributing to statistical significance. Caucasians were more likely to be expansion positive, while Asians and Afro-Caribbean's were more likely to be expansion negative. No statistically significant relationship was found between expansion status and other ethnic groups.

Gender versus Expansion Status Crosstabulation					
			Expansion Status		Total
			Negative	Positive	
Gender	Female	Count	24	130	154
		Expected Count	34.7	119.3	154.0
		Adjusted Residual	-2.8**	2.8**	
	Male	Count	53	135	188
		Expected Count	42.3	145.7	188.0
		Adjusted Residual	2.8**	-2.8**	
Total		Count	77	265	342
		Expected Count	77.0	265.0	342.0

a) Crosstabulation analysis of gender versus expansion status. Crosstabulation analysis of gender versus expansion status provides an observed and expected frequencies in each cell of the table. A statistically significant difference was observed between observed and expected as adjusted residual values were greater than or equal to +/- 2.5 (highlighted cells).

Chi-Square Tests					
	Value	df	Asymptotic Significance (2-sided)	Exact Sig. (2-sided)	Exact Sig. (1-sided)
Pearson Chi-Square	7.713 <sup>a</sup>	1	.005	.006	.004
Likelihood Ratio	7.905	1	.005	.006	.004
Fisher's Exact Test				.006	.004
N of Valid Cases	342				

b) Chi-square statistical analysis of male gender versus expansion status. A statistically significant association was shown between the gender and expansion status (Chi square = 7.71, p < 0.005).

Table 2: Crosstabulation analysis was performed to ascertain the relationship between gender and expansion status. Table (a) shows the distribution of patients and the difference between the expected and actual frequencies of the subjects based on gender and expansion status. An adjusted residual >2.5 was found for both genders (2.8). Table (b) shows Chi Square analysis of the categorical variables of gender and expansion status showed a statistically significant association between gender and expansion status, as male probands are more likely to be expansion positive while female patients are more likely to be expansion negative (Chi square 7.713, p < 0.005).

Statistical Analysis of Association of Ocular Comorbidities with Repeat Expansion Status in FECD Number of valid cases: 342				
Ocular Comorbidity	Chi-Square Test			Fisher's Exact Test
	Value	df	Exact Sig. (1-sided)	
Glaucoma	0.196	1	0.406	0.406
Age Related Macular Degeneration (AMD)	0.01	1	0.610	0.610
Non-AMD Retinal Pathology	0.037	1	0.601	0.601
Keratoconus	0.203	1	0.536	0.536
RCES	0.889	1	0.315	0.315

Table 3: Statistical Analysis of association of ocular comorbidities with repeat expansion status in FECD.

Pearson Chi Square analysis was performed to determine if a statistically significant difference existed between the prevalence of ocular comorbidities in the expansion-positive and expansion-negative FECD cohorts. An additional Fisher exact test was performed given the small cell frequencies to ensure the accuracy of results. No statistically significant association was found between expansion status and the presence of glaucoma [ $\chi^2 = 0.196$   $p = 0.406$ ], Age related macular degeneration [ $\chi^2 = 0.010$   $p = 0.610$ ], non-AMD related retinal pathology [ $\chi^2 = 0.037$   $p = 0.601$ ], keratoconus [ $\chi^2 = 0.203$   $p = 0.536$ ] or recurrent erosion syndrome [ $\chi^2 = 0.889$   $p = 0.315$ ].

(df: degrees of freedom)

Mann-Whitney U Rank Analysis				
	Expansion Status	N	Mean Rank	Sum of Ranks
Age of Surgery	Negative	64	124.69	7980.00
	Positive	198	133.70	26473.00
	Total	262		

Statistical Analysis of Probability	
	Age of Surgery
Mann-Whitney U	5900.000
Wilcoxon W	7980.000
Z	-0.828
Asymp. Sig. (2-tailed)	0.408

Table 4. Statistical analysis of the relationship between age of first corneal transplant surgery and the presence of the repeat expansion. The Mann-Whitney U test was applied to the dependent variable of age of first corneal transplantation and the independent, dichotomous categorical variable of expansion status (repeat expansion positive versus repeat expansion negative). The Mann-Whitney U analysis showed no statistically significant difference was between age of grafting and expansion status (U = 5900, p= 0.408).

Spearman's Rho Correlations Analysis		
Age of Transplant Surgery	Repeat Expansion Length	
	Correlation Coefficient	Sig. (2-tailed)
Repeat Expansion Positive Subjects (N= 198)	-0.251**	0.000
Repeat expansion subjects with NO preceding cataract surgery (N= 112)	-0.254**	0.007
**. Correlation is significant at the 0.01 level (2-tailed)		

Table 5: Statistical analysis of the relationship between TCF4 repeat expansion length and age of first corneal transplantation. Spearman's rho analysis was applied to evaluate the relationship between the relationship of two continuous variables: repeat expansion length and age of corneal transplantation. This nonparametric test showed a weak but statically significant correlation between expansion length and age of grafting, ( $r = -0.251$ ,  $n=198$ ,  $p=0.001$ ). The direction of the relationship association indicated that longer repeat length was associated with a younger age of first corneal transplant surgery. This statistically significant relationship was also noted in the cohort of 112 patients who did not undergo cataract surgery prior to developing corneal decompensation ( $r = -0.254$ ,  $n=112$ ,  $p =0.007$ ).



Ranks				
	Expansion Status	N	Mean Rank	Sum of Ranks
Modified Clinical Grading Score	Expansion Negative	57	135.26	7710.00
	Expansion Positive	198	125.91	24930.00
	Total	255		

Test Statistics	
	Modified Clinical Grading Score
Mann-Whitney U	5229.000
Wilcoxon W	24930.000
Z	-.999
Asymp. Sig. (2-tailed)	.318
Grouping Variable: Expansion Status	

Table 6: Mann Whitney U analysis of the statistical relationship between the Modified Clinical Grading Score and age of first corneal transplant surgery. Analysis of the distribution of Modified Clinical grading score at the time of surgery between the expansion positive and the expansion negative cohort was performed by comparing the mean ranks of both cohorts. No statistically significant relationship was found between the repeat expansion positive and repeat expansion negative cohort (U = 5229, p = 0.318).






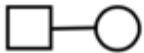
Model Fitting Information				
Model	-2 Log Likelihood	Chi-Square	df	Sig.
Intercept Only	360.053			
Final	356.231	3.822	2	0.148

Table 7: X Chi-Square goodness of fit test assessing the statistical relationship between repeat expansion length and the MCG score. The goodness of fit table for Chi-Square analysis has been used to compare the observed sample distribution with the expected probability distribution of repeat expansion length and MCG score having accounted for age of first corneal transplant. No statistically significant association was noted (p=0.148).

Model Summary									
Model	R	R Square	Adjusted R Square	Std. Error of the Estimate	Change Statistics				
					R Square Change	F Change	df1	df2	Sig. F Change
1	0.079 <sup>a</sup>	0.006	-0.009	77.15064	0.006	0.412	2	132	0.663
ANOVA <sup>a</sup>									
Model			Sum of Squares	Df	Mean Square	F	Sig.		
1	Regression		4904.690	2	2452.345	0.412	0.663 <sup>b</sup>		
	Residual		785693.191	132	5952.221				
	Total		790597.882	134					
Dependent Variable: Central Corneal Thickness									
Predictors: Repeat expansion status, Age of first corneal transplant surgery									

Table 8: Analysis of Variance (ANOVA) assessing the correlation between Central Corneal Thickness (CCT) and age of first corneal graft surgery. ANOVA modelling was performed in order to assess the relationship between eh variable of CCT against the predictor of expansion status, while taking into consideration the effect of age of first corneal transplant surgery. No association was found between the expansion status and CCT after accounting for the age at first grafting ( $p=0.663$ ).

C Legend to pedigree symbols

	Unaffected Male
	Unaffected Female
	Sex Unknown
	Affected Male and Female
	Deceased Individuals
	Non-Consanguineous marriage

## D Moorfields Corneal Cross Linking Guidelines

Ensure that patients have **Pentacam scans** and **refraction** with contact lenses out for a minimum of 2 weeks (RGP) and 1 week (soft).<sup>1</sup>

### Inclusion criteria for patients to be treated on pooled CXL lists (1 or more)

1. *Confirmed progression (based on current understanding of Pentacam measurement repeatability limits)*

Early KC (Kmax < 55D) <sup>2</sup> (1 or more)	Moderate/ advanced KC (Kmax ≥ 55D) <sup>3</sup> (1 or more)
<ul style="list-style-type: none"> <li>• ≥ 1 D increase Kmax</li> <li>• ≥ 1 D increase K2 or K1 front</li> <li>• ≥ 0.5 D increase back K2</li> <li>• ≥ 16 µm decrease minimum thickness</li> </ul>	<ul style="list-style-type: none"> <li>• ≥ 2.5 D increase Kmax</li> <li>• ≥ 2.5 D increase K2 or K1 front</li> <li>• ≥ 22 µm decrease minimum thickness</li> </ul>

2. *High risk of progression (1 or more)*
  - Age ≤ 18 years
  - Age 19 – 30 years (incl.) AND Minimum thickness < 400 µm
  - Age 19 – 30 years (incl.) AND Hydrops/graft fellow eye
3. *History of progression in referral letter based on serial topography or loss of corrected vision – documentation incomplete AND age ≤ 30 years*
4. *Previous LASIK with ectasia*

*NB. Patients who are unable to come out of contact lenses prior to Pentacam scanning (and therefore ineligible for f/u in EKC) may be offered CXL on pooled list if they are considered at risk of progression (i.e. age < 35 years) with continued f/u in Contact Lens clinic.<sup>4</sup>*

### Exclusion criteria

Active surface disease

\*Minimum corneal thickness < 375 µm

†Age < 16 years

\*Cognitive impairment

\*May be treated off pooled lists in laser suite (consultant led) or †main theatres with paediatric anaesthetic cover

**Referring patients to pooled lists:** Please complete provisional booking under OpenEyes 'Bruce Allan (External)' firm. Where both eyes require CXL, patients will be offered same-day bilateral treatments unless specified in the notes. Where available, please include the Pentacam 'compare 2 scans' map for the eye(s) to be treated.

**Treatment protocol:** Epithelium-off, 10 minutes 0.1% riboflavin drops (*Vibex Rapid*), 30mW/cm<sup>2</sup> UVA 4 minutes (pulsed 1.5 seconds on/off).

**Follow-up:** Patients are seen at 1 week for BCL removal. Uptodate refraction at high-street optician advised for those in spectacles at 1 month. Unless consultant input required (e.g. graft fellow eye, uncontrolled AKC etc.), follow-up in the *Early Keratoconus Clinic* at 6 and 12 months, then yearly up to 5 years. Contact lens appointments continue separately as before.

### Retreatment criteria

Treatment failure should be considered no earlier than 12 months post-CXL using the same keratometric indices of progression (Kmax, K2, K1). Pachymetry is not a useful indicator of progression post-CXL since corneal thickness measurements may decrease and/or increase up to 24 months after treatment.

### Notes

1. Maximum 3 scans, or 2 scans if both achieve “OK” quality score (QS). Scans with messages such as “data gaps”, “Fix” (fixation), “Lid” or “Blink” will be less reliable for diagnosing progression and will be recorded with an amber light in the data base, giving the option of filtering these scans out of audit data
2. There is approximately a 95% chance that changes of this magnitude in this group represent real change in the cornea.(Flynn et al. 2015)
3. In this group the 95% limits of agreement for K1 and Kmax are close to 4D. There is approximately an 80% chance that changes of 2.5D in these parameters in this group represent real change.(Flynn et al. 2015) Given that crosslinking is a relatively low-risk treatment, we have chosen this lower value as a compromise to try to avoid missing large changes in corneal shape.
4. Pending increased CXL capacity, this offer initially is restricted to 16 – 18 year olds (inclusive) i.e. those patients at greatest risk of disease progression.  $\geq 375\mu\text{m}$  minimum pachymetry required. If fluorescein has already been instilled during contact lens consultation,(Hirnschall et al. 2012) patients will be re-scanned on the day of treatment to confirm it is safe to proceed.

### References

- Flynn, T. et al., 2015. Differential precision of corneal Pentacam HR measurements in early and advanced keratoconus. *unpublished data*.
- Hirnschall, N. et al., 2012. Effect of fluorescein dye staining of the tear film on Scheimpflug measurements of central corneal thickness. *Cornea*, 31(1), pp.18–20.

## E Clinical Trial Subject Inclusion and Exclusion Criteria

### Inclusion Criteria

The subject is eligible for the study if all the following inclusion criteria are met:

1. Male or female,  $\geq 18$  years of age at Screening
2. Clinical diagnosis of FECD3 with:
  - a. confirmed presence of trinucleotide repeat (TNR) expansion in the *TCF4* gene (50 TNRs or more as determined by polymerase chain reaction (PCR))
  - b. symmetrical disease progression in the opinion of the Investigator necessitating surgical intervention to both eyes
  - c. a clinical indication for DMEK in both eyes is defined as : Best Corrected Visual Acuity (BCVA) worse than 6/12 Snellen, corneal stromal oedema secondary to corneal endothelial failure and patient reported difficulty in performing activities of daily living.
3. BCVA worse than Snellen 6/12 in both eyes. Concomitant cataracts are considered a normal finding however BCVA impairment should not be caused by other ophthalmic disease (e.g., age-related macular degeneration, glaucoma, optic neuropathies).
4. Subjects should be willing and able to provide informed consent, comply with the protocol, follow study instructions, attend study visits as required and able to complete all study assessments, in the opinion of the Investigator.

## Exclusion Criteria

The subject is ineligible for the study if any of the following criteria are met:

1. Presence of any significant ocular or non-ocular disease/disorder (including medication and laboratory test abnormalities) which, in the opinion of the Investigator, may either put the subject at risk because of participation in the study, may influence the results of the study, or the subject's ability to participate in the study.

This includes but is not limited to diagnosis in either eye with:

1. Concurrent cystoid macular oedema (CMO).
2. Neovascular age-related macular degeneration, geographic atrophy, myopic macular degeneration, moderate to severe non-proliferative and proliferative diabetic retinopathy, diabetic macular oedema, macular oedema secondary to retinal vein occlusions, or retinal dystrophies or history of retinal detachments.
3. Visually significant, non-glaucomatous optic neuropathies such as those related to ischemic (both arteritic and non-arteritic), toxic, nutritional, myopic, compression, infective and inflammatory causes.
4. Corneal endothelial disease that is associated with significant stromal scarring to such an extent that will predictably impair post-operative visual recovery after DMEK.
5. Corneal endothelial disease that may possibly be attributed to pathologies other than FECD3, including but not limited to pseudophakic bullous keratopathy, laser-peripheral-iridotomy induced bullous keratopathy, iridocorneal endothelial syndrome, posterior polymorphous corneal dystrophy, Axenfeld Rieger syndrome, congenital hereditary endothelial dystrophy, and any other anterior segment developmental anomalies.
6. History of any form of keratoplasty in either eye.
7. Prior lens replacement in either eye.
8. History or presence of ocular herpetic diseases (including herpes simplex virus, varicella zoster or cytomegalovirus) in either eye.
9. Presence of any active ocular infection in either eye.
10. Receipt within 3 months prior to Screening of any intraocular or periocular surgery (including refractive surgery), or an IVT injection or planned intraocular surgery or procedure (other than lens replacement or DMEK) during the course of the study in either eye.

11. Subjects with glaucoma, pseudoexfoliation syndrome, pigment dispersion syndrome, or ocular hypertension in either eye.
12. Current treatment or treatment within the past 12 months with therapies known to influence the immune system (including but not limited to cytostatics, interferons, Tumour Necrosis Factor-binding proteins, drugs acting on immunophilins, or antibodies with known impact on the immune system). Subjects that have been treated with systemic steroids within the past 12 months or that require intermittent use of topical steroids may be considered for inclusion following approval by the Medical Monitor.
13. Use of any investigational drug or device within 90 days or 5 half-lives of Day 1, whichever is longer, or plans to participate in another study of a drug or device during the study period.
14. Any prior receipt of genetic or stem-cell therapy for ocular or non-ocular disease.
15. History of malignancy within 5 years prior to screening, except adequately treated squamous or basal cell carcinoma of the skin or carcinoma in situ of the cervix that has been successfully treated.
16. Pregnant or breastfeeding subjects. Female subjects of childbearing potential and male subjects must be sexually inactive by abstinence, which is consistent with the preferred and usual lifestyle of the subject, or agree to use highly effective methods of birth control. Women of non-childbearing potential may be included without the use of adequate birth control, provided they meet the criteria.



## SCHEDULE OF EVENTS OF INVESTIGATIONS

Study Eye 1 (Control)								
Procedure	Screening Visit	DMEK+IOL						
		D1	D2	D7	M1	M3 <sup>y</sup>	M6 <sup>y</sup>	M12 <sup>y</sup>
		Wk1			Wk5	Wk13	Wk25	Wk49
Informed consent	X							
Confirm eligibility criteria	X							
Confirmation ExpPos status	X							
DMEK+Phaco+IOL		X						
Adverse Events	X	X	X	X	X	X	X	X
BCVA (both eyes)	X			X	X	X	X	X
Contrast sensitivity (both eyes)	X						X	X
Full-field ERG (both eyes)	X							X
FST <sup>1</sup>	X					X	X	X
Slit-lamp biomicroscopy examination +IOP	X	X	X	X	X	X	X	X
Dilated fundus examination	X			X	X	X	X	X
SD-OCT	X			X	X	X	X	X
Corneal OCT	X	X		X	X	X	X	X
Specular Microscopy	X	X		X	X	X	X	X
Scheimpflug tomography pachymetry	X				X	X	X	X
Microperimetry	X				X	X	X	X
Visual field	X				X		X	X
Fundus and Corneal photography	X							X
Hematology and bichemistry	X							

Study Eye 2 (ASO Treatment)											
Procedure	Screening Visit	IVT			DMEK+IOL within 14 days of ASO						
					D1	D2	D7	M1	M3 <sup>y</sup>	M6 <sup>y</sup>	M12 <sup>y</sup>
		D1	D2	D7	Wk1		Wk5	Wk13	Wk25	Wk49	
Informed consent	X										
Confirm eligibility criteria	X										
Confirmation ExpPos status	X										
ASO IVT injection		X									
DMEK+Phaco+IOL					X						
Adverse Events	X	X	X		X	X	X	X	X	X	X
BCVA (both eyes)	X	X	X				X	X	X	X	X
Contrast sensitivity (both eyes)	X		X	X						X	X
Full-field ERG (both eyes)	X			X							X
FST <sup>1</sup>	X			X					X	X	X
Slit-lamp biomicroscopy examination +IOP	X	X	X	X	X	X	X	X	X	X	X
Dilated fundus examination	X	X	X	X			X	X	X	X	X
SD-OCT	X		X	X			X	X	X	X	X
Corneal OCT	X		X	X	X		X	X	X	X	X
Specular Microscopy	X	X		X	X		X	X	X	X	X
Scheimpflug tomography pachymetry	X	X	X	X							
Microperimetry	X			X				X	X	X	X
Visual field	X			X				X		X	X
Fundus and Corneal photography	X										X
Hematology and biochemistry	X		X	X							

**Abbreviations:**

AE:	adverse event
BCVA:	best-corrected visual acuity
D:	day
DMEK:	Descemet's Membrane Endothelial Keratoplasty
ERG:	electroretinogram
FST:	full-field stimulus threshold
IOP:	intraocular pressure
IVT:	intravitreal
M:	month
SD-OCT:	Spectral domain optical coherence tomography
Wk:	week

## G List Of Common Terms

Allele	A term used to describe the alternative form or versions of a gene
Exon	Coding sequence in a gene
Corneal Dystrophy	A group of rare, genetic diseases that affect the cornea
Gene	A gene is a region of DNA that encodes a functional RNA product
Genotype	An organism's complete set of genes
Haplotype	a set of genetic determinants located on a single chromosome, a combination of linked alleles transmitted together
Homozygous	Having two identical alleles of a particular gene
Heterozygous	Having two different alleles of a particular gene
Intron	A segment of a DNA or RNA molecule which does not code for proteins and interrupts the sequence of genes
Mendelian inheritance	Mendelian inheritance refers to an inheritance pattern that follows the laws of segregation and independent assortment
Messenger RNA (mRNA)	Code for a protein that is formed after splicing and removal of introns
Mutation	Pathological change in the genetic sequence
Penetrance	The extent to which a particular gene or set of genes is expressed in the phenotypes of individuals carrying it, measured by the proportion of carriers showing the characteristic phenotype
Phenotype	Observable characteristics or traits of an organism
Proband	An individual being studied or reported on

Transcription	The process by which the information in a strand of DNA is copied into a new molecule of messenger RNA (mRNA)
Translation	process of translating the sequence of a messenger RNA (mRNA) molecule to a sequence of amino acids during protein synthesis
Variant	Term used to describe an alteration in the gene sequence that may be benign, pathogenic, or of unknown significance.

## H Amino Acid Codes

Amino acid	Three letter code	One letter code
alanine	ala	A
arginine	arg	R
asparagine	asn	N
aspartic acid	asp	D
asparagine or aspartic acid	asx	B
cysteine	cys	C
glutamic acid	glu	E
glutamine	gln	Q
glutamine or glutamic acid	glx	Z
glycine	gly	G
histidine	his	H
isoleucine	ile	I
leucine	leu	L
lysine	lys	K
methionine	met	M
phenylalanine	phe	F
proline	pro	P
serine	ser	S
threonine	thr	T
tryptophan	trp	W
tyrosine	tyr	Y
valine	val	V

## I Abbreviations

AD	Autosomal Dominant
AR	Autosomal Recessive
CECs	Corneal Endothelial Cells
CED	Corneal Endothelial Dystrophy
CHED	Congenital Hereditary Endothelial Dystrophy
<i>COL8A2</i>	$\alpha$ 2 chain of type VIII collagen gene
<i>COL8A1</i>	$\alpha$ 1 chain of type VIII collagen gene
DM	Descemet's Membrane
DM1	Myotonic Dystrophy 1
DMEK	Descemet's Membrane Endothelial Keratoplasty
DNA	Deoxyribonucleic Acid
DSAEK	Descemet's Stripping Automated Endothelial Keratoplasty
ECM	Extracellular Matrix
EDTA	Ethylenediaminetetraacetic Acid
ER	Endoplasmic Reticulum
ExpNeg	Expansion Negative
ExpPos	Expansion Positive
FECD	Fuchs Endothelial Corneal Dystrophy
FISH	Fluorescence <i>in situ</i> hybridisation
GWAS	Genome Wide Association Study
HGP	Human Genome Project
HS	Harboyan Syndrome
KANK4	KN Motif And Ankyrin Repeat Domains 4
<i>LAMC1</i>	Laminin Subunit Gamma 1
MAF	Minor Allele Frequency
MEH	Moorfields Eye Hospital
MET	Mesenchymal-to-epithelial transformation
OMIM	Online Mendelian Inheritance in Men
PCR	Polymerase chain reaction
Polyphen2	Polymorphism phenotyping 2
PPCD	Posterior Polymorphous Dystrophy

PTC	Premature Stop Codon
RAN	Repeat Associated non ATG translation
RNA	Ribonucleic acid
SIFT	Sorting Intolerant From Tolerant
<i>TCF4</i>	Transcription Factor 4
UCLex	University College London exome control data set
WES	Whole Exome Sequencing
<i>ZEB1</i>	Zinc Finger E-box binding homeobox 1 gene